



# Kent Academic Repository

**Cherry, Daniel (2022) *Investigating Resistance to Checkpoint Kinase 1 Inhibitors in Triple Negative Breast Cancer*. Doctor of Philosophy (PhD) thesis, University of Kent,.**

## Downloaded from

<https://kar.kent.ac.uk/95339/> The University of Kent's Academic Repository KAR

## The version of record is available from

<https://doi.org/10.22024/UniKent/01.02.95339>

## This document version

UNSPECIFIED

## DOI for this version

## Licence for this version

CC BY-NC-SA (Attribution-NonCommercial-ShareAlike)

## Additional information

## Versions of research works

### Versions of Record

If this version is the version of record, it is the same as the published version available on the publisher's web site. Cite as the published version.

### Author Accepted Manuscripts

If this document is identified as the Author Accepted Manuscript it is the version after peer review but before type setting, copy editing or publisher branding. Cite as Surname, Initial. (Year) 'Title of article'. To be published in *Title of Journal*, Volume and issue numbers [peer-reviewed accepted version]. Available at: DOI or URL (Accessed: date).

## Enquiries

If you have questions about this document contact [ResearchSupport@kent.ac.uk](mailto:ResearchSupport@kent.ac.uk). Please include the URL of the record in KAR. If you believe that your, or a third party's rights have been compromised through this document please see our [Take Down policy](https://www.kent.ac.uk/guides/kar-the-kent-academic-repository#policies) (available from <https://www.kent.ac.uk/guides/kar-the-kent-academic-repository#policies>).

# **Investigating Resistance to Checkpoint Kinase 1 Inhibitors in Triple Negative Breast Cancer**

**Daniel Lee Cherry**

December 2021

This thesis is submitted to the University of Kent for the  
degree of Doctor of Philosophy



Faculty of Sciences  
School of Biosciences  
University of Kent

# Declaration

No part of this thesis has been submitted in support of an application for any degree or other qualification of the University of Kent, or any other University or institution of learning.

Daniel Lee Cherry

December 2021

# Abstract

Triple negative breast cancer (TNBC) is an aggressive and metastatic disease and is characterised by the absence of three therapeutically relevant receptors commonly found in breast cancers, namely oestrogen, progesterone, and human epidermal growth factor receptor 2. Loss of these targets makes hormone therapies and some targeted therapies ineffective, limiting treatment options available to patients with chemotherapy and surgery remaining the standard care of treatment. Loss of *TP53* gene occurs at high frequency in TNBC making these cancers highly genomically unstable creating a dependency on remaining pathways to regulate the cell cycle and correct replication of DNA. Checkpoint Kinase 1 (CHK1) is a serine/threonine kinase activated in response to DNA damage to induce cell cycle arrest and/or replication fork stalling. DNA damage can be caused by exogenous agents such as genotoxic chemotherapy (e.g., gemcitabine), or innate in cancers with high levels of genomic instability and replication stress. Consequentially, tumours may become dependent on CHK1 for survival, making this kinase a potential therapeutic target. Preclinical data indicates that TNBC cells are sensitive to CHK1 inhibitors (CHK1i) SRA737 and Prexasertib, which are both in clinical trial. Unfortunately, resistance to anticancer drugs can emerge in tumours leading to patient relapse. It is therefore important to address this issue, even before a drug is approved for use. Consequently, this project aims to identify mechanisms, biomarkers, and strategies to overcome CHK1i resistance.

CHK1i resistant cell line models were generated from HCC38 and MDA-MB-468 TNBC cell lines to SRA737 and Prexasertib. HCC38 resistant sublines exhibit cross resistance to inhibitors of the CHK1 activator ATR (Ceralasertib) and cell cycle regulator WEE1 (Adavosertib). WEE1 phosphorylates CDK1/2 at Y15 inhibiting CDK activity and is present at higher levels in resistant sublines. Low doses of Adavosertib in combination with SRA737 resensitise resistant cells to CHK1i. Additionally, CDK2/1 inhibitor Roscovitine but not CDK1 inhibitor RO-3306 rescues the effect of SRA737 and Adavosertib drug combination in HCC38 parental and resistant sublines, suggesting resistant cells are dependent on maintenance of CDK2 inhibition for survival. Furthermore, HCC38 resistant sublines show resistance to the genotoxic agent Gemcitabine, suggesting further resistance mechanisms which may promote resilience to replication stress. However, low concentrations of Gemcitabine strongly resensitise HCC38 resistant sublines to CHK1i SRA737. Additionally, RNA sequencing of HCC38 parental and resistant sublines has identified a number of differentially expressed genes which may play a role in drug resistance.

### **Project Aims**

- Investigate and identify biomarkers and mechanisms of resistance to CHK1 inhibitors SRA737 and Prexasertib in Triple Negative Breast Cancer cell lines.
- Validate identified biomarkers/mechanisms of resistance to CHK1 inhibitors.
- Identify clinically relevant therapeutic strategies to overcome resistance.

### **Project Achievements**

- Generated TNBC cell lines with acquired resistance to CHK1 inhibitors.
- Identified a CDK2 dependent mechanism of CHK1 inhibitor resistance.
- Showed WEE1 overexpression is a potential biomarker and driver of acquired resistance to CHK1 inhibitors.
- Demonstrated the use of either Adavosertib (WEE1i) or Gemcitabine (Anthracycline) can be used in combination with a CHK1 inhibitor to overcome acquired resistance to CHK1 inhibitors in TNBC.

# Acknowledgements

Firstly, I would like to thank Professor Michelle Garrett for her unwavering support, expertise, and patience throughout my PhD. Your advice and encouragement has been instrumental in the development of my skills, knowledge, and confidence as a scientist. I would like to thank the University of Kent for awarding me with the GTA scholarship and for providing the resources to conduct my studies. I would also like to thank the Rosetrees Trust who funded the 4<sup>th</sup> year of my PhD which afforded me crucial time to complete my studies after the impact of the COVID outbreak.

I would like to warmly thank members of the Garrett lab for their amazing support throughout my PhD. Nathan, thanks for always reminding me I was at least in the top 20 of Garrett lab members, and for telling me that I was a “Competent and capable scientist” when I needed to hear it most. Helen, thanks for all your help and support, your ability to outcompete even the most sophisticated cell culture robotics while hungover will be something I will never forget. Jasmine, thank you for your patience and understanding when I asked you endless questions about western blots. A most special thanks must go to Edith Blackburn, without whom our lab would cease to function. The skills and experience you bring to the lab are matched only by your kindness and compassion. You have been indispensable in the completion of my project, and I will always consider you a dear friend.

Additionally, within the School of Biosciences, I would like to thank Eithaar for our entertaining office chats. Nikki, Max, and Nerissa of the Fenton lab for your invaluable assistance with flow cytometry and QPCR. I am also grateful to Ian Reddin for providing his time, expertise, and guidance to assist with my RNA sequencing analysis, your help has been crucial in the completion of my project. I would also like to thank James Budge who provided invaluable advice on transfection optimisation. A huge thankyou goes to Dean Judge and the rest of the Science Supplies team who have kept the School of Biosciences running during what has been a trying time for everyone.

Thanks to all my friends that have put up with my scientific ramblings and have been there for me through everything. I would also like to thank Robert and Corinne Heywood, whose kindness, support, and understanding has been amazing over the last year. I am extremely grateful for all the help you have given me, as well as our catchups over fish and chips.

I would also like to thank my family, but in particular my Mum, Dad, and brother Scott for always being there for me when I needed you. None of this would have been possible without your constant love and support, which has helped make me the person I am today. You all mean the world to me, and I hope I have made you proud.

I would like to reserve a special thank you for Kelly, who's unwavering love and support has given me the strength I needed to push on through the most difficult periods of my PhD. You're the love of my life and my best friend, and I am incredibly thankful and lucky to have you by my side.

Finally, I would like to dedicate this thesis to those in my family who can no longer be with us. To my Grandad Michael, Grandma Josephine, Nanny Anne, Harvey, and Harry. I have been incredibly lucky to have you in my life, and I love and miss you all dearly.

# Table of Contents

Declaration.....	1
Abstract.....	2
Acknowledgements.....	4
Table of contents.....	6
List of Figures.....	12
List of Tables.....	18
Abbreviations.....	19
<b>Chapter 1 Introduction.....</b>	<b>28</b>
1.1 The Hallmarks of Cancer.....	28
1.2 The Cell Cycle.....	29
1.2.1 Phases of the cell cycle.....	29
1.2.2 DNA replication.....	31
1.2.3 Cell cycle checkpoints.....	34
1.2.4 Replication stress.....	36
1.2.5 The replication stress response.....	38
1.3 The CHK1 Kinase.....	43
1.3.1 Checkpoint Kinases.....	43
1.3.2 CHK1 Structure.....	44
1.3.3 Regulation of CHK1 activity.....	45
1.3.3.1 ATR-dependent phosphorylation.....	45
1.3.3.2 CHK1 autophosphorylation of S296.....	46
1.3.3.3 Localisation and degradation of CHK1.....	46
1.3.4 CHK1 Function.....	47
1.3.4.1 CHK1 and the response to replication stress and DNA damage.....	48



1.3.4.2	Transcriptional regulation via CHK1.....	51
1.3.4.3	CHK1 regulation of ribonucleotide reductase (RNR).....	51
1.3.4.4	Regulation of apoptosis via CHK1.....	52
1.3.4.5	CHK1 and the spindle checkpoint.....	52
1.3.5	CHK1 as a target for cancer therapies.....	52
1.3.5.1	CHK1 inhibitors.....	53
1.3.5.2	Use of CHK1 inhibitors as a single agent.....	57
1.3.5.3	Combining CHK1 inhibitors with genotoxic agents.....	58
1.3.5.4	CHK1 and WEE1 inhibitors in combination.....	59
1.4	Resistance to Cancer Therapies.....	61
1.4.1	The challenge of drug resistance.....	61
1.4.2	Mechanisms of drug resistance.....	62
1.4.2.1	Pre-target effects.....	62
1.4.2.2	Pathway reactivation.....	63
1.4.2.3	Pathway bypass.....	65
1.4.2.4	Pathway indifference.....	66
1.5	Triple Negative Breast Cancer.....	67
1.5.1	Introducing TNBC.....	67
1.5.2	Treatment strategies for TNBC patients.....	69
1.6	Overview and aims of thesis.....	72
<b>Chapter 2 Materials and Methods.....</b>		<b>75</b>
2.1	Compounds.....	75
2.2	General Cell Culture.....	76
2.2.1	Cell lines and culture.....	77
2.2.2	Generation of TNBC cell lines with resistance to SRA737 or Prexasertib.....	77
2.2.3	Counting cells with a haemocytometer.....	77
2.2.4	Cryopreservation of cell lines.....	77

2.3 Cell Growth Characterisation.....	78
2.3.1 Seeing density assay.....	78
2.4 Sulforhodamine B cell viability assay.....	79
2.5 Cell lysis and Western Blotting.....	80
2.5.1 Cell Lysis.....	80
2.5.2 Bicinchoninic acid and Bradford assays.....	81
2.5.3 SDS-PAGE.....	82
2.5.4 Western Blotting.....	83
2.6 Cell Cycle Analysis via Flow Cytometry.....	85
2.7 Knockdown of WEE1 Gene Expression via Small Interfering RNA.....	86
2.8 Plasmid Preparation.....	87
2.8.1 Transformation of plasmid DNA and creation of glycerol stocks.....	87
2.8.2 Extraction of plasmid DNA.....	88
2.9 Generation of Transient WEE1 Overexpressing Cell Lines.....	89
2.10 Generation of Stable Cell Lines Expressing Exogenous WEE1.....	89
2.10.1 G418 Kill curve.....	89
2.10.2 Transfection of stable cell lines expressing exogenous WEE1.....	90
2.11 RNA Sequencing.....	91
2.11.1 RNA extraction.....	91
<b>Chapter 3 Generation of CHK1 Inhibitor Resistant Cell Lines.....</b>	<b>93</b>
3.1 Introduction.....	93
3.2 Results.....	98
3.2.1 Growth Characterisation of TNBC cell lines MDA-MB-468 and HCC38.....	99
3.2.2 Response of MDA-MB-468 and HCC38 cell lines to CHK1 inhibitors SRA737 and Prexasertib.....	100
3.2.3 Generation of resistant cell lines by dose escalation.....	102
3.2.4 Determination of growth characteristics of resistant cell lines.....	104

3.2.5 Response of CHK1 inhibitor resistant cell lines to SRA737 and Prexasertib.....	107
3.2.6 Light microscopy of MDA-MB-468 and HCC38 parental and resistant cell lines.....	110
3.2.7 Stability of drug resistance in H737R and HPrexR cell lines.....	112
3.2.8 Multidrug resistance in HCC38 and MDA-MB-468 parental and resistant cell lines.....	114
3.2.9 Cross profiling of parental and resistant cell lines.....	117
3.2.9.1 Inhibition of ATR and WEE1 kinases.....	117
3.2.9.2 Inhibition of ATM and CHK2 kinases.....	121
3.2.9.3 Cross profiling with Cisplatin.....	124
3.2.9.4 Cross profiling with Palbociclib.....	126
3.2.9.5 Cross profiling with Olaparib.....	128
3.2.10 Analysis of basal protein expression by western blot.....	129
3.2.10.1 Basal expression of CHK1 and CHK2 phosphorylated and total protein in HCC38 cell lines.....	129
3.2.10.2 WEE1 protein expression levels in HCC38 parental and resistant cell lines.....	131
3.3 Discussion.....	132
<b>Chapter 4 Investigating the role of WEE1 kinase in resistance to CHK1 inhibition...</b>	<b>142</b>
4.1 Introduction.....	142
4.2 Results.....	146
4.2.1 Investigating the effect of SRA737 on the DNA damage response and the cell cycle.....	146
4.2.2 Investigating the role of WEE1 in CHK1i resistance via targeted inhibitors of WEE1.....	151
4.2.3 Knockdown of WEE1 via Small interfering RNA (SiRNA) in resistant cell	

lines.....	167
4.2.3.1 Optimisation of SiRNA transfection conditions.....	167
4.2.3.2 Knockdown of WEE1 protein in H737R and HPrexR cell lines.....	171
4.2.4 Optimising ectopic expression of WEE1 protein.....	174
4.2.5 Investigating WEE1 expression and CHK1i sensitivity in a TNBC cell line panel.....	179
4.3 Discussion.....	183
<b>Chapter 5 Examining the role of replication stress in CHK1 inhibitor resistance.....</b>	<b>194</b>
5.1 Introduction.....	194
5.2 Results.....	197
5.2.1 Response of H737R and HPrexR to inducers of replication stress.....	197
5.2.2 The effect of CHK1 and WEE1 inhibition of replication stress in H737R and HPrexR cells.....	202
5.2.3 The role of CDK activity in resistance to CHK1 inhibition.....	206
5.3 Discussion.....	215
5.3.1 Investigating the role of replication stress in resistance to CHK1 inhibition.....	215
5.3.2 Investigating the role of Cyclin Dependent kinases in resistance to CHK1 inhibition.....	220
5.3.3 Summary.....	222
<b>Chapter 6 Gene Expression Analysis of HCC38 Parental and Resistant Cell Lines...</b>	<b>225</b>
6.1 Introduction.....	225
6.2 Results.....	227
6.2.1 RNA sequencing and quality control of reads.....	227
6.2.2 Identifying differently expressed genes.....	231
6.2.3 Identifying enriched pathways or biological processes.....	238
6.3 Discussion.....	250

<b>Chapter 7 General Discussion.....</b>	<b>257</b>
7.1 Introduction.....	257
7.2 Summary of the main findings.....	258
7.2.1 Triple Negative Breast Cancer cell lines with acquired resistance to CHK1 inhibition.....	258
7.2.2 Maintenance of CDK inhibition combined with elevated resilience to replication stress may drive CHK1i resistance.....	260
7.2.2.1 The role of WEE1 kinase and CDK inhibitor p21 <sup>Cip1/Waf1</sup> .....	260
7.2.2.2 Understanding the role of CDK activity in resistance to CHK1 inhibition.....	265
7.2.2.3 Replication stress and mechanisms of resistance to CHK1 inhibition.....	268
7.2.2.4 A model of CHK1 inhibitor resistance in H737R and HPrexR cell lines.....	271
7.3 Future Work.....	273
7.4 Clinical impact – Therapeutic strategies to combat CHK1 inhibitor resistance.....	276
7.5 Concluding remarks.....	278
Appendix List.....	279
References.....	281

# List of Figures

Figure 1.1: The cell cycle.....	29
Figure 1.2: Licensing and firing of replication origins.....	33
Figure 1.3: Activation of the replication stress response.....	39
Figure 1.4: Rescue of stalled replication forks.....	40
Figure 1.5: Collapse of the replication fork.....	41
Figure 1.6: Repair of double stranded DNA breaks.....	42
Figure 1.7: Structural domains and function of the CHK1 kinase.....	44
Figure 1.8: Functions of CHK1 in multiple cellular processes.....	48
Figure 1.9: Convergence based framework for cancer drug resistance.....	62
Figure 1.10: Diagram of normal breast duct microenvironment.....	68
Figure 3.1: Characterisation of MDA-MB-468 and HCC38 cell line growth in 96-well plates .....	99
Figure 3.2: Dose-response curves for CHK1 inhibitors Prexasertib and SRA737 in MDA-MB- 468 and HCC38 cell lines.....	101
Figure 3.3: Diagram of resistance generation by dose escalation in T25 flasks.....	102
Figure 3.4: Developing resistance in cell lines HCC38 and MDA-MB-468 to CHK1 inhibitors SRA737 and Prexasertib.....	103
Figure 3.5: Characterisation of H737R and HPrexR cell line growth in 96-well plates.....	105
Figure 3.6: Characterisation of MDA-737R and MDA-PrexR cell line growth in 96-well plates.....	106
Figure 3.7: Determination of GI <sub>50</sub> values for HCC38 parental, H737R and HPrexR cell lines to SRA737 and Prexasertib.....	108
Figure 3.8: Determination of GI <sub>50</sub> values for MDA-MB-468 parental, MDA-737R and MDA- PrexR cell lines to SRA737 and Prexasertib.....	109

Figure 3.9: Light microscopy images of HCC38 and MDA-MB-468 parental and resistant sublines at 40x magnification.....	111
Figure 3.10: H737R and HPrexR long term release from drug experiment.....	113
Figure 3.11: MDR1 (P-glycoprotein) expression levels in MDA-MB-468 and HCC38 parental and resistant cell lines.....	114
Figure 3.12: Dose response of HCC38, HPrexR and H737R cells to Verapamil.....	115
Figure 3.13: Dose response of HCC38, H737R and HPrexR cell lines to a drug combination of SRA737/Prexasertib +/- Verapamil.....	116
Figure 3.14: Determination of GI <sub>50</sub> values for HCC38, H737R and HPrexR cell lines to ATR inhibitor Ceralasertib and WEE1 inhibitor Adavosertib.....	119
Figure 3.15: Determination of GI <sub>50</sub> values for MDA-MB-468 parental, MDA-737R and MDA-PrexR cell lines to ATR inhibitor Ceralasertib and WEE1 inhibitor Adavosertib.....	120
Figure 3.16: Determination of GI <sub>50</sub> values for HCC38, H737R and HPrexR cell lines to ATM inhibitor AZD0156 and CHK2 inhibitor CCT241533.....	122
Figure 3.17: Determination of GI <sub>50</sub> values for MDA-MB-468, MDA-737R and MDA-PrexR cell lines to ATM inhibitor AZD0156 and CHK2 inhibitor CCT241533.....	123
Figure 3.18: Determination of GI <sub>50</sub> values for HCC38 and MDA-MB-468 parental and resistant cell lines to Cisplatin.....	125
Figure 3.19: Determination of GI <sub>50</sub> values for HCC38, H737R and HPrexR cell lines to CDK4/6 inhibitor Palbociclib.....	127
Figure 3.20: Determination of GI <sub>50</sub> values for HCC38, H737R and HPrexR cell lines to PARP inhibitor Olaparib.....	128
Figure 3.21: Basal expression of pCHK1 s296 and pCHK2 s516 in HCC38 parental and resistant cell lines.....	130
Figure 3.22: WEE1 protein expression levels in HCC38 parental and resistant cell lines...	131
Figure 4.1: Hypothesis: WEE1 overexpression compensates for CHK1 inhibition and activation of CDC25 by maintaining inhibitory phosphorylation of CDK1/2.....	145

Figure 4.2: Western blot analysis of SRA737 dose response in HCC38 and H737R cell lines	147
Figure 4.3: Western blot analysis of SRA737 effect over time on HCC38 and H737R cell lines	148
Figure 4.4: Propidium iodide (PI) cell cycle analysis of HCC38 and H737R cell lines +/- SRA737	150
Figure 4.5: Bar chart of Propidium iodide (PI) cell cycle analysis of HCC38 and H737R cell lines +/- SRA737	151
Figure 4.6: Time course of HCC38 and H737R cells incubated with cycloheximide	153
Figure 4.7: Time course of HCC38 and HPrexR cells incubated with cycloheximide	154
Figure 4.8: Western blot analysis of Adavosertib dose response in HCC38 and H737R cell lines	156
Figure 4.9: Western blot analysis of HCC38 and H737R cell lines treated with SRA737, Adavosertib or a combination of both drugs	158
Figure 4.10: Propidium iodide (PI) cell cycle analysis of HCC38 cell lines treated with a drug combination of SRA737 and Adavosertib	160
Figure 4.11: Propidium iodide (PI) cell cycle analysis of H737R cell lines treated with a drug combination of SRA737 and Adavosertib	161
Figure 4.12: Bar chart of Propidium iodide (PI) cell cycle analysis of HCC38 cell lines treated with a drug combination of SRA737 and Adavosertib	162
Figure 4.13: Bar chart of Propidium iodide (PI) cell cycle analysis of H737R cell lines treated with a drug combination of SRA737 and Adavosertib	163
Figure 4.14: SRA737 + Adavosertib drug combination experiment in H737R and HPrexR cell lines	165
Figure 4.15: Dose response of HCC38, H737R and HPrexR cell lines to PD0166285	166
Figure 4.16: SRA737 + PD0166285 drug combination experiment in H737R cell lines	167
Figure 4.17: Optimising conditions for SiRNA knockdown of WEE1	169
Figure 4.18: Further optimisation for SiRNA knockdown of WEE1	170



Figure 4.19: WEE1 knockdown by SiRNA H737R and HPrexR cell lines.....	172
Figure 4.20: Effect of WEE1 knockdown by SiRNA on SRA737 sensitivity in H737R and HPrexR cell lines.....	173
Figure 4.21: Transient expression of ectopic WEE1.....	174
Figure 4.22: Geneticin Kill Curve.....	176
Figure 4.23: Stable transfection of WEE1 expressing plasmid to HCC38 cells.....	177
Figure 4.24: Selection of stable cell lines with Geneticin.....	178
Figure 4.25: Western blots of TNBC cell line panel.....	179
Figure 4.26: Comparison of TNBC GI <sub>50</sub> data to WEE1 expression levels.....	181
Figure 4.27: Comparison of TNBC GI <sub>50</sub> data to WEE1 expression levels.....	182
Figure 5.1: GI <sub>50</sub> determination of HCC38, H737R and HPrexR to Gemcitabine and Ribonucleotide Reductase inhibitor Hydroxyurea.....	198
Figure 5.2: SRA737 + Gemcitabine drug combination experiment.....	200
Figure 5.3: Bar chart of SRA737 + Gemcitabine drug combination experiment.....	201
Figure 5.4: Markers of replication stress and cell death to SRA737 treatment in HCC38 and H737R cells.....	203
Figure 5.5: Markers of replication stress and cell death to Adavosertib treatment in HCC38 and H737R cells.....	204
Figure 5.6: SRA737 + Adavosertib drug combination western blot in HCC38 and H737R cell lines.....	205
Figure 5.7: GI <sub>50</sub> determination of HCC38, H737R and HPrexR cell lines to CDK1 inhibitor RO-3306.....	207
Figure 5.8: RO-3306 + SRA737 drug combination experiment.....	208
Figure 5.9: GI <sub>50</sub> determination of HCC38, H737R and HPrexR cell lines to CDK2/1 inhibitor Roscovitine.....	209
Figure 5.10: HCC38 SRA737 + Adavosertib + Roscovitine drug combination experiment.....	210
Figure 5.11: H737R SRA737 + Adavosertib + Roscovitine drug combination experiment.....	211
Figure 5.12: HPrexR SRA737 + Adavosertib + Roscovitine drug combination experiment.....	211

Figure 5.13: SRA737 + Adavosertib + Roscovitine drug combination western blot in H737R cells.....	213
Figure 5.14: Inhibition of both CHK1 and WEE1 greatly increases CDK activity and leads to reduction of p21 <sup>Cip1/Waf1</sup> and WEE1 protein levels.....	220
Figure 6.1: A) Filtering of raw data to remove poor-quality base calls. B) Alignment of reads to the UCSC Human hg38 reference genome via STAR.....	229
Figure 6.2: A) Identified duplicate reads. B) Assignment of RNA bases to known mRNA features.....	230
Figure 6.3: A) Total read counts. B) Percentage of null counts per sample.....	232
Figure 6.4: Pairwise scatter plot and similarity index.....	233
Figure 6.5: Visualising experimental variability with Principal Component Analysis.....	234
Figure 6.6: Assessment of the estimation of size factors for normalisation of raw counts.....	236
Figure 6.7: Boxplots showing quality of normalisation of raw counts.....	237
Figure 6.8: Volcano plots of differentially expressed genes in H737R and HPrexR cell lines versus the parental HCC38 cell line.....	239
Figure 6.9: Differentially expressed genes shared by H737R and HPrexR differential expression analysis.....	240
Figure 6.10: Volcano plots of shared differentially expressed genes between H737R and HPrexR cell lines versus the parental HCC38 cell line.....	241
Figure 6.11: Top 20 most significantly enriched genesets for 569 shared differentially expressed genes.....	242
Figure 6.12: Top 20 most significantly enriched genesets for up and down shared differentially expressed genes.....	244
Figure 6.13: Top 20 most significantly enriched genesets for all differentially expressed genes in H737R and HPrexR.....	246
Figure 6.14: Expression profile of EMT enriched genes in HCC38 parental and resistant cell lines.....	247

Figure 6.15: Expression profile of Epithelial proliferation enriched genes in HCC38 parental and resistant cell lines.....	249
Figure 7.1: Overexpression of p21 <sup>Cip1/Waf1</sup> may compensate for CHK1 inhibition by maintaining CDK inhibition.....	262
Figure 7.2: Difference in response to WEE1 inhibitors Adavosertib and PD0166285 may be explained by PD0166285 ability to inhibit Myt1.....	264
Figure 7.3: Possible model for CHK1 inhibitor resistance and response to combined treatment of CHK1 + WEE1 inhibitors CHK1 + Gemcitabine.....	272

# List of Tables

Table 1.1: Table of CHK1 inhibitors.....	56
Table 2.1: Summary of compounds used in cell-based experiments.....	75
Table 2.2: Drug maintenance concentrations for CHK1 inhibitor resistant cell lines.....	76
Table 2.3: Summary of components lysis buffer.....	80
Table 2.4: Summary of components for the construction of SDS-PAGE gels.....	83
Table 2.5: List of antibodies used for western blot analysis.....	84
Table 2.6: List of SiRNA oligonucleotides used.....	86
Table 3.1: TNBC mutational background for HCC38 and MDA-MB-468 cell lines.....	98
Table 5.1: Fold change of genes expressed in H737R and HPrexR cell lines from HCC38 cells.....	199
Table 6.1: General statistics for processing of raw RNA sequencing data.....	228
Table 6.2: Scaling factors determined by DESeq2 used to normalise RNA sequencing data.....	235
Table 6.3: Total number of differentially expressed genes for each analysis.....	237
Table 6.4: Numbers of Up and Down differentially expressed genes enriched for EMT.....	247
Table 6.5: Key EMT related genes Log2 fold changes and padj values.....	248

# Abbreviations

9-1-1	RAD9-Hus1-RAD1
ABC	ATP-binding cassette
ABCG2	ATP binding cassette subfamily G member 2
AGTR1	Type-1 angiotensin II receptor
AKT	Protein kinase B
AML	Acute myeloid leukaemia
AND-1	Acidic nucleoplasmic DNA-binding protein
APC/C	Anaphase promoting complex
AR	Androgen receptor
Ara-C	Arabinoside cytarabine
ATM	Ataxia-telangiectasia mutated
ATP	Adenosine triphosphate
ATR	Ataxia-telangiectasia and Rad3 related
ATRIP	ATR-interacting protein
β-TRCP	Beta-transducin repeat containing E3 ubiquitin ligase
BCA	Bicinchoninic acid
BER	Base excision repair
BIR	Break-induced repair
BMP2	Bone morphogenetic protein 2 precursor
BMPER	Ubiquitin protein ligase E3A-like protein
B-RAF	Proto-oncogene B-Raf
BRCA1	Breast cancer type 1 susceptibility protein
BRCA2	Breast cancer type 1 susceptibility protein
BSA	Bovine serum albumin

BubR1	Mitotic spindle checkpoint protein
BLBC	Basal-like Breast Cancer
CADM1	Cell adhesion molecule 1
cAMP	Cyclic adenosine monophosphate
CDC	Cell division cycle
CDDP	Cisplatin
CDH1	Cadherin 1
CDK	Cyclin-dependent kinases
CDNA	Complementary DNA
CDT1	Chromatin licensing and DNA replication factor 1
CDT2	Cell division cycle protein 2
CHK1	Checkpoint kinase 1
CHK2	Checkpoint kinase 2
CHO	Chinese hamster ovary cells
circAKT3	Circular RNA AKT3
CK2	Casein kinase
CMG complex	CDC45-MCM2-7-GINS complex
COL1A2	Collagen alpha-2(I) chain
C-PARP	Cleaved PARP
C-RAF	Proto-oncogene C-RAF
CREB	cAMP-response element binding protein
Cul4A	Culin-4A
dCK	Deoxycytidine kinase
DDK	DBF4-dependent kinase
DDR	DNA damage response
DDT	DNA damage tolerance
DEA	Differential expression analysis

DEG	Differentially expressed genes
DNA	Deoxyribonucleic acid
DNA-PK	DNA-dependent protein kinase
dNTPs	Deoxynucleotides
DPP9	Dipeptidyl Peptidase 9
DSB	Double stranded breaks
E2F	E2 transcription factor
ECL	Enhanced chemiluminescence
EDLI3	EGF like repeats and discoidin domains 3
EDNRB	Endothelin receptor type B
EGFR	Epidermal growth factor receptor
EMT	Epithelial to mesenchymal transition
EOC	Epithelial ovarian cancer
ER	Oestrogen receptor
ERBB2	Receptor tyrosine-protein kinase erbB-2
EXO1	Exonuclease 1
FANCE	Fanconi anemia complementation group E protein
FAP	Focal adhesion protein
FBS	Foetal Bovine Serum
Fbx6	F-Box protein 6
FEN1	Flap endonuclease 1
Gadd45	Growth arrest and DNA damage protein
GAPDH	Glyceraldehyde 3-phosphate dehydrogenase
GEMC1	Geminin coiled-coil domain-containing protein 1
GI <sub>50</sub>	Half maximal inhibition of cell proliferation
GIN5	Go-Ichi-Ni-San complex
GJA1	Gap junction alpha-1 protein
GPCR	G-protein coupled receptor

GR	Glucocorticoid receptor
GSEA	Gene set enrichment analysis
HGSOC	High-Grade serous Ovarian Cancer
HDAC	Histone deacetylase
HER2	Human epidermal growth factor receptor 2
HR	Homologous recombination
HSP90	Heat shock protein 90
HTRA1	HTRA serine peptidase 1
HU	Hydroxyurea
Hus1	Checkpoint protein HUS1
IGF1R	Insulin-like growth factor 1 receptor
IMDM	Iscoe modified Dulbecco medium
IR	Ionising radiation
JWA	PRA1 family protein 3
KIT	KIT proto-oncogene, receptor tyrosine kinase
KLF2	Kruppel-Like Factor 2
K-RAS	Kirsten RAS oncogene homolog
LEF-1	Lymphoid enhancer-binding factor 1
Mad2	Mitotic arrest deficient 2
MAPK	Mitogen-activated protein kinase
MAST1	Microtubule associated Serine/Threonine kinase 1
MCM	Mini-chromosome maintenance helicase
MDAR1	Multidrug resistance protein 1
MDM2	Mouse double minute 2 homolog
MEK	MAPK/ERK kinase
MGP	Matrix Gla protein
MIG6	ERBB receptor feedback inhibitor 1
MMR	Mismatch Repair



MRE11	Meiotic recombination 11 homolog A
MRN complex	MRE11/RAD50/NBS1
mRNA	Messenger RNA
MRP2	Multidrug resistance-associated protein 2
MUS81	Crossover junction endonuclease MUS81
MYC	Myelocytomatosis viral oncogene
MYCN	Myelocytomatosis viral oncogene neuroblastoma
NBS1	Nibrin
NER	Nucleotide excision repair
NES	Nuclear export signal
NF-KB	Nuclear factor kappa-light-chain-enhancer of activated B cells
NGS	Next generation sequencing
NHEJ	Non-homologous end joining
NLS	Nuclear localisation sequence
NRP2	Neuropilin-2
NSCLC	Non-Small Cell Lung Cancer
ORC	Origin recognition complex
p21 <sup>Cip1/Waf1</sup>	Cyclin-dependent kinase inhibitor 1
p27 <sup>Cip/Kip2</sup>	Cyclin-dependent kinase inhibitor 1B
p53	Tumour protein p53 (protein)
PARP	Poly-ADP ribose polymerase
PBS	Phosphate Buffered Saline
PCA	Principal Component Analysis
PCNA	Proliferating cell nuclear antigen
P-GP	P-Glycoprotein
PGR	Progesterone Receptor
PI3K	Phosphoinositide 3-kinase

PI3KR1	Phosphoinositide-3-Kinase Regulator Subunit 1
PIP box	PCNA-interacting protein box
Plk1	Polo like kinase 1
Pol	Polymerase
PP1	Protein phosphatase 1
PP2A	Protein phosphatase 2A
PD-1	Programmed cell death receptor 1
PD-L1	Programmed cell death ligand 1
Pre-RC	Pre-replication complex
Pre-IC	Pre-initiation complex
PrimPol	Primase and DNA Directed Polymerase
PRKD1	Serine/threonine-protein kinase D1
Prrx1	Paired mesoderm homeobox protein 1
PTPRD	Protein tyrosine phosphatase receptor type D
PTPRM	Receptor-type tyrosine-protein phosphatase-like mu
PTPRN	Receptor-type tyrosine-protein phosphatase-like N
PVDF	Pore Immobilon-P polyvinylidene fluoride
qPCR	Quantitative polymerase chain reaction
RAD1	DNA repair protein RAD1
RAD17	DNA repair protein RAD17 homologue
RAD51	DNA repair protein RAD51 homologue
RAD9	DNA repair protein RAD9 homologue
RAF	Rapidly Accelerated Fibrosarcoma
Rb	Retinoblastoma protein
RCCL	Resistance Cancer Cell Line Collection
RECQL4	RECQ like helicase 4
RFC	Replication factor C
RIF1	Replication timing regulator factor 1

RMS	Rhabdomyosarcoma
RNA	Ribonucleic acid
RPTPs	Receptor-type tyrosine-protein phosphatases
RRM1	Ribonucleotide Reductase Catalytic Subunit M1
RRM2	Ribonucleotide Reductase Catalytic Subunit M2
RRM2B	Ribonucleotide Reductase Regulatory <i>TP53</i> inducible subunit M2B
rRNA	Ribosomal RNA
RS	Replication stress
RTK	Receptor tyrosine kinase
S	Serine
SCLC	Small cell lung cancer
shRNA	Short hairpin RNA
siRNA	Small interfering RNA
Skp1	S-phase associated protein 1
SLFN11	Schlafen Family Member 11
SLITRK2-5	SLT and NTRK-like protein 2
Snai1/2	Zinc finger protein Snai1/2
SOX11	SRY-Box Transcription factor
SQ	Serine/Glutamine residues
SRB	Sulforhodamine B
ssDNA	Single stranded DNA
T	Threonine
TCA	Trichloroacetic acid
TCGA	The Cancer Genome Atlas Program
TGF- $\beta$	Transforming growth factor $\beta$
TIM	Timeless

TIPIN	Timeless-interacting protein
Tlks	Tousled-like kinase
TLS	Translesion Synthesis
TNBC	Triple Negative Breast Cancer
TNFRSF11B	TNF receptor superfamily member 11B
TOPBP1	DNA topoisomerase II binding protein 1
<i>TP53</i>	Tumour protein p53 (Gene)
Treslin	TopBP1-interacting protein
UMI	Unique molecular identifiers
UTR	Untranslated regions
UV	Ultraviolet light
WEE1	Mitosis inhibitor protein kinase WEE1
WNT	Proto-oncogene Wnt-1
WT	Wild Type
XRCC1	X-ray repair cross-complimenting protein 1
Y	Tyrosine
yH2AX	H2A histone family member X phosphorylated on S139
ZEB1	Zinc finger E-box binding homeobox 1

---

# **Chapter 1**

## **Introduction**

# 1. Introduction

## 1.1 The Hallmarks of Cancer

Cancer is a collection of related diseases defined by the uncontrolled replication of host cells that develop malignancy, subsequently spreading into surrounding tissues, and there were 17 million cases of cancer diagnosed Worldwide in 2018, (*Worldwide cancer incidence statistics* / *Cancer Research UK*, 2018). In the UK alone there are approximately 367,000 new cancer cases every year and it has been calculated that 1 in 2 people will be diagnosed with cancer in their lifetimes (*Cancer incidence statistics* / *Cancer Research UK*, 2017; Smittenaar *et al.*, 2016). These striking statistics highlight that everyone will be impacted by cancer either directly or indirectly and demonstrates the importance of research to develop our understanding of cancer and improve patient outcome.

An important conceptualisation of cancer as a disease was proposed by Hanahan and Weinberg in their seminal papers on “The Hallmarks of Cancer” and “Hallmarks of Cancer: The Next Generation” (Hanahan and Weinberg, 2000; Hanahan and Weinberg, 2011). The first of these papers discussed six critical hallmarks that dictate malignant growth. These hallmarks categorise important processes that result in tumorigenesis and subsequent malignancy. They include sustained proliferative signalling, evasion of growth suppressors, replicative immortality, induction of angiogenesis, resisting cell death, tissue invasion and metastasis (Hanahan and Weinberg, 2000). In the later publication two additional hallmarks were proposed, deregulating cellular energetics and immune evasion along with two “enabling characteristics” of genomic instability and tumour-promoting inflammation leading to mutations in DNA. These enabling characteristics are said to drive the acquisition of aforementioned hallmarks enabling malignant cell behaviour (Hanahan and Weinberg, 2011). At the heart of sustained cell proliferation and genomic instability is the deregulation of normal cell cycle progression, which is explored in more detail below.

## 1.2 The Cell Cycle

### 1.2.1 Phases of the cell cycle

The cell cycle is an essential process in which cells precisely replicate their DNA before dividing into two genetically identical daughter cells. This process is split into four main cell cycle phases known as G1, S, G2 and M (**Figure 1.1**). DNA replication occurs in S-phase while cell division takes place in M-phase, otherwise known as Mitosis. G1 and G2 are known as “gap” phases in which the cells prepare either for DNA replication (G1) or cell division (G2). Additionally, G0 represents cells that have exited the cell cycle by lying dormant awaiting the conditions required to stimulate cellular proliferation in what’s termed quiescence, or permanently exited from the cell cycle into senescence (Terzi, Izmirli and Gogebakan, 2016). Regulating the transition between cell cycle phases are the cyclin-dependent kinases (CDKs) and the cyclin proteins D, E, A and B, which bind to the CDKs and are required for their full activation.

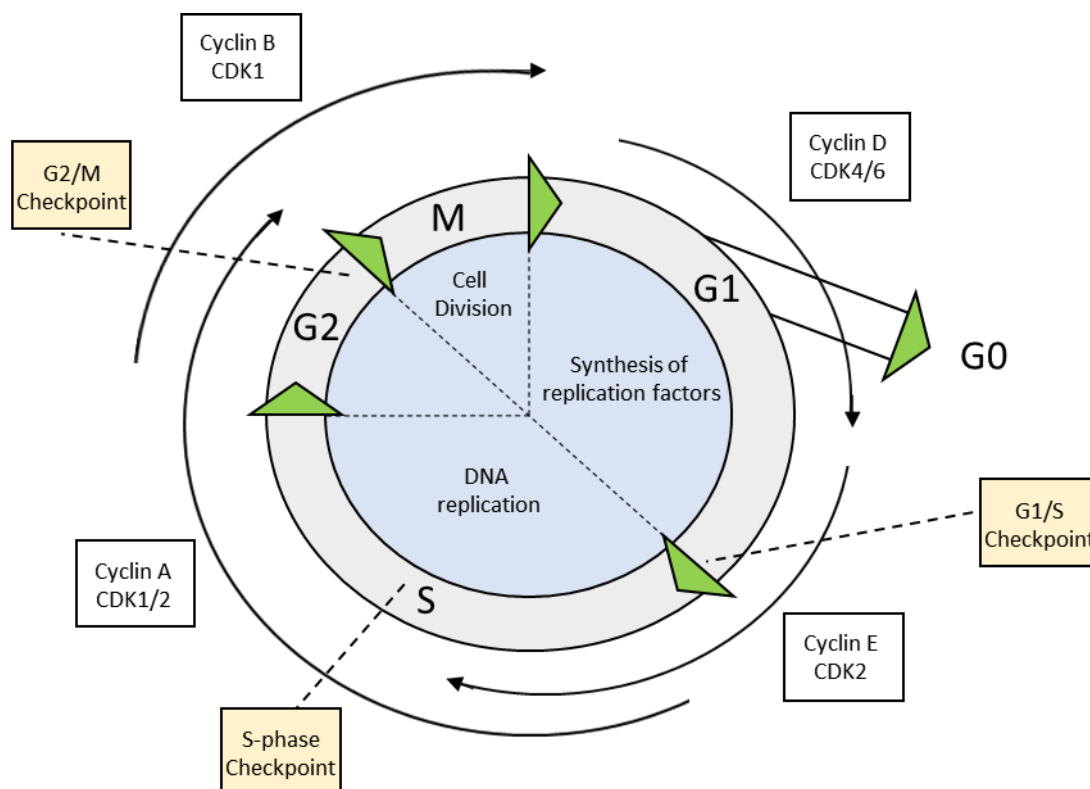


**Figure 1.1: The cell cycle.** During Interphase (G1, S and G2) cells continuously grow and accurately replicate DNA before mitotic cell division.

Cyclins are so named due to their cyclic expression during the cell cycle meaning their CDK binding partners are only activated at specific points in the cell cycle (Steel, 1994; Darzynkiewicz *et al.*, 1996; Schafer, 1998). In response to mitogenic stimuli such as growth factors, cyclin D expression increases and forms a complex with CDK4/6 leading to activation of CDK4/6 and progression through G1 (Donjerkovic and Scott, 2000). Progressively, CDK4/6 phosphorylates retinoblastoma protein (Rb) inhibiting its ability to bind and inactivate transcription factor E2F (Donjerkovic and Scott, 2000). This leads to an increase in cyclin E and subsequent activation of CDK2 which phosphorylates Rb leading to complete dissociation of E2F from Rb, driving the cell cycle from G1 into S-phase and promoting the transcription of Cyclins A and B (Giacinti and Giordano, 2006).

CDK2/Cyclin A regulates the progression of S-phase and replication of DNA via phosphorylation of replication initiation machinery (Girard *et al.*, 1991). CDK1/Cyclin A activity increases in G2 and is rapidly degraded before metaphase and may be involved in the activation of the CDK1/Cyclin B complex (Yam, Fung and Poon, 2002). However, the main controller of mitotic entry is CDK1/Cyclin B (Lindqvist, Rodríguez-Bravo and Medema, 2009), inactivation of which is carefully controlled by the cell via the WEE1 and MYT1 kinases which phosphorylate Y15 and T14 on CDK1 respectively. These inhibitory phosphorylation's are removed by CDC25 phosphatases at the appropriate time to allow entry into mitosis (Timofeev *et al.*, 2010). Additionally, CDK1/Cyclin B is phosphorylated by CDK7/Cyclin H on T161 signalling for its activation (Fujii *et al.*, 2011). Assisting in the timing of cell cycle progression, CDK inhibitors p21<sup>Cip1/Waf1</sup> and p27<sup>Cip/Kip2</sup> regulate the activity of CDK1, 2, 4 and 6 at multiple stages of the cell cycle (Guardavaccaro and Pagano, 2006; Abukhdeir and Park, 2008). Checkpoint Kinase 1 (CHK1) plays a critical role in regulating the activation of CDK1/2 indirectly via the inhibition of CDC25 and is a key kinase in controlling cell cycle progression to ensure accurate replication of DNA and chromosomal segregation during mitosis to maintain genomic stability.



### 1.2.2 DNA replication

Replication of DNA starts with the licensing of replication origins in S-phase, via the recruitment of the six-subunit origin recognition complex (ORC) in the G1 phase of the cell cycle (Fragkos *et al.*, 2015). This recruits the sequential loading of cell cycle division 6 (CDC6) and chromatin licensing and DNA replication factor 1 (CDT1) which act together with ORC to recruit loading of the mini-chromosome maintenance (MCM) helicase. This helicase consists of six subunits (MCM2-7) and binds as an inactive double hexamer around the DNA (**Figure 1.2 A**), licensing the replication origin or pre-Replication Complex (Pre-RC) for formation of the pre-initiation complex (Pre-IC)(Fragkos *et al.*, 2015).

Replication origins are selected for activation via recruitment of the pre-IC complex during the G1-S phase transition. CDK2/Cyclin E and DBF4-dependent kinases (DDK; Composed of Dbf4 and Cdc7 subunits) phosphorylate a number of replication factors promoting their loading onto replication origins which are required for the activation of the MCM2-7 helicase to unwind DNA (**Figure 1.2 B**) (Tanaka *et al.*, 2006; Ilves *et al.*, 2010; Heller *et al.*, 2011). During S-phase the MCM2-7 helicase is activated, the MCM2-7 double hexamer divides into two hexamer units which unwind DNA moving in opposite directions from the replication origin in what is known as firing of the replication origin (Fragkos *et al.*, 2015). Additional proteins known as elongation factors are recruited to the unwound DNA such as replication protein A (RPA), replication factor C (RFC) and proliferating cell nuclear antigen (PCNA) forming the replisome converting the pre-IC into two replication forks (**Figure 1.2 C**) after which B-family polymerases initiate DNA synthesis (Fragkos *et al.*, 2015).

The two steps of DNA replication, namely origin licensing and origin firing are decoupled from one another into different phases of the cell cycle. This ensures no origin firing can be allowed in G1 phase while pre-RC complexes are being assembled stopping under replication of parts of the genome (Siddiqui, On and Diffley, 2013). Equally, no origin licensing may be allowed to occur in S-phase, lest multiple replication forks initiate from the same replication origin, resulting in re-replication of DNA (Siddiqui, On and Diffley, 2013). Only a subset of licensed

replication origins result in active replication forks during unperturbed S-phase while the majority of these sites remain dormant. Replication origins are known to be loaded in excess across the genome and there is a flexibility in which sites will become active. This has been suggested to enable a mechanism which avoids collisions between transcription and replication machinery as firing of MCM helicase was enriched upstream of transcription start sites while most remained inactive (Sugimoto *et al.*, 2018). However, dormant replication origins have also been shown to be involved in recovery of stalled replication forks as a loss of dormant replication origins, even in unperturbed S-phase resulted in an increased number of stalled replication forks (Kawabata *et al.*, 2011). Mice expressing reduced levels of MCM2-7 demonstrate fewer replication origins and show higher susceptibility to genomic instability and cancer formation showing these dormant origins are important in preserving the integrity of the genome (Blow, Ge and Jackson, 2011).

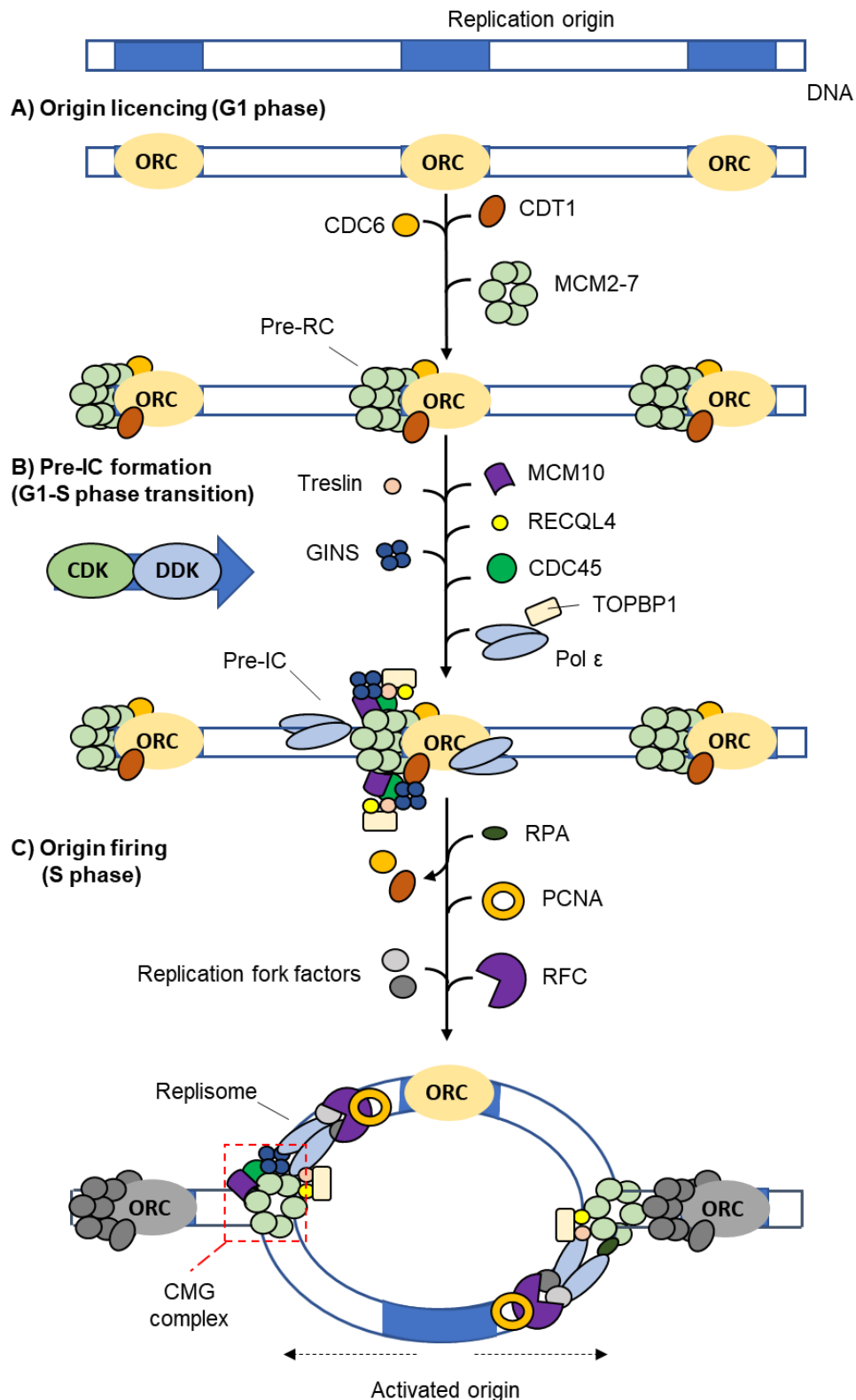


**Figure 1.2: Licensing and firing of replication origins.** **A)** In G1 phase, replication origins (RO) are licensed by the recruitment of the origin recognition complex followed by binding of CDT1 and CDC6 followed by the mini-chromosome maintenance (MCM) helicase complex. Loading of the MCM requires ORC, CDC6 and CDT1 to already be bound to RO. **B)** In the G1/S transition the formation of the pre-initiation complex (Pre-IC) is driven by CDK and DBF4-dependent kinase (DDK) activity via phosphorylation of several replication factors promoting their loading onto replication origins. CDK and DDK also phosphorylate MCM2-7 resulting in activation of the helicase and unwinding of DNA. **C)** Helicase activation induces the recruitment of other proteins that convert the pre-IC into two replication forks that move in opposite directions from the replication origin. Adapted from Fragkos et al., 2015.

### 1.2.3 Cell cycle checkpoints

Cell cycle checkpoints act as surveillance mechanisms that monitor the processes leading up to cell division. In order to successfully complete mitosis, cells must accurately replicate their DNA to ensure each daughter cell acquires a complete set of chromosomes. During replication, the DNA is subjected to exogenous and endogenous sources of damage. Endogenous factors include reactive oxygen species (ROS) and toxic metabolites while exogenous factors consist of ultraviolet (UV) light, ionising radiation (IR) and genotoxic agents (Hakem, 2008). Cells respond to DNA-damage via the DNA damage response (DDR) which co-ordinates DNA repair and checkpoint mechanisms, slowing the progression of the cell cycle to enable sufficient time for DNA repair and replication via the inhibition of CDKs (Kastan and Bartek, 2004). The three DNA damage induced cell cycle checkpoints are at the G1/S phase transition, S-phase, and the G2/M phase transition (Kastan and Bartek, 2004; Bartek and Lukas, 2007).

An important checkpoint protein is the major cellular stress sensor and transcription factor p53, encoded by the *TP53* gene. p53 induces the expression of CDK inhibitor p21<sup>Cip1/Waf1</sup> in response to DNA damage (Ko and Prives, 1996; Levine, 1997). Induced p21<sup>Cip1/Waf1</sup> localises to the nucleus where it inhibits the activity of CDK2 complexes resulting in the activation of the G1/S checkpoint (Gu, Turck and Morgan, 1993; Wade Harper *et al.*, 1993). ATM and Checkpoint Kinase 2 (CHK2) phosphorylate and activate p53 in response to double stranded DNA breaks, phosphorylated p53 exhibits a reduced affinity for its ubiquitin ligase MDM2 increasing its stability and transcriptional activity (Dai and Grant, 2010). Additionally, Checkpoint kinase 1 (CHK1) and CHK2 have also been implicated in the regulation of this checkpoint via their phosphorylation of CDC25A leading to ubiquitin/proteasome dependent degradation of CDC25A, a phosphatase that activates CDK2 via removal of the inhibitory phosphorylation at tyrosine 15 (Y15) (Dai and Grant, 2010). Despite this overlap with CHK1 and CHK2, loss of p21<sup>Cip1/Waf1</sup> is able to abrogate the G1/S phase checkpoint (Abukhdeir and

Park, 2008; Giono and Manfredi, 2006) therefore, the p53/p21<sup>Cip1/Waf1</sup> pathway is considered the dominant regulator of the G1/S phase checkpoint (Kastan and Bartek, 2004).

The S-phase checkpoint is activated during DNA replication predominantly via the stalling of replication forks that have encountered DNA lesions. Activation of the S-phase checkpoint stabilises stalled replication forks and prevents the dissociation of replisome components although it is likely the S-phase checkpoint regulates a wide spectrum of events (Errico and Costanzo, 2012). When the polymerase of the replication fork encounters a lesion, it is unable to proceed, but the MCM2-7 helicase complex continues to unwind DNA. This generates large sections of single stranded DNA (ssDNA) which are coated by replication protein A that signals for the binding of the ATR/ATRIP complex (Namiki and Zou, 2006). ATR then phosphorylates CHK1 leading to its activation and subsequent triggering of the S-phase checkpoint via phosphorylation of downstream substrates. As mentioned previously, CDC25A is phosphorylated and inhibited leading to the inactivation of CDK2/Cyclin E complexes. Inactivated CDK2/Cyclin E can no longer phosphorylate and activate Treslin (Kumagai *et al.*, 2010) which is required for CDC45 loading and the formation of the Pre-IC complex and subsequent origin firing (**Figure 1.2**) stopping unscheduled firing of replication origins during periods of replication stress. Additionally, CHK1 is known to directly regulate CDC45 loading via Treslin inhibition (Guo *et al.*, 2015).

The ATR/CHK1 pathway also regulates the G2/M checkpoint, which stops cells with under replicated or damaged DNA from undergoing mitosis. If the G2/M checkpoint is abrogated and cells commit to mitosis it typically results in mitotic catastrophe, which is a delayed cell death response linked with mitosis (Zhang and Hunter, 2014). Inhibition of CDC25C by the ATR/CHK1 pathway halts removal of Y15 and T14 inhibitory phosphorylation's on CDK1/Cyclin B complexes. Additionally, the WEE1 kinase phosphorylates Y15 on CDK1, while the dual specificity MYT1 kinase phosphorylates both Y15 and T14, maintaining CDK1/Cyclin B in an inactive state (Wang, Decker and Sebolt-Leopold, 2004). This is

maintained until the cell has successfully repaired and replicated its DNA before progressing into mitosis.

#### **1.2.4 Replication stress**

As defined by Zeman and Cimprich, replication stress is the slowing or stalling of replication fork progression and/or DNA synthesis (Zeman and Cimprich, 2013). While this term doesn't encompass all replication defects, such as re-replication or reduced licensing of replication origins, these conditions may contribute to the cell's sensitivity to replication stress. Additionally, replication stress doesn't refer to one physical structure such as double stranded breaks but can be caused by many physical obstacles in the path of the replication machinery. However, long stretches of ssDNA are usually formed when the replicative helicase uncouples from the stalled polymerase (Pacek and Walter, 2004). These long stretches of DNA are bound by RPA, generating a signal for the replication stress response recruiting one of the core replication-stress-response kinases ATR (Zou and Elledge, 2003; MacDougall *et al.*, 2007; Nam and Cortez, 2011).

Frequent sources of replication stress include nicks, gaps and stretches of ssDNA. Nicks and gaps are regularly found in DNA, being natural intermediates of multiple DNA repair pathways (Zeman and Cimprich, 2013) or the products of regular DNA manipulations as seen with the cutting of DNA by topoisomerases to relieve the build-up of topological stress (Bermejo *et al.*, 2009; Tuduri *et al.*, 2009). Additionally, lesions resulting from endogenous and exogenous sources of DNA damage such as reactive oxygen species or IR respectively can cause physical barriers to the progression of replication forks (Ciccia and Elledge, 2010; Zeman and Cimprich, 2013). Other factors include the misincorporation of ribonucleotides (rNTPs) instead of deoxynucleotides (dNTPs) by less stringent polymerases such as Pol  $\delta$  and Pol  $\epsilon$  (Dalgaard, 2012) which stalls progression of the replicative polymerase, requiring RNase H2 to excise ribonucleotides in conjunction with other endonucleases such as FEN1 or EXO1 (Sparks *et al.*, 2012; Zeman and Cimprich, 2013). Secondary DNA structures also prevent progression of replication machinery, such as hairpins and triplexes in trinucleotide repeat

regions or G-quadruplexes in sections of DNA rich in GC nucleotides (Bochman, Paeschke and Zakian, 2012; Paeschke *et al.*, 2013).

Additionally, replication and transcription machinery are likely to collide as both processes require binding to DNA, possibly resulting in fork stalling and subsequent collapse and formation of DSB (Zeman and Cimprich, 2013). These collisions are more frequent in highly transcribed regions during S-phase in sites of DNA known as 'early replicating fragile sites' (Barlow *et al.*, 2013). However, studies in yeast (*S. cerevisiae*) have shown replication stress is caused simply by close proximity of replication and transcription sites and not collision (Bermejo *et al.*, 2011; Bermejo, Lai and Foiani, 2012). This may be due to increases in topological stress in these areas as head-on conflicts with the replication and transcription machinery results in supercoiling of DNA (Lang and Merrikh, 2021). In addition to 'early replicating fragile sites' there are regions known as 'common fragile sites' which may be caused by limited licensing of replication origins in these areas (Debatisse *et al.*, 2012; LeTallec *et al.*, 2013), suggesting stalled forks from collisions or other lesions are less able to be rescued by the firing of backup origins leading to a greater incidence of collapsed replication forks and DSBs (Zeman and Cimprich, 2013).

The overactivation or overexpression of oncogenes such as K-RAS, MYC and cyclin E has been proposed as a source of replication stress. These genes promote cell proliferation and increased initiation and firing of replication origins which can cause an excess of replication forks leading to a depletion of available pools of dNTPs and increased risk of collisions between transcription and replication machinery (Halazonetis, Gorgoulis and Bartek, 2008; Bester *et al.*, 2011; Jones *et al.*, 2012; Srinivasan *et al.*, 2013). Additionally, hypoxic conditions are known to influence the production of dNTPs by ribonucleotide reductase (RNR) which requires oxygen to enable dNTP synthesis (Foskolou and Hammond, 2017; Foskolou *et al.*, 2017). Low levels of oxygen force dNTP production to rely on the less efficient but higher oxygen sequestering subunit RRM2B rather than RRM2 (Foskolou *et al.*, 2017). As a result, less dNTPs are available for DNA replication leading to increased replication stress and a

slower progression of DNA replication (Foskolou *et al.*, 2017). Finally, DNA accessibility may play a role in replication stress as chromatin compaction may interfere with the progression of replication machinery. Tightly compacted areas of heterochromatin have been associated with DNA damage marker  $\gamma$ H2AX and are associated with regions of 'common fragile sites' (Lambert and Carr, no date; Jiang *et al.*, 2009). Relaxation of the chromatin in these areas has been shown to reduce the occurrence of breakages (Jiang *et al.*, 2009). However, it is unknown if these breakages are caused by heterochromatin induced replication stress or due to interference with DNA repair dynamics (Zeman and Cimprich, 2013).

### 1.2.5 The replication stress response

Upon stalling of the replicative polymerase and subsequent unwinding of ssDNA, RPA binds to protect exposed ssDNA and recruits a number of proteins to activate the response to replication stress. The ATR-ATRIP complex and the replication factor C (RFC) in complex with RAD17 are recruited to RPA covered ssDNA which facilitates the binding of the Rad9, Hus1 and Rad1 complex (9-1-1) (Parrilla-Castellar, Arlander and Karnitz, 2004). The 9-1-1 complex subsequently recruits TOPBP1 which physically interacts with and activates ATR (Burrows and Elledge, 2008) (**Figure 1.3**). Additionally, CHK1 is recruited to the stalled replication fork via the binding of the timeless-interacting protein (TIPIN) and Timeless (TIM) complex to RPA which complexes with claspin and promotes the claspin-mediated phosphorylation of CHK1 by ATR and its subsequent activation and dissociation from the chromatin (Kemp *et al.*, 2010) (**Figure 1.3**).

The ATR-CHK1 pathway is important for the regulation of DNA replication in the absence of DNA damage (Shechter, Costanzo and Gautier, 2004; Sørensen *et al.*, 2006; Petermann, Woodcock and Helleday, 2010; Sørensen and Syljuåsen, 2012). Indeed, it has been shown that fluctuations of CDK2 activity triggered by transient ATR signals caused by random replication stress events occur over the course of unperturbed DNA replication (Daigh *et al.*, 2018). This suggests the replication stress response is dynamically regulated to manage innate incidences of replication stress without perturbation from DNA damage and replication



stress inducing agents. Consequently, the ATR-CHK1 pathway is activated at low levels during normal S-phase, and maximal activation of the ATR-CHK1 pathway occurs during high levels of DNA damage/replication stress (Iyer and Rhind, 2017).

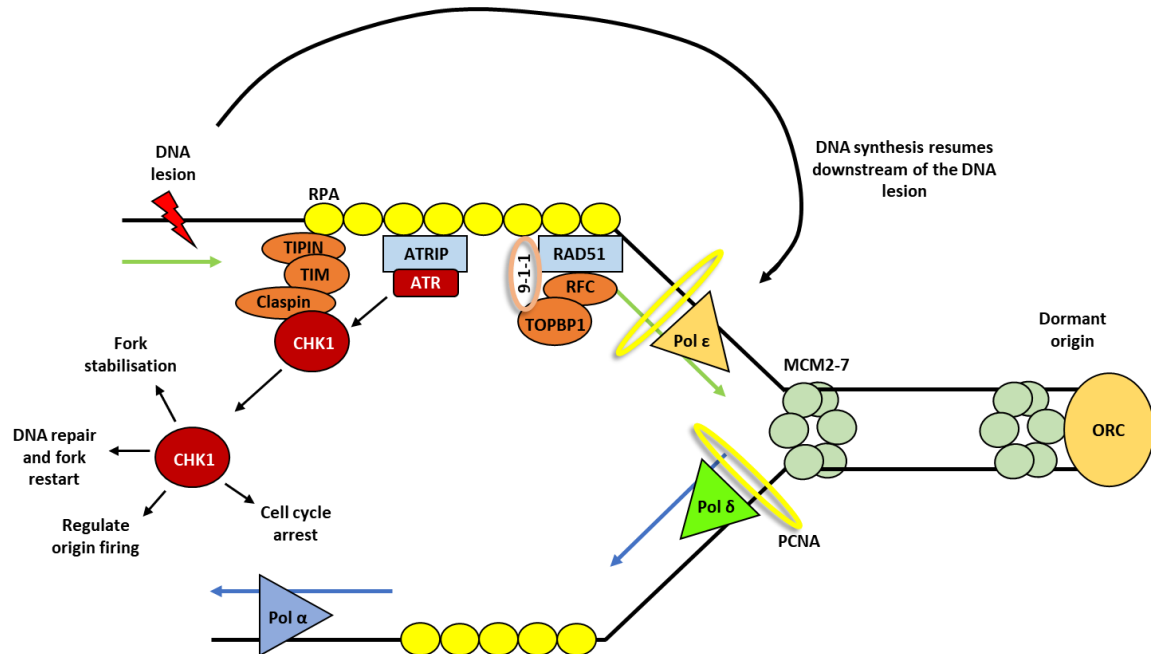


**Figure 1.3: Activation of the replication stress response.** DNA lesions stall the replicative polymerases leading to uncoupling of polymerases ( $\alpha$ ,  $\epsilon$  and  $\delta$ ) from the MCM2-7 helicase resulting in long strands of ssDNA. Subsequently RPA32 binds the ssDNA recruiting replication stress response complexes leading to activation of CHK1 and activation of the S-phase checkpoint. Modified from (Zeman and Cimprich, 2014).

When replication stress persists, alternative mechanisms are initiated to enable to continuation of DNA replication via the protection and repair of stalled or collapsed replication forks. The method of recovery from genomic insults depends on the type of damage caused. DNA lesions may be tolerated via the activation of DNA damage tolerance (DDT) pathways (Branzei and Psakhye, 2016) (**Figure 1.4**). Two strategies in the DDT pathway include translesion synthesis (TLS) (**Figure 1.4 A**) and template switching via homologous recombination (HR)- mediated repair (**Figure 1.4 B**). TLS employs specialised polymerases capable of replicating past certain types of lesions with the caveat of increased risk of mutagenesis due to their inherent low-fidelity (Sale, 2013). In template switching, the sister

chromatid is used as a template for error free replication of the damaged DNA (Zeman and Cimprich, 2013; Branzei and Psakhye, 2016).

An alternative DDT mechanism in the reversal of the replication fork which generate four-way structures resembling holiday junctions (**Figure 1.4 C**). The regressed arm of the replication fork is made up by the nascent strands of DNA which may be altered by nuclease activity and may recruit RAD51, signalling for fork restart by a homologous repair mediated mechanism (Neelsen and Lopes, 2015; Qiu *et al.*, 2021). In addition, DNA lesions may be bypassed on the leading strand of DNA after stalling of the polymerase by repriming with PrimPol (Zeman and Cimprich, 2013) (**Figure 1.4 D**). As the helicase extends past the DNA lesion, unwound ssDNA can be reprimed for association with the polymerase allowing the restart of DNA replication while the gap left behind may subsequently be filled by HR-mediated repair (Lopes, Foiani and Sogo, 2006; Elvers *et al.*, 2011; Mourón *et al.*, 2013).

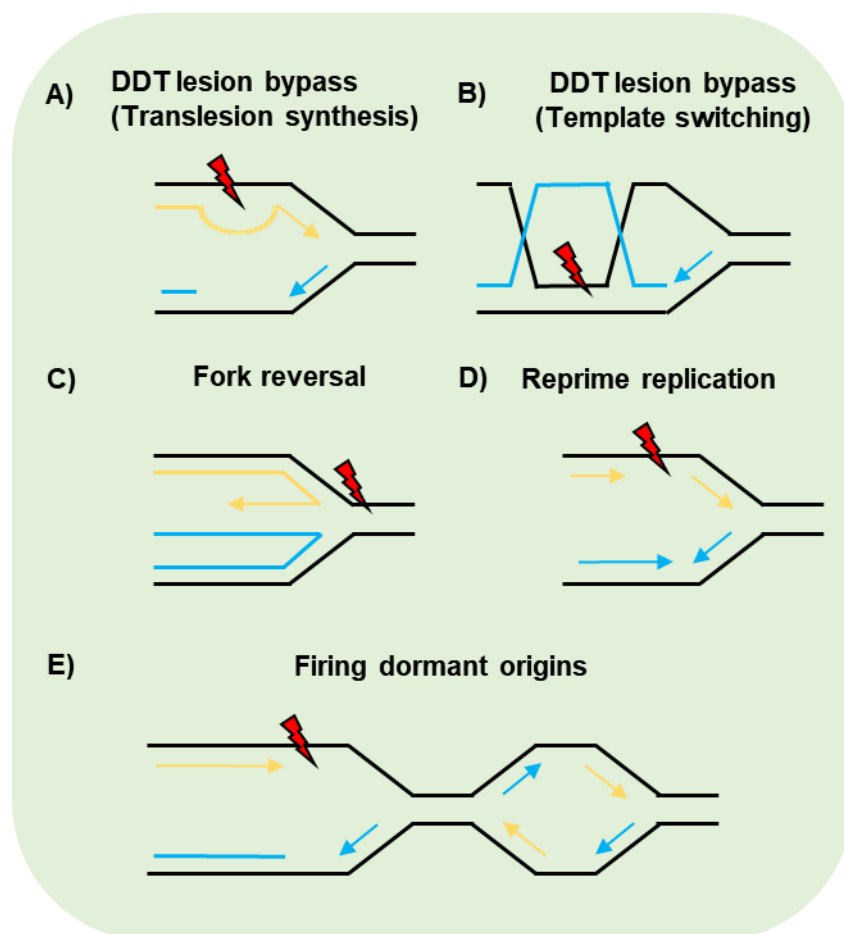


**Figure 1.4: Rescue of stalled replication forks.** DNA damage tolerance (DDT) mechanisms deployed at the replication fork to ensure rescue of stalled replication due to DNA damage. Modified from (Zeman and Cimprich, 2014). Red lightning = DNA Lesion.

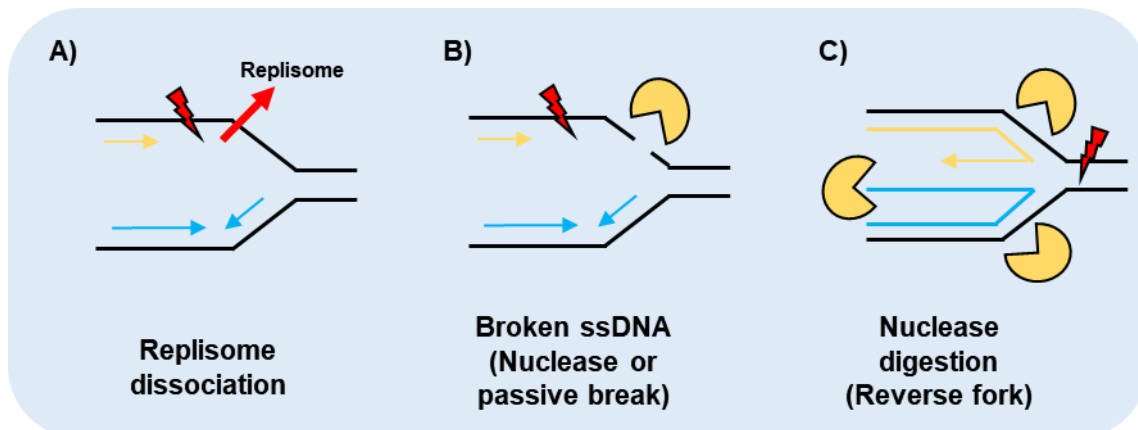


**Figure 1.5: Collapse of the replication fork.** Collapse of the replication fork prevents replication restart. Mechanisms of replication fork collapse include **A)** Dissociation of the replisome **B)** Nuclease digestion of stalled or **C)** reversed replication forks. Modified from (Zeman and Cimprich, 2014). Red lightning = DNA Lesion. Yellow Symbol = Nuclease.

If the various replication fork responses fail to stabilise and restart replication then the replication fork collapses (Zeman and Cimprich, 2014) (**Figure 1.5**), resulting in double stranded breaks which can then be repaired by HR or non-homologous end joining (NHEJ) (**Figure 1.6**). HR repair of DSB has a low error rate due to the use of a homologous sister chromatid as a template for DNA replication/repair (**Figure 1.6 A**), however access to the sister chromatid is limited and so can only take place when the chromatid is accessible, as in S phase and G2 phase (Lieber, 2010). NHEJ does not require a template and therefore does not rely on the sister chromatid, opting instead to directly ligate the two ends of the damaged DNA strands (**Figure 1.6 B**). This can lead to loss or gain of nucleotides and therefore is much more error prone than HR but enables DNA repair when the sister chromatid isn't available (Lieber, 2010). Replication fork collapse may also cause one-ended DSBs which require break-induced replication (BIR) repair, this is a sub pathway of HR DNA repair and also requires a sister chromatid as a template to replace the lost section of DNA which leads to a loss of genetic information and heterozygosity in the repaired DNA (Deem *et al.*, 2011). BIR is highly error prone, demonstrating error rates of up to 2800-fold higher than normal replication, and can result in massive genomic instability, hyper mutagenesis, formation of

mutation clusters and gross chromosomal rearrangements (Li and Heyer, 2008; Deem *et al.*, 2011; Elango *et al.*, 2017) (**Figure 1.6 C**).

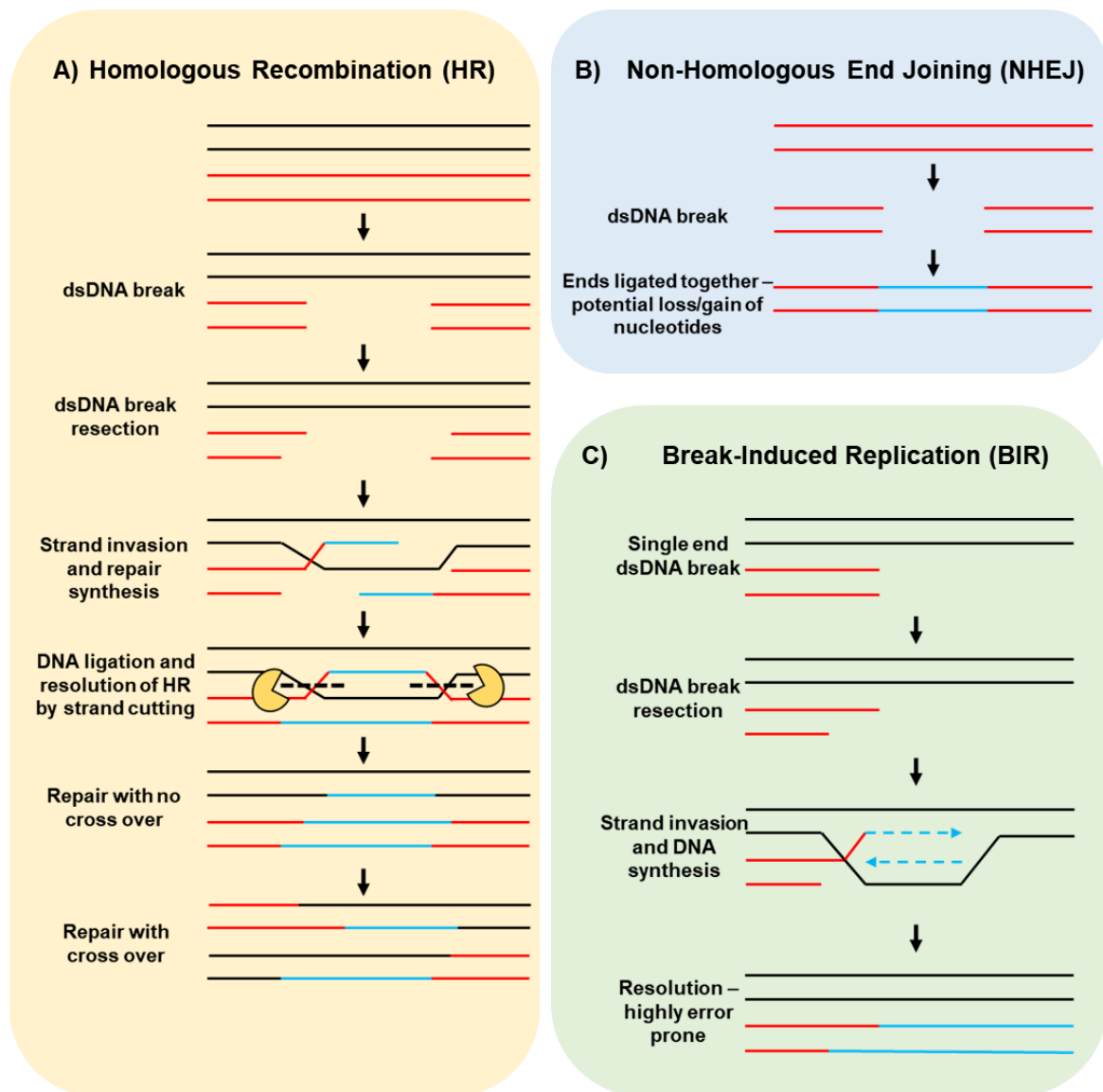


**Figure 1.6: Repair of double stranded DNA breaks.**

Despite multiple pathways to manage replication stress the cell may fail to replicate their DNA. When cells enter mitosis with unrepaired or under replicated DNA this can cause abnormal separation of the chromosomes during anaphase resulting in chromosomal aberrations and genomic instability (Janssen *et al.*, 2011; Wilhelm *et al.*, 2014). As mutations accumulate that induce higher degrees of replication stress (i.e., activation of oncogenes or mutations in DDR proteins) it is likely more mutations will occur as pressure is placed on the replication stress response. Over time this may lead to the progression of diseases such as cancer. Cancers

rely on genomic instability to promote the DNA mutations and alterations required for the emergence of cancer hallmarks (Hanahan and Weinberg, 2011). However, too much genomic instability can still be problematic for cancer cells. Therefore, cancers become reliant on the remaining replication stress response pathways to avoid excessive DNA damage and cell death, such as the ATR-CHK1 pathway.

## 1.3 The CHK1 Kinase

### 1.3.1 Checkpoint Kinases

As discussed briefly in **section 1.2.3** cell cycle checkpoints are mediated by checkpoint kinases and are critical in maintaining genomic stability via control of DNA replication and chromosome segregation. Checkpoint kinases 1 and 2 (CHK1/2) are structurally unrelated but functionally overlapping serine/threonine kinases which are activated by ATR and ATM kinases upon detection of DNA damage (Ronco *et al.*, 2017). Typically, CHK1 is activated by ATR which detects single stranded DNA breakages but can also be phosphorylated by ATM which is activated in response to double stranded DNA breaks (Bartek and Lukas, 2003). CHK2 is mainly activated by ATM but ATR has also been shown to phosphorylate CHK2 in ATM deficient cells (Wang *et al.*, 2006). CHK2 is a stable protein expressed throughout the cell cycle and is typically inactive in the absence of DNA damage whereas CHK1 protein is restricted to S and G2 phases of the cell cycle and shows some activity even in unperturbed cells (Lukas *et al.*, 2001).

Despite the high degree of functional overlap, CHK1 has been shown to be essential to embryo development vs CHK2 as shown by experiments in CHK1<sup>-/-</sup> and CHK2<sup>-/-</sup> null mice. CHK1<sup>-/-</sup> null mice were shown to be non-viable while CHK2<sup>-/-</sup> null mice showed normal development (Takai *et al.*, 2002). Both kinases phosphorylate CDC25C signalling for its degradation stopping the activation of CDK1, however CHK1 is known to be the more prominent regulator of CDK activity (Ronco *et al.*, 2017). CHK2 has been proposed to act as a backup to CHK1 activity but combined inhibition these kinases has not been shown to greatly

enhance the efficacy of DNA-damaging agents vs CHK1 alone (Xiao *et al.*, 2006). An important role of CHK2 is the response to double stranded DNA breakages, signalling for their repair via BRCA1 mediated processes (Lukas *et al.*, 2001). Additionally, CHK2 activates p53 transcription factor and can signal for cell cycle arrest via p21 expression or cell senescence/apoptosis depending on the degree of DNA damage present in the cell (Matthews, Jones and Collins, 2013; Ronco *et al.*, 2017).

### 1.3.2 CHK1 Structure

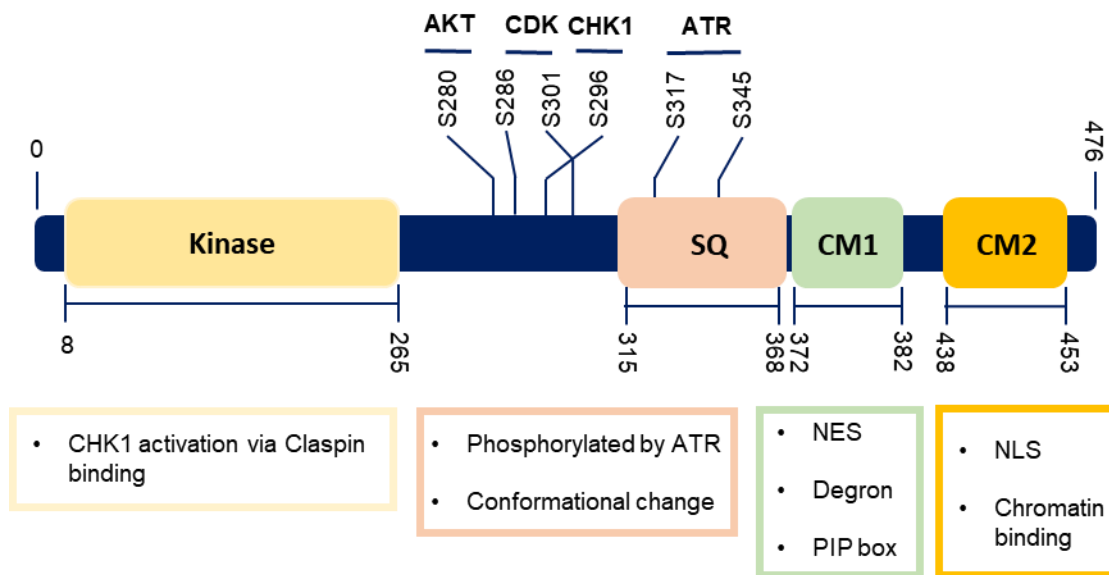


**Figure 1.7: Structural domains and functions of the CHK1 kinase.** Modified from (Zhang and Hunter, 2014).

CHK1 is a Serine/Threonine kinase that controls cell cycle checkpoints and forms part of the DNA damage response. The kinase domain is located at the N-terminus of the protein, while the regulatory C-terminus consists of two conserved motifs (CM) and four Serine/Glutamine (SQ) residues at sites 317, 345, 357 and 366 (**Figure 1.7**). CM1 contains the nuclear export signal (NES), the degron and the PCNA-interacting protein (PIP) box, and CM2 contains the nuclear localisation sequence (NLS) (**Figure 1.7**). The SQ residues S345, S317 and S366 have been shown to be phosphorylated by ATR while no phosphorylation of 357 has been detected (**Figure 1.7**). However, phosphorylation of S366 is much lower than seen with S345 and S317 (Zhang and Hunter, 2014).

### 1.3.3 Regulation of CHK1 activity

#### 1.3.3.1 ATR-dependent phosphorylation

Full activation of the CHK1 kinase requires phosphorylation of the S345 predominantly by ATR (**Figure 1.7**), resulting in an approximately 5-10-fold increase in activity over basal activity (Tapia-Alveal, Calonge and O'Connell, 2009). Cells exhibiting a S345A mutation in CHK1 highly resemble CHK1 null cells suggesting any activity that does not require S345 phosphorylation is likely minimal (Capasso *et al.*, 2002). The C-terminus of CHK1 likely interacts with the kinase domain in absence of S345 phosphorylation physically blocking the interaction between CHK1 and its substrates (Katsuragi and Sagata, 2004; Tapia-Alveal, Calonge and O'Connell, 2009). While inactive, approximately 20% of the total CHK1 pool is associated with chromatin (Smits, Reaper and Jackson, 2006). In response to DNA damage, CHK1 is phosphorylated on S317 and S345 via ATM or ATR resulting in its dissociation from chromatin to the nucleoplasm which is required for downstream signal transduction and mounting of the DNA damage response (Smits, Reaper and Jackson, 2006).

ATR is required for activation of CHK1, however its two phosphorylation sites S317 and S345 appear to have different but connected roles. Phosphorylation of S317 is required to enable S345 phosphorylation, but this alone is not enough to induce maximal phosphorylation and activation of S345 (Wang, Han and Zhang, 2012). Phosphorylation of S345 has been connected to the C-terminus of CHK1 and likely relies on a conformational change to enable maximal phosphorylation, this potentially acts as a mechanism to stop ATR activating CHK1 activity in the absence of DNA damage (Kosoy and O'Connell, 2008; Wang, Han and Zhang, 2012). Additionally, phosphorylated S345 sits within a binding motif for 14-3-3 protein which antagonises the NES in CM1 (**Figure 1.7**), increasing nuclear retention of CHK1 during DNA damage (Jiang *et al.*, 2003). Importantly, ATR requires CHK1 to interact with claspin to enhance CHK1 phosphorylation during replication stress as ATR shows a greater affinity for the CHK1-claspin complex than CHK1 alone (Kumagai and Dunphy, 2000, 2003; Lindsey-Boltz *et al.*, 2009). Consequently, claspin deficiency results in reduced induction of CHK1

phosphorylation via replication stress and compromises the S-phase checkpoint (Kumagai and Dunphy, 2000).

One study showed S317A mutated CHK1 has been shown to exhibit partial proficiency to activate DNA damage induced G2/M and S phase arrests, but this was substantially impaired relative to CHK1 wild type cells (Walker *et al.*, 2009). In another study S317A mutant CHK1 did not induce degradation of CDC25 phosphatase after treatment with IR and replication fork stability and progression was deregulated (Wilsker *et al.*, 2008). However, these events were not as lethal to cells as S345A mutations, suggesting S317 plays a role in checkpoint initiation, but S345 is required for the maximal CHK1 activity (Wilsker *et al.*, 2008; Walker *et al.*, 2009). Additionally, Wilsker *et al.* proposed an essential role for S345 in CHK1 by facilitating the progression of unperturbed mitosis, showing a S317 independent phosphorylation of S345 which only occurred during prophase at the centrosome leading to its dissociation, and likely contributed to the continuation of mitosis (Wilsker *et al.*, 2008).

#### **1.3.3.2 CHK1 autophosphorylation of S296**

After activation of the CHK1 kinase by phosphorylation of S317 and S345 by ATR, CHK1 releases from the chromatin and undergoes autophosphorylation of S296 (Leung-Pineda, Ryan and Piwnica-Worms, 2006; Smits, 2006; Kasahara *et al.*, 2010) (**Figure 1.7**). Following autophosphorylation, S317 and S345 are rapidly dephosphorylated by protein phosphatase 2A (PP2A) which itself is regulated, partially, by CHK1 kinase activity (Leung-Pineda, Ryan and Piwnica-Worms, 2006). S296 provides an additional binding site for the 14-3-3 protein which mediates the interaction between CHK1 and CDC25A, leading to the subsequent phosphorylation and degradation of the phosphatase (Kasahara *et al.*, 2010).

#### **1.3.3.3 Localisation and degradation of CHK1**

During regular growth conditions, CHK1 is predominantly located in the nucleus until the cell is ready to undergo mitosis. At this point CDK1 phosphorylates CHK1 on S286 and S301 leading to nuclear export of CHK1 protein to the cytoplasm stopping CHK1 from inhibiting



CDK1/Cyclin B activity creating a positive feedback loop driving progression through to mitosis (Enomoto *et al.*, 2009). Nuclear export and degradation of CHK1 protein is dependent on CM1 which contains both NES and degron sites. The degron site interacts with the Skp1-Cil1-Fbx6 complex in the cytoplasm signalling for ubiquitination and degradation of CHK1 (**Figure 1.7**) (Zhang *et al.*, 2009; Wang *et al.*, 2012). Additionally, CHK1 is ubiquitinated for proteasomal degradation in the nucleus by the Cul4A-DDB1-CDT2 complex as part of the unperturbed cell cycle, in response to replication stress and on inhibition of heat shock protein 90. Deregulation of this degradation pathway disrupts the G2/M checkpoint induced by ionizing radiation (Van Leung-Pineda, Huh and Piwnica-Worms, 2009; Zhang and Hunter, 2014). It is thought cytoplasmic localisation and degradation of CHK1 serves to allow recovery from the cell cycle checkpoint in addition to keeping CHK1 activity low during an unperturbed cell cycle to avoid inappropriate delay of DNA replication (Zhang *et al.*, 2005; Zhang and Hunter, 2014). Additionally, phosphorylation of s280 by AKT also promotes inactivation of the kinase and subsequent cytoplasmic localisation and ubiquitination (Puc *et al.*, 2005).

#### **1.3.4 CHK1 Function**

CHK1 interacts with a range of different proteins influencing DNA damage and replication checkpoints, DNA repair, the spindle checkpoint in mitosis, apoptosis and gene transcription (**Figure 1.8**) (Dai and Grant, 2010). CHK1 is required for the regular functioning of the cell cycle as well as mounting a response to DNA damage. While the mechanism of CHK1 activation via ATR (predominantly) and ATM (to a lesser extent) remains the same across cellular conditions, the response elicited can be drastically different and is likely reflective of the intensity of CHK1 activation via certain stimulus.

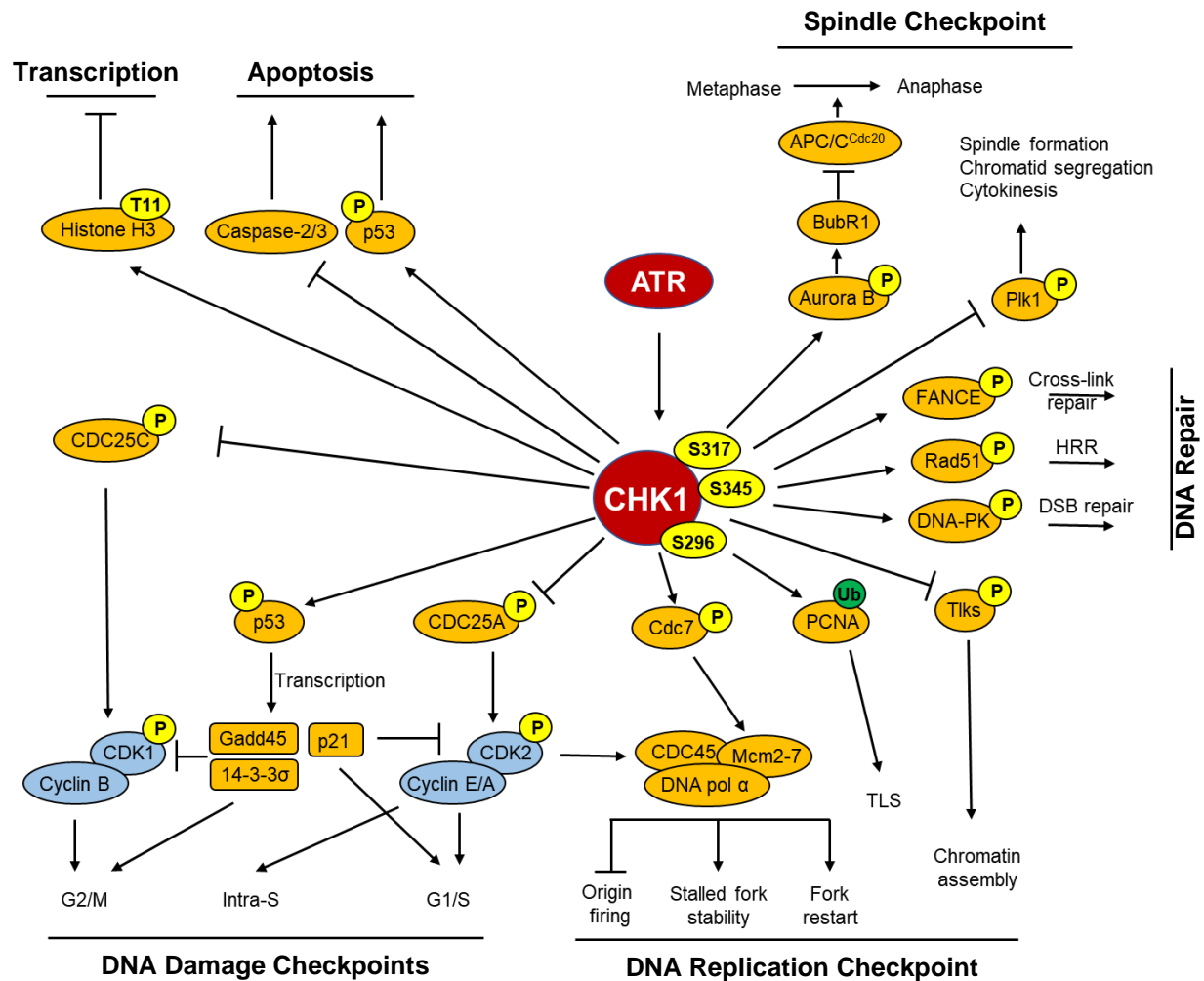


**Figure 1.8: Functions of CHK1 in multiple cellular processes.** Modified from (Dai and Grant, 2010).

#### 1.3.4.1 CHK1 and the response to replication stress and DNA damage

Depletion of CHK1 during unperturbed replication causes slow and asymmetrical movement of the replication fork, increased origin firing, double stranded breaks, genomic instability, and cell death (Syljuåsen *et al.*, 2005; Maya-Mendoza *et al.*, 2007; Besteiro *et al.*, 2019). This shows baseline CHK1 activity during unperturbed S-phase is important for smooth progression of DNA replication. Firing of replication origins is tightly regulated by CHK1 via the regulation of CDC45 loading onto DNA, which is a key subunit of the pre-IC complex required for origin firing. CDK2/Cyclin E phosphorylates Treslin and GEMC1 during unperturbed replication promoting CDC45 loading onto DNA (Balestrini *et al.*, 2010; Kumagai *et al.*, 2010). Upon activation, CHK1 reduces loading of CDC45 via phosphorylation and

degradation of CDC25A stopping the activation of CDK2/Cyclin E complexes. Additionally, the baseline inhibition of CDKs by CHK1 indirectly promotes the interaction between RIF1 and PP1 phosphatase antagonising the CDC7-dependent association of replisome components AND-1 and GINS (Moiseeva *et al.*, 2017, 2019). This is thought to function as a way to limit the overall levels of active replication forks and consequently reducing the likelihood of replication fork collapse and formation of double stranded breaks (Dungrawala *et al.*, 2015; Moiseeva *et al.*, 2017). CHK1 has also been shown to directly phosphorylate Treslin preventing its interaction with TOPB1 also restricting loading of CDC45 (Guo *et al.*, 2015).

The CHK1 kinase must also allow the activation of dormant origins when required to compensate for stalled replication forks, allowing the completion of DNA replication (Ge and Blow, 2010; González Besteiro and Gottifredi, 2015). Replication origins are organised into clusters named replication factories and the firing of these factories is highly regulated. This results in clusters of replication origins classified as early- or late-replicating clusters (Zhao, Watkins and Piwnicka-Worms, 2002; Masai *et al.*, 2010). Within each cluster only a minority of origins are activated while the majority remain dormant until activated by CHK1 to recover DNA replication after a replication fork has stalled. Only replication origins adjacent to the stalled fork should be allowed to fire while origins further away must remain inhibited (Woodward *et al.*, 2006; Ge, Jackson and Blow, 2007; Ibarra, Schwob and Méndez, 2008). This effect may be partially explained by CHK1s tendency to inhibit the initiation of new replication factories, redirecting replication resources to clusters already undergoing DNA replication (Ge and Blow, 2010). However, the exact mechanism of how CHK1 preferentially inhibits new replication factories while selectively allowing dormant origin firing is unknown. One theory is that inactive chromatin bound CHK1 in uninitiated replication factories may act to repress the firing of replication origins, whereas initiated replication factories will have active CHK1 that dissociates from the chromatin that may promote dormant origin firing in the proximity of stalled replication forks (González Besteiro and Gottifredi, 2015).

CHK1 is thought to control the stability of the replication fork. Pharmacological inhibition or depletion via SiRNA leads to the accumulation of replication associated double stranded breaks, CHK1  $-/-$  cell lines and cells treated with a CHK1 inhibitor show reduced ability to resume DNA replication after treatment with aphidicolin (Feijoo *et al.*, 2001; Sørensen *et al.*, 2005; Syljuåsen *et al.*, 2005; Forment *et al.*, 2011). While it is clear that CHK1 is involved in the stability of the replication fork during periods of replication stress, it is unclear if CHK1 prevents dissociation of the replisome directly. It is thought CHK1 may modulate the activity of the replisome rather than recruit different components (De Piccoli *et al.*, 2012; González Besteiro and Gottifredi, 2015).

CHK1 has been shown to promote translesion synthesis (TLS), which is the process in which alternative DNA polymerases are used to replicate across sites of DNA damage (Prakash, Johnson and Prakash, 2005). Replication stress caused by Hydroxyurea (HU), an inhibitor of ribonucleotide reductase (RNR) promotes CHK1-dependent recruitment of Rad18 and DNA polymerase Pol $\eta$  to chromatin and CHK1 has been shown to contribute to the recruitment of Pol $\eta$  to replication factories after UV irradiation (Speroni *et al.*, 2012; Yamada *et al.*, 2013). Rad18 recruitment to chromatin requires phosphorylation of the anaphase promoting complex + adaptor protein CDH1 (APC/C<sup>CDH1</sup>) by CHK1 which recruits DDK followed by Rad18 (Yamada *et al.*, 2013). Additionally, CHK1 potentiates UV-induced PCNA mono-ubiquitination (Yang *et al.*, 2008), a requirement for the post replicative gap filling of UV-induced gaps by Pol $\eta$  (Lehmann and Fuchs, 2006; Edmunds, Simpson and Sale, 2008). CHK1 also prevents the formation of double stranded breaks (DSB) via regulation of the MUS81 and MRE11 nucleases (Syljuåsen *et al.*, 2005; Forment *et al.*, 2011; Thompson, Montano and Eastman, 2012; Murfuni *et al.*, 2013). It is therefore likely CHK1 contributes to replication fork stability by preventing stalling and collapse of replication forks via positive regulation of TLS and inhibition of nuclease activity in perturbed and unperturbed cells.

In cases where replication forks are irreversibly stalled replication fork collapse follows, resulting in DSB via nuclease activity. CHK1 manages the repair response by promoting

homologous recombination (HR), an error-free DNA repair mechanism that requires phosphorylation of Rad51 and BRCA2 by CHK1 to stimulate their recruitment to sites of DNA damage (Sørensen *et al.*, 2005; Bahassi *et al.*, 2008).

#### **1.3.4.2 Transcriptional regulation via CHK1**

Chromatin associated CHK1 during the unperturbed cell cycle phosphorylates histone H3 on T11, which promotes the acetylation of H3 at the promoters of *CDK1* and *Cyclin B1* promoting their transcription and progressing the cell into mitosis (Shimada *et al.*, 2008). However, during periods of replication stress activation of CHK1 and its dissociation from chromatin no longer phosphorylates histone H3 reducing transcription of *CDK1* and *Cyclin B1* delaying mitotic entry (Shimada *et al.*, 2008). Furthermore, CHK1 regulates the activity of E2F transcription factors via inhibitory phosphorylation of the E2F-dependent G1/S transcriptional repressor E2F6. This leads to E2F6 dissociation from promoters allowing association of E2F and subsequent transcription activity (Bertoli *et al.*, 2013). Upregulation of E2F activity leads to increased transcription of CHK1 and claspin and promotes cell survival by preventing DNA damage and cell death (Verlinden *et al.*, 2007; Bertoli *et al.*, 2013).

#### **1.3.4.3 CHK1 regulation of ribonucleotide reductase (RNR)**

In yeast, activation of the S-phase checkpoint has been shown to increase activity of RNR increasing the available pool of dNTPs in times of replication stress promoting cell survival (Iyer and Rhind, 2017). In Ewing Sarcoma cells, CHK1 inhibition has been shown to lead to a CDK2 dependent decrease in the RNR subunit RRM2. CHK1 inhibition increased the DNA damage and replication stress caused by RNR inhibitors, likely due to the depletion of dNTP pools for DNA replication (Koppenhafer *et al.*, 2020). This suggests a regulatory mechanism of CHK1 during replication stress whereby RNR activity is promoted via the inhibition of CDK2-dependent degradation of RNR increasing dNTP pools available for DNA replication.

#### **1.3.4.4 Regulation of apoptosis via CHK1**

The ATR-CHK1 pathway has been shown to suppress a caspase-2 and caspase-3 driven apoptotic response to DNA damage suggesting CHK1 plays a role in suppressing cell death during periods of replication stress (Sidi *et al.*, 2008; Myers *et al.*, 2009). Additionally, during apoptosis CHK1 is cleaved at N299 and N351. The 1-299 fragment of CHK1 has been shown to exhibit elevated kinase activity and may play a role in enhancing the apoptotic process once the cell is committed to apoptosis (Matsuura *et al.*, 2008).

#### **1.3.4.5 CHK1 and the spindle checkpoint**

The spindle checkpoint is activated to delay anaphase and ensure chromosomes are not missegregated. CHK1 helps to regulate this checkpoint via the phosphorylation and activation of Aurora-B kinase, which phosphorylates and recruits BUB1 to the kinetochores of unaligned chromosomes. This helps to inhibit the activity of anaphase promoting complex/cyclosome (APC/C) delaying anaphase and allowing time for correct alignment of chromosomes (Zachos *et al.*, 2007). Additionally, CHK1 has been shown to phosphorylate spindle checkpoint protein Mad2 and inhibition of CHK1 or depletion via SiRNA resulted in depletion of Mad2 protein in cells sensitive to CHK1 depletion. Furthermore, CHK1 was shown to co-localise and physically associate with mad2 in both unstressed and DNA damage conditions (Chilà *et al.*, 2013).

#### **1.3.5 CHK1 as a target for cancer therapies**

Genomic instability is addressed by Hanahan and Weinberg as an enabling characteristic of cancers, promoting the acquisition of malignant cancer hallmarks via the development of mutations (Hanahan and Weinberg, 2011). A major contributor to this characteristic is the deregulation of cell-cycle checkpoints or the disruption of DNA repair mechanisms, however, genomic instability may also be driven by oncogene-induced DNA damage (Hartwell, 1992; Negrini, Gorgoulis and Halazonetis, 2010). Cancer cells with a compromised G1/S checkpoint, as with cancers exhibiting *TP53* mutations, were thought to exhibit an increased dependency on the S-phase and G2/M checkpoints to compensate. As the CHK1 kinase is a key regulator

of these checkpoints, it was hypothesised that CHK1 inhibitors may result in a positive therapeutic outcome.

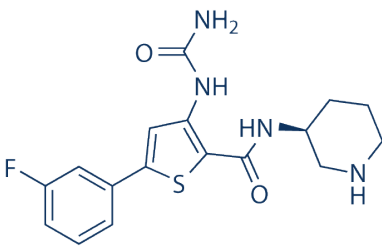
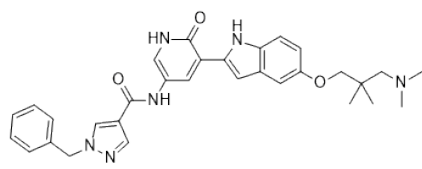
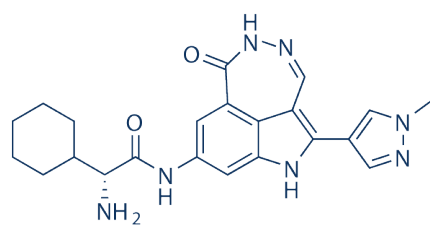
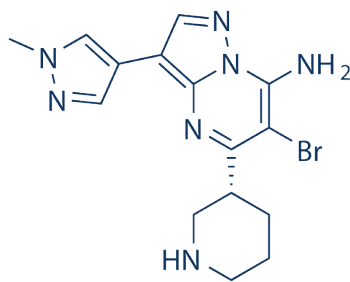
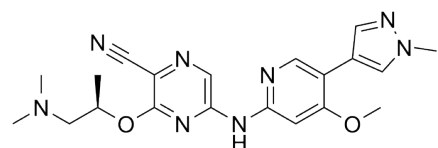
Early validation studies showed depletion or pharmacological inhibition of the CHK1 kinase resulted in sensitivity to DNA damaging agents (Busby *et al.*, 2000; Carrassa *et al.*, 2004; Ganzinelli *et al.*, 2008; Azorsa *et al.*, 2009). However, the role of *TP53* status as a marker of sensitivity to CHK1 inhibitors is unclear as both *TP53* Wild Type (WT) and mutated cell lines have demonstrated sensitivity to CHK1 inhibitors in the past (Flatten *et al.*, 2005; Ganzinelli *et al.*, 2008; Pan *et al.*, 2009; Zenvirt, Kravchenko-Balasha and Levitzki, 2010). It is likely sensitivity to CHK1 inhibitors relies on a combination of factors as other biomarkers of response to CHK1 inhibition have been identified. For example, loss of B-family DNA polymerase function in lung and colorectal cancers has shown synthetic lethality with CHK1 inhibition (Rogers *et al.*, 2020), while high levels of the protein kinase WEE1 (CDK inhibitor) in SCLC or high activity of the epidermal growth factor receptor (EGFR) in TNBC have been associated with resistance to CHK1 inhibition (Lee *et al.*, 2020; Zhao, I. Kim, *et al.*, 2021). Additionally, overexpression of cyclins E and B have been associated with sensitivity to CHK1 inhibition (Xiao *et al.*, 2008; Chen *et al.*, 2018). Therefore, p53 may play a role in response to CHK1, but other pathways involved in cell cycle regulation and growth/survival pathways may be active in cells that can compensate for loss of p53 and CHK1 activity.

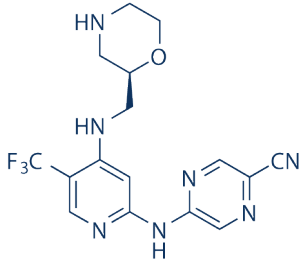
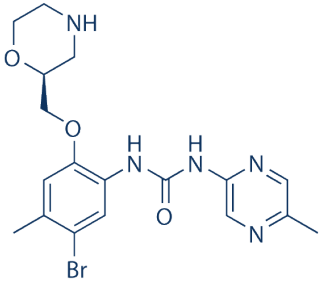
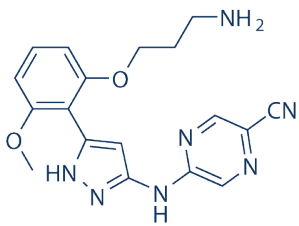
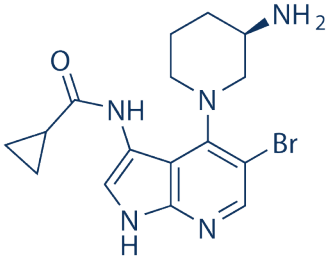
#### 1.3.5.1 CHK1 inhibitors

UCN-01 was the first CHK1 inhibitor, and was an effective tool compound but failed in the clinic due to unfavourable pharmacokinetics, high toxicity, and poor selectivity of CHK1 over other targets such as CHK2, CDK1 and CDK2 (Ma, Janetka and Piwnica-Worms, 2011). Since validation of CHK1 as a clinical target, multiple CHK1 inhibitors have been developed as detailed in **table 1.1**. Most CHK1 inhibitors are ATP-competitive, binding directly with the hinge peptide region forming hydrogen bonds with one or more residues (E85, Y86 or C87) in the region (Matthews, Jones and Collins, 2013), although allosteric inhibitors have also been created which bind outside of the ATP-pocket (Converso *et al.*, 2009; Vanderpool *et al.*, 2009).

Most CHK1 inhibitors have since been discontinued due to toxicity, lack of efficacy or business reasons (Warren and Eastman, 2020). Prexasertib and SRA737 remain as the only two CHK1 inhibitors progressing through clinical trials. However, Prexasertib has been discontinued by Eli Lilly due to excessive neutropenia (Warren and Eastman, 2020), but three clinical trials not sponsored by Eli Lilly are currently recruiting for use of Prexasertib in combination with other drugs. These include, Samotolisib (PI3K and DNA-PK inhibitor) in metastatic TNBC, Irinotecan/Temozolomide (DNA damaging agents) in desmoplastic small round cell tumours (DSRCT) and Rhabdomyosarcoma (RMS), and Cyclophosphamide/Gemcitabine (Antimetabolites) in medulloblastoma (*ClinicalTrials.gov*, 2021). SRA737 has completed phase 1 trials as a monotherapy and in combination with Gemcitabine and exhibited limited neutropenia (Banerji *et al.*, 2019; Plummer *et al.*, 2019; *Clinical Trials.gov*, 2021). Prexasertib inhibits both CHK1 ( $IC_{50} < 1\text{nM}$ ) and CHK2 ( $IC_{50} 8\text{nM}$ ) at low concentrations and is only available intravenously (King, H. B. Diaz, *et al.*, 2015), while SRA737 is orally available and highly selective for CHK1 ( $IC_{50} 1.4\text{nM}$ ) over CHK2 ( $IC_{50} 2.44\mu\text{M}$ ) (Walton *et al.*, 2016a).



Name	Structure	IC <sub>50</sub> /Ki	Selectivity
AZD7762		CHK1 IC <sub>50</sub> = 5nM	Equally potent: CHK1/CHK2
V158411		CHK1 IC <sub>50</sub> = 4.4nM	Equally potent CHK1/CHK2; <b>In cells:</b> 20-fold CHK1 vs. CHK2
PF-0477736		CHK1 Ki = 4.9nM	100-fold CHK1 vs CHK2
MK8776/SCH900776		CHK1 IC <sub>50</sub> = 3nM	500-fold CHK1 vs CHK2
CCT244747		CHK1 IC <sub>50</sub> = 8nM	>1000-fold CHK1 vs CHK2

SRA737		CHK1 IC <sub>50</sub> = 1.4nM	>1500-fold CHK1 vs CHK2
LY2603618		CHK1 IC <sub>50</sub> = 7nM	>1000-fold CHK1 vs CHK2
Prexasertib	 2HCl	CHK1 IC <sub>50</sub> = <1nM	Dual inhibitor of CHK1/CHK2
GDC0575		CHK1 IC <sub>50</sub> = 1.2nM	Kinase selectivity profile at 100nM Residual activity % CHK1 = <1% CHK2 = 50-100% (Tullio et al., 2017)

**Table 1.1: Table of CHK1 inhibitors.** Modified from (Rundle et al., 2017).

### 1.3.5.2 Use of CHK1 inhibitors as a single agent

The accumulation of DNA damage promoted by oncogene induced replication stress in cancers typically acts as a barrier for tumour progression as these cells experience a strong DNA damage response (DDR) and subsequent senescence or apoptosis. For cancer cells to survive the DDR must be downregulated enough to avoid replication stress induced senescence/apoptosis, but not too much that it causes unsustainable DNA damage (Hills and Diffley, 2014). The use of CHK1 inhibitors as a single agent attempts to exploit this precarious balance between genomic instability and an increased dependency on fewer aspects of the DDR. Therefore, CHK1 inhibitors would selectively kill cancer cells with high levels of replication stress while sparing normal cells with an intact DDR that can compensate for CHK1 inhibition, resulting in a potential therapeutic window for patients (Gaillard, García-Muse and Aguilera, 2015).

Single agent use of CHK1 inhibitors has shown cytotoxicity in a number of different cancers exhibiting high levels of replication stress including melanoma, pancreatic, and ovarian cell lines (Garrett and Collins, 2011; Mike I. Walton *et al.*, 2012; Brooks *et al.*, 2013; Parmar *et al.*, 2019). Additionally, lymphoma and neuroblastoma cell lines showing MYCN induced replicative stress have also demonstrated sensitivity to CHK1 monotherapies (Cole *et al.*, 2011; Ferrao *et al.*, 2011; Murga *et al.*, 2011). Furthermore, use of CHK1 inhibitors as a monotherapy has been proposed to treat TNBC, a subtype of breast cancer known for its high genomic instability (Albiges *et al.*, 2014). Depletion by SiRNA and pharmacological inhibition of the CHK1 kinase in TNBC cell lines has demonstrated a marked reduction in cell viability and may be an effective therapeutic strategy for TNBC patients (Albiges *et al.*, 2014; Bryant, Rawlinson and Massey, 2014). In a study carried out by Sakurikar *et al.*, investigating the effect of CHK1 monotherapy on a large panel of different types of cancer cell lines, approximately 15% demonstrated hypersensitivity to the CHK1 inhibitor MK-8776 (Sakurikar *et al.*, 2016). This suggests a subset of patients may be highly responsive to CHK1 monotherapies, providing appropriate patient selection (Ditano and Eastman, 2021).

### 1.3.5.3 Combining CHK1 inhibitors with genotoxic agents

CHK1 has been shown to exhibit synergistic cell killing in combination with other therapeutic agents. Initially, CHK1 inhibitors were developed to enhance the cell killing effects of chemotherapeutic agents. As high levels of DNA damage is caused by agents such as cisplatin and Gemcitabine stalling DNA replication, CHK1 inhibitors should sensitise cells to these drugs by inducing DNA replication and mitosis before cells can repair their DNA (Thompson and Eastman, 2013). Early combination studies with UCN-01 showed a 60-fold increase in cisplatin toxicity in CHO cells (Bunch and Eastman, 1996), this has also been seen with other CHK1 inhibitors Gö6976, PF-0477736 and SB218078 (Blasina *et al.*, 2008; Zenvirt, Kravchenko-Balasha and Levitzki, 2010; Thompson *et al.*, 2012). However, some studies show no sensitisation of cells to cisplatin with AZD7762 or MK-8776 (Wagner and Karnitz, 2009; Montano *et al.*, 2012). Additionally, MK-8776 failed to sensitise cells to topoisomerase I inhibitor SN-38 (active metabolite of irinotecan), whereas both AZD7762 and CHIR-124 have shown synergy with SN-38 (Tse *et al.*, 2007; Zabludoff *et al.*, 2008; Ma *et al.*, 2012). Discrepancies between these CHK1 inhibitors may be reflective of the different degrees of selectivity, or differences in the assays used to determine cytotoxicity (Thompson and Eastman, 2013).

The ribonucleotide reductase (RNR) inhibitors Gemcitabine and Hydroxyurea have shown strong synergistic effects with CHK1 inhibitors. Inhibition of RNR depletes the available pool of dNTPs available for replication, slowing DNA replication and increasing replication stress. In addition to RNR inhibition, Gemcitabine incorporates into replicating DNA followed by one additional nucleotide resulting in a masked chain termination, stopping the addition of further nucleotides and the easy removal of Gemcitabine by exonucleases (Plunkett, Huang and Gandhi, 1995). Numerous CHK1 inhibitors have been shown to increase the cytotoxicity of Gemcitabine/Hydroxyurea including MK-8776, AZD7762, PF-0477736, SAR-020106, CCT244747, SRA737 and Prexasertib (Blasina *et al.*, 2008; Zabludoff *et al.*, 2008; Walton *et al.*, 2010, 2016a; Ma *et al.*, 2012; Mike I Walton *et al.*, 2012; Montano *et al.*, 2012, 2013;

Thompson and Eastman, 2013; Sen *et al.*, 2019; Morimoto *et al.*, 2020). These data suggest CHK1 inhibitors are better used in combination with therapeutics that cause replication stress rather than other types of DNA damaging agents (Montano *et al.*, 2012).

#### **1.3.5.4 CHK1 and WEE1 inhibitors in combination**

WEE1 is a tyrosine kinase which regulates the G1/S transition, S-phase, and G2/M checkpoints alongside CHK1. WEE1 phosphorylates CDK1/2 at Y15 (Heald, McLoughlin and McKeon, 1993; Squire *et al.*, 2005), directly inhibiting its activity, unlike CHK1 which indirectly inhibits CDKs via the phosphorylation and degradation of the phosphatase CDC25, which activates CDKs via removal of phosphorylation at Y15 and T14. Both WEE1 and CHK1 are regulated by 14-3-3 proteins. 14-3-3 promotes nuclear retention of CHK1 and mediates the interaction between CHK1 and CDC25, positively regulating its activity (Jiang *et al.*, 2003; Kasahara *et al.*, 2010). During interphase in *Xenopus* egg extracts, 14-3-3 binds to WEE1, which requires phosphorylation of S549, a site shown to be phosphorylated by CHK1. A S549A mutation of this site stops 14-3-3 binding and reduces the capacity for WEE1 to phosphorylate CDK1 and also effects the distribution of WEE1 across the nucleus (Lee, Kumagai and Dunphy, 2001). In Human cells CHK1 and 14-3-3 has also been shown to regulate WEE1 activity, however it is possible other kinases also phosphorylate WEE1 on S549 to promote 14-3-3 binding to WEE1, as kinase activity is resilient to treatment with CHK1 inhibitor UCN-01 (Rothblum-Oviatt, Ryan and Piwnicka-Worms, 2001; Sarcar *et al.*, 2011).

The use of WEE1 inhibitors has been shown to sensitise cells to CHK1 inhibition and depletion via SiRNA, and has been associated with increased apoptosis (Davies *et al.*, 2011; Carrassa *et al.*, 2012; Chaudhuri, Vincelette, Koh, Naylor, Flatten, Peterson, McNally, Gojo, Karp, Ruben A Mesa, *et al.*, 2014) and high levels of DNA-damage taking place in S-phase, suggesting a high induction of replication stress (Guertin *et al.*, 2012). The strong synergy between CHK1 and WEE1 inhibitors suggested both kinases share unique yet complementary roles in the cell cycle checkpoint that is not just due to higher levels of unscheduled CDK activity (Guertin *et al.*, 2012). Hauge *et al.* showed that the high levels of replication stress and

DNA damage resulted from increased loading of CDC45 and unscheduled firing of replication origins which is regulated in both a CDK2 dependent and independent fashion (Hauge *et al.*, 2017). Independent of CDK2, CHK1 negatively regulates the replication factor Treslin which stimulates loading of CDC45 onto replication origins (Guo *et al.*, 2015), while CDK2 positively regulates Treslin to promote loading of CDC45 (Kumagai *et al.*, 2010). Therefore, combined inhibition of CHK1 and WEE1 results in greater increases in CDK activity than either inhibitor alone. Additionally, loss of CHK1 dependent regulation of Treslin removes the breaks on CDC45 loading resulting in massive deregulation of S-phase and subsequent DNA damage (Hauge *et al.*, 2017).

Currently there are four WEE1 inhibitors in clinical development, namely Adavosertib (NCT02659241; Previously MK-1775/AZD1775), IMP7068 (NCT04768868), ZN-c3 (NCT04158336) and Debio 0123 (NCT05109975, NCT03968653) (*ClinicalTrials.gov*, 2021). Adavosertib is the most clinically progressed undergoing trials both as a monotherapy and in combination with other drugs (NCT03579316, NCT02659241) while IMP7068 and ZN-c3 are currently recruiting for phase 1 clinical trials (*ClinicalTrials.gov*, 2021).

## 1.4 Resistance to Cancer Therapies

### 1.4.1 The Challenge of drug resistance

Drug resistance remains a key limiting factor in the successful treatment of cancer patients, with targeted therapies and chemotherapeutics/radiation therapy. Patients typically relapse after a successful tumour response or fail to respond entirely to available therapies (Garraway and Jänne, 2012). Unfortunately, further attempts to treat these patients are usually unsuccessful. The challenge of drug resistance in cancers is inherently complex due to the genomic instability and heterogeneity within cancers in addition to the flexibility of common oncogenic signalling pathways (Garraway and Jänne, 2012; David J Konieczkowski, Johannessen and Garraway, 2018).

Drug resistance can be either intrinsic or acquired. Intrinsic resistance is when a drug naïve cancer is unresponsive to a given drug (Garraway and Jänne, 2012). Acquired resistance develops over the course of a treatment with tumours showing an initial response but become less responsive over time until the therapeutic is completely ineffective (Garraway and Jänne, 2012). Acquired resistance may be caused by genomic or epigenetic alterations in the cell (Bagrodia, Smeal and Abraham, 2012). Additionally, due to the heterogenous nature of cancers, resistant subpopulations may exist that survive initial treatment enabling the regrowth of the tumour (Turner and Reis-Filho, 2012). This heterogeneity and ability to quickly adapt to the selective pressure of cancer therapies is likely linked to the high genomic instability in most cancers, enabling the accumulation of mutations. each having a chance to alter a gene that may confer drug resistance (Vasan, Baselga and Hyman, 2019). Non-genetic mechanisms can also contribute to resistance, such as alterations in protein phosphorylation or gene expression in ways which alter the activity of signalling pathways and confer resistance (McGranahan and Swanton, 2017). In order to overcome the emergence of resistant cancers, it is critical we develop our understanding of the mechanisms driving drug resistance. It has been suggested that despite the multifaceted nature of drug resistance, resistance

mechanisms to targeted therapies converge into three main patterns being pathway reactivation, pathway by-pass, and pathway indifference (David J. Konieczkowski, Johannessen and Garraway, 2018) (**Figure 1.9**). These are explored in greater detail in the following sections.

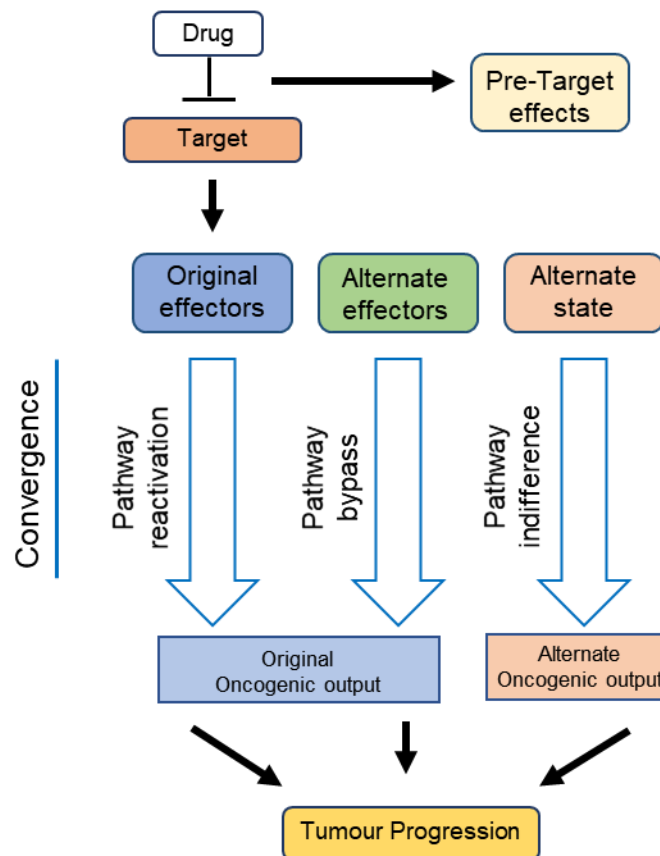


**Figure 1.9: Convergence based framework for cancer drug resistance.**  
Adapted from (David J Konieczkowski, Johannessen and Garraway, 2018)

## 1.4.2 Mechanisms of drug resistance

### 1.4.2.1 Pre-target effects

Although not discussed in Konieczkowski *et al.*, before the therapy can engage the target for the desired therapeutic effect, resistance mechanisms may emerge. Important examples of such mechanisms include the upregulation of drug efflux transporter proteins or alterations in drug metabolism. ATP-binding cassette (ABC) transporters which include Multi Drug resistance protein 1 (MDR1/ABCB1) also known as P-glycoprotein (P-GP), MRP2 (ABCC1) and, ABCG2 can confer multidrug resistance in cancer cells (Gottesman, Fojo and Bates,



2002). Cancers that demonstrate intrinsic resistance to chemotherapy including renal, adrenocorticoid, hepatocellular, pancreatic, and colorectal carcinoma are known to overexpress MDR1 (Filipits, 2004). Additionally, MDR1 overexpression in acute myeloid leukaemia (AML) has been demonstrated as an adaptive response to chemotherapy, as the incidence of MDR1 expression increases from 30% at diagnosis to >50% in relapsed patients and correlates with reduced complete remission rate and shorter duration of survival for patients (Van Den Heuvel-Eibrink, Sonneveld and Pieters, 2000).

In prodrugs, which are biologically inactive compounds prior to metabolic activation by the cancer cell, resistance mechanisms may emerge which alter the metabolic activation of the drug. For example, Gemcitabine requires phosphorylation by deoxycytidine kinase (dCK) which converts Gemcitabine into the active metabolites Gemcitabine diphosphate and triphosphate (Mini *et al.*, 2006). Downregulation of the dCK kinase has been identified as a driver of resistance to Gemcitabine in a drug resistant ovarian cancer cell line model (Al-Madhoun *et al.*, 2004). Additionally, SiRNA knockdown of dCK has also been shown to confer resistance to Gemcitabine (OHHASHI *et al.*, 2008).

#### **1.4.2.2 Pathway reactivation**

Targeted therapeutics act against specific proteins or pathways that have undergone oncogenic dysregulation to exploit cellular dependencies. Consequently, many resistance mechanisms enable reactivation of the pathway despite the presence of the drug. This is one of the most common types of resistance convergence encompassing many different types of mechanisms that can enable pathway reactivation (David J. Konieczkowski, Johannessen and Garraway, 2018).

The simplest way to reactive a pathway downstream of the drug-inhibited target is alter the drug target itself, making them insensitive to the drug. This can arise via point mutations of the target protein stopping the drug from binding the target and eliciting an effect. One of the best-known examples of kinase inhibitor resistance mutations is on the “gatekeeper residue”

(David J. Konieczkowski, Johannessen and Garraway, 2018). Mutation of this residue alters the accessibility of the hydrophobic ATP-binding pocket required for the activity of ATP-competitive kinase inhibitors. Gatekeeper mutations have been identified in EGFR (T790M mutation) and ALK (L1196M mutation) in non-small-cell lung cancers and KIT (T670I mutation) and BCR-ABL (T315I mutation) in gastrointestinal and chronic myeloid leukaemia respectively (Gorre *et al.*, 2001; Demetri *et al.*, 2006; Kobayashi *et al.*, 2009; Choi *et al.*, 2010). Mutations against allosteric inhibitors which are non-ATP-competitive generate mutations outside of the gatekeeper residues, however these may alter the activity of the kinase in addition to stopping drug binding. This was seen with the MEK inhibitor AZD6244 where the majority of mutations were in the allosteric binding pocket while others conferred cross resistance to the B-RAF inhibitor or modulated the activity of MEK itself (Emery *et al.*, 2009). Drug target alterations as drivers of resistance are not only seen in kinases, as inhibitors targeting hormone receptors such as androgen receptor (AR) and oestrogen receptor (ER) have also been rendered ineffective by overexpression of the receptor or mutations that enable constitutive activation of the signalling pathway (Visakorpi *et al.*, 1995; Chen *et al.*, 2003; Robinson *et al.*, 2013; Toy *et al.*, 2013).

Another mechanism by which the target pathway can be reactivated is via the activity of upstream effectors. Upstream effectors are defined by being upstream of the drug target, alterations in these effectors can lead to reactivation of the pathway despite the inhibition of the successful inhibition of the target (David J. Konieczkowski, Johannessen and Garraway, 2018). For example, resistance to the RAF inhibitor PLX4032 in activating B-RAF-mutant melanoma (V600E mutation) was conferred by mutations activating NRAS or by loss of tumour suppressor protein NF1 that negatively regulate RAS (Nazarian *et al.*, 2010; Maertens *et al.*, 2013; Van Allen *et al.*, 2014). Additionally, upstream receptor tyrosine kinases such as EGFR and MET can override RAF inhibition via the activation of RAS and C-RAF, restoring MEK/ERK signalling downstream (Straussman *et al.*, 2012; Wilson *et al.*, 2012; Girotti *et al.*, 2013).

The activity of parallel effectors in a signalling pathway may also confer resistance as seen in resistance to anti-EGFR monoclonal antibodies in colorectal cancer and EGFR tyrosine kinase inhibitors in NSCLC. Resistance can be driven by activation of MET (Engelman *et al.*, 2007; Bardelli *et al.*, 2013), ERBB2 (Yonesaka *et al.*, 2011; Takezawa *et al.*, 2012), and IGF1R receptors (Guix *et al.*, 2008) enabling downstream activation of the pathway via alternative RTKs. Pathways may also be activated downstream of the drug target independent of any upstream or parallel effectors as seen in B-RAF-mutant melanoma exhibiting activating mutations in MEK which drive resistance to inhibition of RAF and MEK (Emery *et al.*, 2009; Carlino *et al.*, 2015). Or as seen in response to EGFR therapies, downstream effector KRAS can generate activating mutations (Diaz *et al.*, 2012; Misale *et al.*, 2012; Van Emburgh *et al.*, 2016).

#### **1.4.2.3 Pathway bypass**

The second type of resistance convergence is pathway bypass, this is when the oncogenic output of the inhibited signalling pathway is instead activated by an alternative pathway thereby facilitating an effective bypass of the drug targets signalling pathway (David J. Konieczkowski, Johannessen and Garraway, 2018). In some cases of BRAF-mutant melanoma resistant to RAF/MEK inhibitors, resistance could be driven by the alternative G protein coupled receptor (GPCR) signalling (Johannessen *et al.*, 2013). GPCR activity triggers an increase in cAMP/protein kinase A signal activating the CREB transcriptional regulator resulting in the activity of RAF/MEK inhibitor resistance conferring transcription factors (Johannessen *et al.*, 2013). Another example of pathway bypass is in prostate cancer in which inhibition of androgen receptor (AR) by enzalutamide can be bypassed via activation of glucocorticoid receptor (GR). The outputs of AR and GR receptors converge at the level of gene expression promoting tumour survival. Therefore, in the event of AR inhibition, GR could become active and rescue the original output of AR, leading to drug resistance (Arora *et al.*, 2013).

#### 1.4.2.4 Pathway indifference

Pathway indifference unlike pathway reactivation and pathway bypass does not rely on the reactivation of the original pathway output inhibited by the drug. Instead, resistance mechanisms arise which are independent of the original oncogenic dependency targeted by the therapy (David J. Konieczkowski, Johannessen and Garraway, 2018). One example of pathway indifference is that of resistance to PARP inhibition in breast cancer patients. The rationale for use of PARP inhibitors against breast cancers was based on the synthetic lethality in cancers with mutated and inactive *BRCA1/2* genes (Turk and Wisinski, 2018). It was shown that secondary mutations in *BRCA1/2* were able to restore function to the protein consequently eliminating synthetic lethality and promoting PARP inhibitor resistance (Edwards *et al.*, 2008; Norquist *et al.*, 2011). This reversion of *BRCA* suggests a shift in cell phenotype from a genetically unstable to stable state (David J. Konieczkowski, Johannessen and Garraway, 2018). In another example, the EGFR-mutant NSCLC treated with EGFR inhibitors demonstrates a shift from a NSCLC type state to a mesenchymal-like or SCLC-like state (Sequist *et al.*, 2011; Piotrowska *et al.*, 2015). The EGFR mutation which conferred sensitivity to EGFR inhibitors was still present in the population of SCLC-like cells. This suggested that within the heterogenous tumour population a small subgroup of SCLC-like cells existed prior to treatment with EGFR inhibitors surviving the treatment before regrowing the tumour, or the switch to a SCLC-like state was the adaptive response of NSCLC cells during treatment with an EGFR inhibitor (Sequist *et al.*, 2011; Oser *et al.*, 2015; Piotrowska *et al.*, 2015; Hata *et al.*, 2016).

## 1.5 Triple Negative Breast Cancer

### 1.5.1 Introducing TNBC

Breast cancer is the second most diagnosed cancer worldwide, with 2,088,849 cases diagnosed in 2018 being only slightly behind lung cancer with 2,093,876 cases (Bray *et al.*, 2018). Breast cancers account for significantly less deaths than lung cancers with 629,679 and 1,761,007 deaths in breast and lung cancer respectively (Bray *et al.*, 2018). Mortality of breast cancers has dropped by approximately 40% between the 1980s and 2020 in high-income countries according to a report by the world health organization (World Health Organization, 2020). This is largely owing to advances in the screening and treatment of breast cancers leading to improved detection rates, patient stratification and effective new treatments.

Triple negative breast cancer (TNBC) accounts for approximately 15% of all breast cancers and is most common in young women and black women (Sharma, 2016). TNBC is called “triple negative” due to the negative expression of three important prognostic receptors called the oestrogen receptor (ER) progesterone receptor (PGR) and human epidermal growth factor receptor 2 (HER2). Due to this molecular phenotype TNBCs are not responsive to endocrine therapies such as Tamoxifen or Fulvestrant which block activation of ER, or targeted therapies like Herceptin which blocks activation of the HER2 receptor (Kumar and Aggarwal, 2015; Wahba and El-Hadaad, 2015). Consequently, treatment options for patients of TNBC is more limited than for regular breast cancer patients leaving surgery and chemotherapy as the main treatment options available for patients.

### 1.5.2 TNBC subtypes

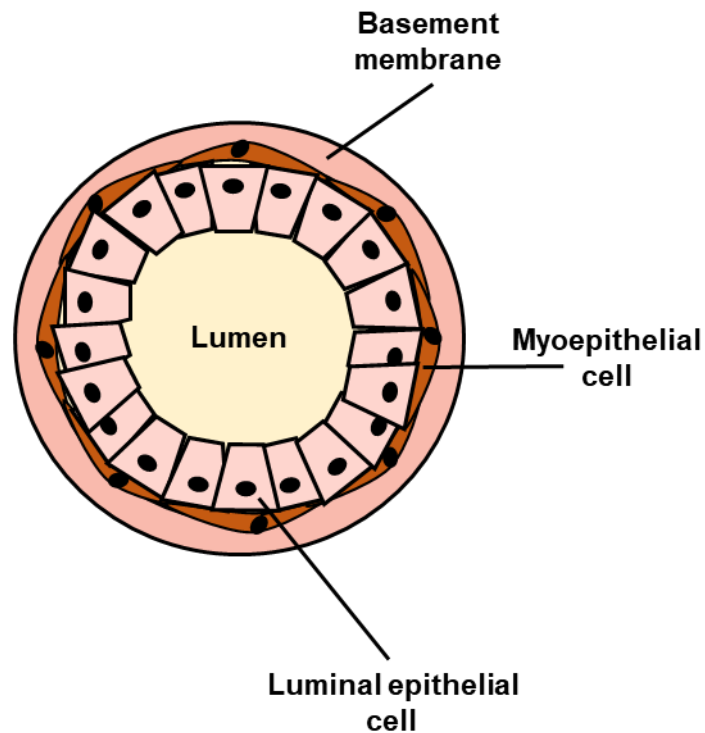


**Figure 1.10: Diagram of a normal breast duct microenvironment.**

Breast cancer is a highly heterogeneous disease. Transcriptomic profiling of breast cancers via microarray analysis established 5 main subtypes of tumour, namely luminal A, luminal B, HER2-enriched, basal-like and normal breast-like (Sørlie *et al.*, 2001). Luminal and basal-like cancers are named due to the consistent expression of genes associated with the epithelial luminal or myoepithelial basal cells respectively (**Figure 1.10**)(Sørlie *et al.*, 2001). Luminal A tumours are the most common subtype representing 50-60% of all breast cancers. These tumours show higher expression of ER but have a good prognosis and lower rate of relapse (Yersal and Barutca, 2014). Luminal B tumours represent 15-20% breast cancer cases and are more aggressive, proliferative and have a worse prognosis than luminal A (Yersal and Barutca, 2014). HER2-enriched tumours lack ER or PGR expression but express HER2. These tumours are typically faster growing than luminal cancers and have a worse prognosis but can be successfully targeted with therapies that target HER2 (Vogel *et al.*, 2002).

TNBC is defined by the lack of ER, PGR and HER2 receptors, but is still a highly heterogenous disease in its own right and gene expression profiles of these tumours can overlap with the main subtypes of breast cancer. Normal breast-like tumours are a poorly characterised subtype accounting for 5-10% of all breast carcinomas but are known to lack expression of ER, PGR and HER2 making them triple negative. These tumours cannot be neatly categorised into luminal or basal-like subtypes by their gene expression profiles. However, there is some contention on the existence of the normal breast-like subtype with critics suggesting contamination of tumour specimens with a high proportion of stromal tissue skews the microarray data (Weigelt *et al.*, 2010). Interestingly, the normal breast-like subtype is typically non-responsive to chemotherapy unlike other TNBCs which are initially responsive (Yersal and Barutca, 2014; Bergin and Loi, 2019).

Basal-like tumours show the greatest overlap with the TNBC subtype. Approximately 50-75% of TNBCs exhibit a basal phenotype with 80% of basal-like tumours showing negative expression of ER and HER2 receptors (Garrido-Castro, Lin and Polyak, 2019). Basal-like tumours are highly aggressive, mitotic, and proliferative and are associated with shorter survival times (Yersal and Barutca, 2014). These tumour subtypes also exhibit a high frequency of *TP53* and *BRCA1* mutations which contribute to the highly genomically unstable phenotype of basal-like breast cancers via deregulation of DNA repair and cell cycle regulatory pathways (Sørli *et al.*, 2001; Turner and Reis-Filho, 2006; Kwei *et al.*, 2010; Yersal and Barutca, 2014).

### **1.5.3 Treatment strategies for TNBC patients**

Historically, TNBC treatment has relied predominantly on chemotherapy and surgery. TNBC typically responds well to surgery and does not demonstrate significantly increased rates of local recurrence at 5 years (Freedman *et al.*, 2009; Wahba and El-Hadaad, 2015). Additionally, TNBC is typically more sensitive to chemotherapies such as anthracycline and taxane-based therapies than ER+ or PGR+ breast cancers (Ismail-Khan and Bui, 2010; Cortazar *et al.*, 2014). Despite this, prognosis for TNBC patients is poor as the disease typically demonstrates

short progression free survival (approximately 4-months) and its highly metastatic and aggressive nature contributes to shortened overall survival (Ismail-Khan and Bui, 2010).

Therapeutic advances have been made in TNBC treatment, particularly in immunotherapies. Current immune therapies tested in TNBC include programmed cell death receptor 1 (PD-1) and programmed cell death ligand 1 (PD-L1) inhibitors. PD-1 is an immune checkpoint protein in T cells which suppresses the T cell immune response when in contact with the PD-L1 ligand (Chinai *et al.*, 2015; Ribas and Wolchok, 2018). Immune therapies such as Pembrolizumab or Atezolizumab work by binding either PD-1 or PD-L1 proteins stopping their interaction and activating T cell immune activity (Chinai *et al.*, 2015). These immune therapies have demonstrated efficacy and tolerable safety in combination with chemotherapies, targeted inhibitors (MEKi, PI3K/AKT, PARP inhibitors) and immune agonists to superior levels than seen with immune checkpoint monotherapy (Ebert *et al.*, 2016; Vinayak *et al.*, 2019; O'Day *et al.*, 2020; Schmid *et al.*, 2021; Chen *et al.*, 2022). More work is still required to understand the difference between PD-1 and PD-L1 antibodies and the most optimal therapeutics for combination treatment. A clear correlation is seen between PD-L1 expression level and therapeutic efficacy. However, some studies have also shown PD-L1 negative patients may still benefit from immunotherapies as high levels of genomic instability has been as a marker of response to immune checkpoint inhibitors (Barroso-Sousa *et al.*, 2020; Zhu *et al.*, 2020).

In addition to immunotherapies, PARP inhibitors have been approved for use against TNBCs harbouring *BRCA* mutations. Approximately 15-20% of TNBCs exhibit germline mutations of *BRCA1/2* (Sharma, 2016). PARP inhibitors have been shown to improve the overall response rate and progression free survival safely and significantly in patients with advanced/metastatic TNBC that exhibit *BRCA1/2* mutations (Liu *et al.*, 2021). Additionally, PARP inhibitors have been shown to significantly improve progression free survival and pathological complete response rates regardless of *BRCA* mutation status in TNBC patients (Rugo *et al.*, 2016; Liu *et al.*, 2021). Questions remain to be answered with PARP inhibitors such as how to practically select patients with TNBC who will experience the most benefit from PARP inhibition and more



biomarkers of response are required to achieve this. Low levels of the DNA damage repair protein RAD51, high levels of tumour infiltrating lymphocytes (T/B cells), and high PD-L1 expression have also been associated with PARP inhibitor response in TNBC. This shows markers of reduced homologous recombination capacity and immunological signatures may be useful as predictive biomarkers for PARP inhibitor response (Cruz *et al.*, 2018; Liu *et al.*, 2021).

In addition to PARP inhibitors, CHK1 inhibitors hold the potential to exploit highly deregulated DNA repair pathways common in TNBCs. Mutation or loss of *TP53* occurs at a high frequency in TNBC with 68% of tumours in The Cancer Genome Atlas program found to exhibit *TP53* mutations, in addition 3% of tumours demonstrated homozygous deletion of the gene (Koboldt *et al.*, 2012; Sharma, 2016). While only 15-20% of TNBCs exhibit a BRCA1/2 germline mutation, 45% of TNBCs exhibit a BRCAness phenotype which is defined by a deficiency in the homologous recombination DNA repair pathway in cells (Sharma, 2016). These mutations in the DDR and cell cycle regulatory pathways increase genomic instability and reliance on CHK1 for maintenance of cell cycle checkpoints and genomic integrity (Ma *et al.*, 2012). CHK1 inhibitors have already shown effectiveness against TNBC cell lines with pCHK1 S296 being identified as a predictive biomarker of CHK1 inhibitor sensitivity (Ma *et al.*, 2012; Albiges *et al.*, 2014; Bryant, Rawlinson and Massey, 2014). Clinical trials for CHK1 inhibitors are currently ongoing and these inhibitors show great potential to treat patients of genomically unstable cancers such as TNBC.

## 1.6 Overview and aims of thesis

As mentioned previously, TNBC is an aggressive sub-type of breast cancer with currently very limited therapeutic options. TNBC is also known to be highly genomically unstable, exhibiting multiple defects in the DNA damage response such as high incidence of *TP53* mutations and *BRCA* mutations. CHK1 inhibitors may be able to tackle the currently unmet clinical need of TNBC patients as some TNBC cancers may be highly dependent on CHK1 to maintain sufficient genomic stability. Multiple studies have already demonstrated single agent usage of CHK1 inhibitors are capable of reducing cell viability via the induction of DNA damage, apoptosis, and mitotic catastrophe (Ma *et al.*, 2012; Turner *et al.*, 2013; Albiges *et al.*, 2014; Bryant, Rawlinson and Massey, 2014). While CHK1 inhibitors may be effective at treating TNBC, the likelihood resistance will emerge is high. With CHK1 inhibitors currently progressing through clinical trials, it is important to understand how resistance mechanisms to CHK1 inhibitors may arise over the course of a patient's therapy. Pre-clinical cell line models have proved very effective at identifying clinically relevant mechanisms of drug resistance in the past and helped generate therapeutic strategies to overcome resistance (Nazarian *et al.*, 2010; Garraway and Jänne, 2012; David J Konieczkowski, Johannessen and Garraway, 2018). To this end, this project will generate CHK1 inhibitor resistant TNBC cell line models using the two most progressed CHK1 inhibitors SRA737 and Prexasertib in HCC38 and MDA-MB-468 TNBC cell lines. Newly generated CHK1 inhibitor cell line models will be characterised and investigated to identify resistance mechanisms, biomarkers of resistance and potential therapeutic strategies to overcome CHK1 inhibitor resistance.

### **Aims and objectives:**

- Investigate and identify biomarkers and mechanisms of resistance to CHK1 inhibitors SRA737 and Prexasertib in Triple Negative Breast Cancer cell lines.
  - Generate models of acquired resistance in HCC38 and MDA-MB-468 cell lines via a dose escalation method and characterise resistant cell lines.
  - Biased approach: Cross-resistance profiling of parental and resistant cell lines with a range of targeted inhibitors and chemotherapeutic agents.
  - Hits identified via cross-resistance profiling to be investigated at the molecular level – investigate changes in cell signalling in response to targeted inhibitors.
  - Un-biased approach: RNA sequencing analysis of HCC38 parental and resistant cell lines.
- Validate identified biomarkers/mechanisms of resistance to CHK1 inhibitors.
- Identify clinically relevant therapeutic strategies to overcome resistance.
  - Identify targeted inhibitors/chemotherapeutics that can restore sensitivity to CHK1 inhibitors via drug combination experiments.

# **Chapter 2**

## **Materials and Methods**

## 2. Materials and Methods

### 2.1 Compounds

Compounds used on cell lines shown in **table 2.1** were prepared and diluted in either dimethyl sulfoxide (DMSO; Sigma-Aldrich, Germany) or sterile dH<sub>2</sub>O under sterile conditions and stored at -20°C in aliquots.

Inhibitor/drug	Target(s)	Catalogue Number	Supplier
SRA737	CHK1	N/A	Institute of Cancer Research, UK
Prexasertib	CHK1/CHK2	A13684	Adooq Bioscience, USA
Verapamil	L-Type calcium channel/P-gp	S4202	Selleckchem, DE
Ceralasertib	ATR	A15794	Adooq Bioscience, USA
Adavosertib	WEE1	A10599	Adooq Bioscience, USA
AZD0156	ATM/ATR	S8375	Selleckchem, DE
CCT241533	CHK2	N/A	Institute of Cancer Research, UK
Cisplatin	DNA damage	P4394	Sigma, Aldrich, DE
Olaparib	PARP	A10111	Adooq Bioscience, USA
Bleomycin	DNA damage	13877	Cayman Chemical, USA
Cyclohexamide	Protein Synthesis	357420010	ThermoFisher Scientific, USA
PD0166285	WEE1/Myt1/CHK1	A15863	Adooq Bioscience, USA
G418	Anitbiotic	G0175	Melford Laboratories, UK
MK-8776	CHK1	A11167	Adooq Bioscience, USA
Rabusertib	CHK1	A11036	Adooq Bioscience, USA
Gemcitabine	DNA damage	S1149	Selleckchem, DE
Hydroxyurea	RNR	S1896	Selleckchem, DE
RO-3306	CDK1/CDK2	SML0569	MerckMillipore, DE
Roscovitine	CDK1/CDK2/CDK5	S1153	Selleckchem, DE

**Table 2.1: Summary of compounds used in cell-based experiments.**

## 2.2 General Cell Culture

### 2.2.1 Cell lines and culture

HCC38 and MDA-MB-468 human triple negative breast cancer (TNBC) cell lines were kindly provided by the Resistant Cancer Cell Line collection (RCCL, Frankfurt, Germany). SRA737 and Prexasertib resistant cell lines H737R, HPrexR, MDA-737R and MDA-PrexR cell lines were generated as shown in **section 2.2.2**. All cell lines were cultured in Iscove Modified Dulbecco Medium (IMDM), which contains L-Glutamine, HEPES and Sodium Bicarbonate (3.024g/L) (Gibco, UK). Media is supplemented with 10% (v/v) Foetal Bovine Serum (FBS; Gibco, UK) and 1% (v/v) Penicillin Streptomycin solution (Penstrep; Life technologies, UK). Cells were cultured in either T25, T75 or T175 flasks and incubated at 37°C in a humidified 5% CO<sub>2</sub> incubator. All cell culture was carried out in sterile conditions in a class II biological safety cabinet.

Before passaging cells, all reagents were pre-warmed to 37°C. Cells were passaged at approximately 70-90% confluency. In T25 flasks, cell culture medium was aspirated off and discarded before rinsing cells in 2ml of phosphate-buffered saline (PBS; Oxoid, UK). 1ml of 0.25% Trypsin-EDTA (ThermoFisher Scientific, UK) was added to cells which were then allowed to incubate at 37°C until cells had detached. Detached cells were suspended in IMDM and typically split at either 1:10-1:5 into a new flask and topped up with IMDM to a final volume of 5ml. IMDM was added to the remaining cells in the old flask up to 5ml and kept as a backup flask. For culture in T75 and T175 flasks volumes were adjusted by 3- and 7-fold respectively. Resistant cell lines were routinely maintained in either SRA737 or Prexasertib at the concentrations shown in **table 2.2**.

	Prexasertib (μM)	SRA737 (μM)
HPrexR	0.5	-
H737R	-	4
MPrexR	1.75	-
M737R	-	17.2

**Table 2.2: Drug maintenance concentrations for CHK1 inhibitor resistant cell lines.**

### **2.2.2 Generation of TNBC cell lines with resistance to SRA737 or Prexasertib.**

HCC38 and MDA-MB-468 parental cell lines were used to generate sublines with resistance to SRA737 or Prexasertib via dose escalation. Specifically, HCC38 and MDA-MB-468 cell lines were seeded in T25 flasks and allowed to adhere overnight in standard growth conditions. Preliminary half maximal growth Inhibitory ( $GI_{50}$ ) values of SRA737 and Prexasertib in HCC38 and MDA-MB-468 cell lines (provided by Dr Helen Grimsley (Garrett lab) via the MTT cell viability assay) were used to establish starting concentrations for dose escalation. Cells were grown in standard growth conditions in their preliminary  $GI_{50}$  of either SRA737 or Prexasertib until reaching approximately 70% confluency. At 70% confluency HCC38 and MDA-MB-468 cell lines were passaged, and the drug concentration was increased 2-fold. This was repeated over a period of 140 days and stopped if resistant cell lines were unable to survive in higher concentrations of the drug or if the  $GI_{50}$  of the resistant cell lines was at least 5-fold greater than the parental  $GI_{50}$ . Untreated cell lines were cultured over the same period. This led to the generation of HCC38 sublines H737R and PrexR with resistance to SRA737 and Prexasertib respectively and generation of MDA-MB-468 sublines MDA-737R and MDA-PrexR with resistance to SRA737 and Prexasertib respectively.

### **2.2.3 Counting cells with a haemocytometer**

Cell number was determined via haemocytometer. Cells were trypsinised and suspended in 5-10ml of IMDM. Resuspended cells were diluted 1:2 in trypan blue and 20 $\mu$ l added to the chambers of a BRAND® haemocytometer to count the number of cells. After counting, resuspended cells were diluted in IMDM at the required seeding density.

### **2.2.4. Cryopreservation of cell lines**

Every 3-6 months passaged cells would be replaced with fresh cryopreserved cells to avoid genetic drift. Once cells grown in a T75 flask reached 70% confluency they were trypsinised and resuspended in 15 ml of IMDM. Cells were then separated into 5 ml aliquots and centrifuged at 270 x g for 5 minutes to pellet the cells. Media was aspirated off and discarded

and pellet was resuspended in 0.5 ml IMDM. Freeze down medium was then prepared with 20% DMSO and 80% FBS. 0.5 ml of freeze medium was added to 0.5 ml of suspended cells bringing the final concentration of DMSO to 10%. 1 ml of cells suspended in freeze medium was then placed in each cryovial and cells were left overnight in a -80°C freezer. The next day cryovials were transferred to a liquid nitrogen tank for long term storage.

For revival of cryopreserved cell lines cryovials were thawed rapidly by placing them in a 37°C water bath until completely thawed. Cells were then added to a T25 flask containing 9 ml of media to dilute the DMSO in the freeze medium and incubated overnight to adhere to the flask. The next day media was aspirated off and discarded and replaced with fresh IMDM media. Within 5 passages cells were expanded to T75 flasks and fresh cells were cryo-preserved before too many passages were accumulated.

## **2.3 Cell Growth Characterisation**

Understanding growth characteristics of cell lines is important for determining optimal seeding conditions for assays. Ideally cells should be in log phase growth throughout the assay so that data collected represents changes caused by the independent variable and not by changes in growth characteristics potentially caused events such as contact inhibition or depletion of media.

### **2.3.1 Seeding density assay**

Cells were plated in seven 96-well plates in 200µl of IMDM at multiple seeding densities and allowed to grow normally. Every 24 hours one plate was fixed with 10% (w/v) trichloroacetic acid (TCA) using 70 µl per well. Cells were then stained with Sulforhodamine B (SRB; Sigma-Aldrich, Germany) and analysed as described in **section 2.4**.



## 2.4 Sulforhodamine B cell Viability Assay

Cross-profiling of parental and resistant cell lines with a range of targeted inhibitors and cancer drugs is carried out using a cell viability assay. The Sulforhodamine B (SRB) assay is a method for measuring the cellular protein content of cells. SRB dye binds to cellular protein and so can be used to estimate cellular density and measure cell viability (Skehan et al., 1990). Cells were plated in 96-well plates and at the end of the assay media was flicked out of the wells and cells were fixed with 70  $\mu$ l of 10% (w/v) TCA per well for 30 minutes. After fixation, plates were washed with distilled water and cells were stained with 70  $\mu$ l of 0.4% (w/v) SRB (Sigma-Aldrich, Germany) in 1% (v/v) acetic acid per well for 30 minutes before washing in 1% (v/v) acetic acid until all excess dye was removed. Plates were placed in a 37°C oven until completely dry overnight before the addition of 100  $\mu$ l of 10 mM Tris-base per well to solubilise bound SRB-dye. Plates were left on a shaker until dye was completely solubilised and absorbances were read at a wavelength of 490 nm using a Victor X4 multi-label plate reader (PerkinElmer Life Sciences, USA). Raw absorbances were adjusted with a blank calculated from the mean absorbance of the media control wells, which contained no cells. The mean was subtracted from the absorbance of all wells and dose response values were percentage normalised to the mean absorbance of the untreated control wells. Results were then plotted in Graphpad Prism 6 (Graphpad Software Inc, USA) and the GI<sub>50</sub> values were determined via non-linear regression.

In cell viability assays measuring the effects of drugs/compounds, cells were plated in 160  $\mu$ l of IMDM media per well at the indicated seeding densities and allowed to grow for 48 hours. 200  $\mu$ l of PBS was placed in the outermost wells at the edge of the plate in addition to a background/media control with no cells. Drugs and compounds that were tested on plated cell lines were first serially diluted in IMDM at 5x the required concentration to account for dilution of drug when added to the plate. 40  $\mu$ l of IMDM containing drug was then added in triplicate

to the required wells. For vehicle control wells 40 µl of IMDM + maximum concentration of vehicle used in drug dilution was added to cells, while 40 µl of IMDM was added to untreated control wells.

## 2.5 Cell lysis and Western Blotting

Western blot analysis is an effective method for detecting specific protein molecules within a cell lysate. This technique is used to identify changes in protein levels and cell signalling via protein specific antibodies for targets in the CHK1 pathway and other related pathways in parental and resistant cell lines.

### 2.5.1 Cell Lysis

Lysis buffer (**Table 2.3**) was prepared in advance of cell lysis and stored in aliquots at –20°C.

Cells were seeded in 10cm or 7cm dishes and grown for 24-48 hours until approximately 50-60% confluent prior to drug treatment. IMDEM Media was refreshed, and drug or vehicle was added at the desired concentration and cells were incubated for up to 24 hours. Media control plates were incubated in fresh IMDM for the same amount of time. After drug incubation, plates were put on ice and media aspirated off before washing twice in ice cold PBS, all PBS removed and from this point plates were either frozen at -80°C for lysis later or lysed immediately.

Reagent	Concentration	Manufacturer
HEPES pH 7.4	50 mM	Sigma-Aldrich, DE
NaCl	250 mM	Sigma-Aldrich, DE
Nonidet-P40 substitute	0.1% (v/v)	Roche, CH
DTT	1 mM	Melford Laboratories, UK
EDTA	1 mM	FisherScientific, UK
NaF	1 mM	Sigma-Aldrich, DE
β-Glycerophosphate	10 mM	Sigma-Aldrich, DE
Sodium orthovanadate	0.1 mM	Sigma-Aldrich, DE
Complete™ protease inhibitor cocktail	1 tablet per 50 ml	Roche, CH

**Table 2.3: Summary of components lysis buffer.** HEPES: 4-(2-hydroxyethyl)-1-piperazineethanesulfonic acid, DTT: Dithiothreitol, EDTA: Ethylenediaminetetraacetic acid.

For lysis, 50-100 µl of ice-cold lysis buffer was added to plates depending on the plate size and cells were scraped off the surface of the plate into lysis buffer. Lysis buffer containing scraped cells was then moved into a pre-cooled 1.5 ml Eppendorf and incubated on ice for 30 minutes. Lysates were centrifuged at 14,000 x g for 10 minutes at 4°C and supernatant was collected in a separate pre-cooled 1.5 ml Eppendorf and kept on ice or snap-frozen in dry ice and stored at -80°C. 10 µl of lysate would be transferred to a microcentrifuge tube for protein quantification via Bicinchoninic acid or Bradford assay.

### **2.5.2 Bicinchoninic acid and Bradford assays**

Determination of total protein content by bicinchoninic acid assay (BCA) was performed using Pierce™ BCA protein assay kit (ThermoFisher Scientific, UK; Smith *et al.*, 1985). Lysates prepared as shown in **section 2.5.1** were diluted 10- to 20-fold in lysis buffer (**Table 2.3**) and 10µl of each lysate was added in triplicate in a 96-well plate. In each plate, 10µl of bovine serum albumin (BSA) protein standards at concentrations of 0.1-1mg/ml and a blank of 10µl lysis buffer were also added in triplicate to each plate. A copper (II) sulfate solution was added to BCA at a 1:50 ratio and 200µl of the solution was added to each plate. Plates were mixed on a microplate shaker for 30 seconds before incubation at 37°C for 30 minutes. After incubation, absorbances were measured at a wavelength of 560nm using the Victor X4 multi-label plate reader (PerkinElmer Life Sciences, USA). The mean absorbance of the blank control was subtracted from the raw absorbances of all samples, total protein concentration was determined using a BSA protein standard curve.

In cases where total protein concentration was anticipated to be low (< 0.1mg/ml in diluted lysate), the BCA standards and the plate incubation steps were modified to increase assay sensitivity. BCA standards were diluted to 5-500µg/ml and plates were incubated at 60°C for 30 minutes.

Determination of total protein content by Bradford assay was performed using the Bio-Rad Protein assay dye concentrate kit (Bio-Rad, UK; Bradford, 1976). Bradford reagent was diluted 1:5 in dH<sub>2</sub>O for a working solution. BSA standards were prepared between 50-500µg/ml in lysate buffer (**Table 2.3**) and 10µl added in triplicate to a 96-well plate. Samples were diluted 10- to 2-fold in lysis buffer as mentioned previously and 10µl added to the plate in triplicate. 10µl of lysis buffer was added as a blank in triplicate and 200µl of Bradford reagent was pipetted into each well. Plates were mixed on a microplate shaker for 30 seconds before absorbances were measured at 595nm on the Victor X4 multi-label plate reader (PerkinElmer Life Sciences, USA). Total protein concentration and deduction of the average background absorbance was carried out as described above for the BCA assay.

### 2.5.3 SDS-PAGE

Lysates were thawed on ice and normalised to equal protein concentrations (usually 30-50ug/well) with lysis buffer. 5x sample buffer (0.3M Tris pH 6.8, 50% (v/v) glycerol (ThermoFisher Scientific, UK) 25% (v/v) β-mercaptoethanol, 10% (w/v) SDS (ThermoFisher Scientific, UK) and 0.05% (v/v) bromophenol blue) was added to normalised lysates at a 1/5 dilution. Normalised lysates containing sample buffer were vortexed and spun down on a benchtop centrifuge before heating for 5 minutes at 95°C and spinning down a final time. Samples were then loaded on a sodium dodecyl sulphate-polyacrylamide gel electrophoresis (SDS-PAGE) gel or stored either -20°C or -80°C.

SDS-PAGE resolving and stacking gels were produced as shown in **table 2.4**. Equal amounts of protein (5-70 µg) were loaded into the wells of the stacking gel in addition to 7 µl of PageRuler™ Plus Prestained protein ladder (ThermoFisher Scientific, UK). SDS-PAGE gel was run with a Tris-Glycine running buffer (25 mM Tris-HCl, 192 mM Glycine, 0.1% SDS) and electrophoresis was carried out over a 60- to 90-minute period using a Hoefer SE250 electrophoresis unit (Hoefer, USA) at a constant voltage of 100V until samples had entered the resolving gel when voltage was increased to 150V. When double loading was necessary the gel was run at 100V until samples left the wells and entered the stacking gel, additional

sample was loaded, and the gel was run as normal. Gel electrophoresis was stopped when the bands of interest reached the middle of the resolving gel or once the dye front was approximately 1cm from the bottom of the gel.

Reagent	Resolving gel concentration	Stacking gel concentration	Manufacturer
Acrylamide/Bis (29:1)	8-12% (v/v)	4% (v/v)	Bio-Rad, USA
Tris-HCl pH 8.8	0.375 M	-	Sigma-Aldrich, DE
Tris-HCl pH 6.8	-	0.125 M	Sigma-Aldrich, DE
SDS	0.1% (v/v)	0.1% (v/v)	Sigma-Aldrich, DE
TEMED	0.2% (v/v)	0.1% (v/v)	Sigma-Aldrich, DE
APS	0.1% (w/v)	0.1% (w/v)	Bio-Rad, USA

**Table 2.4: Summary of components for the construction of SDS-PAGE gels.** SDS: Sodium lauryl sulfate, TEMED: Tetramethylethylenediamine, APS: Ammonium persulfate.

#### 2.5.4 Western Blotting

After gel electrophoresis, protein was transferred from the SDS/polyacrylamide gel to a 0.2 µm pore Immobilon-P polyvinylidene fluoride (PVDF) (Millipore, USA) using a wet blotting system Mini Trans-Blot® Cell. Before blotting, PVDF was activated in methanol and protein was transferred for 90 minutes in pre-cooled transfer buffer (25 mM Tris-HCl, 192 mM Glycine and 10% (v/v) methanol) under a constant voltage of 100V. Once transfer was completed the gel was discarded and the membrane was reactivated in methanol and stained with ponceau S solution (0.1% (w/v) ponceau S in 5% (v/v) acetic acid) for protein detection. This confirmed successful transfer, equal loading of protein, and assisted in accurate cutting of PVDF membrane to isolate protein targets. After cutting membranes were blocked in blocking buffer (Tris-buffered-saline + Tween (TBS-T; 5 mM Tris-HCl pH 8.0 and 15 mM NaCl + 0.1% (v/v) Tween-20) with 5% (w/v) milk (Marvel, UK)) on an orbital shaker.

After blocking membranes were incubated overnight in primary antibody in blocking buffer at 4°C. Following primary antibody incubation membranes were washed for 10 minutes 2x in TBS-T before an hour incubation in horseradish peroxidase conjugated secondary antibody in blocking buffer. Antibody specifications and concentrations are listed in **table 2.5**. After

secondary incubation membranes were washed for 4x 5 minutes in TBS-T. Detection of protein signal was performed with Clarity™ western enhanced chemiluminescence (ECL) substrate (Bio-Rad, USA) and visualised by exposure of Hyperfilm ECL (GE healthcare, UK) and developed using an Optimax™ 2010 film processor (Protec, Germany).

Antibodies were stripped from membranes before they were re-probed by incubating methanol activated membranes in stripping buffer (50 mM Glycine, 1% (w/v) SDS, pH 2.0) for 2x 5 minutes and then washing in TBS-T for 2x 5 minutes. Membranes were then blocked for 1 hour in blocking buffer and primary and secondary incubation steps carried out as mentioned previously. To store membranes after use, blots were stripped and washed in TBS-T before air drying at room temperature. Once dry membranes were labelled and stored at -20°C.

Primary Antibody	Supplier	Catalogue number	Species	Dilution
MDR1	Santa Cruz, USA	SC-55510	Mouse	1:100
pCHK1 s345	CST, USA	2348	Rabbit	1:500
pCHK1 s296	CST, USA	2349	Rabbit	1:500
T-CHK1	CST, USA	2360	Mouse	1:1000
pCHK2 s516	CST, USA	2996	Rabbit	1:500
T-CHK2	CST, USA	6334	Rabbit	1:1000
WEE1	Santa Cruz, USA	SC-5285	Mouse	1:1000
pCDK1/2 Y15	CST, USA	9111	Rabbit	1:2000
T-CDK1	Santa Cruz, USA	SC-8395	Mouse	1:4000
C-PARP	CST, USA	9541	Rabbit	1:1000
GFP	Santa Cruz, USA	SC-9996	Mouse	1:1000
pRPA32 s4-8	Bethyl, USA	A300-245A	Rabbit	1:2000
RPA32	Abcam, UK	EPR2877Y	Mouse	1:2000
γH2AX	MerckMillipore, DE	05-636	Mouse	1:1000
p21 <sup>Cip1/Waf1</sup>	CST, USA	2947	Rabbit	1:1000
α-Tubulin	Bio-Rad, USA	150028	Rabbit	1:1000
GAPDH	MerckMillipore, DE	MAB374	Mouse	1:200,000
Secondary - Anti Rabbit	Bio-Rad, USA	170-6516	Goat	1:10,000
Secondary - Anti Mouse	Bio-Rad, USA	170-6515	Goat	1:10,000

**Table 2.5: List of antibodies used for western blot analysis.** CST: Cell Signalling Technology.

## 2.6 Cell Cycle Analysis via Flow Cytometry

Analysis of the cell cycle distribution via flow cytometry is used identify differences in response to targeted inhibitors affecting the cell cycle in both parental and resistant cell lines. Cells were seeded in T75 flasks and allowed to adhere overnight before drug treatment. Cells were incubated in drug for 24 hours before collection. Media was discarded and cells were washed in PBS, trypsinised and suspended in 5ml IMDM before counting via hemocytometry as shown in **section 2.2.3**. Approximately  $1 \times 10^6$  cells per sample were collected for fixing and cell cycle analysis.

After counting cells, 4.5ml of cells suspended in IMDM was centrifuged at  $270 \times g$  for 5 minutes to pellet the cells. IMDM was removed and replaced with 5ml PBS and centrifuged again at  $270 \times g$  for 5 minutes to wash the cells. PBS was removed and cells were gently suspended in 0.5ml of PBS and pipetted up and down to achieve a single cell suspension. Approximately 4.5ml of ice cold 70% ethanol was added in a drop-wise fashion to the single cell solution while gently vortexing to avoid cell aggregates. After fixation, cells were incubated in fixative for at least 2 hours at room temperature or stored at  $-20^{\circ}\text{C}$ .

After fixation, cells were centrifuged at  $270 \times g$  for 5 minutes and ethanol removed. Cells were washed in 5ml PBS and re-centrifuged. PBS was removed and cells were suspended in 0.25ml of PBS +  $5\mu\text{l}$  of 10mg/ml RNase A (ThermoFisher Scientific, UK) to a final concentration of 0.2 mg/ml and incubated at  $37^{\circ}\text{C}$  for 1 hour. 1mg/ml Propidium Iodide (PI) stain (Sigma-Aldrich, Germany) was added to a final concentration of  $10\mu\text{g/ml}$  and incubated at  $4^{\circ}\text{C}$  in the dark until analysis. Sample was then analysed on a BD Accuri™ C6 Plus Flow Cytometer (BD Biosciences, UK) at 488nm and data processed using BD Csample Plus software (BD Biosciences, UK).

## 2.7 Knockdown of WEE1 Gene Expression via Small Interfering RNA

To validate WEE1 overexpression as a potential mechanism of resistance WEE1 protein expression was knocked down using SiRNA. Small interfering RNAs (siRNAs) were used for the transient knockdown of WEE1 gene expression in the HCC38 cell line, via reverse transfection with Lipofectamine 2000 (ThermoFisher Scientific, UK), a lipid-based transfection reagent. Non-targeting control and death control siRNA were used to determine transfection efficiency and toxicity. All siRNAs used are listed in **table 2.6**.

SiRNA	Target Gene	Target Sequence	Manufacturer
#1 J-005050-05	WEE1	AAUAGAACAUCUCGACUUA	Dharmacon, USA
#2 J-005050-06	WEE1	AAUAUGAAGUCCCGGUAUA	Dharmacon, USA
#3 J-005050-07	WEE1	GAUCAUAUGCUUAUACAGA	Dharmacon, USA
#4 J-005050-08	WEE1	CGACAGACUCCUCAAGUGA	Dharmacon, USA
AllStars Negative Control siRNA	Non-Targeting	Sequence validated by QIAGEN	QIAGEN, DE
AllStars HS Death Control siRNA	Death Control	Sequence validated by QIAGEN	QIAGEN, DE

**Table 2.6: List of SiRNA oligonucleotides used.**

Lipofectamine 2000 and siRNA were diluted and mixed together in Opti-MEM™ reduced serum medium which contains HEPES, Sodium Bicarbonate (2.4g/L), and L-Glutamine (ThermoFisher Scientific, UK), and incubated for 15 minutes at room temperature to complex. Cells were trypsinised and counted as described in **section 2.2.3** and diluted in IMDM medium. For 96-well SRB assays, 50µl of SiRNA/lipid complex was added per well followed by 110µl of cells in complete IMDM medium per well and incubated at 37°C for 24 hours before treatment with 40µl of IMDM +/- drug treatment. After treatment, cells were grown for an additional 72hrs prior to analysis via SRB assay as shown in **section 2.4**.

To determine the level of WEE1 knockdown achieved by siRNA, western blot analysis was performed alongside SRB cell viability assays. SiRNA/lipid complexes were prepared as shown previously and 500µl of the mixture was added per well of a 6-well plate. 1.1ml of cells were then added to the 6-well plate at the seeding density indicated and incubated in standard growth conditions for 24 hours before the addition of 400µl IMDM medium. Cells were then



incubated for another 24-72 hours in standard growth conditions, depending on the timepoint before cell lysis and analysis via western blot (**Section 2.5**).

## **2.8 Plasmid Preparation**

To validate WEE1 overexpression as a resistance mechanism in resistant cell lines WEE1 expression vectors were transfected into parental cell lines. To carry out these experiments the appropriate stocks of DNA were required. Expression vectors were transformed into *E.coli* and grown overnight prior to extraction and purification.

### **2.8.1 Transformation of plasmid DNA and creation of glycerol stocks**

The WEE1 + Myc tag expressing plasmid pCDNA3Myc-P71 and Myc tag only vector pCDNA3Myc, were a kind gift from Dr Helen Piwinica-Worms (University of Texas, MD Anderson Cancer Centre, Houston, USA; original publication: Rothblum-Oviatt, Ryan and Piwnica-Worms, 2001), which was provided on a piece of filter paper. Spotted plasmid DNA filter paper was placed in a microcentrifuge tube with 200µl of Tris-EDTA buffer (TE; 10mM Tris pH 8.0, 1mM EDTA), vortexed briefly, and allowed to incubate at room temperature for 10 minutes. 5µl of recovered plasmid DNA was used to transform 50µl of Subcloning Efficiency™ DH5α Competent *E. coli* cells (ThermoFisher Scientific, UK) and incubated on ice for 30 minutes. Cells + plasmid DNA were heat shocked in a 42°C water bath for 45 seconds before incubation on ice for 2 minutes. Afterwards, 250µl of S.O.C medium (2% tryptone, 0.5% yeast extract, 10mM NaCl, 2.5mM KCl, 10mM MgCl<sub>2</sub>, 10mM MgSO<sub>4</sub>, and 20mM glucose; ThermoFisher Scientific, UK) was added to *E. coli* DNA mixture and incubated in a shaking incubator at 37°C and 180rpm. Following incubation, transformed *E. coli* was spread on LB agar plates (1% (w/v) bacto-tryptone, 0.5% (w/v) yeast extract, 1% (w/v) NaCl and 1.2% (w/v) agar) containing 100µg/ml Ampicillin and incubated overnight at 37°C. The following day colonies were picked and used to inoculate 10ml of LB broth (1% (w/v) bacto-tryptone, 0.5% (w/v) yeast extract and 1% (w/v) NaCl) + 100µg/ml Ampicillin and incubated at 37°C in a shaking incubator overnight at 180rpm. After overnight culture, glycerol stocks were prepared

by mixing 500µl of transformed *E. coli* from the overnight culture with 500µl of glycerol in a cryovial and stored at -80°C for future use.

### **2.8.2 Extraction of plasmid DNA**

Due to the low yield of plasmid DNA, large volumes of transformed *E. coli* was required to produce sufficient DNA. 5ml LB + 100µg/ml Ampicillin starter cultures were inoculated with a scraping of a glycerol stock (**Section 2.8.1**) and incubated in a shaking incubator at 37°C and 180rpm for 5 hours. After incubation, 250ml of LB broth in a 3L conical flask was inoculated with the 500µl of the starter culture and incubated overnight at 37°C and 180rpm. *E. coli* cells were pelleted by centrifugation at 6,000 x g for 15 minutes at 4°C followed by extraction of plasmid DNA using the EndoFree® Plasmid Maxi Kit (QIAGEN, UK), following the manufacturer's instructions. Plasmid DNA was eluted in a final volume of 200µl of TE buffer and left to dissolve overnight at 4°C. Plasmid DNA concentration was determined using a Nanodrop ND-1000 UV/Vis spectrophotometer (Nanodrop, USA).

## **2.9 Generation of Transient WEE1 Overexpressing Cell Lines**

Transient expression of WEE1 protein was used to confirm successful exogenous expression of WEE1 protein in the HCC38 cell lines. HCC38 cells were plated in a 6-well plate at  $1 \times 10^5$  cells per well and allowed to grow overnight under standard growth conditions, seeding densities were selected to ensure cells were approximately 60-80% confluent prior to transfection. 2 $\mu$ g of pCDNA3Myc (Myc tag only), pCDNA3Myc-P71 (WEE1 gene + Myc tag) and pEGFP\_N1 (GFP expressing plasmid; kindly provided by the Fenton Lab, University of Kent) were mixed with lipofectamine 2000 in ratios of 1:0.5 and 1:1 (Plasmid/Lipo  $\mu$ g/ $\mu$ l) in Opti-MEM™ reduced serum medium to a total volume of 200 $\mu$ l and incubated for 10 minutes at room temperature. Media was removed from HCC38 cells in 6-well plates and replaced with 1.8ml normal IMDM medium without antibiotic. 200 $\mu$ l of plasmid/lipid complexes was added to their respective wells and cells were incubated at standard growth conditions for a following 4 hours before removal of the transfection reagent and replaced with 2ml IMDM medium +1% (v/v) Penicillin Streptomycin solution. Cells were incubated in standard growth conditions for a following 24 hours before lysis and analysis via western blot (**Section 2.5**).

## **2.10 Generation of Stable Cell Lines Expressing Exogenous WEE1**

Stable cell lines were required to validate WEE1 overexpression as a mechanism of resistance to CHK1 inhibition. To this end, HCC38 cells were transfected with a WEE1 expression vector or a control vector that only expressed a Myc tag and stable clones selected using a G418 kill curve.

### **2.10.1 G418 Kill curve**

pCDNA3Myc and pCDNA3Myc-P71 plasmids contain a neomycin resistance gene for selection of stably transfected cells making them resistant to G418 treatment. The optimal concentration for selection of stably transfected cells was determined. An optimal concentration of G418 kills all non-resistant cells between 5-7 days. HCC38 cells were plated

at  $1 \times 10^5$  cells per well and grown overnight under standard growth conditions, seeding densities were selected to ensure cells were approximately 60-80% confluent prior to treatment with Geneticin (G418). The following day, media was removed and replaced with IMDM + G418 at a range of concentrations (between 0.25-1.5mg/ml) or just IMDM media as a control. Cells were then incubated at standard growth conditions for a week and IMDM +/- G418 was refreshed every 2 days or when media showed signs of depletion. 1mg/ml was selected as an optimal concentration of G418 for selection of stable cells.

### **2.10.2 Transfection of stable cell lines expressing exogenous WEE1**

HCC38 cells were plated in a T25 flasks at  $2.6 \times 10^5$  cells per flask and allowed to grow overnight under standard growth conditions, seeding densities were selected to ensure cells were approximately 60-80% confluent prior to transfection. 6.5µg of pCDNA3Myc (Myc tag only) and pCDNA3Myc-P71 (WEE1 gene + Myc tag) was mixed with lipofectamine 2000 in a 1:1 ratio (Plasmid/Lipo µg/µl) in Opti-MEM™ reduced serum medium to a total volume of 650µl and incubated at room temperature for 10 minutes. IMDM media was replaced with 4.4ml of IMDM medium without antibiotic and 600µl of plasmid/lipo mixture was added to cells. Cells were then incubated at standard growth conditions for 4 hours before removal of IMDM + transfection reagent and replacement with IMDM medium without antibiotic before further incubation overnight at standard growth conditions. The following day cells showed high levels of cell death in both pCDNA3Myc and pCDNA3Myc-P71 transfected cells and were incubated for a further 96 hours in standard growth conditions. Following the extended incubation, transfected cells were trypsinised and counted as seen in **section 2.2.3** and plated into 6-well plates at a density of  $1 \times 10^5$  cells per well in a total of 2ml IMDM media +1% (v/v) Penicillin Streptomycin solution and incubated overnight in standard growth conditions. The following day media was refreshed in each well with 2ml IMDM + 1mg/ml G418 for selection of stable expressing cells.

## 2.11 RNA Sequencing

To investigate acquired resistance via an unbiased approach RNA was extracted from HCC38, HPrxR, and H737R cell lines and sequenced by UCL Genomics. Following initial analysis carried out by UCL Genomics expression data was investigated to identify genes or pathways which may play a role in resistance.

### 2.11.1 RNA extraction

HCC38, H737R and HPrxR cell lines were plated in T25 flasks at  $2.6 \times 10^5$  cells per flask and allowed to grow for 24 hours in standard growth conditions, three biological replicates were plated for each sample on different days. After 24 hours cells were approximately at 60-70% confluency and trypsinised before suspension in 5ml IMDM medium and pelleted via centrifugation at  $270 \times g$  for five minutes. After centrifugation, IMDM was removed and pellet was washed with 2ml PBS and spun again at  $270 \times g$  for a further 5 minutes. Afterwards, PBS was removed, and the cell pellets were snap frozen in dry ice and stored at  $-80^\circ\text{C}$  until RNA extraction.

Extraction of RNA was carried out using the Monarch<sup>®</sup> Total RNA Miniprep kit (New England Biolabs<sup>®</sup>, UK) following the manufacturer's instructions. RNA was eluted in 60 $\mu$ l of Nuclease-free water and sample concentration was determined using a Nanodrop ND-1000 UV/Vis spectrophotometer (Nanodrop, USA). Samples were stored at  $-80^\circ\text{C}$  before shipping on dry ice to UCL Genomics () who carried out the CDNA synthesis, RNA sequencing and subsequent differential expression analysis, reports generated by UCL Genomics can be found in **appendix 6.1 & 6.2**.

# **Chapter 3**

## **Generation of CHK1 inhibitor Resistant Cell Lines**

# 3. Generation of CHK1 Inhibitor Resistant Cell Lines

## 3.1 Introduction

Resistant cell line models can be used to study cancer drug resistance *in vitro*. Resistance to cancer therapies is a major obstacle in the successful treatment of patients. Resistance can be innately present in the tumour or acquired over time by a drug sensitive tumour with successive treatments. Acquired resistance can result from mutations or deliberate adaptive responses which may allow cells to compensate for, or recover from, the effects of a cancer drug (Longley and Johnston, 2005). As tumours are known to be highly heterogeneous, drug resistance may arise via selection of resistant sub-populations within drug treated tumours (Swanton, 2012).

The study of tumour samples taken from patients with drug resistant disease provides the most clinically relevant data. Unfortunately, these patient samples are often difficult to acquire and do not allow for proactive research as scientists must wait for resistance to form in patients (Garraway and Jänne, 2012). Therefore, *in vitro* and *in vivo* models have been developed using both established cancer cell lines and human tumour xenografts in mice. While these models are less clinically relevant, they still provide useful data to help inform new therapeutic strategies and identify resistance mechanisms which are later shown to be present in the clinic. Cell line models are the cheapest and easiest approach but are less clinically relevant versus human tumour xenografts grown *in vivo* that can reproduce the tumour microenvironment, stromal cells and match the cancer type with the organ of origin. Despite the limitations inherent in cell line models, there are many ways to develop models of cancer drug resistance.

A common and successful approach in the generation of resistant cell lines is the culture of cancer cells in the presence of a drug over a period of time (Garraway and Jänne, 2012). Generation of resistance can take from 3-18 months in the laboratory and changes can be made to the methodology depending on the desired outcome. Cells cultured with a pulsed treatment strategy allowing for recovery in drug free media and generally lower drug concentrations are used to create low levels of resistance that aim to mimic patient conditions. These tend to have lower fold-resistance compared to models adapted to higher drug concentrations and resistance may be lost after a period in no drug. Adaptations tend to be subtler making them potentially more difficult to identify. However, these models are more clinically relevant (McDermott *et al.*, 2014). High-level drug resistant models are cells exposed to very high doses or escalating doses of drug in concentrations unlikely to be achievable in a patient tumour. While these models are less clinically relevant, they are helpful in identifying potential resistance mechanisms. These high-level models are often more stably resistant making them easier to maintain in culture while exhibiting a generally higher level of resistance. As a result molecular changes in these cell lines become more pronounced and may be easier to identify than more clinically relevant models (McDermott *et al.*, 2014).

A phase 1 clinical trial of the WEE1 inhibitor Adavosertib was used to inform development of a resistant cell line model through low concentration dose escalation with clinically relevant drug concentrations (Leijen, Van Geel, Pavlick, *et al.*, 2016; Garcia *et al.*, 2020). WEE1 is an important kinase, which like CHK1 is involved in regulation of CDK1 activity. It was shown that increased HDAC activity in the Adavosertib resistant leukaemia cell lines led to an increase in c-MYC expression and activity, the authors suggested this may increase the levels of nucleotides available for DNA replication thus reducing replication stress and promoting survival in the presence of drug (Garcia *et al.*, 2020). Another study in gastric cancer cell lines reported resistance to the drug cisplatin acquired via dose escalation. In this case the protein JWA, which blocks the activity of casein kinase (CK2), was shown to be down regulated in cisplatin resistant cells allowing for CK2 to phosphorylate XRCC1, stabilising the protein and



allowing it to carry out its DNA repair function. This highlighted CK2 and JWA as potentially useful drug targets and JWA expression as a possible resistance biomarker (Xu *et al.*, 2014).

Biomarkers and resistance mechanisms can also be investigated through high-throughput screening of cancer cell lines using either drug panels or knockdown/overexpression technologies to modulate the activity of target genes (Garraway and Jänne, 2012). RNA interference (RNAi) technology such as short hairpin RNA (shRNA) or small interfering RNA (siRNA) have been used in many studies to target genes of interest and silence their expression. While transfection of cDNA in the appropriate vector can result in transient or permanent overexpression of a selected gene. (Garraway and Jänne, 2012). These studies can be used to identify genes that may confer resistance or sensitivity to a drug of interest. A study investigating cisplatin resistance in the KB-3-1 cisplatin-resistant human carcinoma cell line used shRNA targeting a range of different genes followed by sublethal doses of cisplatin. This study showed that the MAST1 kinase replaced c-RAF mediated activation of the MAPK pathway allowing for cisplatin resistance and cell proliferation (Jin *et al.*, 2018). Lestaurtinib, an inhibitor of MAST1 was found to sensitise resistant cells to cisplatin treatment in addition to synergistically attenuating cancer cell proliferation. This was also seen in patient-derived xenograft models (Jin *et al.*, 2018).

Another approach has been to use large panels of existing cancer cell lines with known gene expression, DNA mutational profile and drug response data. These data can then be analysed to identify genes expression profiles or mutations associated with resistance or sensitivity to certain drug treatments. The US National Cancer Institute (NCI) collection sixty of cancer cell lines (NCI-60) derived from multiple tissue types, was used to identify Schlafen 11 (SLFN11), as the unanticipated genomic determinant of response to topoisomerase (Top) 1 inhibitors, Top 2 inhibitors, alkylating agents and DNA synthesis inhibitors (Zeeberg *et al.*, 2012; Sousa *et al.*, 2015; Zoppoli *et al.*, 2012; Nogales *et al.*, 2016). SLFN11 had previously been identified as a biomarker for Top 1 inhibitors in the Cancer Cell Line Encyclopaedia (CCLE) (Barretina *et al.*, 2012). In a later study SLFN11 was implicated in PARP inhibitor response, as loss of

SLFN11 allowed continued DNA replication through to G2, whereas expression of SLFN11 resulted in prolonged S-phase arrest and cell death. Cells with loss of SLFN11 were also shown to rely on activity of the DNA damage response kinase ATR, to maintain checkpoint integrity at G2 and therefore inhibition of ATR in combination with PARP inhibition was shown to reverse resistance to PARP inhibitors in cell lines lacking SLFN11 expression (Murai *et al.*, 2016). Thus, there are many approaches that can be used to identify mechanisms and biomarkers of acquired drug resistance.

CHK1 inhibitors are of substantial interest in oncology. This is due to their ability to potentiate the effect of DNA damaging chemotherapeutics and evidence of their efficacy as single agents in certain genomically unstable cancers. This is exemplified by their synthetic lethality with cancers expressing dysfunctional p53 (Wang *et al.*, 1996; Levesque *et al.*, 2005; Gurpinar and Vousden, 2015). Triple Negative Breast Cancers (TNBC) are a subgroup of breast cancer that exhibit a high rate of mutations in the *TP53* gene and therefore are potential candidates for CHK1 inhibitor therapy (Ma *et al.*, 2012). TNBC does not express oestrogen receptor (ER), progesterone receptor (PGR) or human epidermal growth factor 2 receptor (HER2) proteins, limiting treatment options to chemotherapy, as existing targeted therapies for these receptors are ineffective in this breast cancer type. Unfortunately, tumour drug resistance and subsequent patient relapse is often an inevitable outcome following treatment with chemotherapeutics and targeted inhibitors. This highlights the importance in understanding resistance to Chk1 inhibitors before they enter the clinic.

The aim of this chapter was to generate TNBC cell line models with acquired resistance to the CHK1 inhibitors SRA737 and Prexasertib and investigate changes in drug response to a panel of cancer drugs and targeted inhibitors. Differences in signalling of targets within the DNA damage response and cell cycle regulatory pathways were also investigated by western blotting, as these may identify potential resistance mechanisms and biomarkers of resistance.

## **Chapter aims and objectives**

- Generate models of acquired resistance in HCC38 and MDA-MB-468 cell lines via a dose escalation method to SRA737 and Prexasertib.
- Characterise parental and resistant cell lines.
  - Changes in cell doubling time.
  - Determine stability of drug resistance.
- Identify potential resistance mechanisms.
  - Cross-resistance profiling of parental and resistant cell lines with a range of targeted inhibitors and chemotherapeutic agents.
  - Investigate basal protein expression and cell signalling of CHK1 and related proteins in parental and resistant cell lines.

## 3.2 Results

### 3.2.1 Growth Characterisation of TNBC cell lines MDA-MB-468 and HCC38

Treatment of p53 defective cancers with a CHK1 inhibitor have demonstrated synthetic lethality (Gurpinar and Vousden, 2015). TNBC is highly associated with mutations in *TP53* and so is an ideal candidate for treatment with a CHK1 inhibitor (Turner *et al.*, 2013). TNBC cell lines HCC38 and MDA-MB-468 both harbour a substitution missense mutations in the *TP53* gene (**Table 3.1**) at amino acid residue 273 in the DNA binding domain of p53, leading to its disfunction (Olivier, Hollstein and Hainaut, 2010). Therefore HCC38 and MDA-MB-468 cell lines were selected for the development of models of acquired resistance to CHK1 inhibition (Chavez, Garimella and Lipkowitz, 2010).

	Site of Origin	Pathology	Grade	Molecular Classification	<i>TP53</i> status	AA Muatation	Type	<i>BRCA1</i> status
HCC38	Primary Tumour	IDC	3	Basal B	Mutated	p.R273L	Subsitution - Missense	Wild Type
MDA-MB-468	Plerual Effusion	AC	NA	Basal A	Mutated	p.R273H	Subsitution - Missense	Wild Type

**Table 3.1: TNBC mutational background for HCC38 and MDA-MB-468 cell lines.** Cell lines were selected for the mutational status of *TP53*, a common mutation in TNBC (Chavez, Garimella and Lipkowitz, 2010). AC: Adenocarcinoma IDC: Infiltrating ductal carcinoma.

Seeding density assays were conducted to determine growth characteristics and optimal growth conditions for HCC38 and MDA-MB-468 human TNBC cell lines. Cells were plated at multiple densities in seven 96-well plates and then one plate was fixed per cell line every 24 hours over 7 days and analysed via SRB assay. Growth curves generated were used to determine the doubling time of each cell line. MDA-MB-468 cell lines have a considerably shorter doubling time than HCC38 cells, doubling every 27 hours and 47 hours respectively. Seeding densities were selected to ensure cells were in log phase growth over the 96-hour period indicated (**Figure 3.1**). This ensures constant cell growth during the drug incubation period of dose response assays. Initially a seeding density of 6400 cells/well was selected for HCC38 parental and resistant cell lines, later experiments in the project reduced these seeding

densities to 3200 cells/well and then 1600 cells/well as it was noted that media began to deplete before the end of the 96-hour drug incubation time. While a slight reduction in  $GI_{50}$  across HCC38 parental and resistant cell lines was seen the effect did not drastically alter the results, seeding densities used for each experiment can be found in the figure legends. MDA-MB-468 cell lines were plated at 3200 cells/well consistently throughout the study.

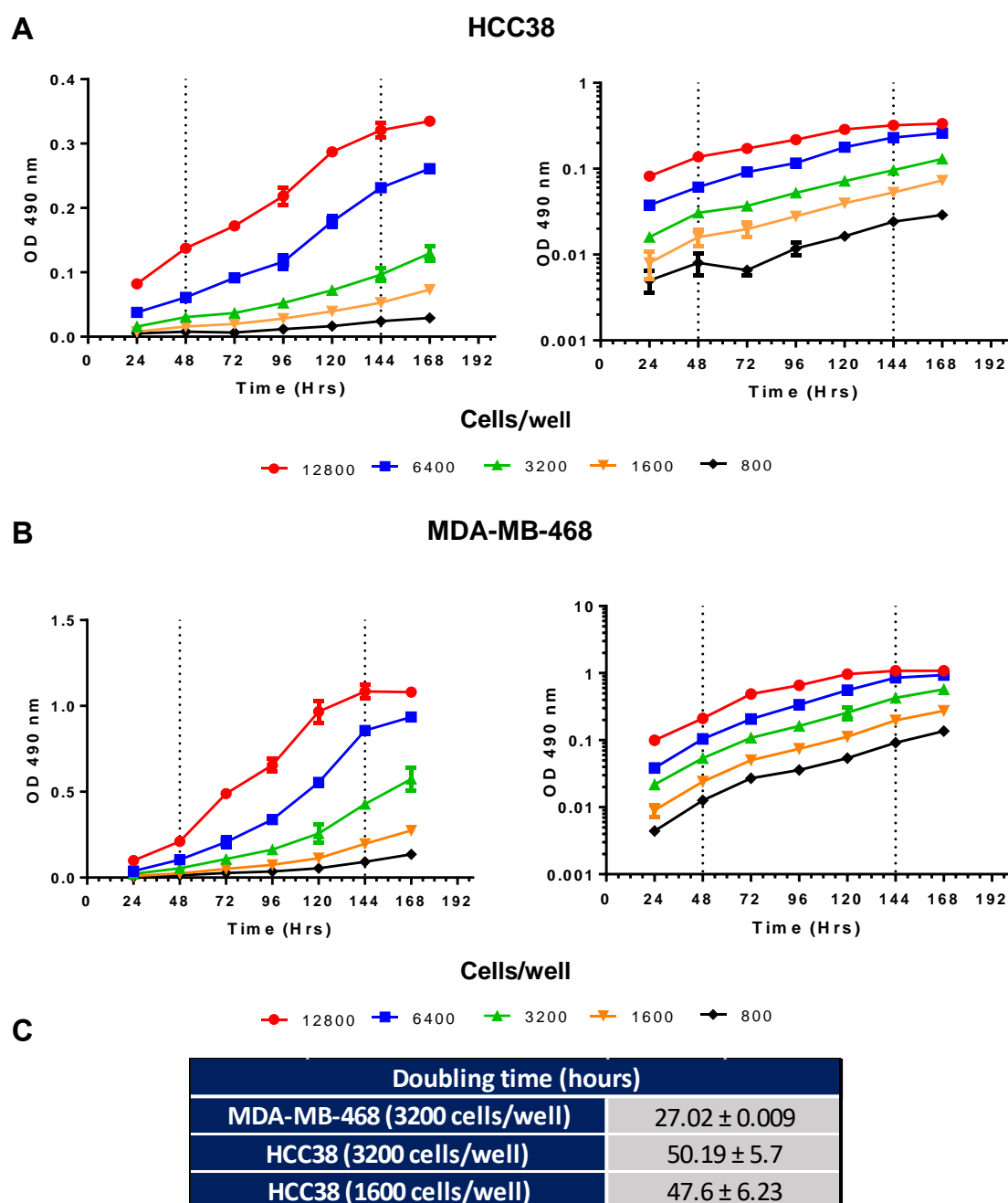


**Figure 3.1: Characterisation of MDA-MB-468 and HCC38 cell line growth in 96-well plates.** Cells were plated at the densities indicated above in 96-well plates. One plate was fixed every 24 hours and analysed via SRB assay. Dotted lines indicate the 96-hour period of drug exposure for cells in a standard SRB cytotoxicity assay. Growth curves were generated using GraphPad Prism 6. **A)** HCC38 cell-line. **B)** MDA-MB-468 cell-line. **C)** Average doubling time +/- the standard deviation was calculated using data from  $n \geq 2$  independent experiments. Linear and log scales on the Y-axis in left and right graphs respectively.

### 3.2.2 Response of MDA-MB-468 and HCC38 cell lines to CHK1 inhibitors SRA737 and Prexasertib

The dose response of HCC38 and MDA-MB-468 TNBC cell lines to the CHK1 inhibitors SRA737 and Prexasertib was investigated. Cells were plated in 96-well plates at the densities indicated and allowed to grow for 48 hours before addition of either Prexasertib or SRA737 for 96-hours. Cells were fixed at 144 hours and analysed via SRB assay. Dose response curves were plotted and the  $GI_{50}$  value for each drug per cell line was determined by non-linear regression.

**Figure 3.2** shows that the  $GI_{50}$  values for SRA737 and Prexasertib in the HCC38 cell line were 0.28 $\mu$ M and 4.3nM, respectively. The MDA-MB-468 cell lines were more resistant to both drugs with  $GI_{50}$  values of 16.99 $\mu$ M for SRA737 and 0.15 $\mu$ M for Prexasertib. Interestingly both cell lines show greater sensitivity to Prexasertib, which is a dual inhibitor of CHK1 and CHK2 (King, H Bruce Diaz, *et al.*, 2015) compared to SRA737 which selectively inhibits CHK1 (Walton *et al.*, 2016a). In contrast, the high  $GI_{50}$  value of 16.99 $\mu$ M for SRA737 in the MDA-MB-468 cell line suggests it may be intrinsically resistant to this CHK1 selective drug.

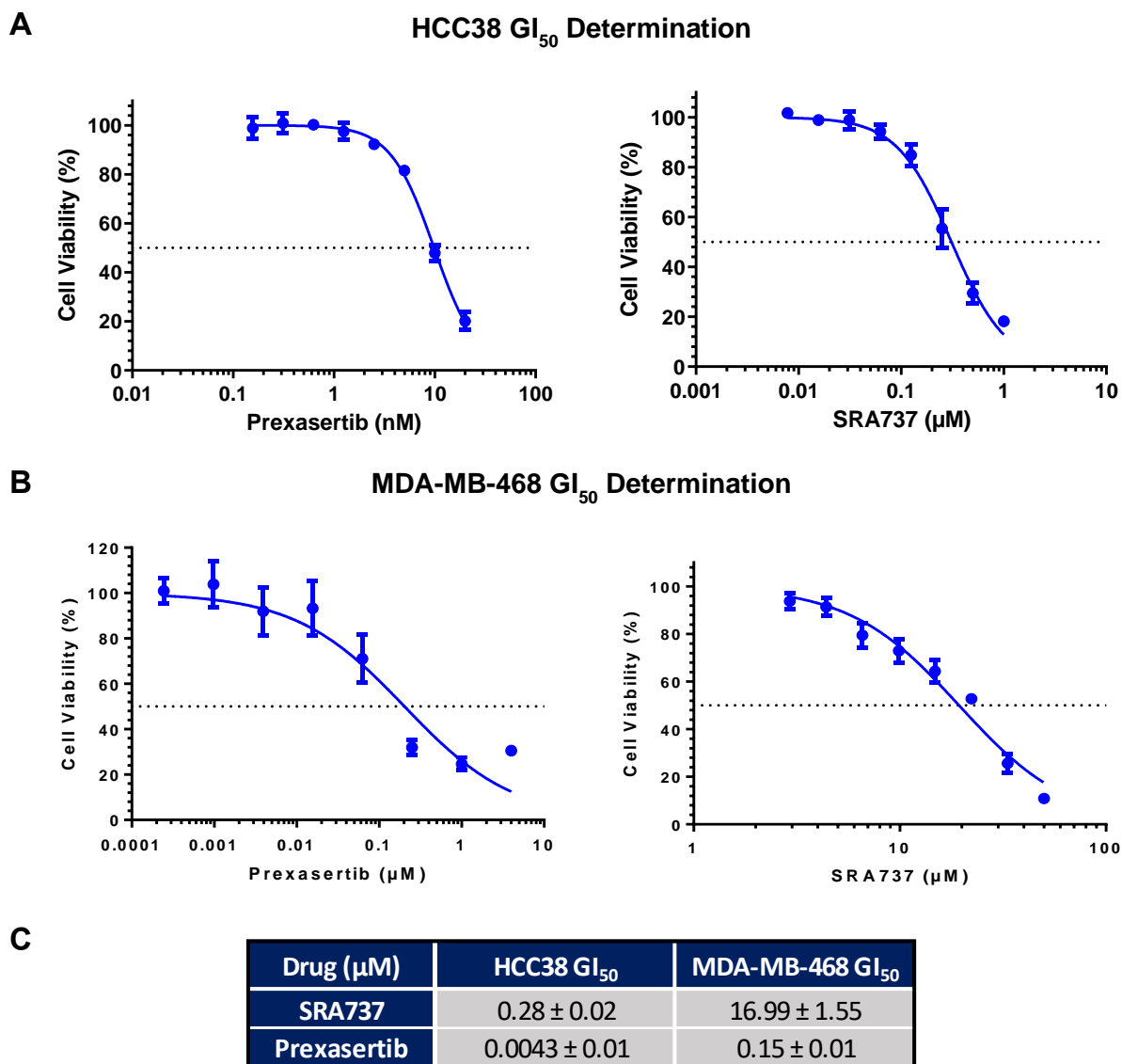


**Figure 3.2: Dose-response curves for CHK1 inhibitors Prexasertib and SRA737 in MDA-MB-468 and HCC38 cell lines.** HCC38 cells were plated at 6400 cells/well and MDA-MB-468 cell lines were plated at 3200 cells/well in a 96-well plate and grown for 48 hours before treatment with a serial dilution of Prexasertib or SRA737 for 96 hours. **A)** MDA-MB-468 and **B)** HCC38 Dose response curves generated using GraphPad Prism 6 and fitted using non-linear regression. Dotted line marks the GI<sub>50</sub> of Prexasertib or SRA737. Data points represent the mean ± SD from one representative experiment. **C)** Table summarises the mean ± SD GI<sub>50</sub> of MDA-MB-468 and HCC38 cell lines treated with Prexasertib and SRA737 of at least n= 3 independent experiments.

### 3.2.3 Generation of resistant cell lines by dose escalation

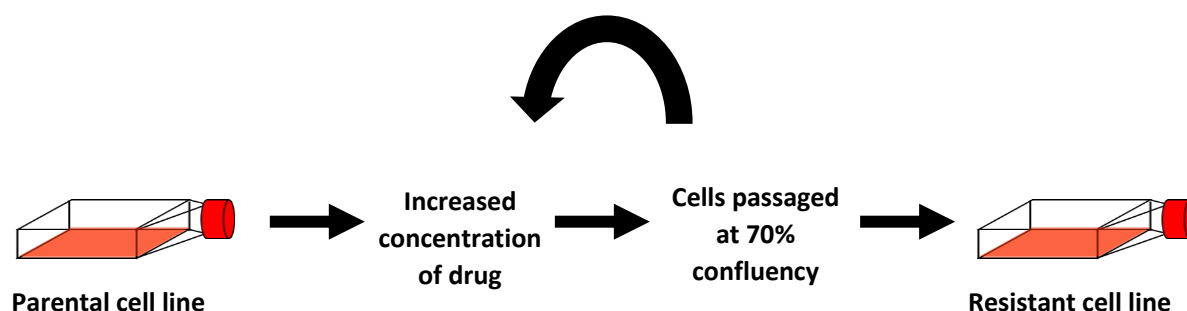


**Figure 3.3: Diagram of resistance generation by dose escalation in T25 flasks.**

HCC38 and MDA-MB-468 cell lines with acquired resistance to either SRA737 or Prexasertib were generated by dose escalation in T25 flasks (**Figure 3.3**). Preliminary  $GI_{50}$  data from the Garrett lab was used to inform the starting concentrations of Prexasertib and SRA737 for dose escalation before the actual  $GI_{50}$  data (**Figure 3.2**) could be produced. Cells were passaged into T25 flasks and allowed to adhere overnight. The following day SRA737 or Prexasertib was added to cells at the concentrations indicated (**Figure 3.4**). Cells were passaged and transferred to new flasks and left to adhere overnight before doubling the concentration of drug. This process was repeated for approximately 140 days until cells could either no longer survive in higher concentrations of drug or showed a  $GI_{50}$  at least 5x that of the parental cell line.

**Figure 3.4** shows how the drug concentration was increased over time. During the first 1-100 days both SRA737 & Prexasertib treated HCC38 and the Prexasertib treated MDA-MB-468 cell lines struggled to survive in concentrations higher than the  $GI_{50}$  of their respective drug. Eventually these cell lines adapted and continued to proliferate in higher drug concentrations. MDA-MB-468 treated with SRA737 initially grew well in the starting drug concentration but were unable to survive concentrations higher than the  $GI_{50}$ . This is likely due to the preliminary  $GI_{50}$  data used to start the dose escalation process being artificially low compared to the actual  $GI_{50}$ . In addition, the inability for cells to survive in doses much higher than the  $GI_{50}$  of 16.99 $\mu$ M



supports the suggestion that the MDA-MB-468 cell line may be intrinsically resistant to SRA737 inhibition. Once resistance was generated, new resistant cell lines were named H737R, HPrexR, MDA-737R and MDA-PrexR (H; HCC38, MDA; MDA-MB-468) with respect to the drugs used in their dose escalation SRA737 and Prexasertib.

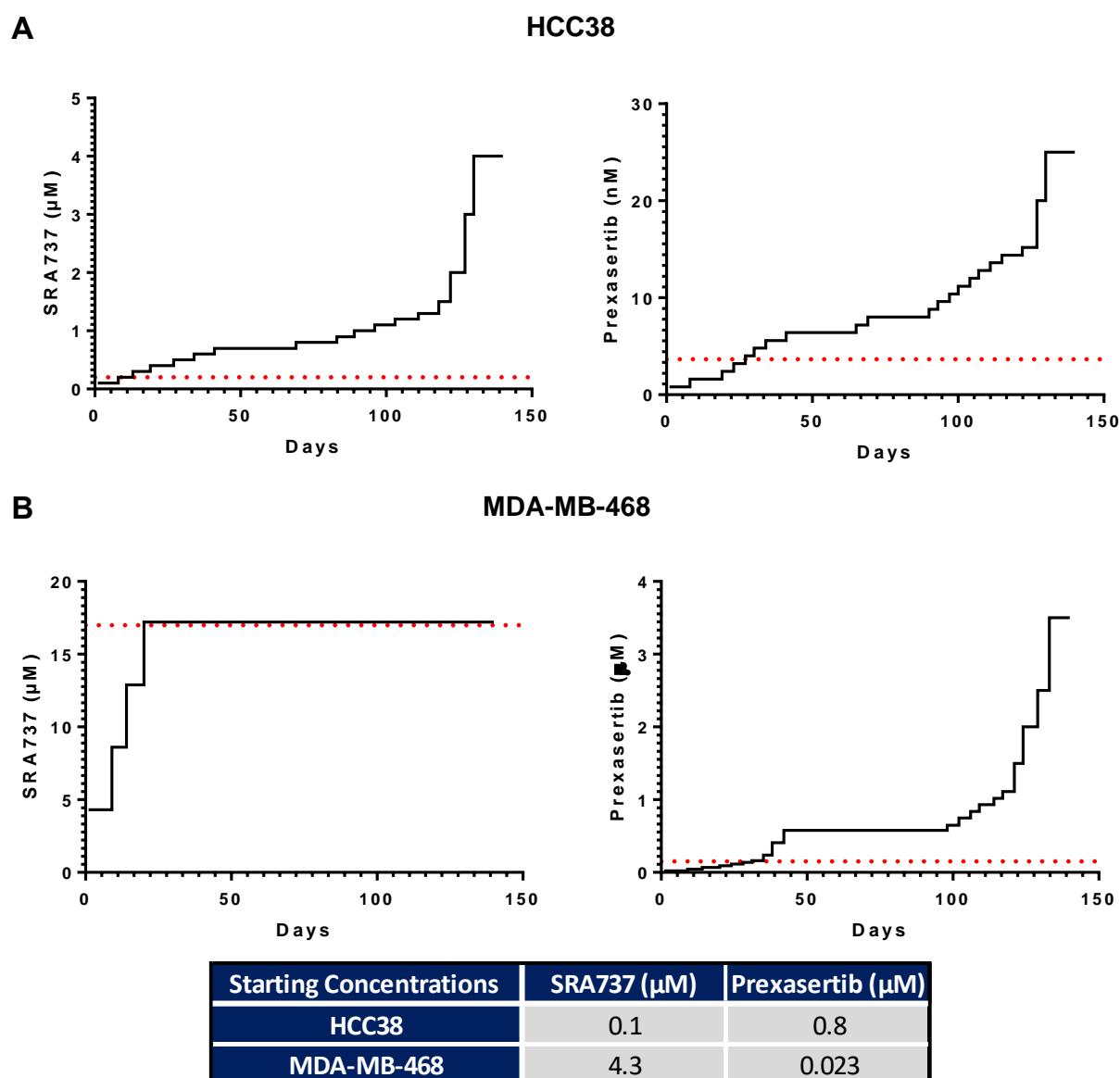


**Figure 3.4: Developing resistance in cell lines HCC38 and MDA-MB-468 to CHK1 inhibitors SRA737 and Prexasertib.** Graphs demonstrating the increases in inhibitor concentration during the generation of resistant cell lines for **A)** HCC38 and **B)** MDA-MB-468 cells. Red dotted line represents the  $GI_{50}$  of the parental cell line to the respective drug. **C)** Table showing starting concentrations used for dose escalation.

### 3.2.4 Determination of growth characteristics of resistant cell lines

After resistant cell lines were generated, the growth characteristics were investigated to determine whether any changes had occurred. At 1600 cells/well HCC38, H737R and HPrexR cell lines showed doubling times of approximately 43.2, 31.3 and 35.2 hours respectively (**Figure 3.5**). At 3200 cells/well MDA-MB-468, MDA-737R and MDA-PrexR cell lines showed doubling times of approximately 27, 30.6 and 29.9 hours respectively (**Figure 3.6**). In HCC38 parental and resistant cell lines doubling times were longer at 3200 cells/well versus 1600 cells/well this is likely due to cells approaching high confluency/depleting media at later stages of the assay, showing seeding densities greater than 1600 cells/well were likely not optimal.

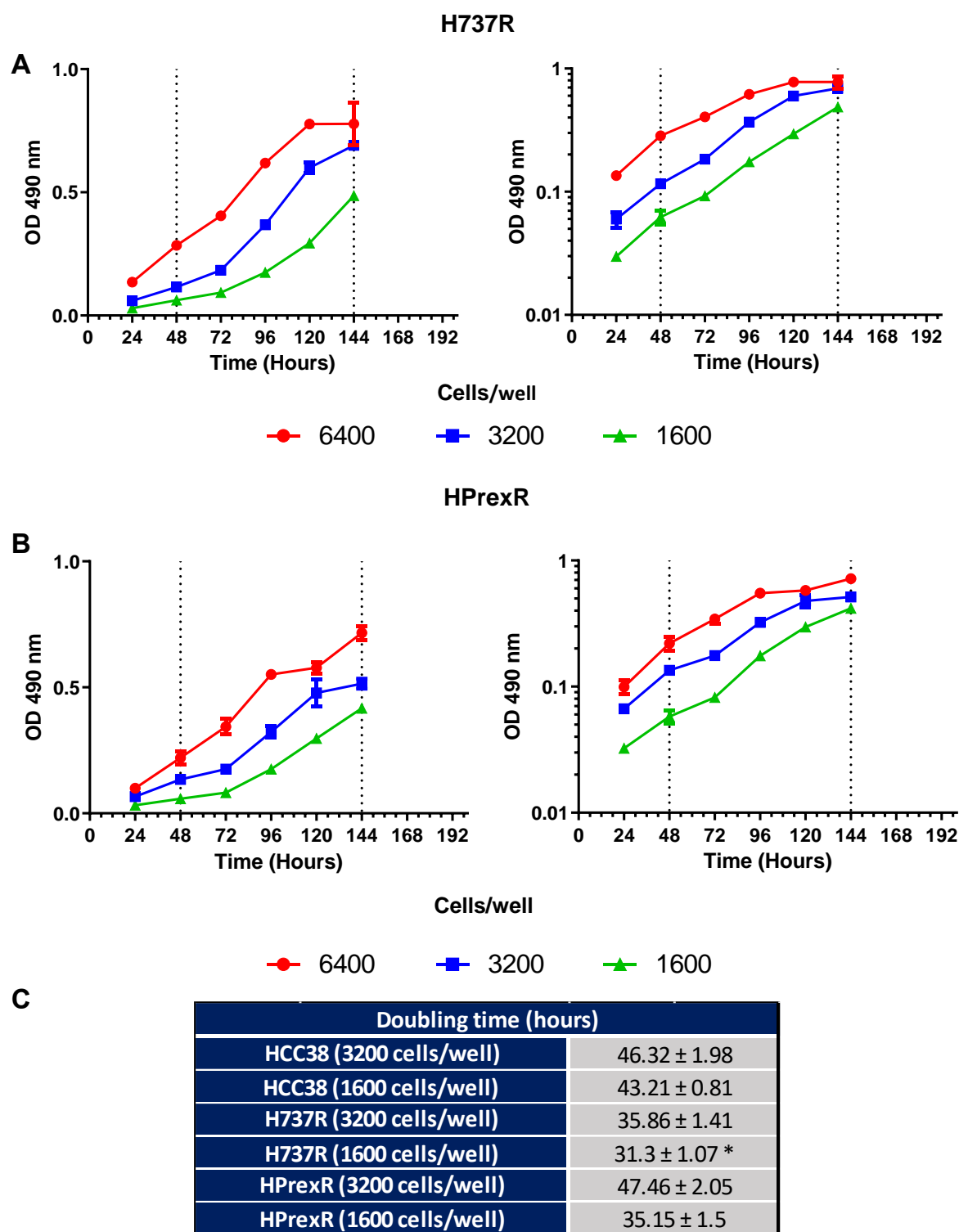


**Figure 3.5: Characterisation of H737R and HPrexR cell line growth in 96-well plates.** Cells were plated at the densities indicated above in 96-well plates. One plate was fixed every 24 hours and analysed via SRB assay. Dotted lines indicate the 96-hour period of drug exposure for cells in a standard SRB cytotoxicity assay. Growth curves were generated using GraphPad Prism 6. **A)** H737R cell-line. **B)** HPrexR cell-line. **C)** Average doubling time +/- the standard deviation was calculated using data from n=2 independent experiments. Statistical significance was calculated using a student's t-test, \* =  $p \leq 0.05$ . Linear and log scales on the Y-axis in left and right graphs respectively.

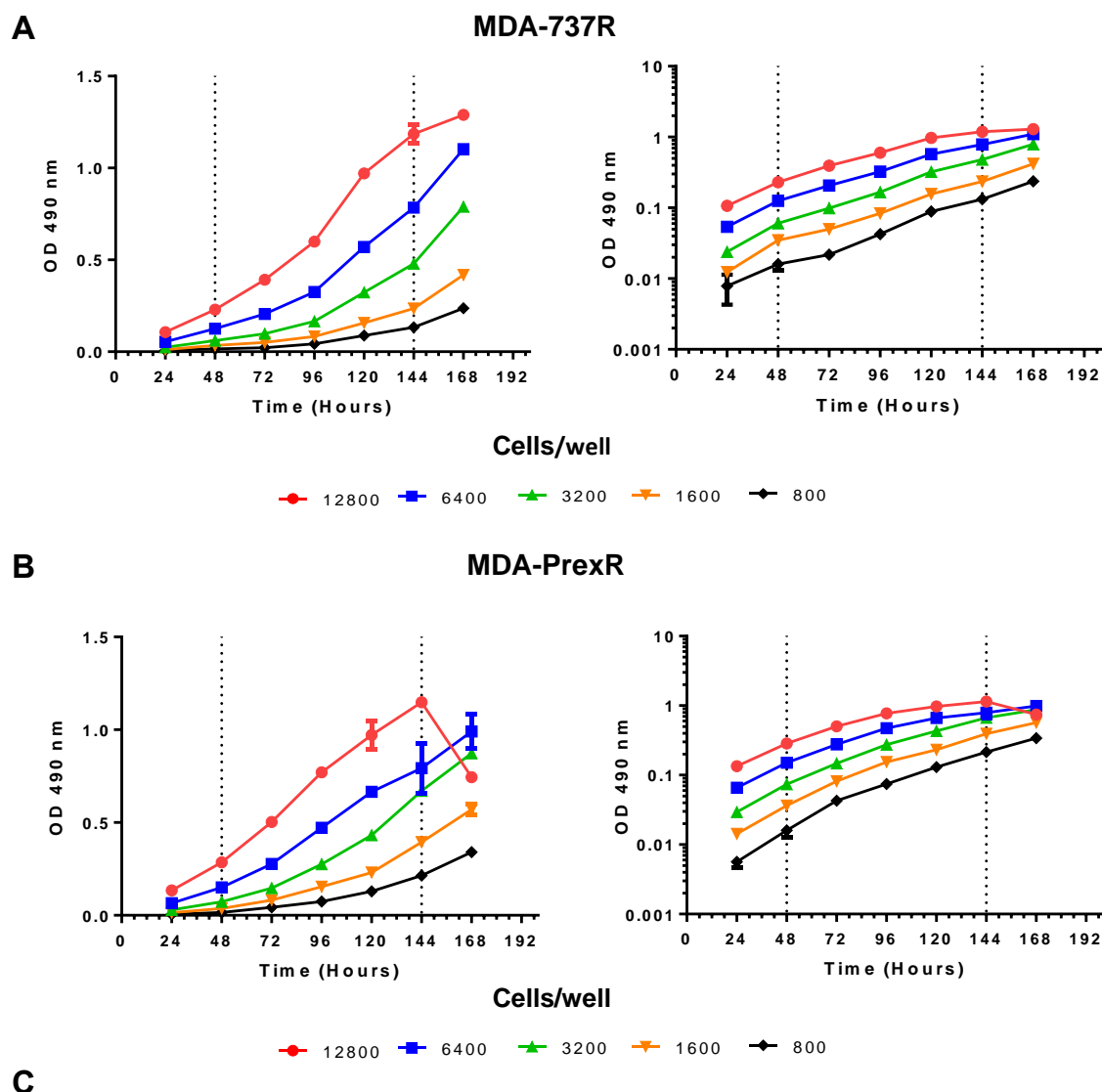


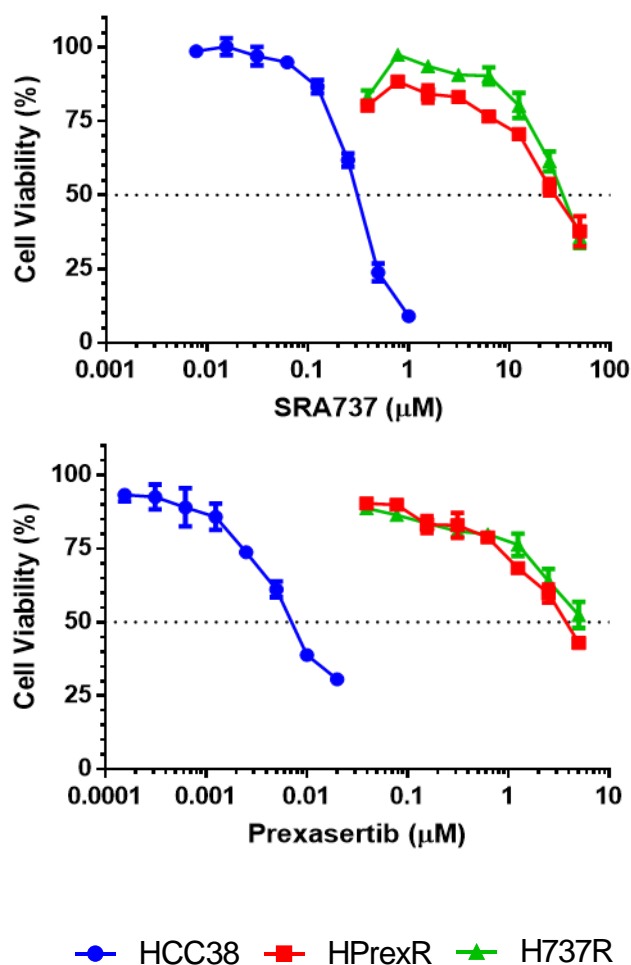
**Figure 3.6: Characterisation of MDA-737R and MDA-PrexR cell line growth in 96-well plates.** Cells were plated at the densities indicated above in 96-well plates. One plate was fixed every 24 hours and analysed via SRB assay. Dotted lines indicate the 96-hour period of drug exposure for cells in a standard SRB cytotoxicity assay. Growth curves were generated using GraphPad Prism 6. **A)** MDA-737R cell-line. **B)** MDA-PrexR cell-line. **C)** Average doubling time +/- the standard deviation was calculated using data from n=2 independent experiments. Statistical significance was calculated using a student's t-test, \* =  $p \leq 0.05$ . Linear and log scales on the Y-axis in left and right graphs respectively.

### 3.2.5 Response of CHK1 inhibitor resistant cell lines to SRA737 and Prexasertib

Resistant and parental cell lines were plated at the seeding densities indicated and treated with a titration of either SRA737 or Prexasertib after 48 hours of growth. Cells were left to grow in drug after 96 hours and analysed via SRB assay. H737R and HPrexR are highly resistant to both SRA737 (121-fold and 133-fold respectively) and Prexasertib (>1250-fold for both H737R and HPrexR) (**Figure 3.7**). Interestingly, MDA-737R which was adapted to SRA737 and failed to survive in drug concentrations higher than the  $GI_{50}$  (**Figure 3.4**), showed limited resistance to SRA737 (1.5-fold) but shows high resistance to Prexasertib (>33-fold) (**Figure 3.8**). This is also true for the MDA-PrexR cell line which shows high resistance to Prexasertib (>33-fold) but limited resistance to SRA737 (1.5-fold) (**Figure 3.8**). In addition, MDA-PrexR and MDA-737R show different dose response curves to Prexasertib but both respond similarly to SRA737, with MDA-737R showing less resistance to Prexasertib than MDA-PrexR (**Figure 3.8 A**). Unfortunately, it was not possible to accurately determine  $GI_{50}$  values for resistant cell lines to Prexasertib as viability barely dropped below 50% at the highest concentration of drug. Despite inaccurate  $GI_{50}$  values it was clear that all drug adapted cell lines were resistant to Prexasertib.

A

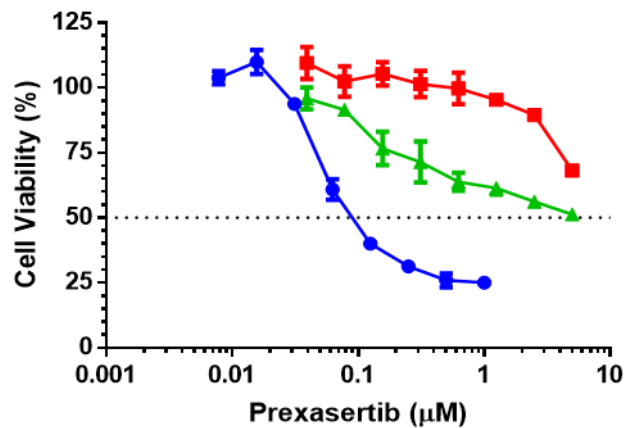
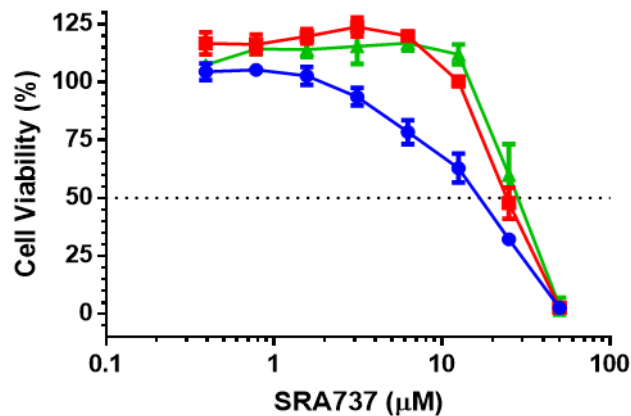
HCC38



B

HCC38		Parental	H737R		HPrexR	
		$\text{GI}_{50} \pm \text{SD}$	$\text{GI}_{50} \pm \text{SD}$	RF	$\text{GI}_{50} \pm \text{SD}$	RF
SRA737 ( $\mu\text{M}$ )	CHK1	$0.28 \pm 0.02$ (n=4)	$33.84 \pm 5.61$ (n=3) *	121.0	$37.32 \pm 3.32$ (n=3) **	133.0
Prexasertib ( $\mu\text{M}$ )	CHK1/CHK2	$0.0043 \pm 0.01$ (n=6)	$>5$ (n=4) **	1250	$>5$ (n=4) **	1250

**Figure 3.7: Determination of  $\text{GI}_{50}$  values for HCC38 parental, H737R and HPrexR cell lines to SRA737 and Prexasertib.** Cells were plated at 6400 cells/well in a 96-well plate and grown for 48 hours before treatment with a serial dilution of Prexasertib or SRA737 for 96 hours. **A)** HCC38 dose response curves generated using GraphPad Prism 6 and fitted using non-linear regression. Dotted line marks the  $\text{GI}_{50}$  of Prexasertib or SRA737. Data points represent the mean  $\pm$  SD from one representative experiment. **B)** Table summarises the mean  $\pm$  SD of all experiments conducted. Statistical significance was calculated using a student's t-test, \* =  $p \leq 0.05$ , \*\* =  $p \leq 0.01$ . (n) indicates the number of independent experiments.

**A****MDA-MB-468**

● MDA-MB-468    ■ MDA-PrexR    ▲ MDA-737R

**B**

MDA-MB-468		Parental	MDA-737R		MDA-PrexR	
		GI <sub>50</sub> ± SD	GI <sub>50</sub> ± SD	RF	GI <sub>50</sub> ± SD	RF
SRA737 (μM)	CHK1	16.99 ± 1.55 (n=4)	25.98 ± 0.36 (n=4) **	1.5	24.93 ± 0.15 (n=4) **	1.5
Prexasertib (μM)	CHK1/CHK2	0.15 ± 0.01 (n=4)	>5 (n=3) ***	>33	>5 (n=3) ***	>33

**Figure 3.8: Determination of GI<sub>50</sub> values for MDA-MB-468 parental, MDA-737R and MDA-PrexR cell lines to SRA737 and Prexasertib.** Cells were plated at 3200 cells/well in a 96-well plate and grown for 48 hours before treatment with a serial dilution of Prexasertib or SRA737 for 96 hours. **A)** MDA-MB-468 dose response curves generated using GraphPad Prism 6 and fitted using non-linear regression. Dotted line marks the GI<sub>50</sub> of Prexasertib or SRA737. Data points represent the mean ± SD from one representative experiment. **B)** Table summarises the mean ± SD of all experiments conducted. Statistical significance was calculated using a student's t-test, \*\* =  $p \leq 0.01$ , \*\*\* =  $p \leq 0.001$ . (n) indicates the number of independent experiments.

### 3.2.6 Light microscopy of MDA-MB-468 and HCC38 parental and resistant cell lines

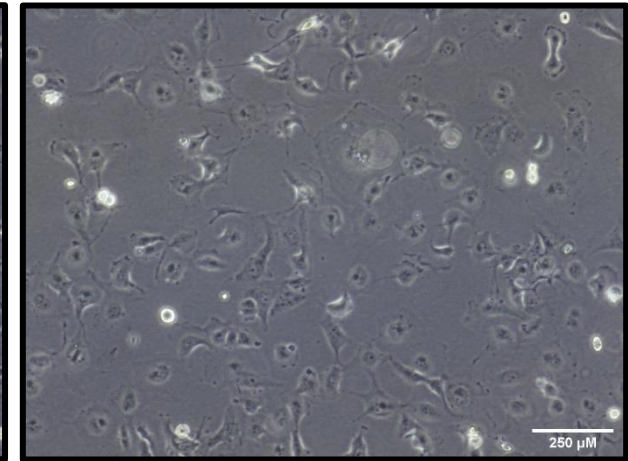
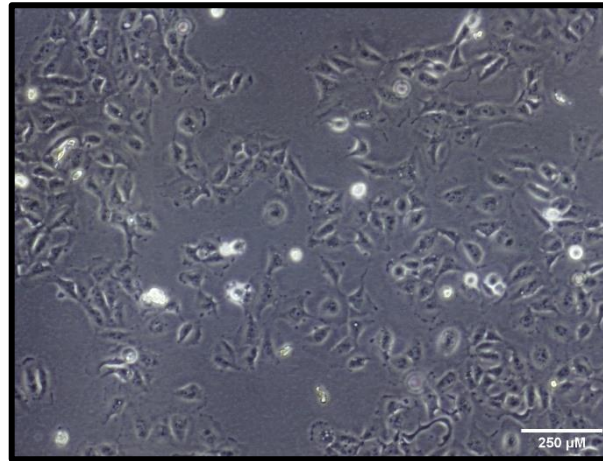
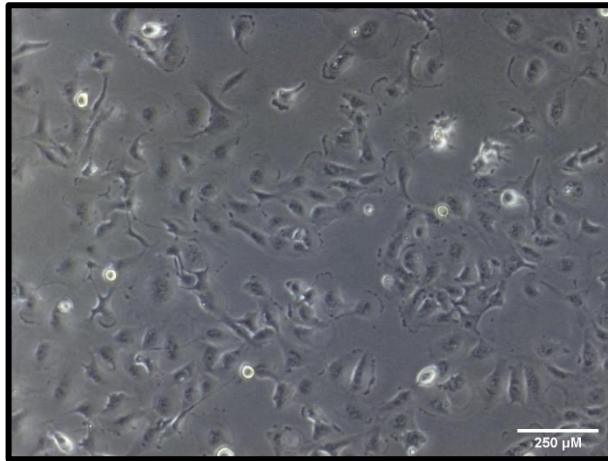
Images of HCC38 and MDA-MB-468 parental and drug resistant cell lines were taken to compare differences in morphology (**Figure 3.9**). HCC38 and MDA-MB-468 exhibit very different morphologies. HCC38 cells are large and elongated with a flat oval body like a fibroblastic or mesenchymal phenotype. MDA-MB-468 cells are much smaller than HCC38 cells, more rounded and grow together in clusters presenting a more epithelial phenotype. H737R cells appear smaller than HCC38 cells and less flat, with less spindle structures emanating from the main body of the cell. Also, H737R cells appear to grow in tighter clusters. These features are less noticeable in HPrexR cells. MDA-737R and MDA-PrexR cells appear morphologically unchanged.



HCC38

H737R

HPrexR



MDA-MB-468

MDA-737R

MDA-PrexR

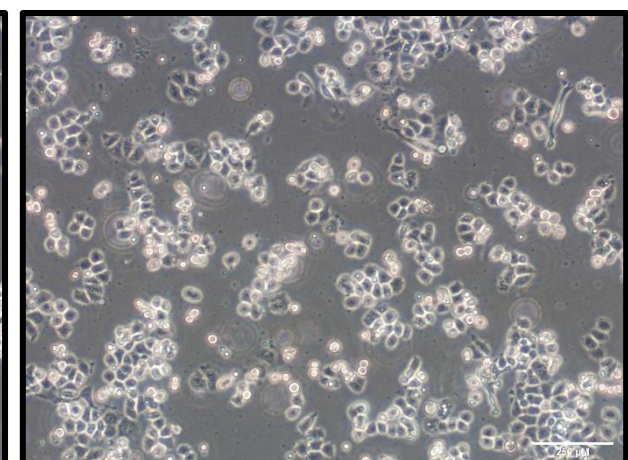
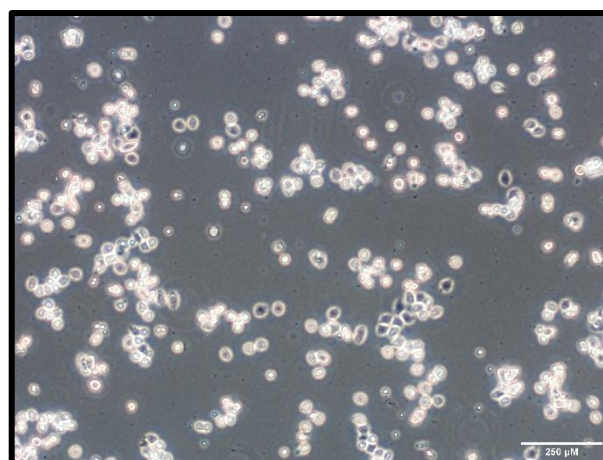
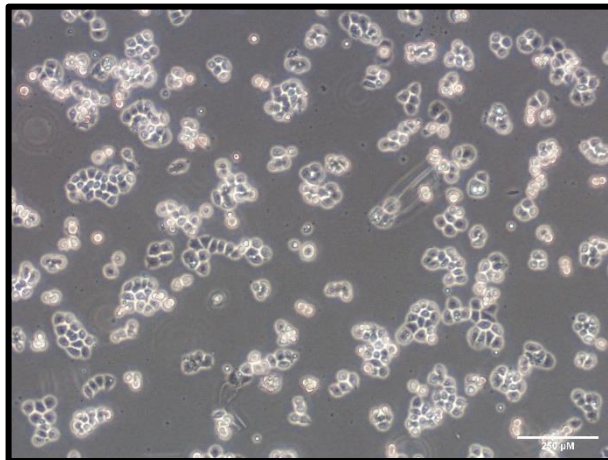


**Figure 3.9: Light microscopy images of HCC38 and MDA-MB-468 parental and resistant sublines at 40x magnification.**  
Cell images taken to compare differences in morphology.

### 3.2.7 Stability of drug resistance in H737R and HPrexR cell lines

H737R and HPrexR cell lines were maintained in 4 $\mu$ M SRA737 or 500nM Prexasertib, respectively to maintain a selection pressure from CHK1 inhibitor resistance in these cell lines. To see if drug resistance was preserved in the absence of a CHK1 inhibitor, cells were cultured in drug free media for 9-weeks. Regular SRB assays were conducted over this time to see if resistance to CHK1i SRA737 was lost. The GI<sub>50</sub> values for H737R and HPrexR were maintained over the 9-week period indicating that drug resistance was preserved over this time frame (**Figure 3.10**). It is important to note the GI<sub>50</sub> of H737R and HPrexR cell lines (**Figure 3.10 C**) were slightly lower than shown in previous SRB assays, with H737R and HPrexR cell lines showing GI<sub>50</sub> of 21.03 $\mu$ M and 27.06 $\mu$ M (**Figure 3.10**) versus original GI<sub>50</sub> values of 33.84 $\mu$ M and 37.32 $\mu$ M respectively (**Figure 3.7**). This difference is likely due to changes in seeding densities between experiments.

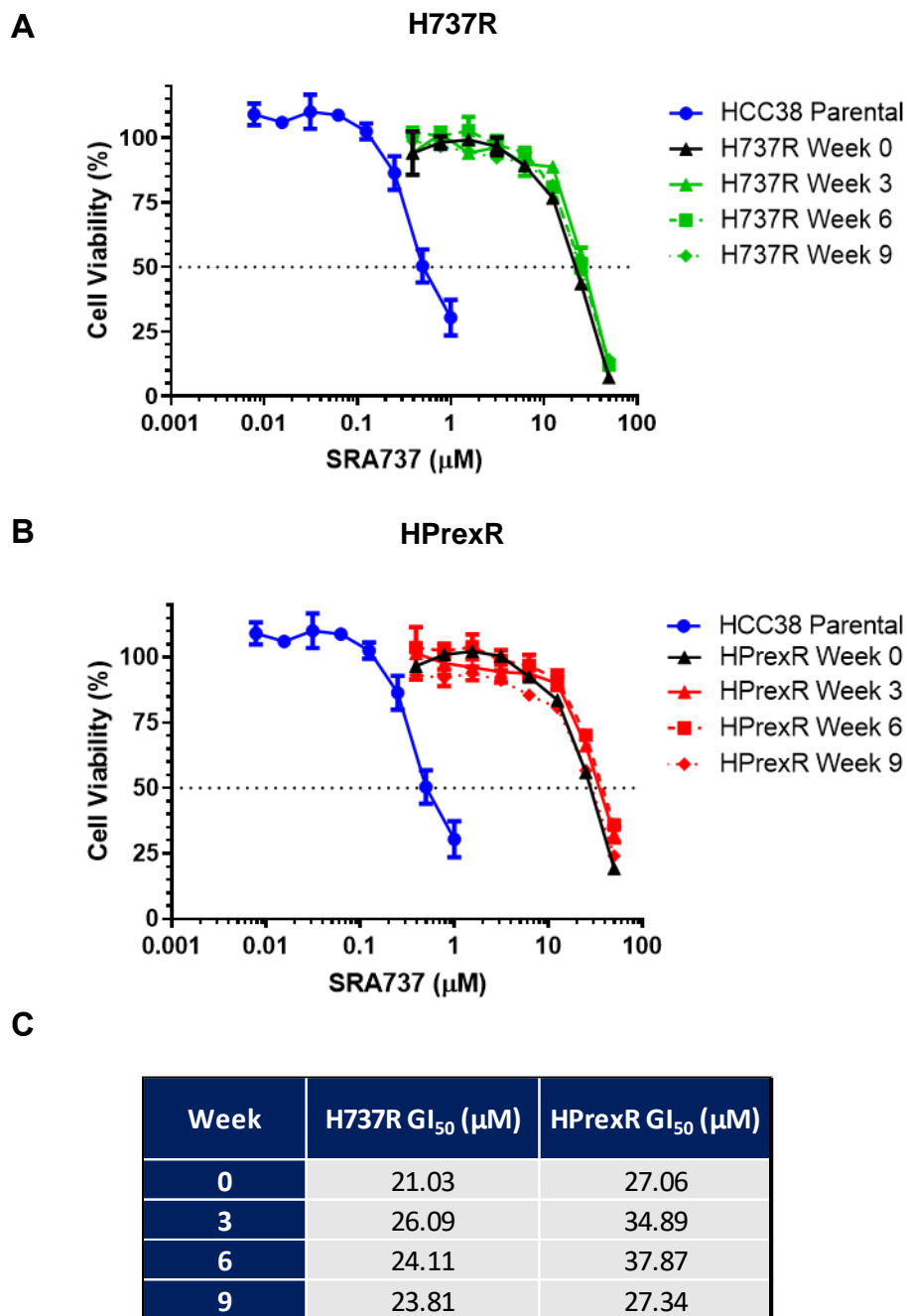


**Figure 3.10:** H737R (**A**) and HPrexR (**B**) long term release from drug experiment. Cells were released from drug and routinely cultured for a period of 9 weeks to see if resistance to SRA737 was maintained. Cells were plated in a 96-well plate at 1600 cells/well and grown for 48 hours before treatment with a serial dilution of SRA737 for 96 hours. Dose response curves generated using GraphPad Prism 6 and fitted using non-linear regression. Dotted line marks the GI<sub>50</sub> of SRA737. Data points represent the mean  $\pm$  SD from 1 experiment. **C**) Table shows the GI<sub>50</sub> of SRA737 for weeks 0-9. Data for weeks 3-9 representative of n=1 independent experiment, data for HCC38 parental and Week 0 representative of n  $\geq$  3 independent experiments.

### 3.2.8 Multidrug resistance in HCC38 and MDA-MB-468 parental and resistant cell lines

*MDR1* encodes for P-glycoprotein, an efflux protein located in the cells plasma membrane and has been implicated in multidrug resistance (Amin, 2013). Both HCC38 and MDA-MB-468 parental and resistant cell lines were investigated for changes in expression of P-glycoprotein. However, relative to a subline of the human UKF-NB-3 neuroblastoma cell line generated with resistance to vincristine and shown to express MDR1 (a kind gift from the Michaelis laboratory, University of Kent) no signal was found in parental or resistant cells suggesting the protein was not expressed or expression is too low to detect via this method (**Figure 3.11**).

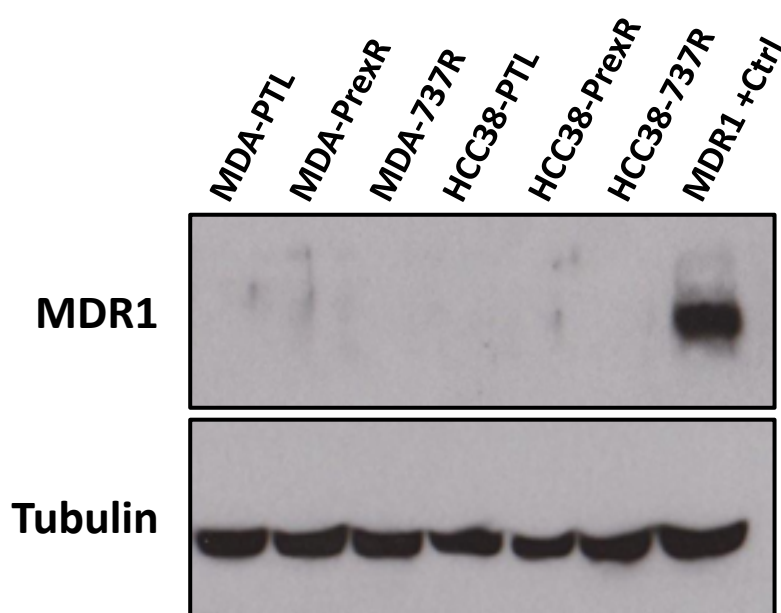


**Figure 3.11: MDR1 (P-glycoprotein) expression levels in MDA-MB-468 and HCC38 parental and resistant cell lines.** Cells were plated in 10cm dishes and left to grow for 24 hours before lysis and analysis by western blot. An NB3-Vincristine resistant cell line, provided by the Resistant Cancer Cell line collection (Frankfurt, Germany), was used as a positive control for MDR1 expression. Tubulin was included as a loading control. Blot is representative on n=2 independent experiments.

The calcium channel blocker verapamil has been shown to reverse multidrug resistance via inhibition of P-glycoprotein (Tsuruo *et al.*, 1981; Yusa and Tsuruo, 1989). To confirm that P-glycoprotein is not responsible for drug efflux and subsequent resistance to CHK1i, H737R and HPrexR cells were treated with Verapamil and SRA737 or Prexasertib in combination. To select the appropriate dose of Verapamil a dose response curve was generated via SRB assay (**Figure 3.12**). Tsuruo *et al.*, showed Verapamil concentrations between 2.2-6.6 $\mu$ M were used to reverse resistance to Vincristine in P388/VCR cell line. 5 $\mu$ M Verapamil concentration was selected as it was shown to be non-lethal in HCC38, H737R and HPrexR cell lines (**Figure 3.12**) and fell within the range used by Tsuruo *et al.* Verapamil failed to sensitise H737R and HPrexR cell lines to SRA737 or Prexasertib suggesting CHK1i resistance is not due to drug efflux (**Figure 3.13**).

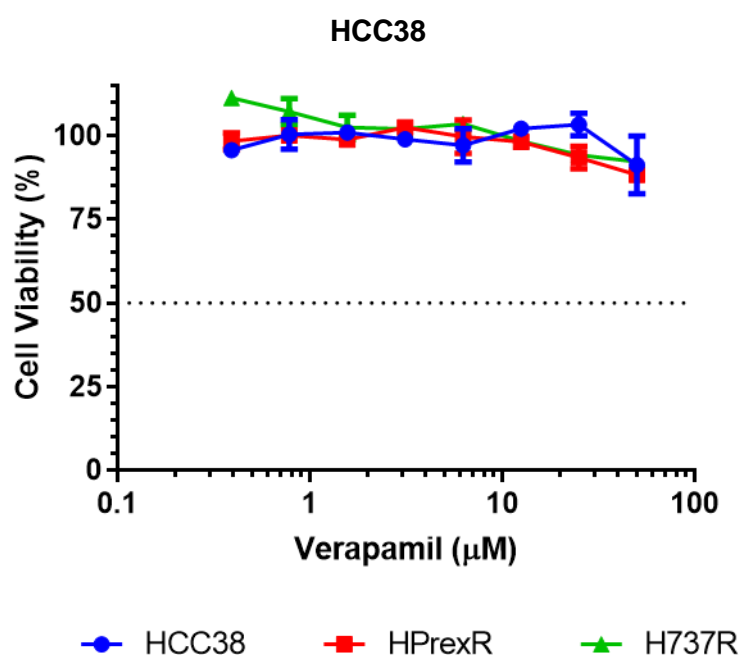
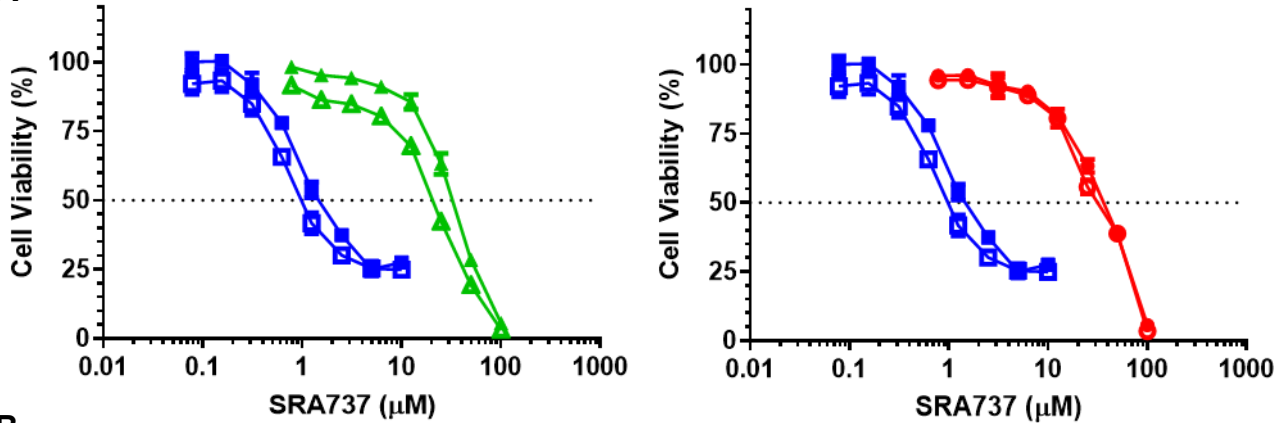


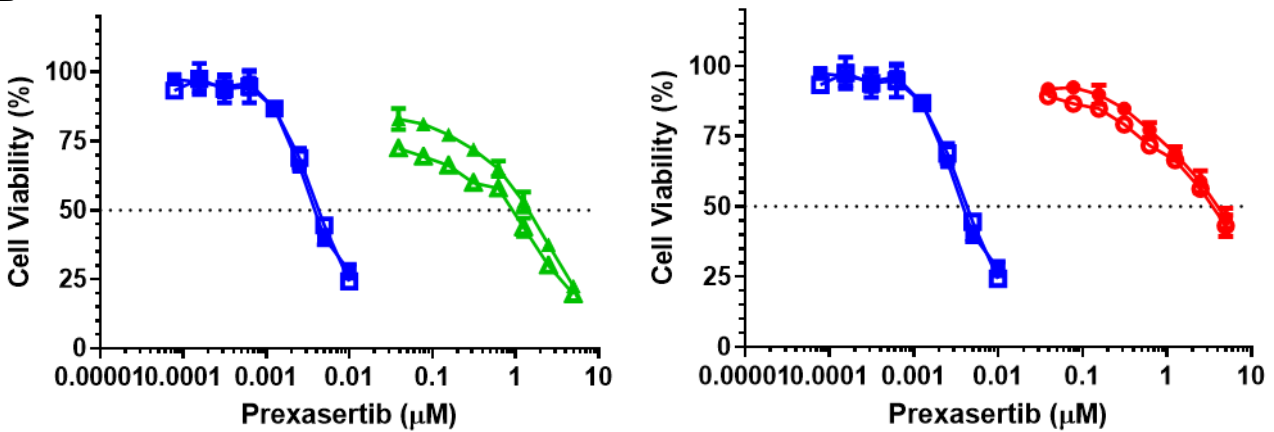
**Figure 3.12: Dose response of HCC38, HPrexR and H737R cells to Verapamil.** Cells were plated at 1600 cells/well in a 96-well plate and grown for 48 hours before treatment with a serial dilution Verapamil for 96 hours. Dose response curves generated using GraphPad Prism 6. Dotted line marks the  $GI_{50}$  but was not achievable in these cell lines are the concentrations tested. Data points represent the mean  $\pm$  SD from one experiment. Data representative of n=2 independent experiments for H737R cell line and n=3 independent experiments for HCC38 and HPrexR cell lines.

## HCC38

**A**



**B**



■ HCC38    □ HCC38 + Verapamil    ● HPrexR    ○ HPrexR + Verapamil    ▲ H737R    △ H737R + Verapamil

**Figure 3.13: Dose response of HCC38, H737R and HPrexR cell lines to a drug combination of SRA737/Prexasertib +/- Verapamil.** Cells were plated at 1600 cells/well in a 96-well plate and grown for 48 hours before treatment with a serial dilution of **A)** SRA737 **B)** Prexasertib +/- 5  $\mu$ M Verapamil for 96 hours. Dose response curves generated using GraphPad Prism 6. Dotted line marks the  $GI_{50}$  of SRA737 or Prexasertib +/- Verapamil. Data points represent the mean  $\pm$  SD from one experiment. Data representative of  $n \geq 3$  independent experiments.



### 3.2.9 Cross profiling of parental and resistant cell lines

HCC38 and MDA-MB-468 parental and drug resistant cell lines were cross profiled with various cancer drugs and tool compounds and their  $GI_{50}$  values determined. Differences in  $GI_{50}$  value between parental and resistant cell lines can be used to highlight changes in cell signalling and provide clues for potential resistance mechanisms.

#### 3.2.9.1 Inhibition of ATR and WEE1 Kinases

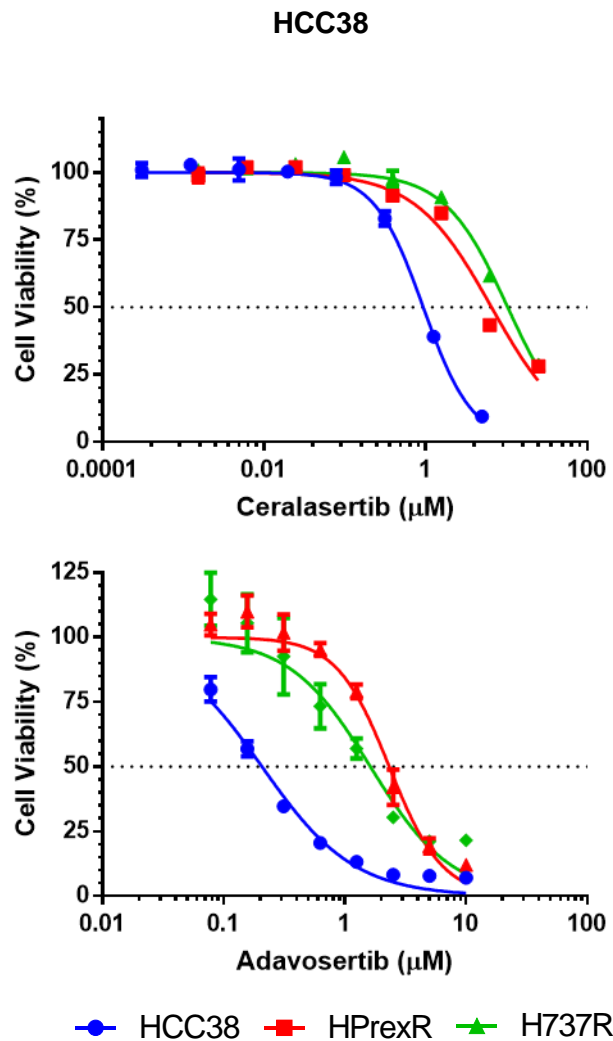
Ataxia telangiectasia and RAD3-related protein (ATR) and WEE1 kinases are critical for an effective DNA damage response and cell cycle checkpoint control. While ATR is required for activation of CHK1 through signal transduction from sites of ssDNA breaks (Zhang and Hunter, 2014) Wee1 acts as an inactivator of Cyclin Dependent Kinase 1 and 2 (CDK1/2) by inhibitory phosphorylation of Y15 (Parker and Piwnica-Worms, 1992). WEE1 acts in conjunction with CHK1 which regulates CDK1/2 by sequestration or ubiquitination of the CDC25 phosphatases that remove the inhibitory Y15 phosphorylation (Medema and Macuerek, 2012). Both ATR and WEE1 kinases are important for successful activation of the G2/M checkpoint and S-phase DNA replication and may contribute to resistance of CHK1 inhibitors. Therefore, parental and resistant cell lines were profiled with the selective ATR kinase inhibitor Ceralasertib (Vendetti *et al.*, 2015), and selective WEE1 inhibitor Adavosertib (Hirai *et al.*, 2009).

For Ceralasertib, HCC38 resistant cells show resistance factors of 8.4-fold for H737R and 5.2-fold for HPrexR versus the parental HCC38 cells, (**Figure 3.14**) but MDA-PrexR and MDA-737R show lower resistance factors of 3.4 and 2.0-fold resistance respectively versus MDA-MB-468 cells (**Figure 3.15**). MDA-737R show no resistance to Adavosertib with no change in  $GI_{50}$  versus the parental cells. However, there is a slight and significant increase in  $GI_{50}$  values and resistance of 1.7-fold for MDA-PrexR cells versus the parental cell line (**Figure 3.15**). Both H737R and HPrexR cell lines demonstrate resistance to Adavosertib with resistance factors of 7.8-fold and 10.9-fold respectively versus the HCC38 parental cells (**Figure 3.14**). These data show cross resistance to ATR inhibitor Ceralasertib in both HCC38 and MDA-MB-468

resistant cell lines, suggesting potential reactivation of the CHK1 pathway downstream of CHK1 or activation of a compensatory pathway may play a role in CHK1 inhibitor resistance. Cross resistance to WEE1 inhibitor Adavosertib in H737R and HPrexR cell lines suggests the locus of resistance may be related to CDK1/2 activity, as cells are resilient to perturbations of the two main regulators of this kinase, CHK1 and WEE1. The lack of resistance to Adavosertib in MDA-PrexR and MDA-737R suggests CHK1i resistance in these cell lines may be related to an alternate pathway.



A



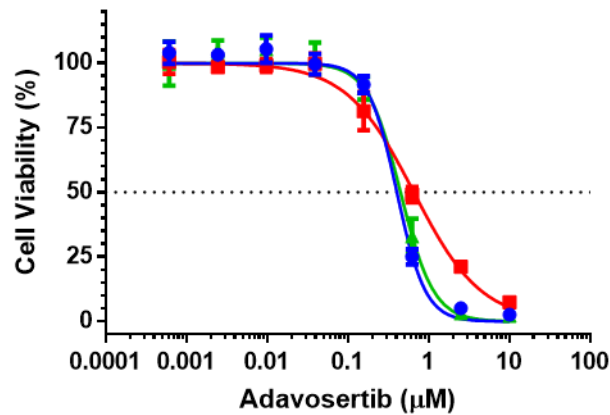
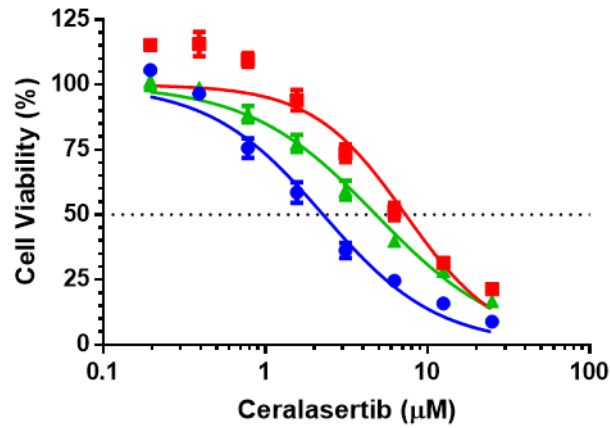
B

HCC38		Parental	H737R		HPrexR	
		GI <sub>50</sub> ± SD	GI <sub>50</sub> ± SD	RF	GI <sub>50</sub> ± SD	RF
Ceralasertib (μM)	ATR	1.32 ± 0.51 (n=4)	11.16 ± 1.11 (n=4) ***	8.4	6.82 ± 0.16 (n=4) ***	5.2
Adavosertib (μM)	WEE1	0.2 ± 0.03 (n=3)	1.55 ± 0.34 (n=3) *	7.8	2.18 ± 0.17 (n=3) **	10.9

**Figure 3.14: Determination of GI<sub>50</sub> values for HCC38, H737R and HPrexR cell lines to ATR inhibitor Ceralasertib and WEE1 inhibitor Adavosertib.** Cells were plated at 6400 cells/well for Ceralasertib and 3200 cells/well for Adavosertib in a 96-well plate and grown for 48 hours before treatment with a serial dilution of Ceralasertib or Adavosertib for 96 hours. **A)** HCC38 dose response curves generated using GraphPad Prism 6 and fitted using non-linear regression. Dotted line marks the GI<sub>50</sub> of Ceralasertib or Adavosertib. Data points represent the mean ± SD from one representative experiment. **B)** Table summarises the mean ± SD of all experiments conducted. (n) indicates the number of independent experiments. Statistical significance was calculated using a student's t-test, \* =  $p \leq 0.05$ , \*\* =  $p \leq 0.01$ , \*\*\* =  $p \leq 0.001$ .

**A**

**MDA-MB-468**



● MDA-MB-468 ■ MDA-PrexR ▲ MDA-737R

**B**

MDA-MB-468		Parental	MDA-737R		MDA-PrexR	
		GI <sub>50</sub> ± SD	GI <sub>50</sub> ± SD	RF	GI <sub>50</sub> ± SD	RF
Ceralasertib (μM)	ATR	2.41 ± 0.58 (n=4)	4.87 ± 0.56 (n=4) **	2.0	8.20 ± 0.94 (n=3) **	3.4
Adavosertib (μM)	WEE1	0.39 ± 0.04 (n=3)	0.39 ± 0.07 (n=3)	1.0	0.68 ± 0.02 (n=3) **	1.7

**Figure 3.15: Determination of GI<sub>50</sub> values for MDA-MB-468 parental, MDA-737R and MDA-PrexR cell lines to ATR inhibitor Ceralasertib and WEE1 inhibitor Adavosertib.** Cells were plated at 3200 cells/well in a 96-well plate and grown for 48 hours before treatment with a serial dilution of Ceralasertib or Adavosertib for 96 hours. **A)** MDA-MB-468 dose response curves generated using GraphPad Prism 6 and fitted using non-linear regression. Dotted line marks the GI<sub>50</sub> of Ceralasertib or Adavosertib. Data points represent the mean ± SD from one representative experiment. **B)** Table summarises the mean ± SD of all experiments conducted. (n) indicates the number of independent experiments. Statistical significance was calculated using a student's t-test, \*\* = p ≤ 0.01.

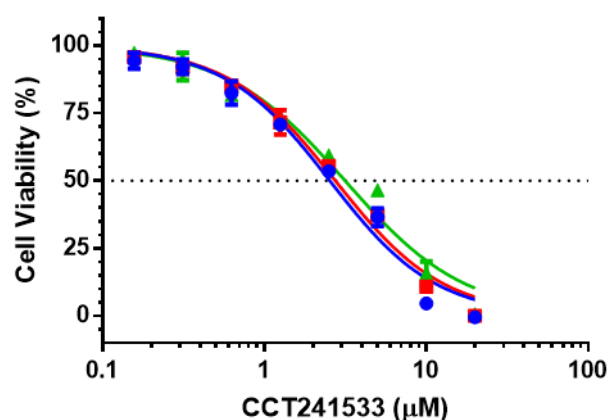
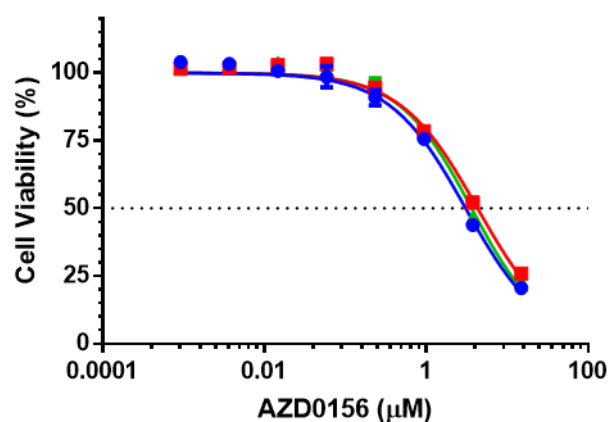
### 3.2.9.2 Inhibition of ATM and CHK2 kinases

Ataxia telangiectasia mutant (ATM) and Checkpoint kinase 2 (CHK2) play important roles in the cell response to double stranded DNA breaks (DSBs). ATM is activated by DSBs and phosphorylates CHK2 at Thr-68 leading to its activation (Bartek and Lukas, 2003). CHK2 is structurally different from CHK1 but can phosphorylate and inhibit CDC25 phosphatases (Benada and Macurek, 2015). However, CHK2 is not thought to have a dominant role in the G2/M checkpoint and may act as a signal booster rather than the main driving force (Takai *et al.*, 2002). CHK2 may also play a role in DNA repair by promoting pathways such as the error-free homologous recombination (HR) and suppressing the error-prone pathway non-homologous end joining (NHEJ)(Antoni *et al.*, 2007). As ATM and CHK2 operate within the areas of DNA repair and cell cycle control it would be prudent to consider that changes in these pathways may contribute to CHK1i resistance. As a result, HCC38 and MDA-MB-468 parental and resistant cell lines were profiled with the selective ATM inhibitor AZD0156 (Pike, 2016) and the selective CHK2 inhibitor CCT241533 (Anderson *et al.*, 2011).

In H737R and HPrexR cell lines no significant difference was detected in response to either AZD0156 or CCT241533 inhibitors versus the parental HCC38 cells (**Figure 3.16**). However, MDA-737R cells were significantly more sensitive to treatment with the ATM inhibitor AZD0156 with a resistance factor of 0.5 versus the parental cell line i.e., 2-fold sensitivity (**Figure 3.17**). A resistance factor of 0.8 was seen in the MDA-PrexR cell line in response to AZD0156 but this was non-significant. No significant differences were recorded in MDA-737R and MDA-PrexR sublines versus the parental cell line to CCT241533 treatment. Sensitivity seen in MDA-737R to AZD0156 suggests this cell line may be more reliant on signalling from ATM and perhaps double stranded break repair as a coping mechanism for CHK1 inhibition.

**A**

**HCC38**



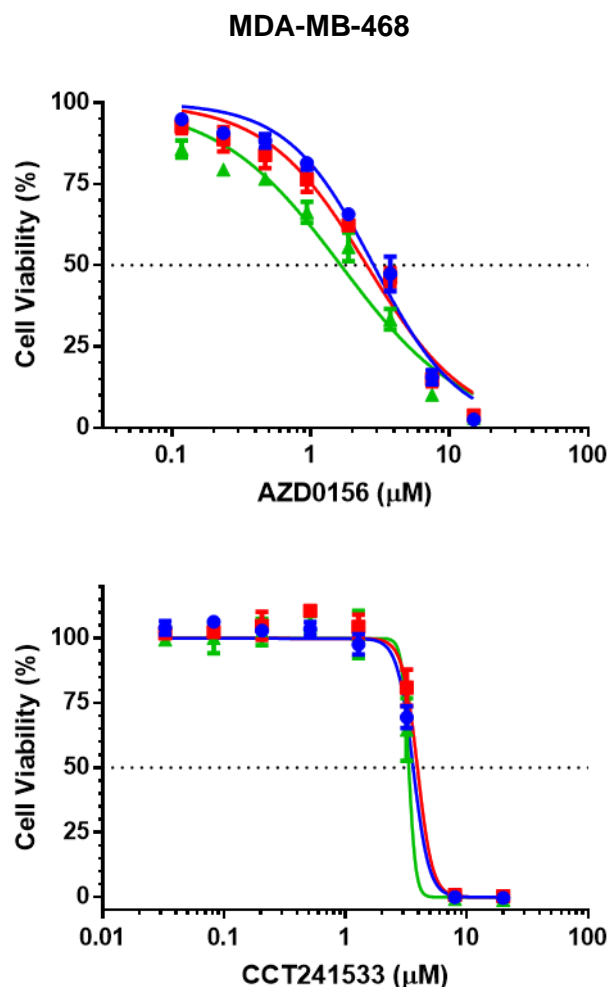
**B**

● HCC38    ■ HPrexR    ▲ H737R

HCC38		Parental	H737R		HPrexR	
		GI <sub>50</sub> ± SD	GI <sub>50</sub> ± SD	RF	GI <sub>50</sub> ± SD	RF
AZD0156 (μM)	ATM	2.96 ± 0.55 (n=3)	3.11 ± 0.49 (n=3)	1.1	3.23 ± 0.54 (n=3)	1.1
CCT241533 (μM)	CHK2	2.58 ± 0.46 (n=3)	3.39 ± 1.27 (n=3)	1.3	2.87 ± 0.63 (n=3)	1.1

**Figure 3.16: Determination of GI<sub>50</sub> values for HCC38, H737R and HPrexR cell lines to ATM inhibitor AZD0156 and CHK2 inhibitor CCT241533.** Cells were plated at 6400 cells/well in a 96-well plate and grown for 48 hours before treatment with a serial dilution of AZD0156 or CCT241533 for 96 hours. **A)** HCC38 dose response curves generated using GraphPad Prism 6 and fitted using non-linear regression. Dotted line marks the GI<sub>50</sub> of AZD0156 or CCT241533. Data points represent the mean ± SD from one representative experiment. **B)** Table summarises the mean ± SD of all experiments conducted. (n) indicates the number of independent experiments. Statistical significance was calculated using a student's t-test, but no significant difference was found.

**A**



**B**

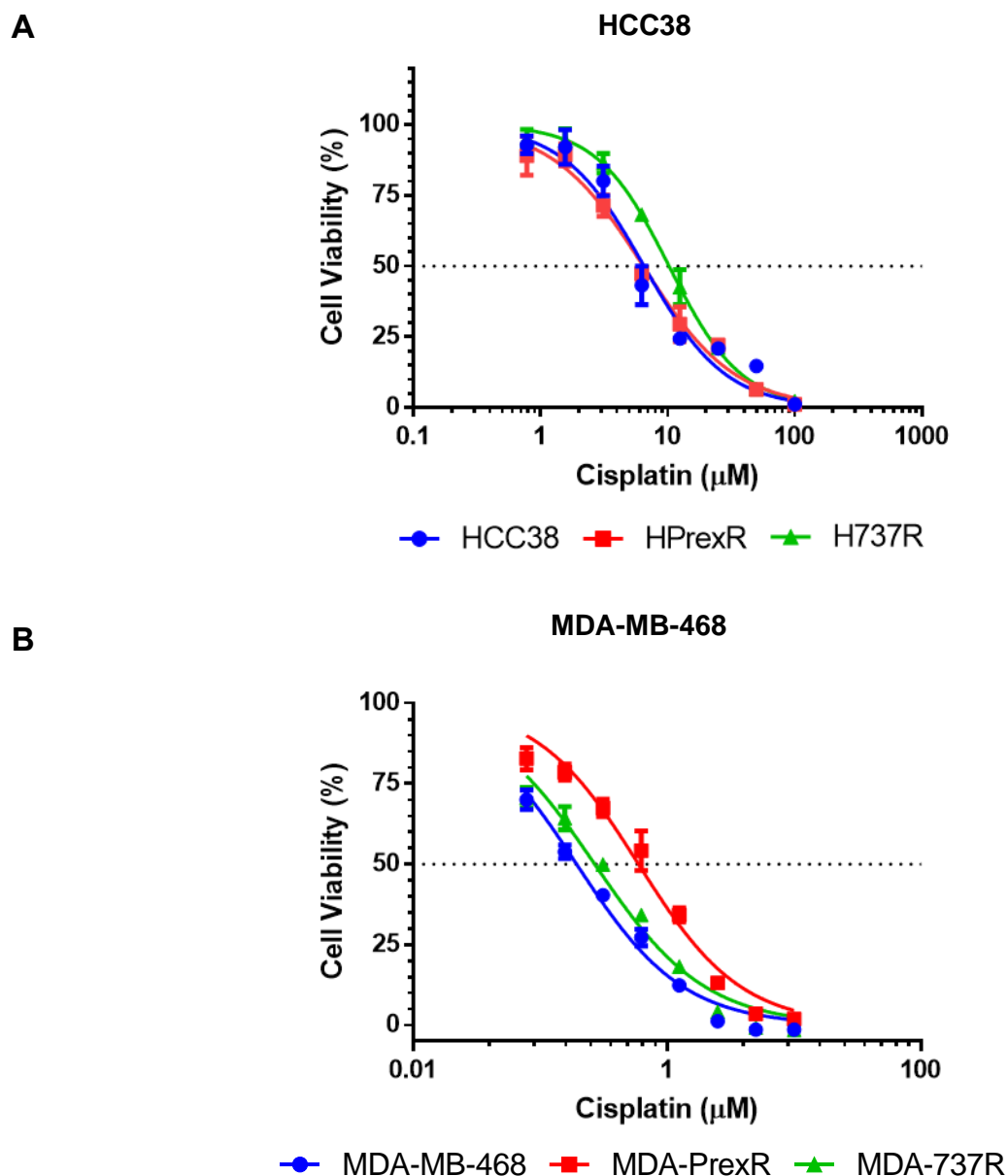
● MDA-MB-468    ■ MDA-PrexR    ▲ MDA-737R

MDA-MB-468		Parental	MDA-737R		MDA-PrexR	
		GI <sub>50</sub> ± SD	GI <sub>50</sub> ± SD	RF	GI <sub>50</sub> ± SD	RF
AZD0156 (μM)	ATM	2.83 ± 0.17 (n=3)	1.46 ± 0.18 (n=3) **	0.5	2.34 ± 0.21 (n=3)	0.8
CCT241533 (μM)	CHK2	3.91 ± 0.84 (n=3)	3.31 ± 0.49 (n=3)	0.9	4.32 ± 0.36 (n=3)	1.1

**Figure 3.17: Determination of GI<sub>50</sub> values for MDA-MB-468 parental, MDA-737R and MDA-PrexR cell lines to ATM inhibitor AZD0156 and CHK2 inhibitor CCT241533.** Cells were plated at 3200 cells/well in a 96-well plate and grown for 48 hours before treatment with a serial dilution of AZD0156 or CCT241533 for 96 hours. **A)** MDA-MB-468 and dose response curves generated using GraphPad Prism 6 and fitted using non-linear regression. Dotted line marks the GI<sub>50</sub> of AZD0156 or CCT241533. Data points represent the mean ± SD from one representative experiment. (n) indicates the number of independent experiments. **B)** Table summarises the mean ± SD of all experiments conducted. Statistical significance was calculated using a student's t-test, \*\* = p ≤ 0.01.

### 3.2.9.3 Cross profiling with Cisplatin

Cisplatin is a highly potent DNA damaging agent that primarily forms intrastrand crosslink adducts that interfere with the successful replication of DNA (Turner *et al.*, 2013). DNA damage in tumour cells leads to activation of the DNA damage response leading to either to apoptosis or DNA repair and cell survival (Siddik, 2003). As HCC38 and MDA-MB-468 sublines have been generated with resistance to CHK1 inhibition it is possible that the response to DNA damaging agents may also have changed as cells become more/less fit to manage insults to their DNA. Therefore, HCC38 and MDA-MB-468 parental and resistant sublines were profiled with Cisplatin. **Figure 3.18** shows HCC38 and MDA-MB-468 cell lines treated with Cisplatin. Neither HCC38 nor MDA-MB-468 parental or resistant cell lines showed significant differences in the response to Cisplatin.



**C**

HCC38		Parental	H737R		HPrexR	
		$GI_{50} \pm SD$	$GI_{50} \pm SD$	RF	$GI_{50} \pm SD$	RF
Cisplatin ( $\mu\text{M}$ )	DNA Damage	$5.38 \pm 1.23$ (n=4)	$7.87 \pm 2.23$ (n=4)	1.5	$7.46 \pm 2.23$ (n=4)	1.4

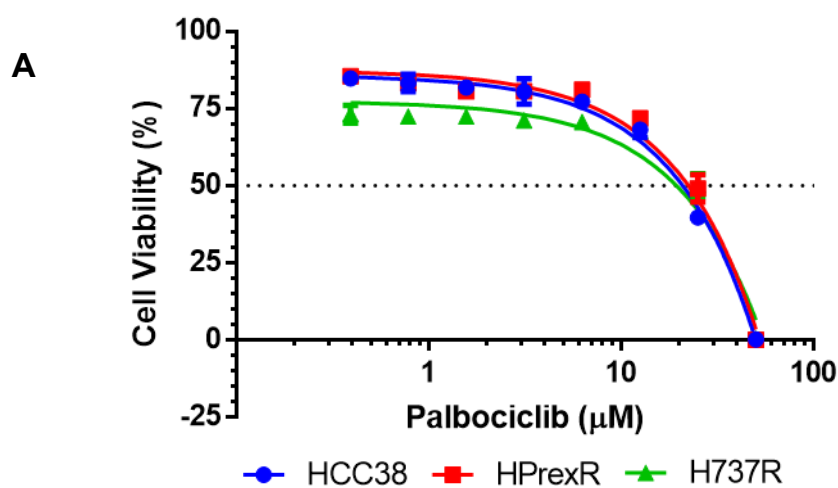
MDA-MB-468		Parental	MDA-PrexR		MDA-737R	
		$GI_{50} \pm SD$	$GI_{50} \pm SD$	RF	$GI_{50} \pm SD$	RF
Cisplatin ( $\mu\text{M}$ )	DNA Damage	$0.21 \pm 0.05$ (n=3)	$0.22 \pm 0.04$ (n=3)	1.0	$0.42 \pm 0.14$ (n=3)	2.0

**Figure 3.18: Determination of  $GI_{50}$  values for HCC38 and MDA-MB-468 parental and resistant cell lines to Cisplatin.** Cells were plated at 6400 cells/well for HCC38 cells and 3200 cells/well for MDA-MB-468 cells in a 96-well plate and grown for 48 hours before treatment with a serial dilution of Cisplatin for 96 hours. **A)** MDA-MB-468 and **B)** HCC38 Dose response curves generated using GraphPad Prism 6 and fitted using non-linear regression. Dotted line marks the  $GI_{50}$  of Cisplatin. Data points represent the mean  $\pm$  SD from one representative experiment. **C)** Table summarises the mean  $\pm$  SD of all experiments conducted. (n) indicates the number of independent experiments. Statistical significance was calculated using a student's t-test but no significant difference was found.

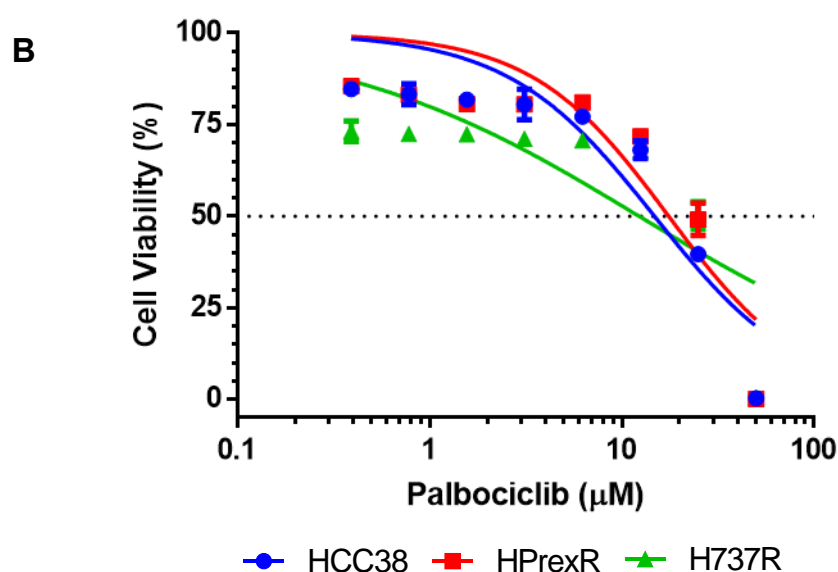
#### 3.2.9.4 Cross profiling with Palbociclib

Palbociclib is an ATP competitive inhibitor of CDK4 and CDK6 kinase activity (CDK4/6) (Fry *et al.*, 2004). As CDK4/6 are important regulators of the cell cycle it seemed plausible that CHK1i resistant cell lines may demonstrate changes in their response to inhibitors of other cell cycle related proteins. **Figure 3.19** shows two types of regression analysis performed with this data as the usual non-linear regression (**Figure 3.19 B**) does not strongly fit the data. The linear regression (**Figure 3.19 A**) provides stronger  $R^2$  values for each data set and a more consistent prediction of  $GI_{50}$  values between experiments. Nevertheless, **figure 3.19** demonstrates that there is no significant difference in response to Palbociclib between HCC38, H737R and HPrexR cell lines.





Linear Regression			
Cell Line	$\text{GI}_{50}$ ( $\mu\text{M}$ )	RF	$R^2$
HCC38	$18.81 \pm 1.59$ n=3	N/A	$0.94 \pm 0.03$
H737R	$17.6 \pm 1.35$ n=3	0.94	$0.91 \pm 0.02$
HPrexR	$20.42 \pm 1.52$ n=3	1.09	$0.94 \pm 0.03$



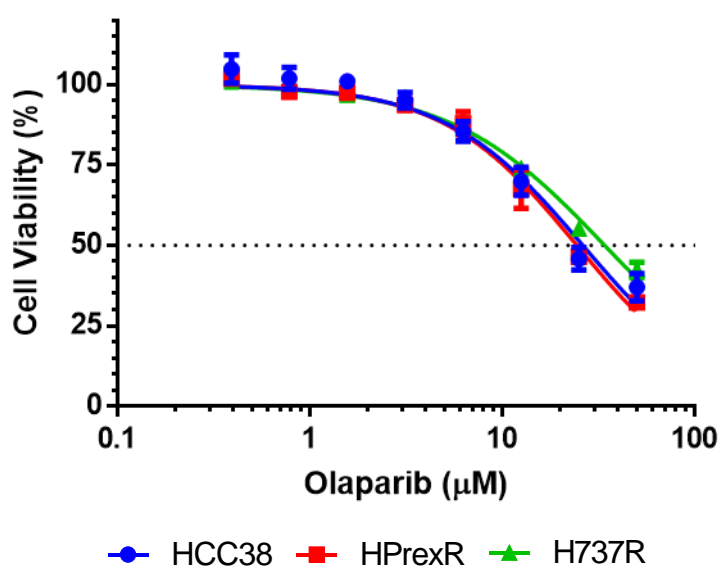
Non-linear Regression			
Cell Line	$\text{GI}_{50}$ ( $\mu\text{M}$ )	RF	$R^2$
HCC38	$17.85 \pm 2.45$ n=3	N/A	$0.82 \pm 0.02$
H737R	$19.66 \pm 5.94$ n=3	1.15	$0.69 \pm 0.07$
HPrexR	$21.2 \pm 3.22$ n=3	1.18	$0.8 \pm 0.03$

**Figure 3.19: Determination of  $\text{GI}_{50}$  values for HCC38, H737R and HPrexR cell lines to CDK4/6 inhibitor Palbociclib.** Cells were plated at 3200 cells/well in a 96-well plate and grown for 48 hours before treatment with a serial dilution of Palbociclib for 96 hours. **A)** Dose response curves calculated with Graphpad Prism 6 using a linear regression. **B)** Dose response curves calculated with Graphpad Prism 6 using non-linear regression. Dotted line marks the  $\text{GI}_{50}$  of Palbociclib. Data points represent the mean  $\pm$  SD from one representative experiment. (n) indicates the number of independent experiments. Both tables summarise the mean  $\pm$  SD of all experiments conducted. Statistical significance was calculated using a student's t-test, but no significant difference was found.

### 3.2.9.5 Cross profiling against Olaparib

Olaparib is a selective inhibitor of poly (ADP-ribose) polymerase 1/2 (PARP1/2), an important protein in a cell's response to DNA damage and subsequent DNA repair (Kummar *et al.*, 2012). As CHK1 is also involved in the DNA damage response HCC38, H737R and HPrexR cell lines were cross profiled with this inhibitor (**Figure 3.20**). No significant differences were found between parental and drug resistant cell lines to inhibition with Olaparib.

**A**



**B**

HCC38		Parental	H737R		HPrexR	
		GI <sub>50</sub> ± SD	GI <sub>50</sub> ± SD	RF	GI <sub>50</sub> ± SD	RF
Olaparib (μM)	PARP	26 ± 2.4 (n=3)	31.99 ± 7.12 (n=3)	1.2	23.55 ± 2.66 (n=3)	0.9

**Figure 3.20: Determination of GI<sub>50</sub> values for HCC38, H737R and HPrexR cell lines to PARP inhibitor Olaparib.** Cells were plated at 3200 cells/well in a 96-well plate and grown for 48 hours before treatment with a serial dilution of Olaparib for 96 hours. **A)** Dose response curves calculated with Graphpad Prism 6 using non linear regression. Dotted line marks the GI<sub>50</sub> of Olaparib. Data points represent the mean ± SD from one representative experiment. **B)** Table summarises the mean ± SD of all experiments conducted. (n) indicates the number of independent experiments. Statistical significance was calculated using a student's t-test but no significant difference was found.

### 3.2.10 Analysis of basal protein expression by western blot

#### 3.2.10.1 Basal expression of CHK1 and CHK2 phosphorylated and total protein in HCC38 cell lines

CHK1 and CHK2 are structurally unrelated serine/threonine kinases that overlap in functionality by both responding to DNA damage. Upstream signalling by ATR in response to single stranded DNA breaks and ATM from double stranded DNA breaks activate CHK1 and CHK2 respectively, however, crosstalk between these kinases has been documented (Bartek and Lukas, 2003). Basal signalling of pCHK1 S296 and pCHK2 S516 was investigated in HCC38 parental and resistant cell lines (**Figure 3.21**). The residues selected are autophosphorylation sites and are markers of activity for their respective kinases (Wu and Chen, 2003; Smits, 2006; Walton *et al.*, 2010). Unexpectedly both pCHK1 and pCHK2 show bands above the expected molecular weight that do not correspond with the total CHK1 and CHK2 bands. These bands may be due to non-specific binding of the antibody or extra banding may be due to highly phosphorylated CHK1 and CHK2 protein migrating at a slower rate through the SDS-PAGE gel. The lack of double banding for T-CHK1 and T-CHK2 could be explained by the blocking of epitopes for total CHK1 and CHK2 antibodies in highly phosphorylated proteins. This is supported by SRA737, and Adavosertib dose response experiments carried out in **chapter 4**. These show a dose dependent increase in pCHK1 s345 double banding with increased DNA damage and is discussed in greater detail in **chapter 4**. Alternatively, these extra bands may be due to cross-reactivity of the antibody with other phospho-proteins phosphorylated alongside CHK1 or due to post-translational modification of CHK1. Basal signalling for these targets proved inconsistent with no strong discernible pattern emerging between repeated experiments, in some cases bands were very faint or imperceptible and in others strong differences could be seen between cell lines (**Figure 3.21**).

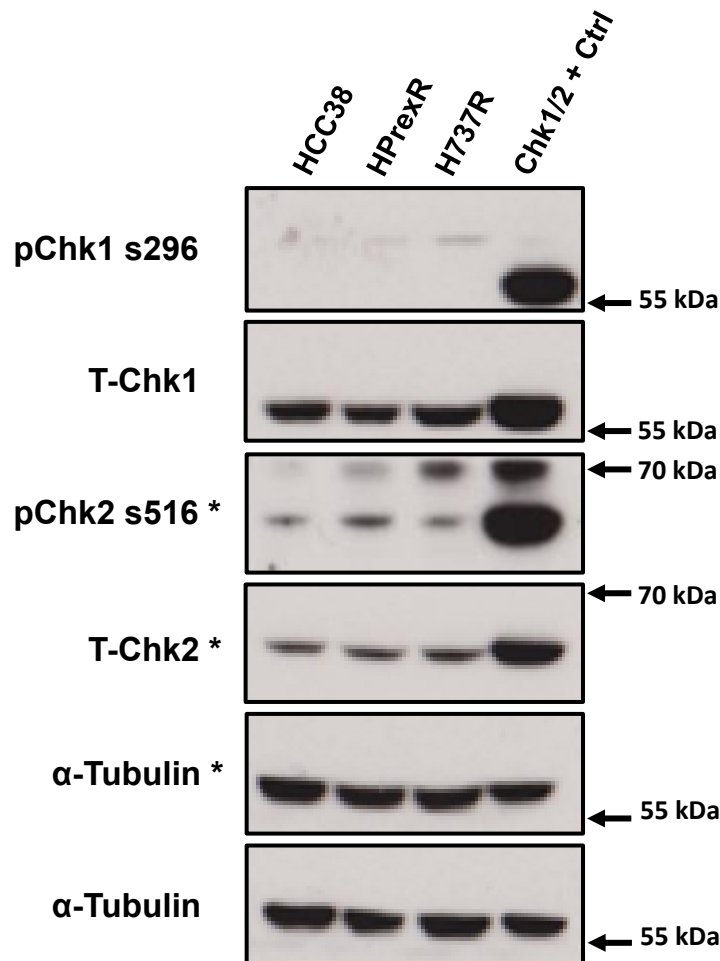


**Figure 3.21: Basal expression of pChk1 s296 and pChk2 s516 in HCC38 parental and resistant cell lines.** Cells were plated in 10cm dishes and left to grow for 48 hours before lysis and analysis by western blot. α-Tubulin was included as a loading control. HEK293 cells were treated with bleomycin for 24 hours as a positive control for pChk1/2 S296. \* Indicates which loading control corresponds to which antibody. Blots are representative of n=3 independent experiments.

### 3.2.10.2 WEE1 protein expression levels in HCC38 Parental and resistant cell lines

WEE1 is an important protein involved in cell cycle regulation and phosphorylates CDK1/2 on the Y15 residue, maintenance of which is critical for activation of the G2/M checkpoint and regulation of S-phase. Strong resistance to the WEE1 inhibitor Adavosertib was seen in H737R and HPrexR cell lines (**Figure 3.14**). It was hypothesised that changes in WEE1 protein levels may allow cells to compensate for CHK1 inhibition by maintaining the G2/M checkpoint or better regulate S-phase during CHK1 inhibition and result in resistance to WEE1 inhibition due to the increased level of the of drug target. Basal expression of the WEE1 protein was investigated via western blot. As shown in **Figure 3.22** WEE1 levels in H737R and HPrexR are both higher than the parental cell line. This suggests that an increase in WEE1 protein may be driving resistance to CHK1 inhibition in these cell lines.

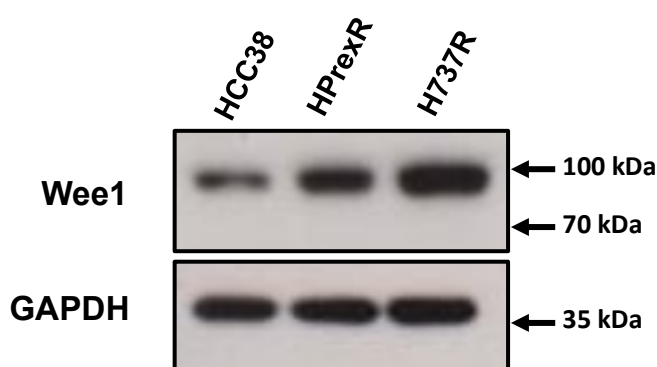


**Figure 3.22: WEE1 protein expression levels in HCC38 parental and resistant cell lines.** Cells were plated in 10cm dishes and left to grow for 48 hours before lysis and analysis by western blot. GAPDH was included as a loading control. Blots are representative of n=3 independent experiments.

### 3.3 Discussion

In this chapter resistant cell lines were successfully generated from MDA-MB-468 and HCC38 parental cell lines to both SRA737 and Prexasertib (**Figure 3.4**). H737R and HPrexR show over 100-fold resistance to SRA737 and over 1000-fold resistance to Prexasertib (**Figure 3.7**). Likewise, MDA-737R and MDA-PrexR cell lines show over 30-fold resistance to Prexasertib but only 1.5-fold resistance to SRA737 (**Figure 3.8**) although MDA-MB-468 cells appeared intrinsically resistant to SRA737 relative to the HCC38 cell line (**Figure 3.2**). Additionally, cross profiling with targeted inhibitors revealed cross-resistance to WEE1 inhibitor Adavosertib and ATR inhibitor Ceralasertib in H737R and HPrexR cell lines (**Figure 3.14**). Growth rates of resistant and parental cell lines were successfully characterised showing an increase in MDA-PrexR doubling times and a decrease in H737R doubling times vs their parental cell lines (**Figure 3.5 & 3.6**). Long term drug release experiments showed resistance was stable for at least 9-weeks in the absence of drug (**Figure 3.10**) and MDR1 blots and verapamil drug combination experiments suggest drug efflux is not likely to be the cause of drug resistance (**Figure 3.11-3.13**). Furthermore, western blot analysis reveals an increase in WEE1 protein levels in H737R and HPrexR cell lines (**Figure 3.22**). These results of this chapter are discussed in more detail below.

Initial screening revealed that the parental HCC38 and MDA-MB-468 cell lines were more sensitive to Prexasertib than SRA737 (**Figure 3.2**). This may be due to Prexasertib inhibiting both CHK1 and CHK2 kinases with  $IC_{50}$  values of <1nM and 8nM respectively (King, H Bruce Diaz, *et al.*, 2015) compared to SRA737 which only inhibits CHK1 with an  $IC_{50}$  of 1.4nM (Walton *et al.*, 2016a). In addition, MDA-MB-468 exhibits  $GI_{50}$  values of 0.15 $\mu$ M and 16.99 $\mu$ M to Prexasertib and SRA737 respectively compared to HCC38 which has  $GI_{50}$  values of 4.3nM to Prexasertib and 280nM to SRA737, suggesting that the former is more intrinsically resistant to both inhibitors versus the latter (**Figure 3.2**). It is notable that the SRA737  $GI_{50}$  value for MDA-MB-468 is very high and suggesting a high level of innate resistance to SRA737 in this cell line.

Resistance generation occurred over a 5-month period in which cells were routinely cultured with an escalating concentration of each drug, with each subsequent passage (dose escalation). On occasion, during dose escalation, cells appeared unhealthy and struggled to proliferate. Cells would then be maintained in the existing drug concentration until they appeared healthier and continued to grow. All cell lines went through a period where they were maintained at a fixed concentration of drug over several weeks as seen in **Figure 3.4**. H737R, HPrexR and MDA-PrexR struggled to grow in concentrations approximately 2-3 times greater than the parental GI<sub>50</sub> but eventually recovered and were able to survive higher concentrations of drug. However, MDA-737R which already had an innately high GI<sub>50</sub> to SRA737 was unable to survive in higher drug concentrations than the parental GI<sub>50</sub> despite being cultured in approximately 17  $\mu$ M of drug for 5 months. Towards the end of the dose escalation process resistant cell lines were profiled with both SRA737 and Prexasertib.

Other studies that have generated resistant cell line models by dose escalation describe similar processes. In a lapatinib (HER2i) drug resistance study, breast cancer cell lines SUM149 and SUM190 were cultured over a minimum period of 3-months in increasing concentrations of drug (Aird *et al.*, 2010). Following an increase in drug concentration SUM149 & SUM190 cells demonstrated increased cell death and decreased growth prior to the growth of small viable colonies after 2 weeks of drug incubation (Aird *et al.*, 2010). Another study investigating acquired resistance to Prexasertib in SCLC cell lines GLC4 and NCI-H792 escalated drug concentrations from 100nM to 1 $\mu$ M over a period of at least 3 months (Zhao, I. K. Kim, *et al.*, 2021). The new drug resistant cell lines demonstrated >100-fold resistance to Prexasertib vs their parental cell lines (Zhao, I. K. Kim, *et al.*, 2021). These studies mirror our own experience in generating drug resistant cell lines and support the use of dose escalation as an effective method to generate cell line models of acquired drug resistance.

Growth characteristics of resistant cell lines were measured via a seeding density assay and compared with parental cell lines (**Figure 3.5 & 3.6**). H737R and HPrexR cell lines had a shorter doubling time of 31.3 and 35.15 hours respectively compared with 47.58 hours in

HCC38 cell lines. There is a noticeable difference in doubling time between seeding densities shown in **figure 3.5**. As mentioned in **section 3.2.1** seeding densities were reduced from 6400 to 3200 and again to 1600 cells/well for later experiments in all HCC38 cell lines as it was noted that media was depleted towards the end of an assay, suggesting conditions were not optimal. At both 6400 and 3200 cells/well it was likely cells were not in log phase growth in the last stages of drug incubation, which would also explain why doubling times appear longer at 3200 cells/well than 1600 cells/well as estimation of cell doubling assumes cells are in log phase growth. Regardless, **figure 3.5** demonstrates reduced doubling times in H737R and HPrexR cell lines relative to HCC38, however only H737R at 1600 cells/well is significantly different from HCC38 cells. MDA-737R and MDA-PrexR show increased doubling times of 30.59 and 29.9 hours respectively relative to MDA-MB-468 27.02 hours but only MDA-PrexR is significantly different from MDA-MB-468 cells (**Figure 3.6**). P-values for HPrexR and MDA-737R cell lines were non-significant. However, this was only based on n=2 biological repeats of the experiment and the data collected is likely inadequate to identify potential subtle but significant changes in growth rate. These experiments should be repeated to identify if HPrexR and MDA-737R growth rates are significantly different from their parental cell lines.

Changes in doubling time may be indicative of deeper morphological changes. Cells that have a more epithelial phenotype are associated with increased proliferation, while a shift to a mesenchymal phenotype may demonstrate increased cell migration but reduced proliferation (Liu *et al.*, 2014). This is seen between HCC38 and MDA-MB-468 cell lines as HCC38 cells present a more mesenchymal cell morphology and are also slower to proliferate while MDA-MB-468 are much more rounded epithelial like cells and have a faster doubling time. The faster doubling times seen in H737R and HPrexR versus the HCC38 parental cell line may be explained by a shift to a more epithelial phenotype as cells appear smaller, rounder and grow in tighter clusters compared with parental cells (**Figure 3.9**). Although this is more apparent in H737R than HPrexR.



Resistant cell lines have significantly higher  $GI_{50}$  values for either SRA737 or Prexasertib compared to the parental cell line (**Figure 3.7 & 3.8**). Both H737R and HPrexR show similar dose response curves to Prexasertib and SRA737 and similar  $GI_{50}$  values. (**Figure 3.7**) This could suggest that adaptations within these cell lines may be similar. However, the  $GI_{50}$  values of HCC38 resistant cells are very similar to MDA-MB-468 resistant cells showing 35  $\mu$ M to SRA737 and a >5  $\mu$ M to Prexasertib (**Figure 3.7**) compared with MDA-MB-468 cell lines at 25  $\mu$ M and >5  $\mu$ M for SRA737 and Prexasertib respectively (**Figure 3.8**). This would suggest that there is an upper limit of resistance to these CHK1 inhibitors that may be due to a build-up of off target effects at higher concentrations. Despite similar  $GI_{50}$  values HCC38 CHK1 inhibitor resistant cell lines show much greater fold resistance versus the MDA-MB-468 CHK1 inhibitor resistant cell lines, potentially due to the greater sensitivity of the HCC38 parental cell line to CHK1 inhibitor treatment versus the MDA-MB-468 parental cell line.

Interestingly both MDA-737R and MDA-PrexR show a small but significant fold change in their  $GI_{50}$  values for SRA737 versus the parental cell line, while showing large increases against Prexasertib. Resistance levels to Prexasertib exceeded the maximum dose available without high levels of vehicle related toxicity. This made it difficult to determine accurate  $GI_{50}$  values. Dose response curves reveal MDA-737R cells are more sensitive to Prexasertib than the MDA-PrexR cells, as viability almost reaches 50% at 5  $\mu$ M in MDA-PrexR cells while MDA-737R cells are around 70% viability (**Figure 3.8**). The differences in response to Prexasertib between MDA-737R and MDA-PrexR suggest differing mechanisms of resistance and could be related to the ability of Prexasertib to inhibit both CHK1 and CHK2 kinases with similar  $IC_{50}$  values. This indicates that CHK1 inhibitor resistance in the MDA-PrexR cell line may be in part due to a mechanism that compensates for inhibition of CHK2. The MDA-737R cell line may have also developed adaptive responses to CHK2 inhibition, perhaps serendipitously while cell lines were adapted to a continuous exposure of SRA737. In addition, adaptations carried out by both MDA-737R and MDA-PrexR may only have been able to slightly improve fitness

to SRA737 as innate resistance is already very high to this drug as demonstrated by the very high parental GI<sub>50</sub> values.

Multidrug resistance resulting from the upregulation of drug efflux transporters such as MDR1 (P-Glycoprotein) is a known resistance mechanism to cancer therapeutics (Gillet and Gottesman, 2010). It is possible resistance to CHK1i may arise through upregulation of these drug efflux proteins. Western blotting was unable to detect expression of the drug transporter MDR1 in HCC38 and MDA-MB-468 parental or resistant cell lines (**Figure 3.11**). Reversal of MDR1 related multidrug resistance has been shown with the MDR1 inhibitor Verapamil (Tsuruo *et al.*, 1981; Yusa and Tsuruo, 1989). No reversal of resistance to SRA737 or Prexasertib was seen in H737R and HPrexR cell lines with the addition of Verapamil (**Figure 3.13**). This suggests drug efflux is an unlikely candidate for resistance to CHK1 inhibitors SRA737 and Prexasertib in these cell lines.

To investigate further changes to resistant cell lines, cells were profiled with several targeted inhibitors and existing cancer drugs. Differences in GI<sub>50</sub> between parental and resistant cell lines provide clues about changes in biological pathways related to the drug target. Ceralasertib is a selective inhibitor of Ataxia-telangiectasia and RAD3-related (ATR) protein which is a member of the phosphoinositide 3-kinase (PI3K)-related family of protein kinases (Vendetti *et al.*, 2015). ATR responds to single stranded DNA coated with RPA which is essential for localisation and subsequent activation of ATR by its binding partner ATR-interacting protein (ATRIP) (Zou and Elledge, 2003). Activation of ATR allows phosphorylation of CHK1 on S317 and S345 leading to activation of CHK1 and the CHK1 pathway (Zhang and Hunter, 2014). As ATR is directly upstream of CHK1 and is required for its activation it was hypothesised that CHK1i resistant cell lines may respond differently to an ATR inhibitor. CHK1i resistant cell lines do indeed demonstrate significant resistance to ATR inhibition via Ceralasertib with resistance factors of 5.2 for HPrexR and 8.4 for H737R (**Figure 3.14**) while MDA-PrexR and MDA-737R show lower levels of resistance of 3.4- and 2.0-fold resistance respectively (**Figure 3.15**). Cross resistance of HCC38 and MDA-MB-468 CHK1i resistant cell

lines to ATR inhibitor Ceralasertib suggests activity of the CHK1 pathway, or its downstream effectors, are resilient to loss of activation signalling from ssDNA through ATR and CHK1 kinase activity. This helps to partially rule out the potential resistance mechanism of point mutations in the CHK1 protein which may interfere with CHK1i binding affinity in the ATP binding pocket of the kinase. If such a mutation were to exist it would be unlikely that cells would also exhibit cross resistance to a selective ATR inhibitor. However, without sequencing data of the CHK1 gene we cannot be certain of the mutational status.

Adavosertib is a selective inhibitor of WEE1 kinase (Hirai *et al.*, 2009). WEE1 phosphorylates Cyclin Dependent Kinase 1/2 (CDK1/2) on Y15 inhibiting its activity resulting in activation of the G2/M checkpoint and deregulation of S-phase (Parker and Piwnica-Worms, 1992; Leijen *et al.*, 2016). As the CHK1 pathway also helps to regulate CDK1/2 Y15 phosphorylation by the regulation of CDC25 phosphatases (Medema and Macuerek, 2012), it was hypothesised changes in the activity of WEE1 protein kinase could allow cells to compensate for loss of CHK1 activity and therefore resistant cell lines may respond differently to a WEE1 inhibitor when compared to their parental counterparts. H737R and HPrexR cell lines demonstrate resistance to Adavosertib with resistance factors of 10.9- and 7.8-fold respectively (**Figure 3.14**). Interestingly MDA-MB-468 cell lines show little to no resistance to Adavosertib with no change in GI<sub>50</sub> value between MDA-737R and the parental cells. However, there is a slight and significant increase of GI<sub>50</sub> values and a fold resistance of 1.7 for MDA-PrexR cells (**Figure 3.15**). Cross resistance to WEE1 inhibitor Adavosertib in HCC38 resistant cell lines suggests the locus of resistance may be related to CDK1/2 activity, as cells are resilient to perturbations of the two main regulators of this kinase. MDA-MB-468 resistant cell lines show little no difference in their response to Adavosertib compared to the parental cell line suggesting this part of the pathway is unchanged. This may indicate that the resistance mechanism for MDA-MB-468 cell lines is due to the change in a separate pathway, or a CHK1 specific interaction that does not affect CDK1/2 activity.

Cell lines were profiled with inhibitors targeting ataxia-telangiectasia mutated (ATM) and Checkpoint kinase 2 (CHK2). ATM is related to ATR as a member of the PIKKs family of serine/threonine kinases and plays a role in DNA double stranded break (DSB) repair. The MRN complex, consisting of Mre11, Rad50 and Nbs1 proteins binds to double stranded breaks and is required for the subsequent activation and signalling of ATM to activate Chk2 (Uziel *et al.*, 2003). CHK2 is involved in the DNA damage response and once activated signals down to multiple effectors such as CDC25, BRCA1, E2F1 and p53 (Perona *et al.*, 2008). As a result, it can play a significant role in control of cell cycle checkpoints and DNA repair. It was therefore hypothesised that CHK2 and ATM signalling may play an important role in resistance to SRA737 and Prexasertib, especially as Prexasertib also inhibits CHK2.

**Figures 3.16 and 3.17** show no significant difference in GI<sub>50</sub> values in between HCC38 and MDA-MB-468 parental and resistant cell lines against the CHK2 inhibitor CCT241533. However, significant sensitivity was seen in MDA-737R against the ATM inhibitor AZD0156 with an RF of 0.5 which means this cell line was twice as sensitive to AZD0156 than the parental cell line, but no significant difference was detected in MDA-PrexR cells. As mentioned earlier, cross profiling of MDA-MB-468 resistant cell lines with CHK1 inhibitors suggested differences in dose response to Prexasertib may be CHK2 related. If MDA-PrexR cells had undergone changes to compensate for loss of CHK2 activity by Prexasertib then we might see resistance to a CHK2 inhibitor. Surprisingly, this is not the case and suggests that resistance may not be CHK2 related. However, sensitivity to ATM inhibitor AZD0156 in MDA-737R suggests there may be some level of dependency on signalling through ATM to maintain cell viability in this SRA737 resistant cell line. It is important to note that as Prexasertib is a dual inhibitor of CHK1 and CHK2, perhaps any changes related to either signalling pathway may only be apparent during inhibition of both kinases and may be missed when profiling with a CHK2 inhibitor alone.

Both HCC38 and MDA-MB-468 cell lines were profiled against the DNA damaging agent Cisplatin. Upon entering the cell Cisplatin is hydrolysed allowing for its activation and

subsequent DNA damaging activity. Cisplatin damages DNA by binding to purine residues to form intrastrand crosslinks blocking DNA replication and cell cycle division (Dasari and Bernard Tchounwou, 2014). Repair of DNA damage caused by Cisplatin relies on nucleotide excision repair (NER) (Reardon *et al.*, 1999). NER has been implicated in drug resistance to Cisplatin in the past and removes DNA adducts by cleaving the DNA strand around the damage, removing the damaged section of DNA and allowing DNA polymerase to fill the gap using the undamaged strand as a template (Duan *et al.*, 2020). No significant differences in dose response were detected in HCC38 or MDA-MB-468 resistant cell lines (**Figure 3.18**). It is unlikely that changes in NER would confer cross resistance to CHK1 inhibitors as DNA damage caused by CHK1i is attributed to replication fork collapse (Syljuåsen *et al.*, 2005) and likely relies on homologous recombination (HR) for DNA repair (Toledo, Neelsen and Lukas, 2017).

Olaparib, an inhibitor of PARP, an important protein in Base excision repair (BER) has demonstrated synthetic lethality in cells with inactive *BRCA* genes (Lord and Ashworth, 2017). PARP1 and PARP2 are important for cells to manage replication stress in S-phase and may also play a role in HR by stabilising RAD51 at double stranded breaks (Ronson *et al.*, 2018). No difference was observed in dose response to Olaparib in H737R or HPrexR cell lines compared with HCC38 parental cells (**Figure 3.20**). These data suggests that PARP does not play a role in resistance to CHK1 inhibitors in H737R and HPrexR cells. However, changes in the DDR pathway may not be apparent in resistant cells when treated with a single agent, as active CHK1 in H737R and HPrexR cells may be compensating for PARP inhibition. Masking differences between parental and resistant cell lines. H737R and HPrexR cells treated with a drug combination of CHK1i and Olaparib may show differences in response to HCC38 cell lines.

WEE1 regulates both CDK1 and CDK2 activity through the phosphorylation of Y15, leading to inactivation of these two kinase (Do, Doroshov and Kummar, 2013). Western blotting revealed an increase in WEE1 protein in H737R and HPrexR cell lines (**Figure 3.22**). Paired with dose

response data showing resistance to WEE1 inhibitor Adavosertib in H737R and HPrexR cell lines (**Figure 3.14**) this suggests changes in WEE1 protein expression could be compensating for loss of CHK1 signalling via inhibition of CDK1/2. Increased protein expression may also account for the increase in resistance to WEE1 inhibitor Adavosertib as higher concentrations may be required to achieve the same inhibitory effect.

To summarise, in this chapter two TNBC cell lines HCC38 and MDA-MB-468 were drug adapted to both CHK1 inhibitors SRA737 and Prexasertib through the process of dose escalation, and resistant sub lines generated. HCC38 resistant cell lines showed strong resistance to both SRA737 and Prexasertib while MDA-MB-468 cell lines were unable to adapt to SRA737 with high initial GI<sub>50</sub> values suggesting intrinsic resistance to this drug. Cross profiling of parental and resistant cell lines was carried out revealing resistance to the ATR inhibitor Ceralasertib and WEE1 inhibitor Adavosertib in HCC38 resistant sublines. MDA-MB-468 resistant sublines demonstrated resistance to the ATR inhibitor but not the WEE1 inhibitor. WEE1 protein levels were checked by western blot analysis in HCC38 cell lines showing an increase in the WEE1 protein in resistant sublines. This was consistent with the increase in Adavosertib GI<sub>50</sub> values in these cells. As WEE1 is an important regulator of CDK1 and CDK2 activity the G2/M checkpoint and S-phase it was thought that changes in WEE1 protein levels may contribute to the CHK1 inhibitor resistance phenotype of H737R and HPrexR cells. The following chapter investigates the potential role of WEE1 kinase in CHK1 inhibitor resistance.

---

# **Chapter 4**

## **Investigating the role of WEE1 kinase in resistance to CHK1 inhibition**

## 4. Investigating the Role of WEE1 Kinase in Resistance to CHK1 Inhibition

### 4.1 Introduction

The WEE1 tyrosine kinase was first identified in *Schizosaccharomyces pombe* as an important gene in timing cell division and acquired its name due to WEE1 mutant *S. pombe* cells exhibiting significantly reduced cell size (P, 1979). The human WEE1 kinase is a key enforcer of the G2-M cell cycle checkpoint allowing cells with damaged DNA time to repair before progressing through to mitosis (Do, Doroshov and Kummar, 2013). Single agent activity of the WEE1 inhibitor Adavosertib (MK-1775) revealed that WEE1 also regulates S-Phase as inhibition of the kinase caused DNA damage that relied on active replication of DNA (Guertin *et al.*, 2013).

Progression through the cell cycle is controlled by the family of cyclin-dependent kinases (CDKs) which consist of 14 serine/threonine protein kinases that associate with different cyclin subunits (Malumbres and Barbacid, 2009). The CDK1/Cyclin B complex controls progression from G2 into mitosis (Lindqvist, Rodríguez-Bravo and Medema, 2009), while CDK2/Cyclin E promotes the transition from G1 into S-phase (Giacinti and Giordano, 2006) and CDK2/Cyclin A regulates S-phase related processes (Girard *et al.*, 1991). WEE1 controls CDK activity via inhibitory phosphorylation of Y15 on CDK1/2 (Elbæk, Petrosius and Sørensen, 2020). WEE1 works in opposition to the CDC25 phosphatases, which dephosphorylate CDK1/2 leading to their activation (Gabrielli *et al.*, 1992; J, 2007). CDC25s are regulated by CHK1, which when activated by DNA damage phosphorylates CDC25 leading to its subsequent sequestration or degradation (Zhang and Hunter, 2014). Therefore, WEE1 and CHK1 work together to maintain CDKs in an inactive state until their activity is required.



WEE1 is regulated by controlling stability of the protein and mRNA levels. Kinase activity of WEE1 remains active throughout the life of the protein, unlike many kinases which require phosphorylation to modulate their activity (Elbæk, Petrosius and Sørensen, 2020). Degradation of WEE1 is reduced by 14-3-3 $\beta$  which binds to the C-terminus of the protein, increasing the half-life of WEE1 and subsequently its kinase activity due to the increased levels of WEE1 protein. 14-3-3 $\beta$  potentially increases WEE1 half-life by inducing a conformational change in WEE1 which blocks a degradation motif located on the N-terminus (Wang *et al.*, 2000; Lee, Kumagai and Dunphy, 2001; Rothblum-Oviatt, Ryan and Piwnica-Worms, 2001). Heat shock protein 90 (HSP90) and MIG6 (also known as ERBB receptor feedback inhibitor 1 (ERRFI1)) have also been shown to interact with WEE1 reducing the rate of protein degradation (Aligue, Akhavan-Niak and Russell, 1994; M *et al.*, 2018). Polo-like kinase 1 (PLK1) and CDK1 have also been shown to phosphorylate WEE1 on s53 and s123 leading to its degradation by  $\beta$ -TrCP E3 ubiquitin ligase (N *et al.*, 2004). Kruppel-Like Factor 2 (KLF2) and microRNA miR-195 have been shown to negatively regulate WEE1 mRNA levels through transcriptional repression (Wang *et al.*, 2005; Bhattacharya *et al.*, 2012).

WEE1 is highly expressed in a number of cancer types including breast, cervical, lung and ovarian cancers and is associated with tumour progression and poor disease-free survival (Matheson, Backos and Reigan, 2016). However, downregulation of WEE1 has also been seen in cancers such as non-small cell lung cancer and colon cancer and was also associated with poor prognosis in patients (Backert *et al.*, 1999; Yoshida *et al.*, 2004) suggesting the impact of WEE1 levels on patient survival is context dependent. Due to WEE1's critical role in the cell cycle and regulation of CDK activity, it has become an important target for treatment of cancer. Inhibitors of WEE1 have been reported to potentiate the effects of DNA damaging agents (Hirai *et al.*, 2009, 2010) and shown potential as a single agent (Guertin *et al.*, 2013; Do *et al.*, 2015). The WEE1 inhibitor Adavosertib has also been shown to enhance the effect of CHK1 inhibitors (Russell *et al.*, 2013; Chilà *et al.*, 2015). In addition to Adavosertib, three

other WEE1 inhibitors are in clinical development, namely IMP7068, ZN-c3 and DEbio 0123 (*ClinicalTrials.gov*, 2021).

In the previous chapter, TNBC cell lines HCC38 and MDA-MB-468 were drug adapted to CHK1 inhibitors SRA737 and Prexasertib. MDA-MB-468 cells were innately more resistant to both CHK1 inhibitors compared with the HCC38 cell line (**Figures 3.7 & 3.8**). H737R and HPrexR cells demonstrated high fold-resistance to CHK1 inhibition relative to MDA-737R and MDA-PrexR cell lines, suggesting they have undergone significant phenotypic changes. In addition, H737R and HPrexR demonstrated cross resistance to the WEE1 inhibitor Adavosertib, which was not seen in MDA-MB-468 CHK1i adapted cell lines. Subsequently, western blot analysis identified high WEE1 expression in H737R and HPrexR cell lines. I hypothesised increased expression of WEE1 protein may compensate for CHK1 inhibition via increased phosphorylation of the inhibitory Y15 on CDK1/2 (**Figure 4.1**). Therefore, this chapter investigates WEE1 and its role in resistance to CHK1 inhibition in H737R and HPrexR cells.

### Chapter aims and objectives

- Investigate the role of WEE1 in resistance to CHK1 inhibitors.
  - Western blot DDR cell signalling in response to CHK1 and WEE1 inhibitors.
  - Measure WEE1 degradation by cycloheximide time course experiment.
- Validate increased levels of WEE1 protein as a mechanism of CHK1i resistance.
  - Combined inhibition of CHK1 and WEE1 kinases to overcome resistance.
  - Knockdown WEE1 levels via SiRNA.
  - Overexpress WEE1 in parental cell lines to artificially generate resistance.
  - Compare levels of WEE1 protein and CHK1i GI<sub>50</sub> data across a panel of TNBC cell lines.

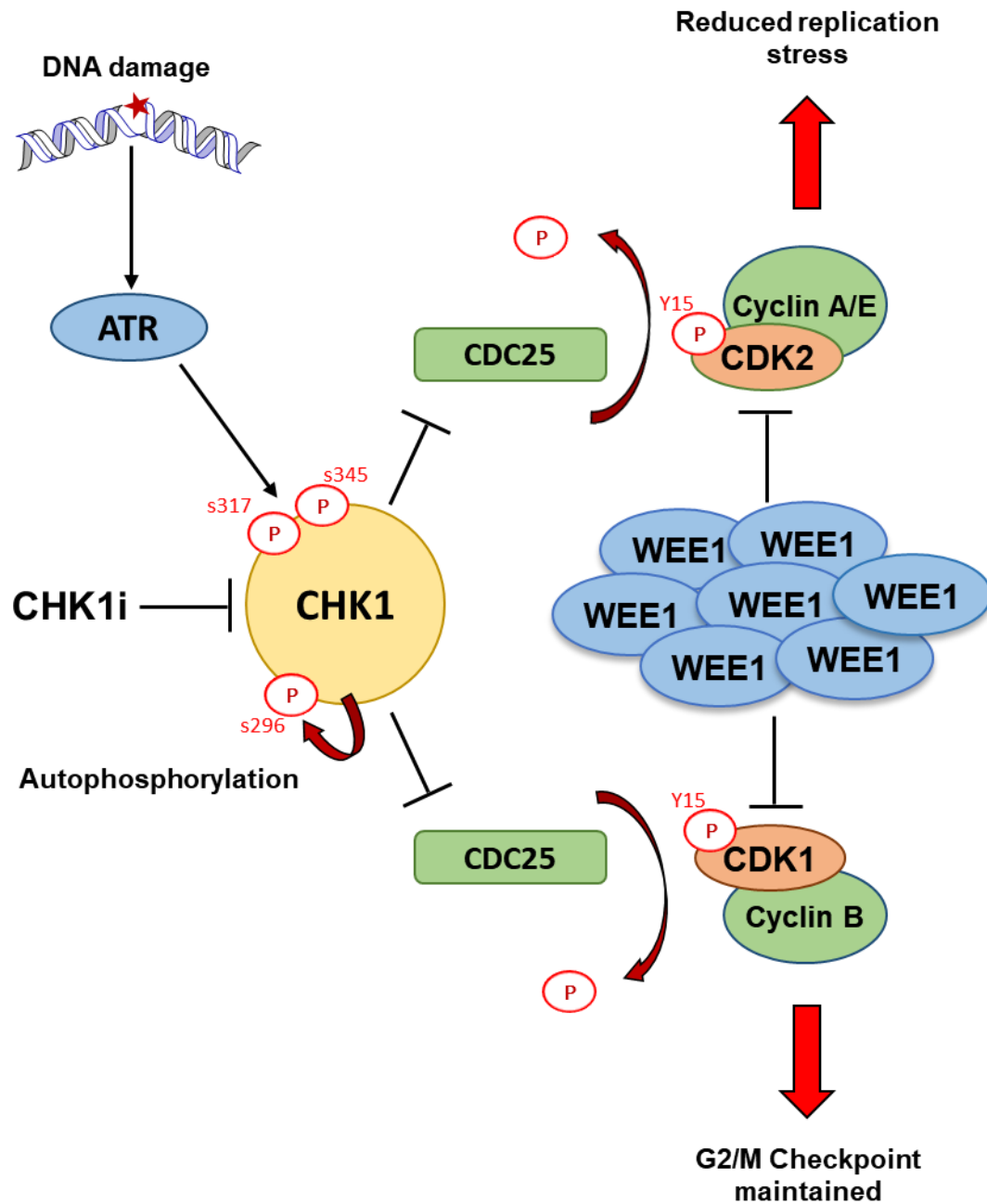


**Figure 4.1: Hypothesis: WEE1 overexpression compensates for CHK1 inhibition and activation of CDC25 by maintaining inhibitory phosphorylation of CDK1/2.**

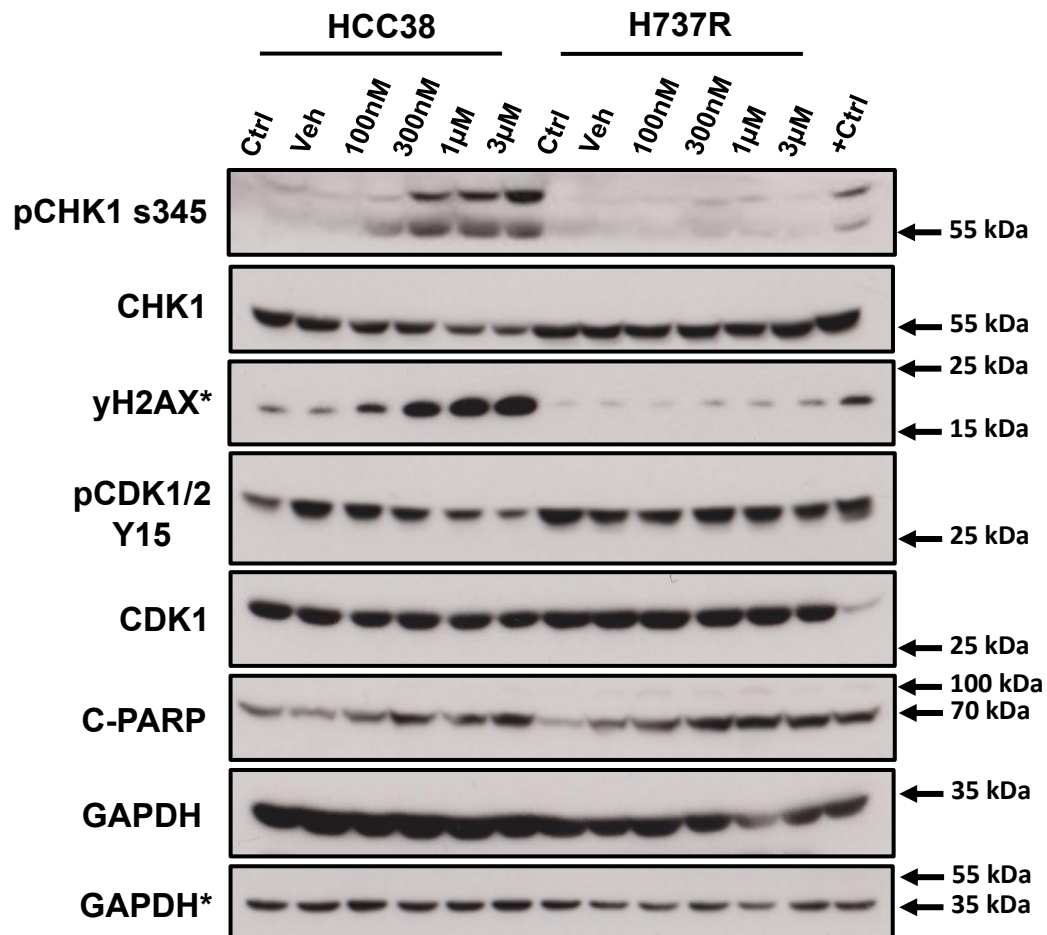
## 4.2 Results

### 4.2.1 Investigating the effect of SRA737 on the DNA damage response and the cell cycle

Cross profiling experiments revealed resistance to WEE1 inhibitor Adavosertib in HCC38 resistant cell lines (**Figure 3.14**). These experiments highlighted CDK1/2 activity as a potential locus of resistance. This is because both CHK1 and WEE1 both regulate CDK1/2 by controlling Y15 phosphorylation, inhibiting the activity of these kinases in response to DNA damage and replication stress. We hypothesised H737R and HPrexR cell lines may be maintaining phosphorylation of CDK1/2 Y15 during CHK1 inhibition to either uphold the G2/M checkpoint or regulate replication stress in S-phase. To investigate this, HCC38 and H737R cells were treated with a titration of the CHK1 inhibitor SRA737 for 24 hours (**Figure 4.2**) or treated with 1 $\mu$ M SRA737 at multiple time points (**Figure 4.3**) followed by lysis and analysis of protein content via western blot. CDK1/2 Y15 and other targets involved in the DNA damage response, apoptosis, and regulation of cell cycle checkpoints were investigated.

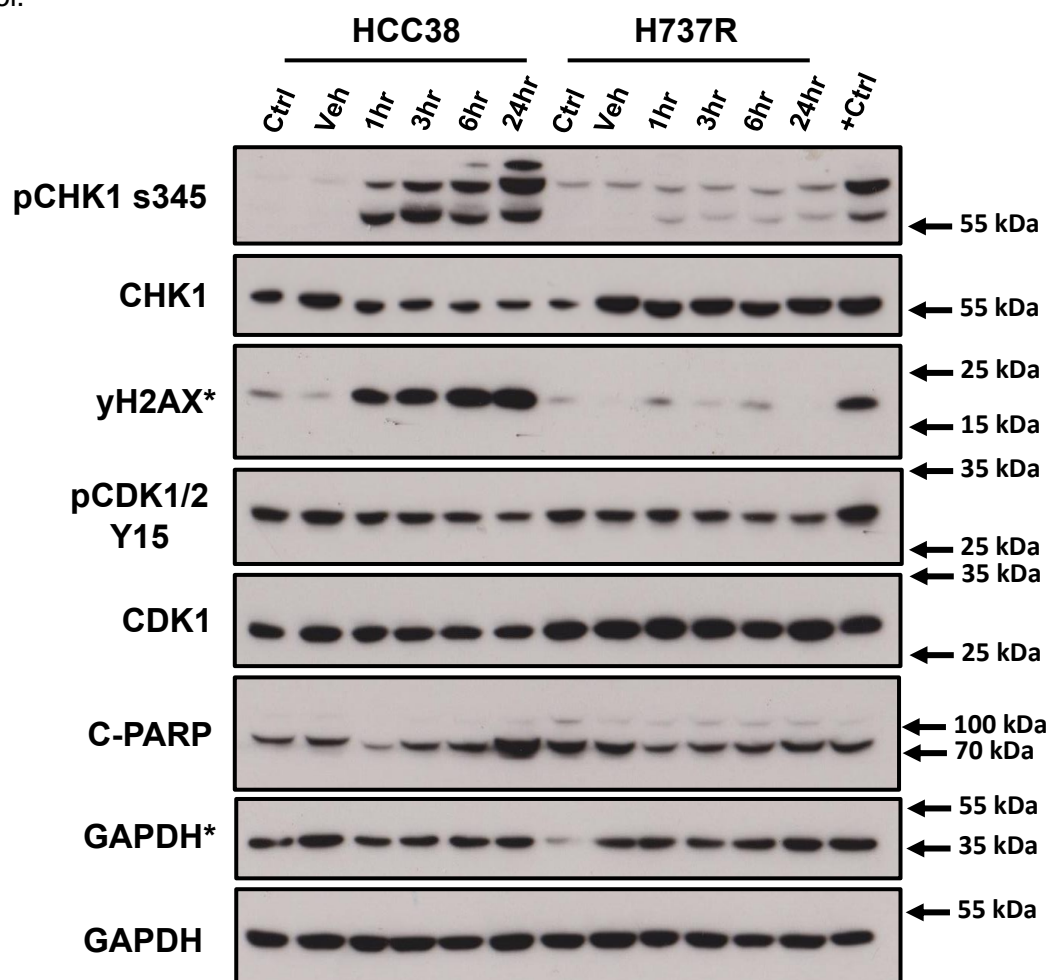
The western blot showing the dose response to SRA737 in HCC38 and H737R cell lines show CHK1 is phosphorylated on S345 in HCC38 cells in response to SRA737 but not in H737R and increases with increasing SRA737 concentration in HCC38 cells (**Figure 4.2**).  $\gamma$ H2AX levels, a marker of DNA damage also increases with higher concentrations of SRA737 in HCC38 but not H737R cells (**Figure 4.2**). H737R cells maintained pCDK1/2 Y15 phosphorylation during SRA737 treatment compared with HCC38 cells which showed reduced pCDK1 Y15 at drug concentrations of 1 & 3 $\mu$ M (**Figure 4.2**). It is important to note that the antibody recognising pCDK1 Y15 also recognises pCDK2 Y15. As the molecular weights of these proteins are very similar it is not possible to distinguish between either signal in this blot. Cleaved PARP (C-PARP) a marker of apoptosis, does not show a clear distinction between HCC38 and H737R cell lines (**Figure 4.2**), however this is potentially due to technical error. A comparison of C-PARP levels between SRA737 dose response westerns is shown in

**Appendix 4.1.** This shows a slightly higher levels of C-PARP in HCC38 cells relative to H737R at higher doses of SRA737 in 2 out of 3 experiments.



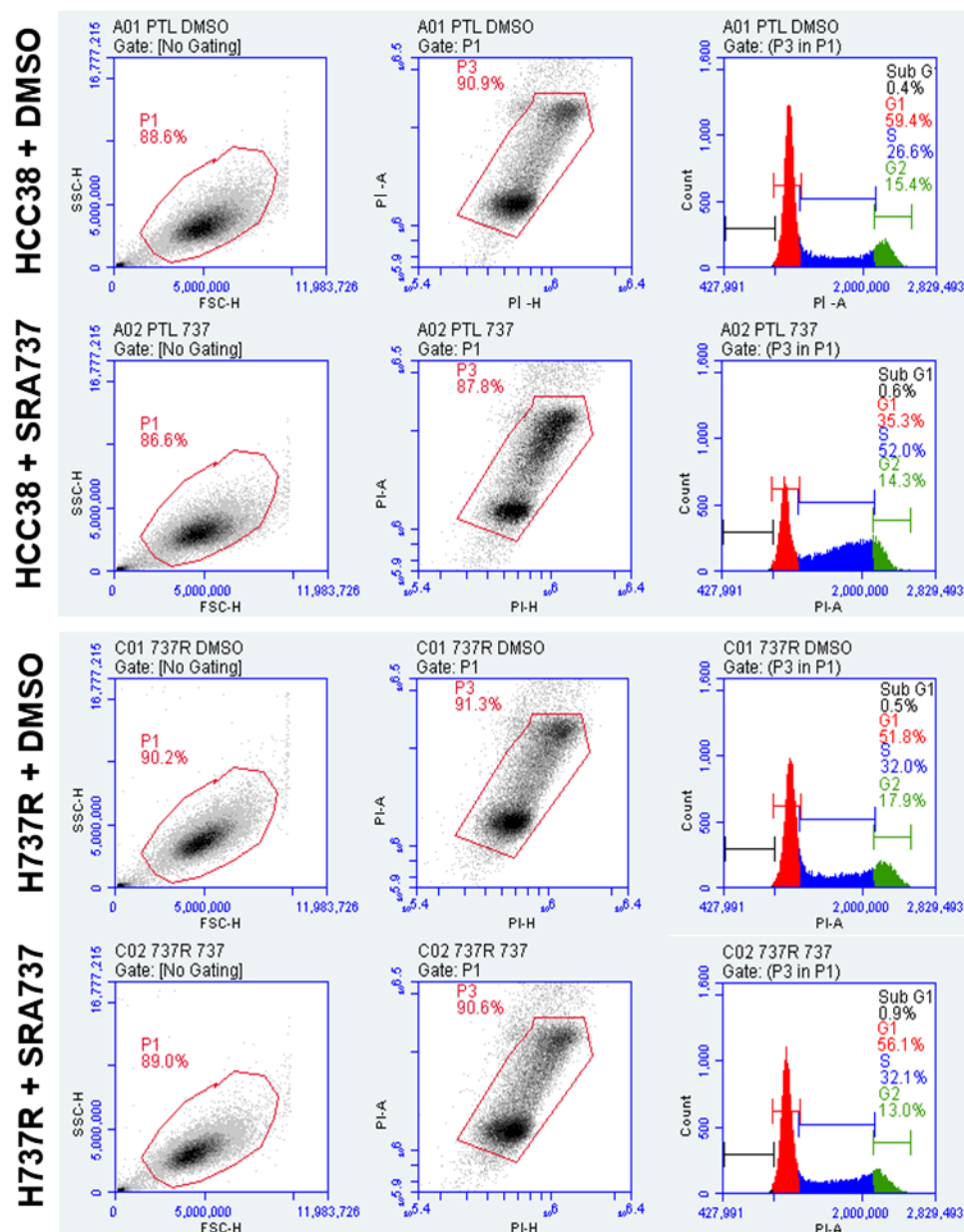
**Figure 4.2: Western blot analysis of SRA737 dose response in HCC38 and H737R cell lines.** Cells were plated in 7cm dishes and left to adhere overnight before incubation with SRA737 at the concentrations indicated for 24 hours before lysis and analysis via western blot. GAPDH = loading Control. Ctrl = Untreated cells. Veh = Vehicle control (DMSO). +Ctrl = HCC38 cells treated with 5μM Cisplatin for 24 hours as a positive DNA damage control. \* Indicates which loading control corresponds with each target. Blots are representative of n=3 experiments.

Analysis of SRA737 dose response across multiple timepoints showed CHK1 phosphorylation at S345 occurs as soon as 1 hour after drug treatment in HCC38 but not H737R cells (**Figure 4.3**). The DNA damage marker  $\gamma$ H2AX is also increased within an hour of SRA737 treatment in HCC38 but not H737R cells (**Figure 4.3**). Maintenance of pCDK1/2 Y15 in H737R cells is less pronounced in **figure 4.3** compared with **figure 4.2**. Interestingly, C-PARP signal decreased 1hr after treatment with SRA737 but shows a net increase at 24hrs relative to the control in HCC38 cells (**Figure 4.3**). This decrease in C-PARP is also seen in H737R cells but after 24 hours incubation with SRA737, C-PARP signal does not exceed that of the untreated control.



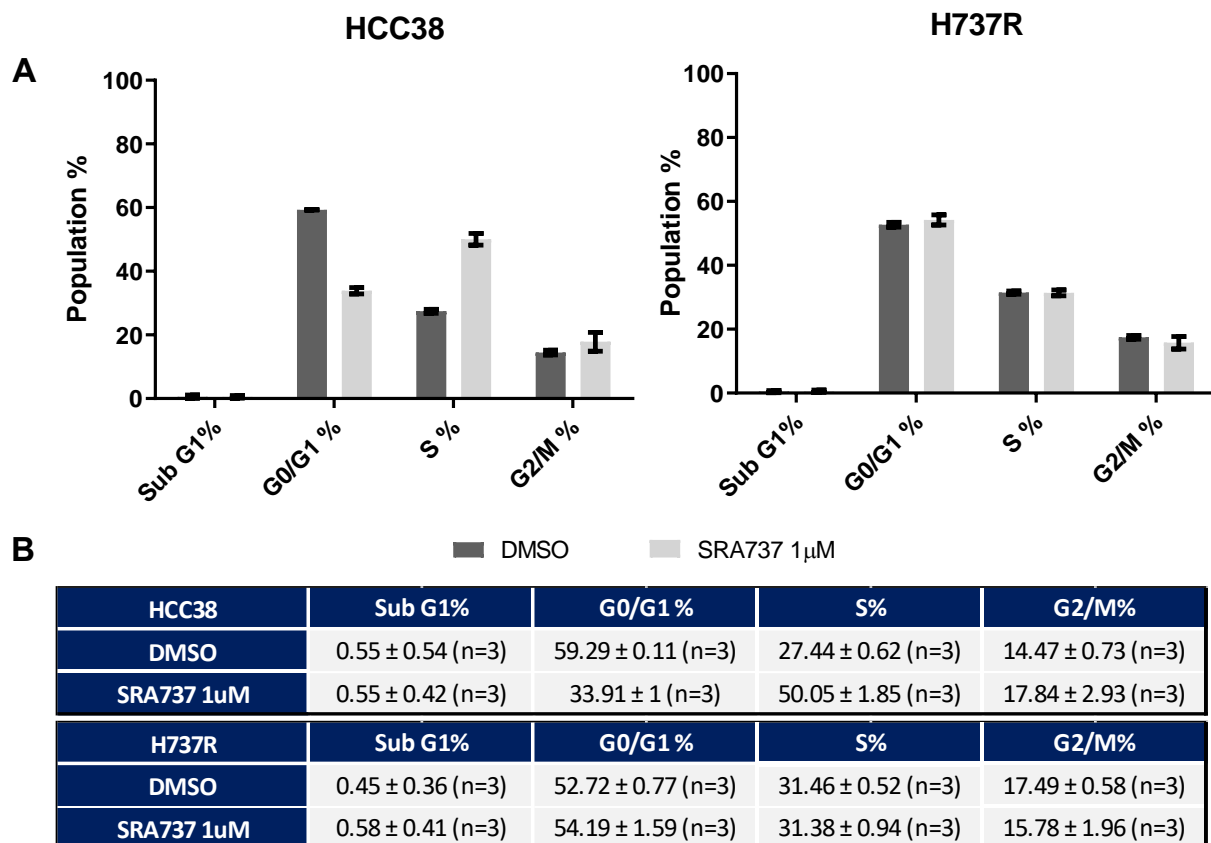
**Figure 4.3: Western blot analysis of SRA737 effect over time on HCC38 and H737R cell lines.** Cells were plated in 7cm dishes and left to adhere overnight before incubation in  $1\mu\text{M}$  SRA737 for the time stated before lysis and analysis via western blot. GAPDH = loading Control. Ctrl = Untreated cells. Veh = Vehicle control (DMSO). +Ctrl = HCC38 cells treated with  $5\mu\text{M}$  Cisplatin for 24 hours as a positive DNA damage control. \* Indicates which loading control corresponds with each target. Blots are representative of  $n=3$  experiments.

As CHK1 is a critical regulator of multiple checkpoints in the cell cycle, it was considered important to investigate the effects of SRA737 on the cell cycle distribution. Therefore, HCC38 and H737R cells were treated with 1 $\mu$ M SRA737 or a DMSO control for 24 hours before cell cycle analysis via propidium iodide (PI) staining and flow cytometry. 1 $\mu$ M SRA737 was used as this concentration increased DNA damage marker  $\gamma$ H2AX and signalling for activation of CHK1 by phosphorylation of S345 in HCC38 cells, suggesting an activation of the DNA damage response which may affect progression through the cell cycle. Cell cycle analysis revealed that HCC38 cells accumulated in S-phase after treatment with SRA737, but this was not seen in the H737R cell line (**Figures 4.4 & 4.5**). On average, the S-phase population of cells increased by approximately 25% from 27.44% to 50.05% in HCC38 cells after treatment with 1 $\mu$ M SRA737 while H737R maintained an S-phase population of approximately 31% (**Figure 4.5**). The G0/G1 population in HCC38 decreased by approximately 30% from 59.29% to 33.81% with 1 $\mu$ M SRA737 treatment while for H737R cells there was little difference between DMSO and SRA737 treatments in G0/G1 population (**Figure 4.5**). The Sub G1 and G2/M populations showed no changes for either HCC38 or H737R with 1 $\mu$ M SRA737 (**Figure 4.5**).



**Figure 4.4: Propidium iodide (PI) cell cycle analysis of HCC38 and H737R cell lines +/- SRA737.** Analysis of cell cycle distribution in HCC38 and H737R cell lines via flow cytometry. Cells were plated in T25 flasks and left to adhere overnight before 24hr incubation in 1 $\mu$ M SRA737 or DMSO control. Cells were fixed in ethanol and DNA stained with PI before analysis on a BD Accuri™ C6 flow cytometer. G1 = G1/G0 and G2 = G2/M phases. Representative forward versus side scatter plots, PI-Area versus PI-Height plots and PI density histograms showing gating of cell cycle populations. Data representative of n=3 experiments.



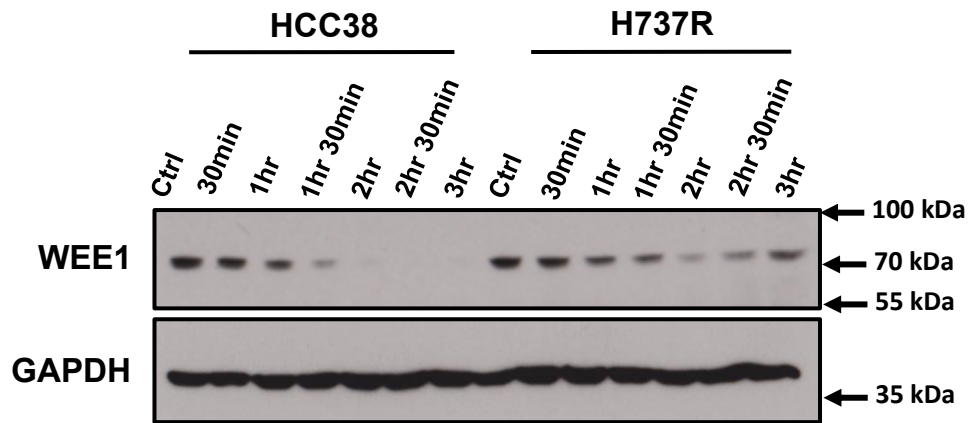
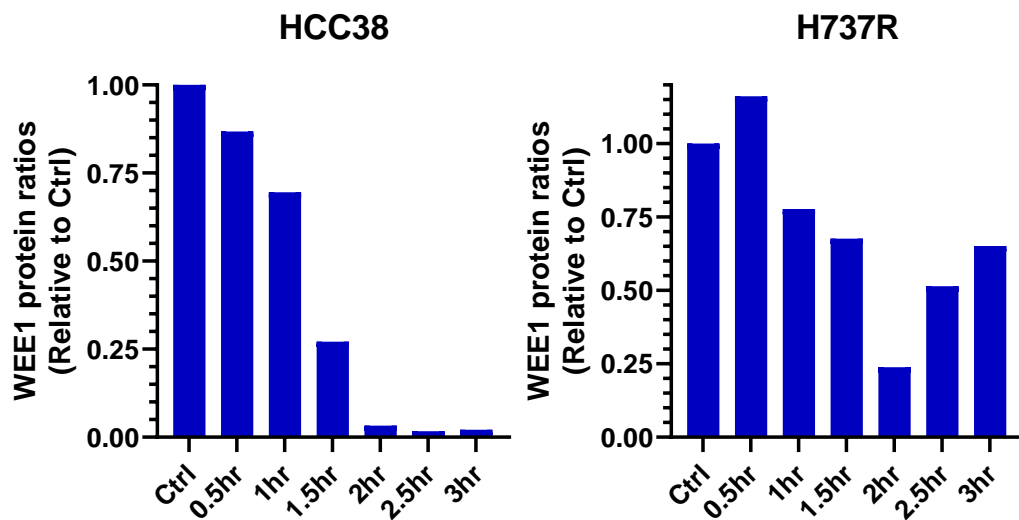


**Figure 4.5: bar chart of Propidium iodide (PI) cell cycle analysis of HCC38 and H737R cell lines +/- SRA737. A)** Bar chart showing the average percentage +/- the standard deviation of cells in each stage of the cell cycle. **B)** Table showing average percentages +/- the standard deviation of cell cycle populations shown in **A**. (n) indicates the number of independent experiments.

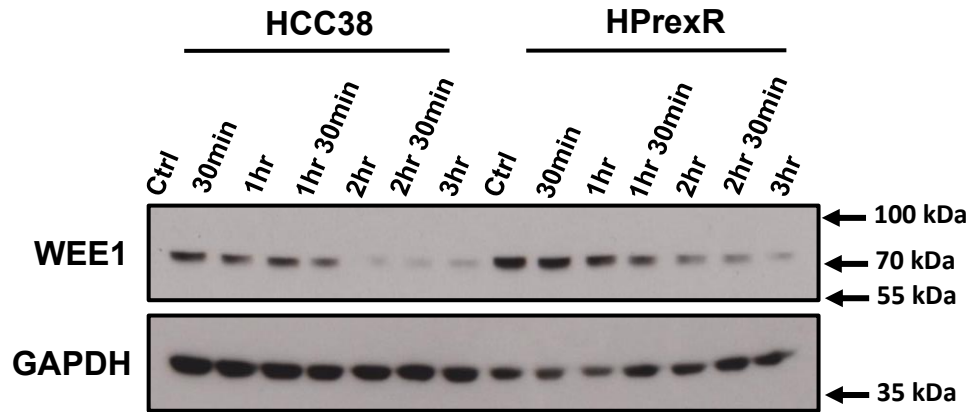
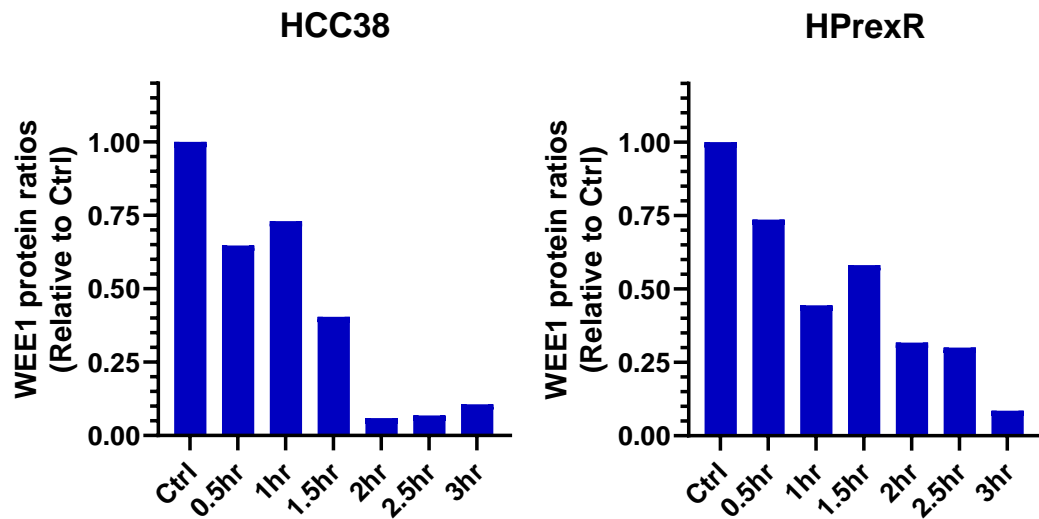
#### 4.2.2 Investigating the role of WEE1 in CHK1i resistance via targeted inhibitors of WEE1

WEE1 protein may be overexpressed due to changes in protein degradation leading to increased protein stability. To investigate this, WEE1 protein levels in HCC38, H737R and HPrexR cell lines were measured by western blot after incubation in the presence of cycloheximide, which inhibits protein synthesis by stopping translocation elongation of the ribosome and blocking formation of the polypeptide chain (Schneider-Poetsch *et al.*, 2010). As new protein can no longer replace degraded protein, it is possible to measure protein stability (Buchanan *et al.*, 2016).

Interestingly, H737R cell lines appear to degrade WEE1 at a slower rate than HCC38 cells (**Figure 4.6**). By the 3-hour timepoint < 10% of WEE1 protein signal remains in HCC38 cells while >50% remains in H737R cells (**Figure 4.6**). Generally, H737R WEE1 expression is variable but remains high relative to HCC38 cells across the period of the experiment suggesting the rate of WEE1 degradation is decreased in H737R cells (**Figure 4.6 A**). On the other hand, WEE1 degradation in HPrexR cells appears similar to that of the HCC38 cell line (**Figure 4.7**). By the 3-hour time point both cell lines show approximately 10% of WEE1 signal relative to their respective controls (**Figure 4.7**). However, HPrexR remains at around 25% relative expression at 2 & 2.5-hour timepoints while HCC38 remains at approximately 10%. This suggests HPrexR cells also show a decreased rate of WEE1 degradation. It is important to note that the quality of the GAPDH loading controls make it difficult to accurately quantify via densitometry. Nevertheless, WEE1 degradation does appear to be decreased relative to parental cells.

**A****B**

**Figure 4.6: Time course of HCC38 and H737R cells incubated with cycloheximide.** HCC38 and H737R cell lines were plated in 6-well plates and allowed to adhere overnight. Cells were then incubated in media containing 300µg/ml cycloheximide for the time stated before lysis and analysis via western blot for the proteins indicated. **A)** Representative western blot of n=2 experiments. GAPDH = loading control, Ctrl = No treatment with cycloheximide. **B)** Densitometry of **A)** carried out on ImageJ. Each sample was normalised to the corresponding GAPDH loading control. Bar graphs are representative of n=2 experiments.

**A****B**

**Figure 4.7: Time course of HCC38 and HPrexR cells incubated with cycloheximide.** HCC38 and HPrexR cell lines were plated in 6-well plates and allowed to adhere overnight. Cells were then incubated in media containing 300 $\mu$ g/ml cycloheximide for the time stated before lysis and analysis via western blot for the proteins indicated. **A)** Representative western blot of n=2 experiments. GAPDH = loading control, Ctrl = No treatment with cycloheximide. **B)** Densitometry of **A)** carried out on ImageJ. Each sample was normalised to the corresponding GAPDH loading control. Bar graphs are representative of n=2 experiments.

As H737R and HPrexR cell lines appear to demonstrate resistance to the WEE1 inhibitor Adavosertib (**Figure 3.14**) and overexpress WEE1 protein (**Figure 3.22**), we investigated the effects of Adavosertib on DDR, apoptosis, and cell cycle related proteins (**Figure 4.8**). HCC38 and H737R cell lines were treated with a titration of Adavosertib and incubated for 24 hours before lysis and analysis via western blot. pCHK1 S345 was induced with increasing concentrations of Adavosertib in the HCC38 cell line but to a lesser degree in H737R cells (**Figure 4.8**). At low doses of Adavosertib (50nM), the yH2AX signal increased in the HCC38 cell line but not in H737R cells (**Figure 4.8**). yH2AX signal in H737R cells only increased at much higher concentrations of Adavosertib (1 $\mu$ M and 2 $\mu$ M) in the same range as the SRA737 resistant cell line GI<sub>50</sub> value of 1.55  $\mu$ M for Adavosertib (**Figures 3.14 & 4.8**). Interestingly pCDK1/2 Y15 was not maintained in either HCC38 or H737R cell lines in the presence of Adavosertib (**Figure 4.8**) while for H737R cells treated with SRA737, pCDK1/2 Y15 was maintained (**Figure 4.2**). Additionally, CDK1 protein decreases in HCC38 in 1-2 $\mu$ M of Adavosertib which is not seen in H737R (**Figure 4.8**). C-PARP signal increased with an increasing Adavosertib concentration but to a lesser extent in H737R versus HCC38 cells (**Figure 4.8**). Total WEE1 protein also decreased at high concentrations of Adavosertib in both cell lines (**Figure 4.8**). Interestingly Adavosertib seems to have similar molecular effects to SRA737 on HCC38 cells, as both drugs induce yH2AX and pCHK1 S345 and a loss of pCDK1 Y15 in addition to increased C-PARP (**Figures 4.2 & 4.8**). On the other hand, H737R is much more responsive to Adavosertib exposure than SRA737, which is to be expected as H737R is 17 times more resistant to SRA737 than Adavosertib. However, H737R is still more resistant than HCC38 to the effects of Adavosertib showing minimal induction of yH2AX and pCHK1 S345 at 40-200nM.

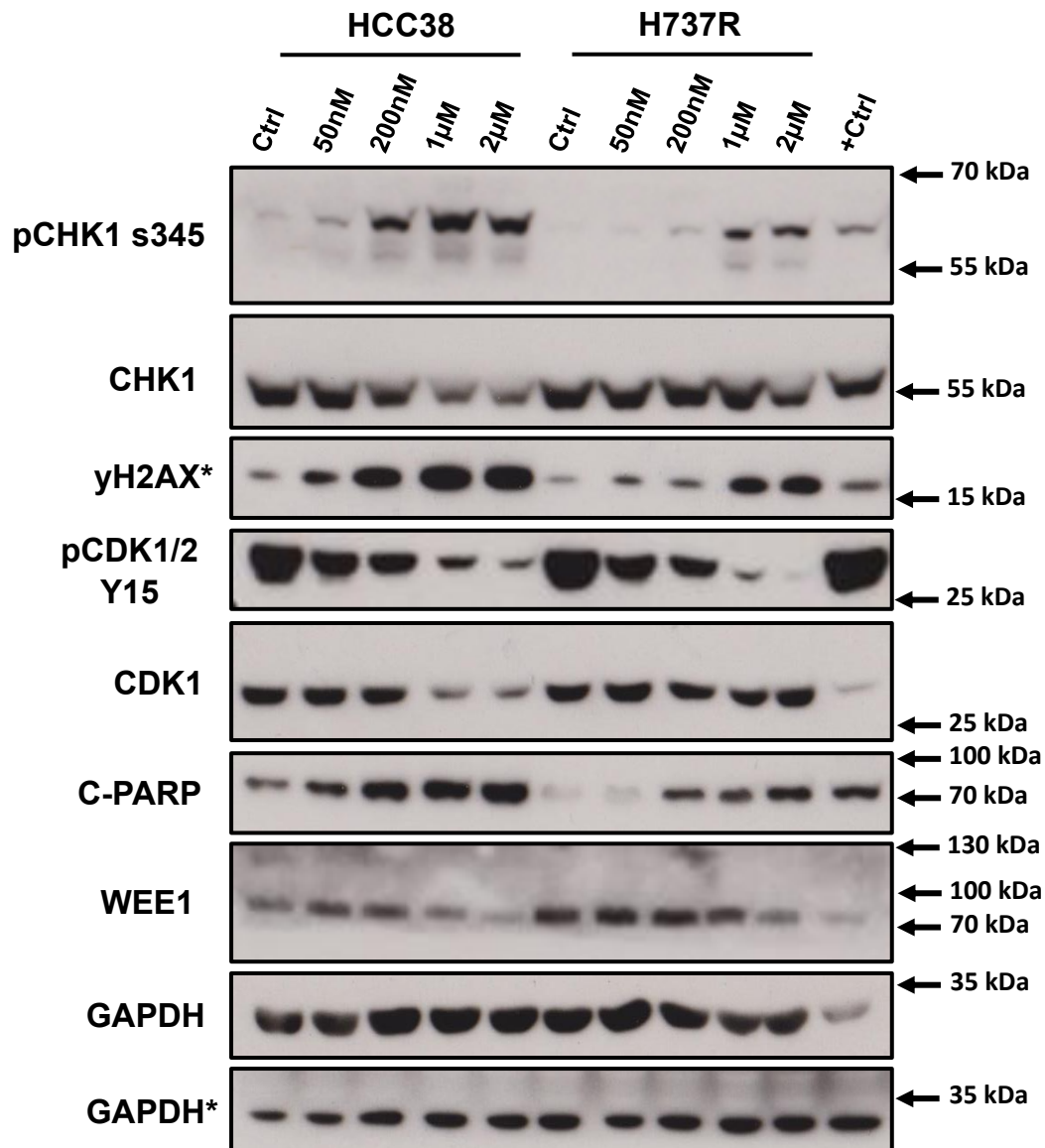


**Figure 4.8: Western blot analysis of Adavosertib dose response in HCC38 and H737R cell lines.** Cells were plated in 7cm dishes and left to adhere overnight before incubation with Adavosertib at the concentrations indicated for 24 hours before lysis and analysis via western blot for the proteins indicated above. GAPDH = loading control. Ctrl = untreated cells. +Ctrl = HCC38 cells treated with Cisplatin 5μM for 24 hours as a positive control for DNA damage. \* Indicates which loading control corresponds with each target. Blots are representative of n=3 experiments.

We hypothesised increased levels of WEE1 protein may be compensating for CHK1 inhibition by maintaining the inhibitory phosphorylation on CDK1/2. Increased WEE1 protein levels may also explain resistance to the WEE1 inhibitor Adavosertib as higher concentrations may be required to achieve the same inhibitory effect. If this is the case, treatment of resistant cell lines with Adavosertib in combination with SRA737 may be able to sensitise resistant cells to

SRA737. To test this theory, we treated HCC38 and H737R cells with a combination of SRA737 1 $\mu$ M and either the GI<sub>10</sub> or GI<sub>20</sub> of Adavosertib for H737R for 24 hours and analysed changes in protein expression and signalling by western blot (**Figure 4.9**).

HCC38 cells treated with the drug combination show higher induction of  $\gamma$ H2AX and pCHK1 S345 than cells treated with SRA737 alone (**Figure 4.9**) suggesting SRA737 and Adavosertib are acting synergistically to increase DNA damage. H737R cells also show a much higher level of  $\gamma$ H2AX and pCHK1 S345 signals with the drug combination versus with SRA737 treatment alone, but these signals are still lower than seen in HCC38 cells treated with the drug combination (**Figure 4.9**). Interestingly, the  $\gamma$ H2AX signal in H737R cells treated with the drug combination are similar to that seen in HCC38 treated with 1 $\mu$ M SRA737, suggesting cells may be re-sensitised to SRA737 treatment (**Figure 4.9**). Both cell lines exhibit loss of pCDK1/2 Y15 and increased levels of C-PARP (**Figure 4.9**) suggesting CDK activity is increased, and cells may be undergoing apoptosis.

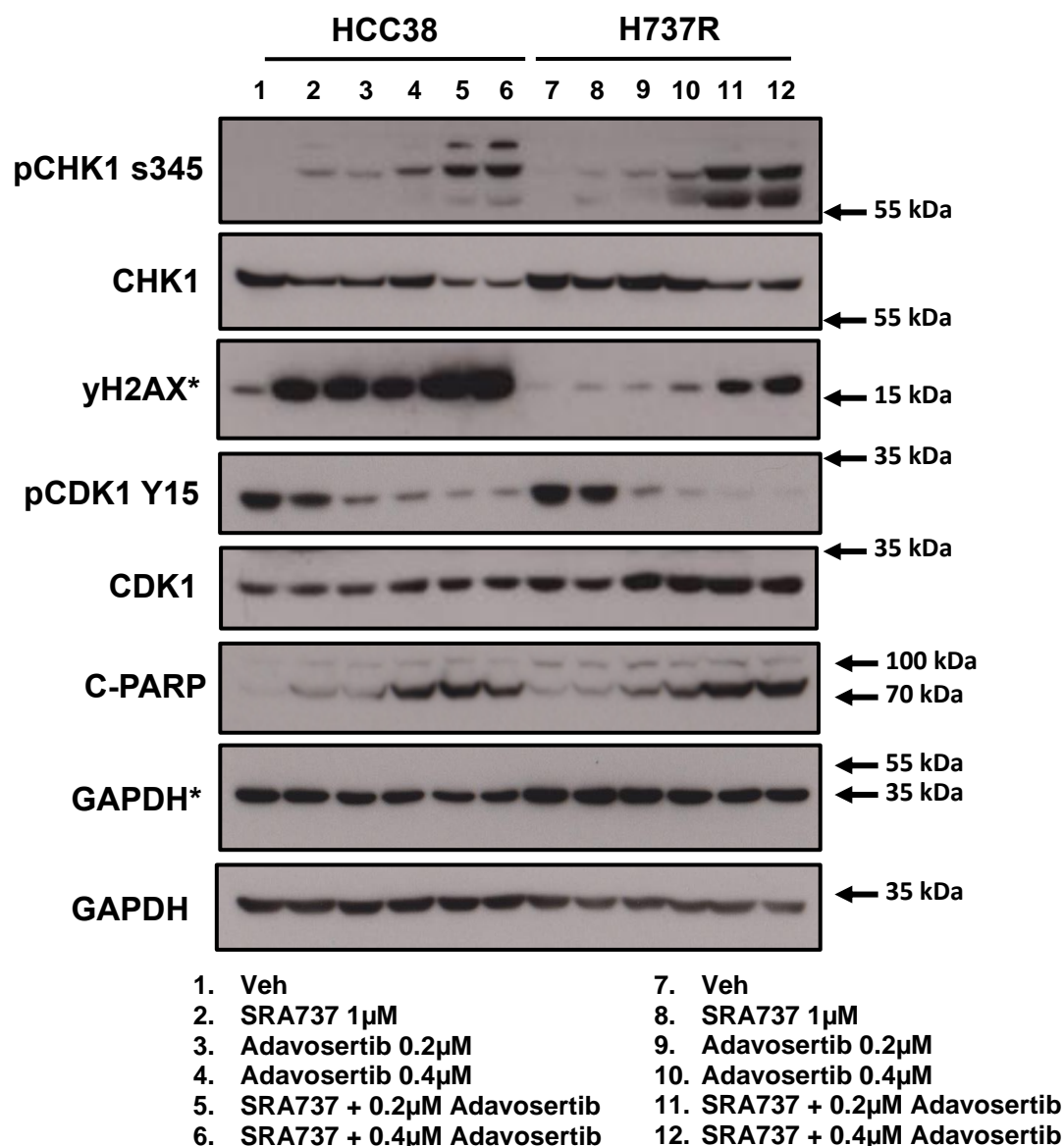


**Figure 4.9: Western blot analysis of HCC38 and H737R cell lines treated with SRA737, Adavosertib or a combination of both drugs.** Cells were plated in 7cm dishes and left to adhere overnight before incubation with SRA737, Adavosertib or a combination of both drugs at the concentrations indicated for 24 hours before lysis and analysis via western blot of proteins indicated above. GAPDH = loading control. Veh = Vehicle control (DMSO). \* Indicates which loading control corresponds with each target. Blots are representative of n=3 experiments.

To identify the effects Adavosertib and SRA737 may be having on the cell cycle, cells were treated with either drug alone or a combination of both drugs for 24 hours and analysed via PI staining and flow cytometry (**Figures 4.10-4.13**). In HCC38 cells, treatment with Adavosertib alone greatly increased the S-phase population and reduced the G0/G1 population of cells in a dose-dependent manner relative to the DMSO control. The G0/G1 population percentage dropped from 59% to 40% and 27% with treatment of 0.2 $\mu$ M and 0.4 $\mu$ M Adavosertib respectively. Whilst S-phase increased from 27% to 41% and 49% with 0.2 $\mu$ M and 0.4 $\mu$ M



respectively (**Figures 4.10 & 4.12**). The percentage of HCC38 cells in G2/M also increased from 14% to 26% in cells treated with 0.4 $\mu$ M Adavosertib (**Figures 4.10 & 4.12**). The drug combination of Adavosertib and SRA737 had a strong effect on the cell cycle in HCC38 cells leading to almost 80% of cells being in S-phase while the G0/G1 population was reduced to below 10% (**Figures 4.10 & 4.12**). The G2/M population of HCC38 cells was slightly increased from approximately 14% in the untreated control up to approximately 17-19% of cells in G2/M during treatment with the drug combination (**Figures 4.10 & 4.12**). No discernible differences were detected in the sub-G1 population of cells (**Figures 4.10 & 4.12**).

H737R cells show little difference in response to Adavosertib on its own but do show a decrease in G0/G1 population with the drug combination from 53% down to 30%. H737R cells appeared more resistant to the drug combination than HCC38 cells but showed a significant increase in cells in S-phase from approximately 31% in the DMSO control up to approximately 55% with the drug combination (**Figures 4.11 & 4.13**). The G2/M population of cells shows a small decrease from 17% down to 14% in H737R cells in response to the drug combination (**Figures 4.11 & 4.13**). No differences in the Sub-G1 population of H737R cells was detected between conditions (**Figures 4.11 & 4.13**). The increase in S-phase of H737R cells in response to the drug combination mirrors that of HCC38 cells treated with SRA737 alone (**Figures 4.4 & 4.5**). This suggests that while H737R is more resistant to the drug combination of SRA737 and Adavosertib, use of this WEE1 inhibitor can restore sensitivity to SRA737 treatment at least in terms of the phenotypic response seen in the cell cycle (**Figures 4.10-4.12**) and molecular signalling (**Figure 4.9**).

## HCC38

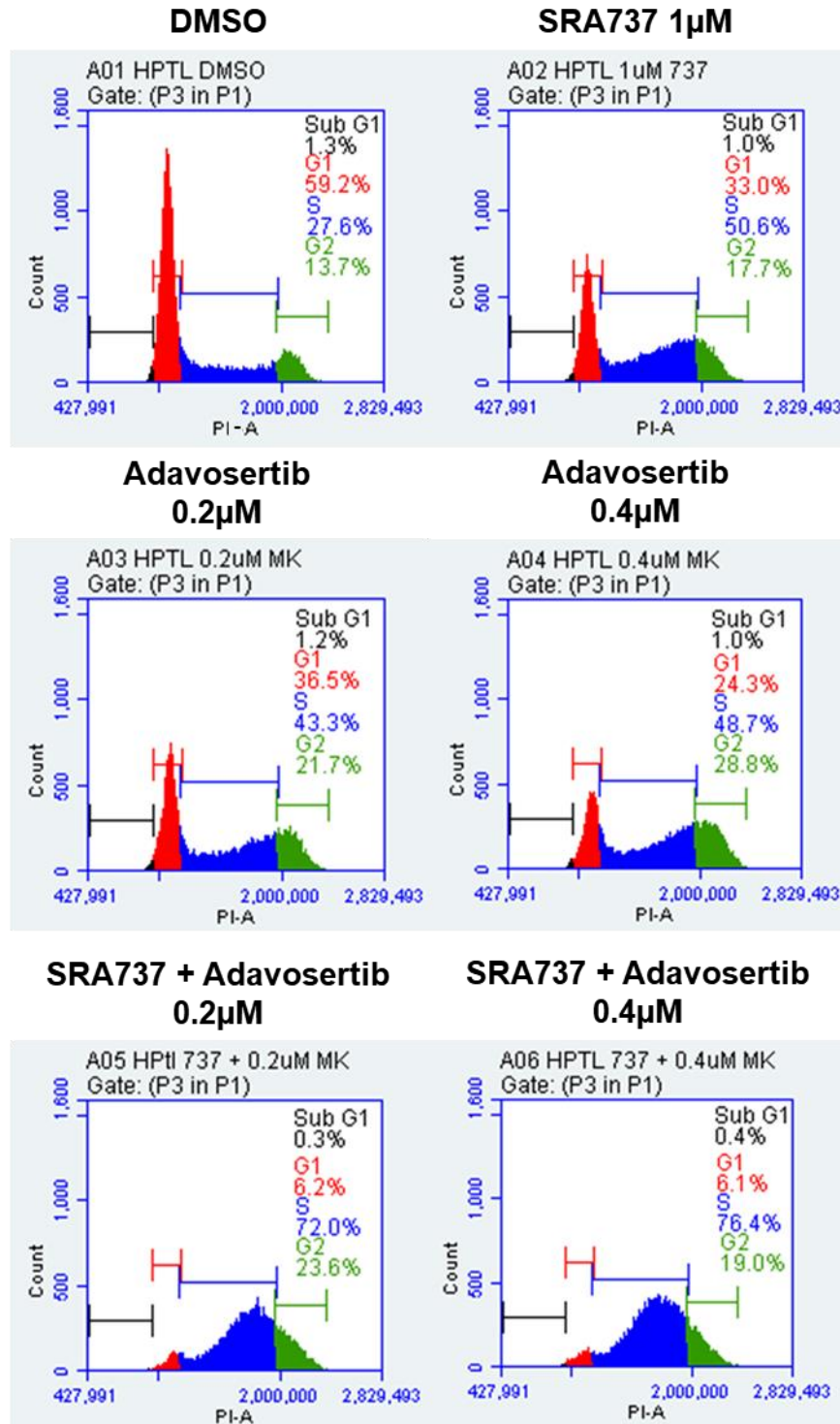


**Figure 4.10: Propidium iodide (PI) cell cycle analysis of HCC38 cell lines treated with a drug combination of SRA737 and Adavosertib.** Analysis of cell cycle distribution in HCC38 cell lines via flow cytometry. Cells were plated in T25 flasks and left to adhere overnight before 24hr incubation in DMSO control SRA737, Adavosertib or a combination of both drugs. Cells were fixed in ethanol and DNA stained with PI before analysis on a BD Accuri™ C6 flow cytometer. G1= G1/G0 and G2= G2/M phases. Representative PI density histograms showing gating of cell cycle populations. Data is representative of n ≥2 independent experiments.

## H737R

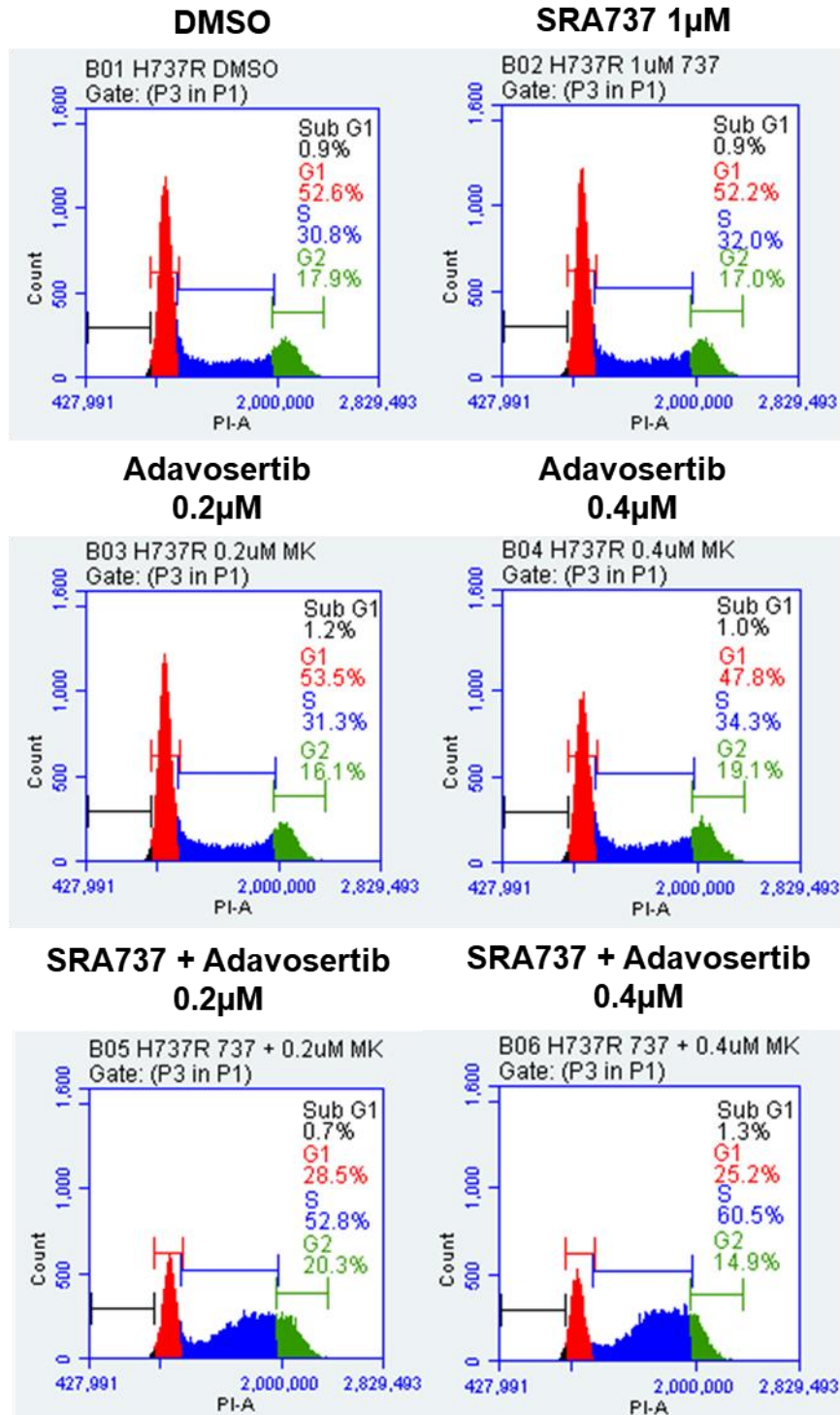


**Figure 4.11: Propidium iodide (PI) cell cycle analysis of H737R cell lines treated with a drug combination of SRA737 and Adavosertib.** Analysis of cell cycle distribution in H737R cell lines via flow cytometry. Cells were plated in T25 flasks and left to adhere overnight before 24hr incubation in DMSO control SRA737, Adavosertib or a combination of both drugs. Cells were fixed in ethanol and DNA stained with PI before analysis on a BD Accuri™ C6 flow cytometer. G1= G1/G0 and G2= G2/M phases. Representative PI density histograms showing gating of cell cycle populations. Data is representative of n ≥ 2 independent experiments.

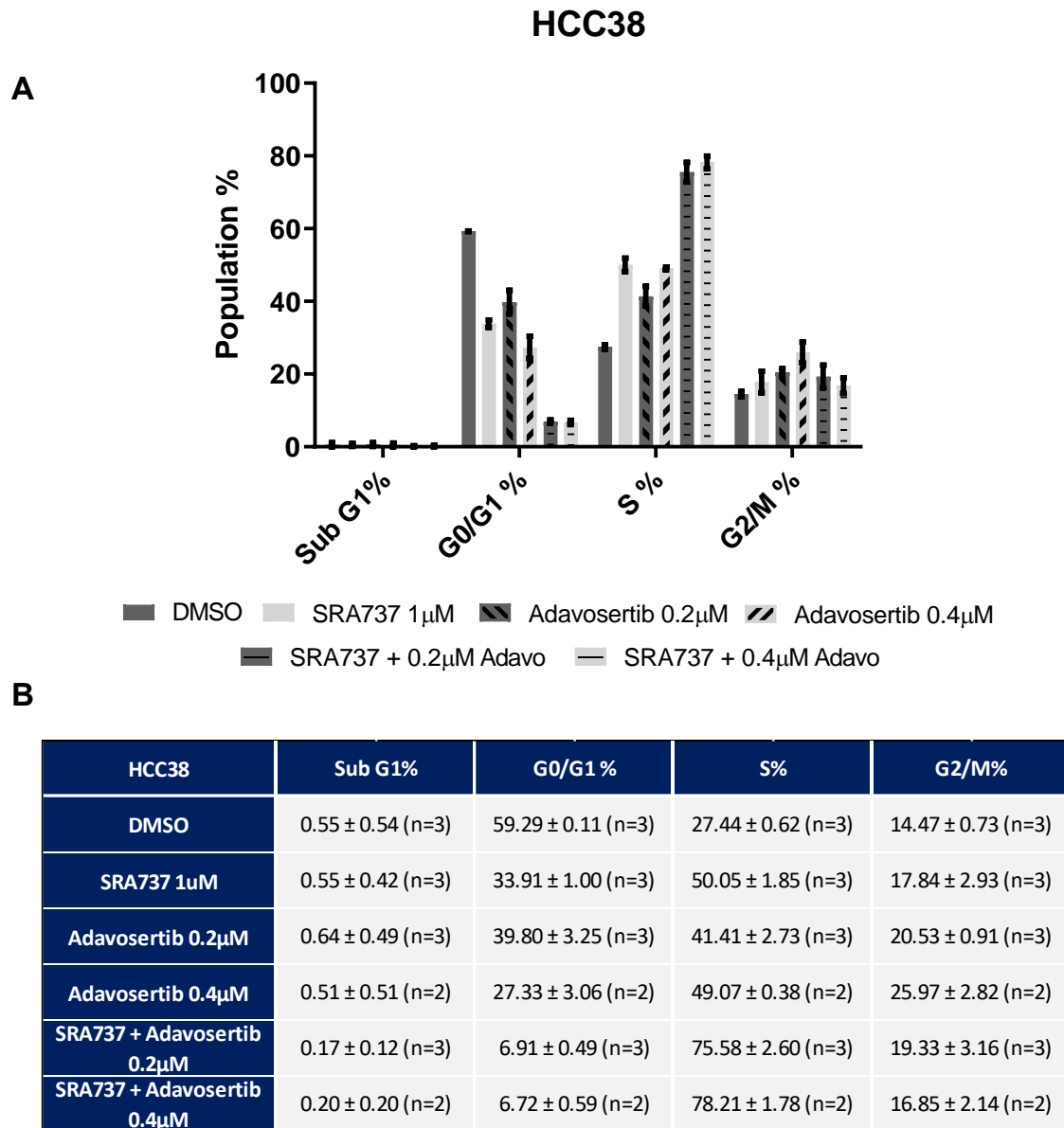
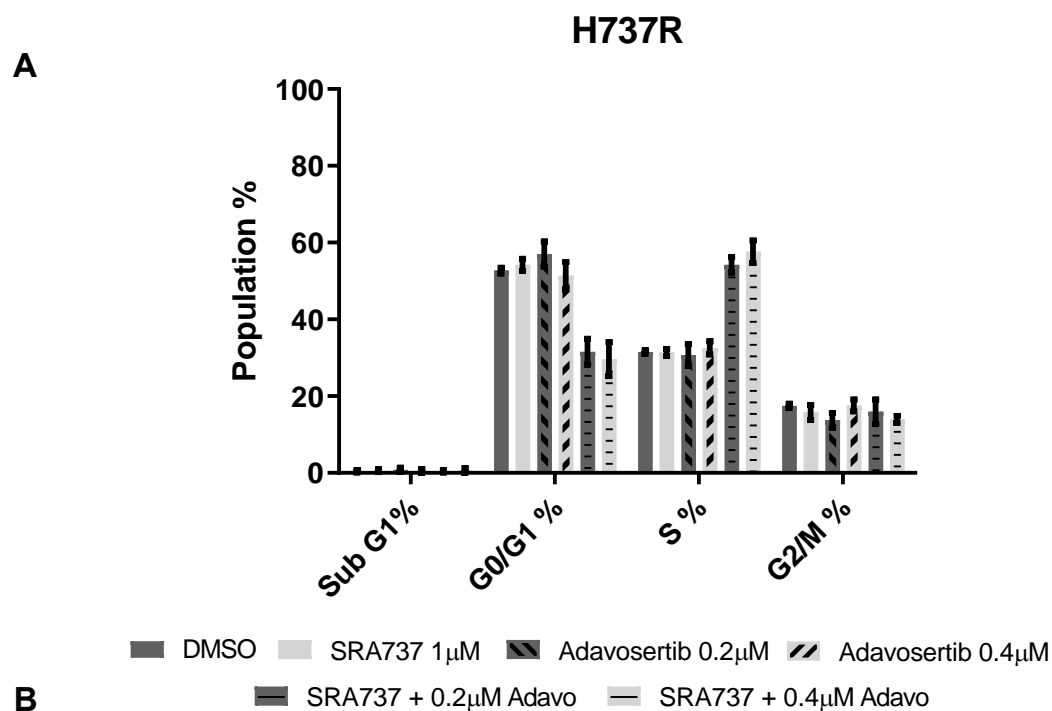


**Figure 4.12: Bar chart of Propidium iodide (PI) cell cycle analysis of HCC38 cell lines treated with a drug combination of SRA737 and Adavosertib. A)** Bar chart showing the average percentage +/- the standard deviation of cells in each stage of the cell cycle. **B)** Table showing average percentages +/- the standard deviation of cell cycle populations shown in **A**. (n) indicates the number of independent experiments.



H737R	Sub G1%	G0/G1 %	S%	G2/M%
DMSO	0.45 ± 0.36 (n=3)	52.72 ± 0.77 (n=3)	31.46 ± 0.52 (n=3)	17.49 ± 0.58 (n=3)
SRA737 1µM	0.58 ± 0.41 (n=3)	54.19 ± 1.59 (n=3)	31.38 ± 0.94 (n=3)	15.78 ± 1.96 (n=3)
Adavosertib 0.2µM	0.81 ± 0.57 (n=3)	56.99 ± 3.27 (n=3)	30.70 ± 2.80 (n=3)	13.67 ± 1.96 (n=3)
Adavosertib 0.4µM	0.52 ± 0.52 (n=2)	51.38 ± 3.55 (n=2)	32.58 ± 1.73 (n=2)	17.55 ± 1.55 (n=2)
SRA737 + Adavosertib 0.2µM	0.41 ± 0.30 (n=3)	31.56 ± 3.37 (n=3)	54.23 ± 1.99 (n=3)	15.93 ± 3.19 (n=3)
SRA737 + Adavosertib 0.4µM	0.64 ± 0.64 (n=2)	29.66 ± 4.42 (n=2)	57.60 ± 2.90 (n=2)	13.94 ± 0.92 (n=2)

**Figure 4.13: Bar chart of Propidium iodide (PI) cell cycle analysis of H737R cell lines treated with a drug combination of SRA737 and Adavosertib. A)** Bar chart showing the average percentage +/- the standard deviation of cells in each stage of the cell cycle. **B)** Table showing average percentages +/- the standard deviation of cell cycle populations shown in A. (n) indicates the number of independent experiments.

To determine the effect of the drug combination on cell viability H737R and HPrexR cell lines were analysed via a dose response SRB assay. HCC38 Parental and drug resistant cell lines were treated with a titration of SRA737 alone in combination with Adavosertib at concentrations matching their respective  $GI_{20}$  (**Figure 4.14**). H737R showed a stronger response to the drug combination than HPrexR cells reaching approximately 30% viability at 1 $\mu$ M of SRA737 (**Figure 4.14 A**) while HPrexR cells did not drop below 50% viability at the same SRA737 concentration (**Figure 4.14 B**). However, it is important to note that there was some variability with response to the drug combination in other assays (**Appendix 4.2**) which may be due to technical error. Despite this, Adavosertib does appear to resensitise H737R and HPrexR cell lines to SRA737 suggesting the drugs are having a synergistic effect on cell viability.

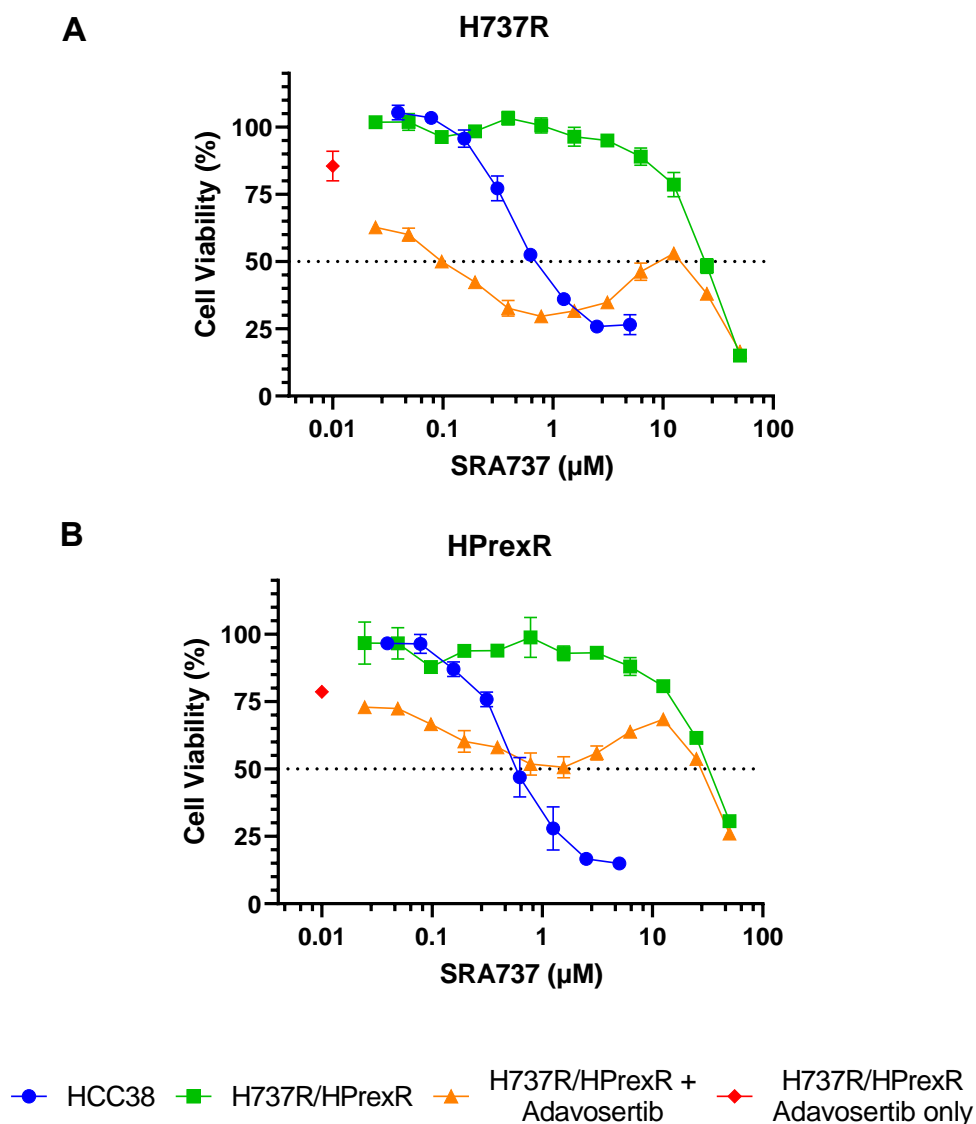


**Figure 4.14: SRA737 + Adavosertib drug combination experiment in H737R and HPrexR cell lines.** Cells were plated at 3200 cells/well in a 96-well plate and grown for 48 hours before treatment with a serial dilution SRA737 +/-  $GI_{20}$  of Adavosertib for 96 hours and analysed via SRB assay. **A)** H737R Adavosertib  $GI_{20}$  = 443nM **B)** HPrexR Adavosertib  $GI_{20}$  = 825nM. Data points represent the mean  $\pm$  SD from one representative experiment. Graphs are representative of n=3 individual experiments.

To test if the synergistic effects seen with SRA737 and Adavosertib could be replicated with another WEE1 inhibitor, we ran a drug combination experiment with WEE1i PD0166285. PD0166285 is a WEE1 inhibitor which also inhibits MYT1 kinase at low concentrations and also inhibits CHK1 at much higher concentrations of the drug (Wang *et al.*, 2001). PD0166285  $GI_{50}$  was determined in HCC38, H737R and HPrexR cell lines via SRB cell viability assay (**Figure 4.15**). Surprisingly H737R and HPrexR did not exhibit resistance to PD0166285 despite showing resistance to the WEE1 inhibitor Adavosertib (**Figure 3.14**). Furthermore, the

synergistic effect observed with Adavosertib and SRA737 was not seen in H737R cells treated with a drug combination of SRA737 and PD0166285 (**Figure 4.16**). While the drug combination of PD0166285 and SRA737 does shift the dose response curve to the left slightly, the effect is not as strong as seen with SRA737 and Adavosertib in combination (**Figure 4.16**).

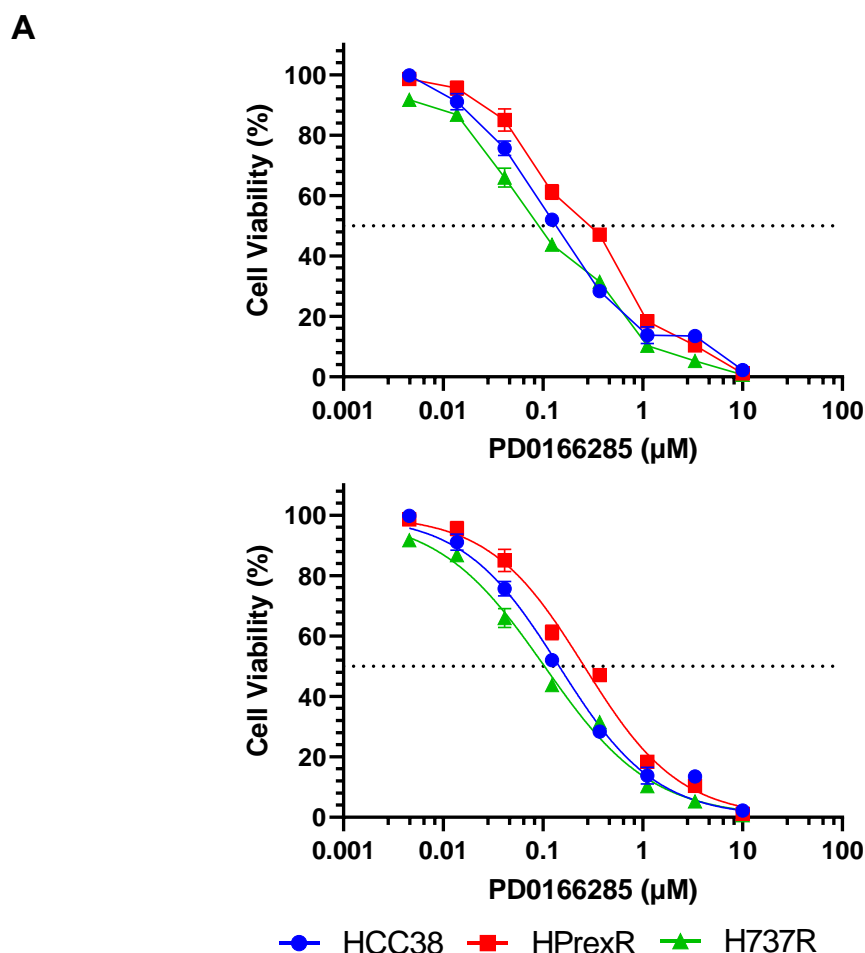


**Figure 4.15: Dose response of HCC38, H737R and HPrexR cell lines to PD0166285.** Cells were plated at 1600 cells/well in a 96-well plate and grown for 48 hours before treatment with a serial dilution of PD0166285 for 96 hours and analysed via SRB assay. **A**) Dose response curves generated using GraphPad Prism 9 and fitted using non-linear regression. Dotted line marks the GI<sub>50</sub> of PD0166285. Data points represent the mean ± SD from one representative experiment. **B**) Table summarises the mean ± SD of all experiments conducted. Statistical significance was calculated using a student's t-test but no significant difference was found.



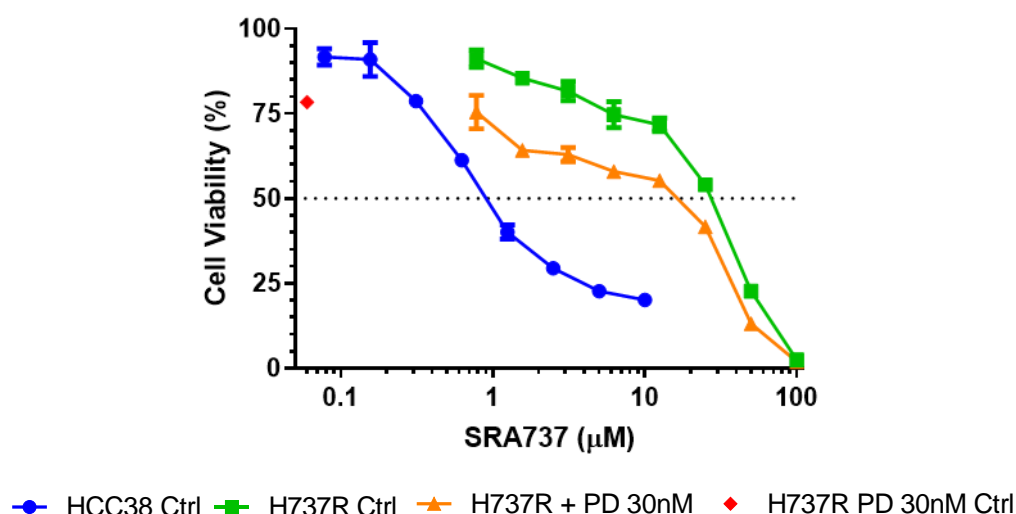


**Figure 4.16: SRA737 + PD0166285 drug combination experiment in H737R cell lines.** Cells were plated at 1600 cells/well in a 96-well plate and grown for 48 hours before treatment with a serial dilution SRA737 +/- 30nM of PD0166285 for 96 hours and analysed via SRB assay. Data points show mean  $\pm$  SD from one representative experiment from  $n \geq 3$  independent experiments.

### 4.2.3 Knockdown of WEE1 via Small interfering RNA (SiRNA) in resistant cell lines

Overexpression of WEE1 protein and partial re-sensitisation of H737R and HPrexR cell lines to SRA737 with Adavosertib suggested WEE1 may play a role in CHK1i resistance. However, as the WEE1 inhibitor PD0166285 does not strongly sensitise H737R cells to SRA737, this suggests that sensitivity caused by Adavosertib may not be due to inhibition of WEE1. To test if loss of WEE1 protein is enough to restore sensitivity to SRA737 we knocked down WEE1 protein levels in the cell via small interfering RNA (SiRNA).

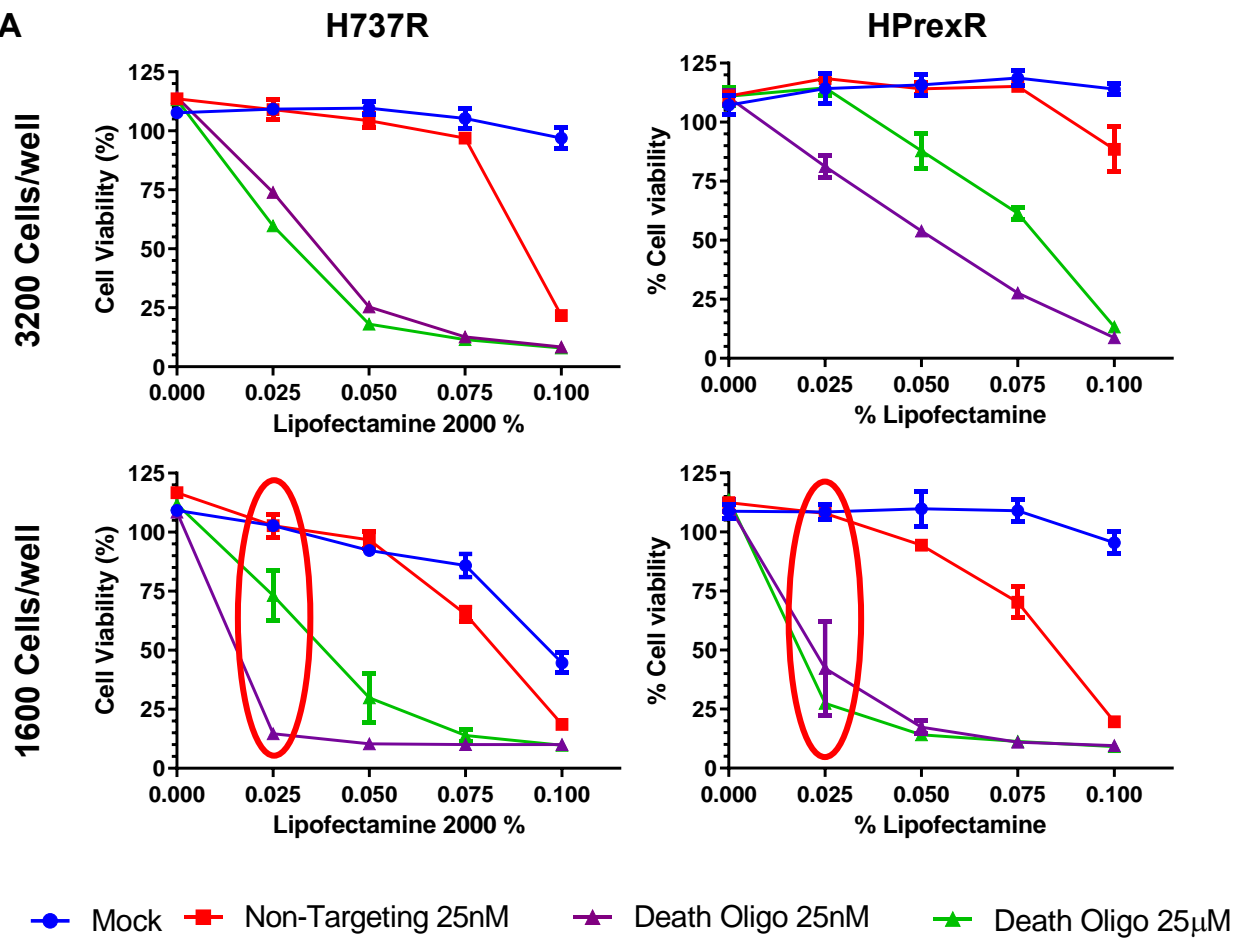
#### 4.2.3.1 Optimisation of SiRNA transfection conditions

Transfection conditions were optimised in H737R and HPrexR cell lines. Initially cells were plated in 96-well plates at either 1600 or 3200 cells/well and reverse transfected with 0.025% to 0.1% Lipofectamine 2000 combined with death control siRNA (positive control for transfection), non-targeting SiRNA (negative control for siRNA off target effects), or no SiRNA (mock transfection control). Successful uptake of SiRNA indicated by a cell death inducing

oligonucleotide was balanced with the inherent toxicity of transfection shown by the mock and non-targeting SiRNA controls. The optimal conditions allowed for the greatest uptake of SiRNA with minimal transfection induced toxicity. Seeding density greatly impacted the transfection efficiency requiring much higher concentrations of Lipofectamine to successfully transfect death oligo into cells at 3200 cells/well, therefore 1600 cells/well was selected (**Figure 4.17 A**). H737R and HPrexR were highly sensitive to lipofectamine 2000, therefore 0.025% lipofectamine was selected for initial experiments although this concentration still appeared to show some toxicity (**Figure 4.17 A**).

Four WEE1 targeting SiRNAs were reverse transfected into cells in 6-well plates plated at 48,000 cells/well. Cells were reverse transfected with either the mock control, non-targeting SiRNA or SiWEE1 #1-4 at two different concentrations and lysed after 48 hours before analysis via western blot. SiWEE1 #1 and #4 achieved the highest levels of knockdown and were taken forward for later experiments (**Figure 4.17 B**). Initial experiments showed unacceptable levels of toxicity (**Appendix 4.3**) and an additional optimisation assay was carried out using a lower concentration of lipofectamine in H737R cells (**Figure 4.18**). The lower lipofectamine concentrations still showed sufficient transfection efficiency and demonstrated less toxicity at 10nM of SiRNA (**Figure 4.18**). Based on this assay the final transfection conditions of 0.0125% Lipofectamine 2000, 10nM SiRNA and 1600 cells/well were selected in H737R and HPrexR cell lines.

**A**



**B**

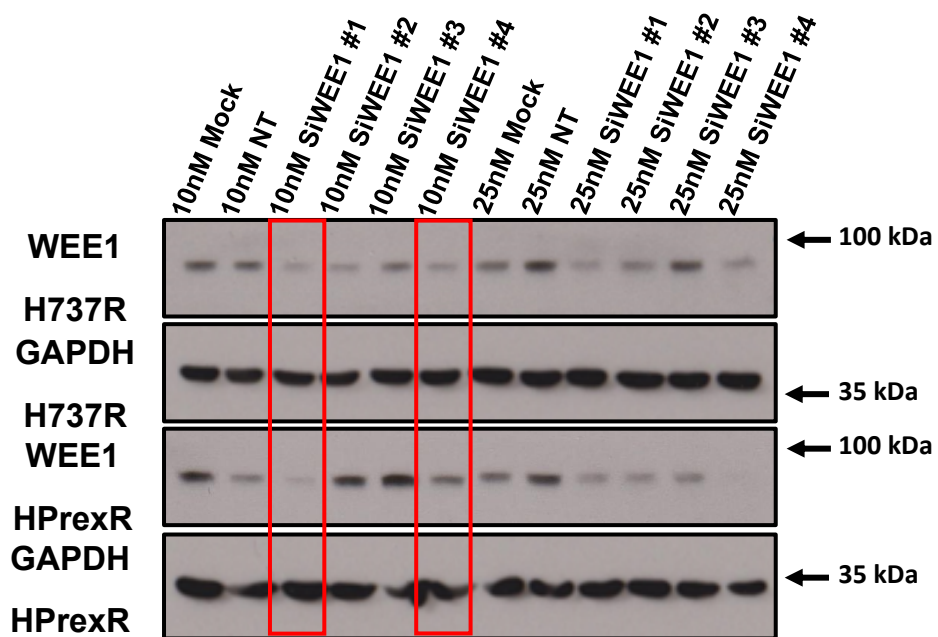


**Figure 4.17: Optimising conditions for SiRNA knockdown of WEE1.** **A)** H737R and HPrexR cells were reverse transfected in duplicate into 96-well plates at the seeding densities shown. Lipofectamine 2000 was used at the concentration indicated in a total volume of 160µl. After 24hrs incubation 40µl media was added, cells were incubated for another 72hrs before analysis. Initial optimisation shows Lipofectamine 2000 concentrations alone (mock), 25nM of Allstars non-targeting siRNA and Allstars cell death control SiRNA at either 25nM or 5nM. Red circles indicate lipofectamine concentration selected for initial WEE1 knockdown experiment. Only n=1 independent experiment conducted. **B)** H737R and HPrexR cells were reverse transfected in 6-well plates at  $4.8 \times 10^4$  cells per well in a total volume of 1.6ml and incubated for 24hrs before addition of 0.4ml media. Cells were lysed at the 48hr timepoint and analysed via western blot. Red boxes indicate SiRNA WEE1 #1 and #4 at 10nM were taken forward for later experiments. Western blot is representative of n=2 independent experiments.

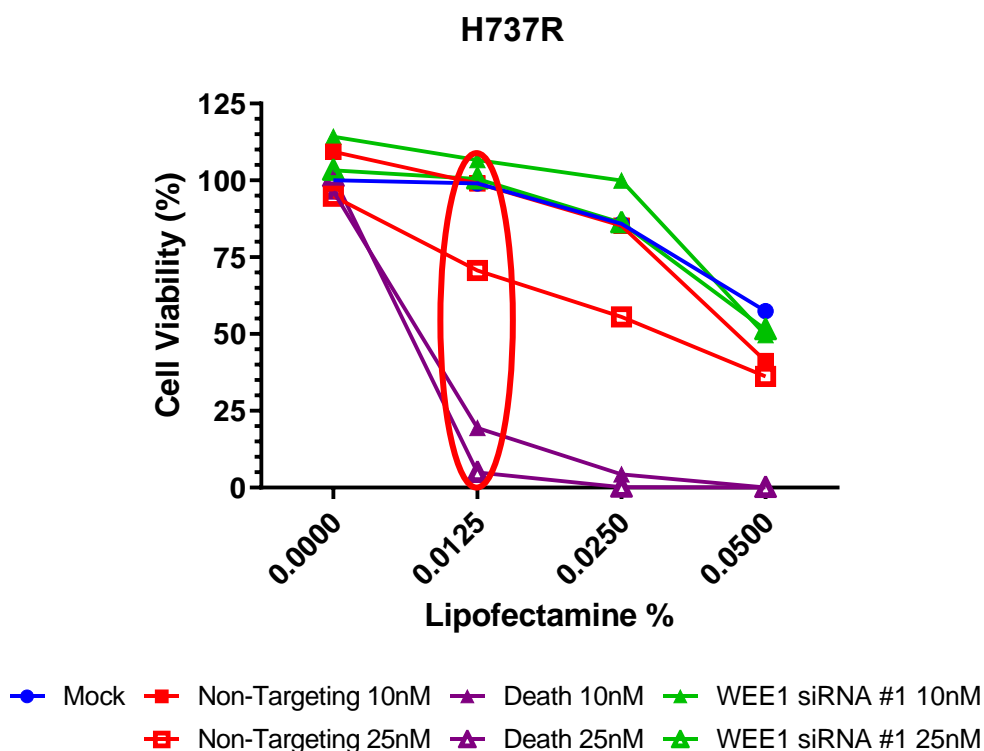


**Figure 4.18: Further optimisation for SiRNA knockdown of WEE1.** H737R cells were reverse transfected in duplicate into 96-well plates at 1600 cells/well. Lipofectamine 2000 was used at the concentrations indicated in a total volume of 160µl. After 24hrs incubation 40µl media was added, cells were incubated for another 72hrs before analysis. Initial optimisation shows Lipofectamine 2000 concentrations alone (mock), 10nm & 25nM of Allstars non-targeting siRNA, 10nm & 25nM of Allstars cell death SiRNA, and 10nm & 25nM Dharmacon SiWEE1 #1 SiRNA. Red circle indicates the new lipofectamine 2000 concentration taken forward for all further knockdown experiments. Only n=1 independent experiment conducted.

#### 4.2.3.2 Knockdown of WEE1 protein in H737R and HPrexR cell lines

After identifying optimal SiRNA transfection conditions WEE1 SiRNA knockdown was performed on H737R and HPrexR cell lines to investigate if loss of WEE1 could sensitise resistant cell lines to CHK1 inhibitors. As SiRNA only transiently blocks gene expression a 4-day SRB assay was performed to ensure WEE1 was knocked down over the course of the experiment. H737R and HPrexR cells were reverse transfected in a 96-well plate with SiWEE1 #1, SiWEE1 #4 or non-targeting SiRNA and incubated for 24 hours before the addition of a serial dilution of SRA737. Cells were also reverse transfected in 6-well plates alongside the SRB assay and lysed at 48- and 96-hour timepoints to check WEE1 protein knockdown over the course of the experiment.

WEE1 was successfully knocked down relative to mock and non-targeting controls in both cell lines (**Figure 4.19**). However, WEE1 levels in H737R and HPrexR knockdown samples still appears greater than HCC38 WEE1 levels suggesting knockdown is not reducing protein expression to levels seen in the parental phenotype (**Figure 4.19**). Strangely WEE1 expression across all 96-hour samples is much lower than seen at 48 hours (**Figure 4.19**). As this effect is seen in both control and knockdown samples it is likely independent of SiRNA activity. It is difficult to explain the cause of this effect but technical error during sample preparation and protein concentration determination could be a cause. However, the GAPDH loading control is relatively stable across all samples making this unlikely. Another explanation may be due to less-than-optimal growth conditions of cells leading up to the 96-hour timepoint. Seeding densities for 6-well plates were scaled up from the 96-well format of 1600 cells/well by a factor of 30 to  $4.8 \times 10^4$  cells/well. This was based on the difference in surface area between 96-well ( $0.32\text{cm}^2$ ) and 6-well plates ( $9.6\text{cm}^2$ ) but conditions seen in a 96-well format may not be completely comparable to 6-well format even when scaling seeding densities due to the differences in surface area to volume ratio.

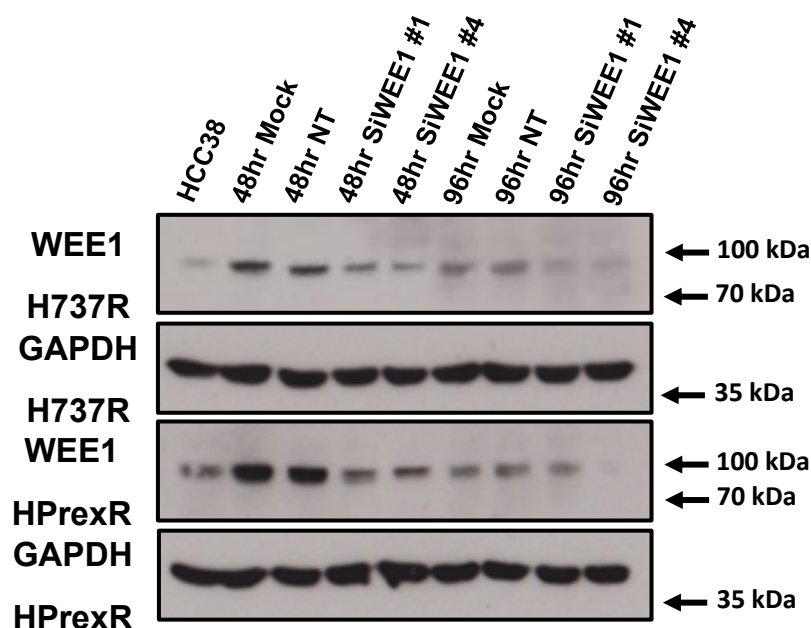
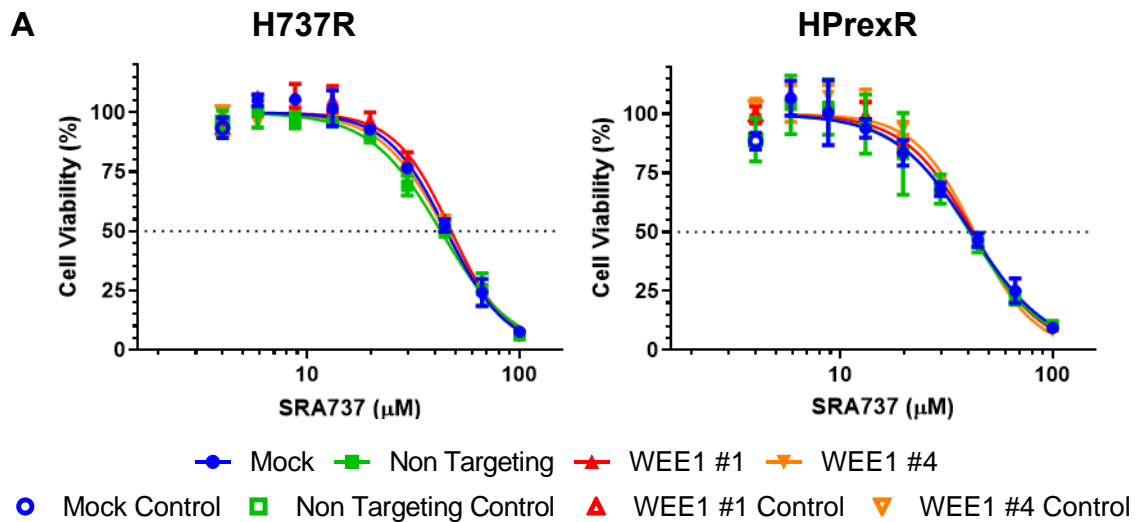


**Figure 4.19: WEE1 knockdown by SiRNA H737R and HPrexR cell lines.** H737R and HPrexR cells were reverse transfected in 6-well plates at  $4.8 \times 10^4$  cells per well in a total volume of 1.6ml and incubated for 24hrs before addition of 0.4ml media. Cells were lysed at 48hr and 96hr timepoints and analysed via western blot for the proteins indicated above with GAPDH as a loading control. Only n=1 independent experiment conducted.

Dose response SRB assays showed no significant difference between control and WEE1 knockdown cells in either H737R or HPrexR cell lines to a serial dilution of SRA737 (**Figure 4.20**). This suggests that resistance to the CHK1i SRA737 is not dependent on high expression of WEE1 protein. It is important to consider that while WEE1 was significantly knocked down in both H737R and HPrexR, it was not as low as seen in HCC38 parental cell lines. However, if resistance to CHK1i was highly dependent on increased WEE1 expression one might expect some level of sensitisation to occur equivalent to the loss of active WEE1 protein, even if resistant cell lines do not return completely to the levels of sensitivity seen in HCC38 cells.



**B**

	H737R	HPrexR
<b>GI<sub>50</sub> Mock</b>	34.97 ± 10.48 (n=2)	32.92 ± 8.47 (n=2)
<b>GI<sub>50</sub> Non-Targeting</b>	34.32 ± 8.33 (n=2)	32.24 ± 8.5 (n=2)
<b>GI<sub>50</sub> WEE1 #1</b>	34.74 ± 13.02 (n=2)	32.47 ± 9.74 (n=2)
<b>GI<sub>50</sub> WEE1 #4</b>	33.63 ± 11.26 (n=2)	33.24 ± 9.59 (n=2)

**Figure 4.20: Effect of WEE1 knockdown by SiRNA on SRA737 sensitivity in H737R and HPrexR cell lines.** H737R and HPrexR cells were plated in duplicate into 96-well plates at 1600 cells/well with 0.0125% lipofectamine 2000. Cells were reverse transfected with 10nM of Allstars non-targeting SiRNA as a control and Dharmacon SiWEE1 #1 & #4 SiRNA in a total volume of 160μl. After 24hrs incubation 40μl of a serial dilution of SRA737 was added to cells. Cells were incubated for a further 72hrs and analysed via SRB assay. **A)** Dose response curves were generated in Graphpad Prism 9 and fitted using non-linear regression. Graphs are representative of n=2 independent experiments. **B)** Table showing average GI<sub>50</sub> ± SD in H737R and HPrexR for each condition from n=2 independent experiments. Statistical significance was calculated using a student's t-test, but no significant difference was found.

#### 4.2.4 Optimising ectopic expression of WEE1 protein

Along with SiRNA KD in CHK1i resistant cells we aimed to carry out the inverse experiment on the HCC38 cell line to ectopically overexpress WEE1 and see if this drives resistance to CHK1 inhibitors. Unfortunately, due to difficulties with optimisation and time constraints the work did not reach completion. However, significant progress was made on optimising transfection conditions for future experiments. Constructs pCDNA3myc-p71 (WEE1+Myc tag) and pCDNA3myc (Myc tag only) kindly provided by Dr Piwnica-Worms (Rothblum-Oviatt, Ryan and Piwnica-Worms, 2001) were used to ectopically express WEE1+Myc tagged protein or Myc-tag only as a control. To check if these plasmids express WEE1 in our cell line a transient transfection experiment was carried out (**Figure 4.21**). WEE1 was successfully expressed ectopically and so these plasmids were used for generation of stable cell lines.

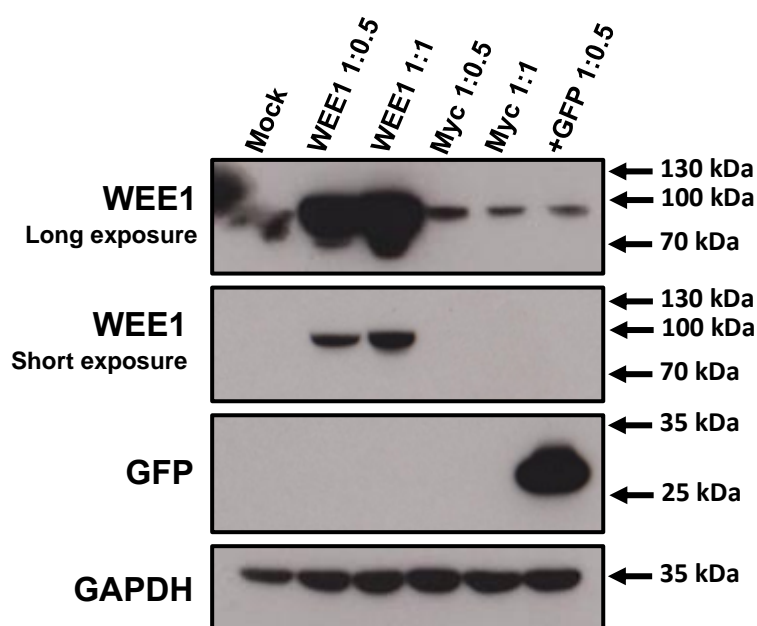


**Figure 4.21: Transient expression of ectopic WEE1.** HCC38 cell lines were plated in 6-well plates at  $1 \times 10^5$  cells/well and incubated overnight. Media was replaced with 1.8ml fresh medium (IMDM + FBS no PenStrep). 2 $\mu$ g of plasmid expressing Myc tagged WEE1 or a Myc tag control was mixed in either a 1:1 or 1:0.5 ratio with Lipofectamine 2000 (DNA:Lipofectamine) in 200 $\mu$ l of Opti-MEM reduced serum Medium and added to cells after a 10 minute incubation. Cells were incubated in IMDM + transfection mixture for 4 hours before media was replaced with 2ml of fresh IMDM and incubated for a further 24 hours before lysis and analysis via western blot. Plasmid expressing GFP tag (pEGFP\_N1) was used as a + control for transfection. Only n=1 independent experiment conducted.



The pCDNA3 expression vectors contain a Neomycin resistance gene allowing for cell selection via Geneticin (G418). To successfully select stable expressing cell lines a concentration of G418 was determined by a G418 kill curve. Cells were plated in 6-well plates and left to adhere overnight before constant exposure to a range of G418 concentrations over the course of a week (**Figure 4.22**). An optimal G418 concentration was selected that killed all cells within 5-7 days of exposure, therefore 1mg/ml G418 was taken forward for selection of stable expressing cell lines (**Figure 4.22**). Transfection of HCC38 cells was carried out in T25 flasks seeded at  $2.6 \times 10^5$  cells per flask and left to adhere overnight. Cells were transfected for 4hrs before media was replaced with fresh medium. Transfected cells showed high levels of cell death in both WEE1+Myc and Myc-tag only cells and so cells were allowed to recover for 96 hours before G418 selection (**Figure 4.23**). After 96 hours cells were trypsinised and seeded into 6-well plates at  $1 \times 10^5$  cells per well and allowed to adhere overnight before treatment with 1mg/ml G418. Unfortunately, after 196 hours only Myc-tag cells formed resistant colonies while WEE1+Myc colonies did not emerge (**Figure 4.24**).

As stable colonies were formed from Myc-tag only controls but not WEE1 expressing colonies it is likely that transfection conditions, albeit rather sub-optimal as indicated by transfection induced toxicity (**Figure 4.23**), are not the reason why colonies failed to emerge. More likely, HCC38 cells failed to survive selection due to excessive ectopic expression of WEE1 protein, as indicated during the transient transfection (**Figure 4.21**). As WEE1 controls G2 and S-phase checkpoints in the cell cycle, it is possible excessively high WEE1 expression led to prolonged cell cycle arrest and cell death. Future attempts to generate stable cell lines expressing ectopic WEE1 should firstly look to reduce the excessive WEE1 expression, either through titration of the expression vector or changing the gene promoter to one that demonstrates weaker expression of the gene. Further optimisation should also be carried out to reduce toxicity seen in both WEE1-Myc and Myc-tag only transfection, either by reducing the concentration of Lipofectamine 2000, or trying different transfection reagents known to be less toxic to cells.

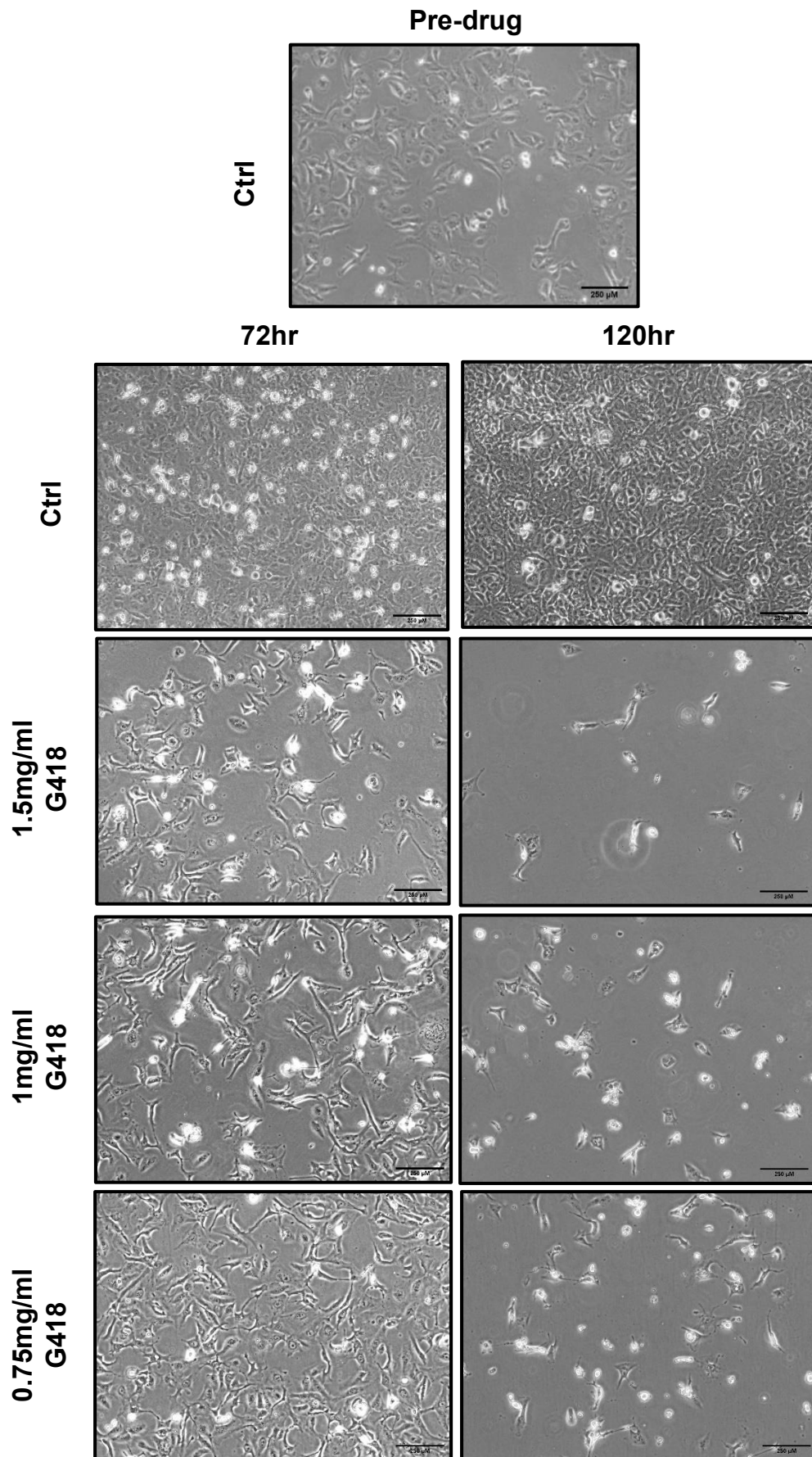


**Figure 4.22: Geneticin Kill Curve.** To select stably expressing cell lines with Neomycin resistance a concentration must be determined which kills all non-resistant cells within 5-7 days. HCC38 cells were seeded in 6-well plates at  $1 \times 10^5$  cells/well and left to adhere overnight. The following day media was replaced with 2ml IMDM + Geneticin (G418) at stated concentrations and incubated for a week. Media + G418 was replaced every 2 days or when the media showed signs of depletion. Pictures of cells taken at 40x magnification.

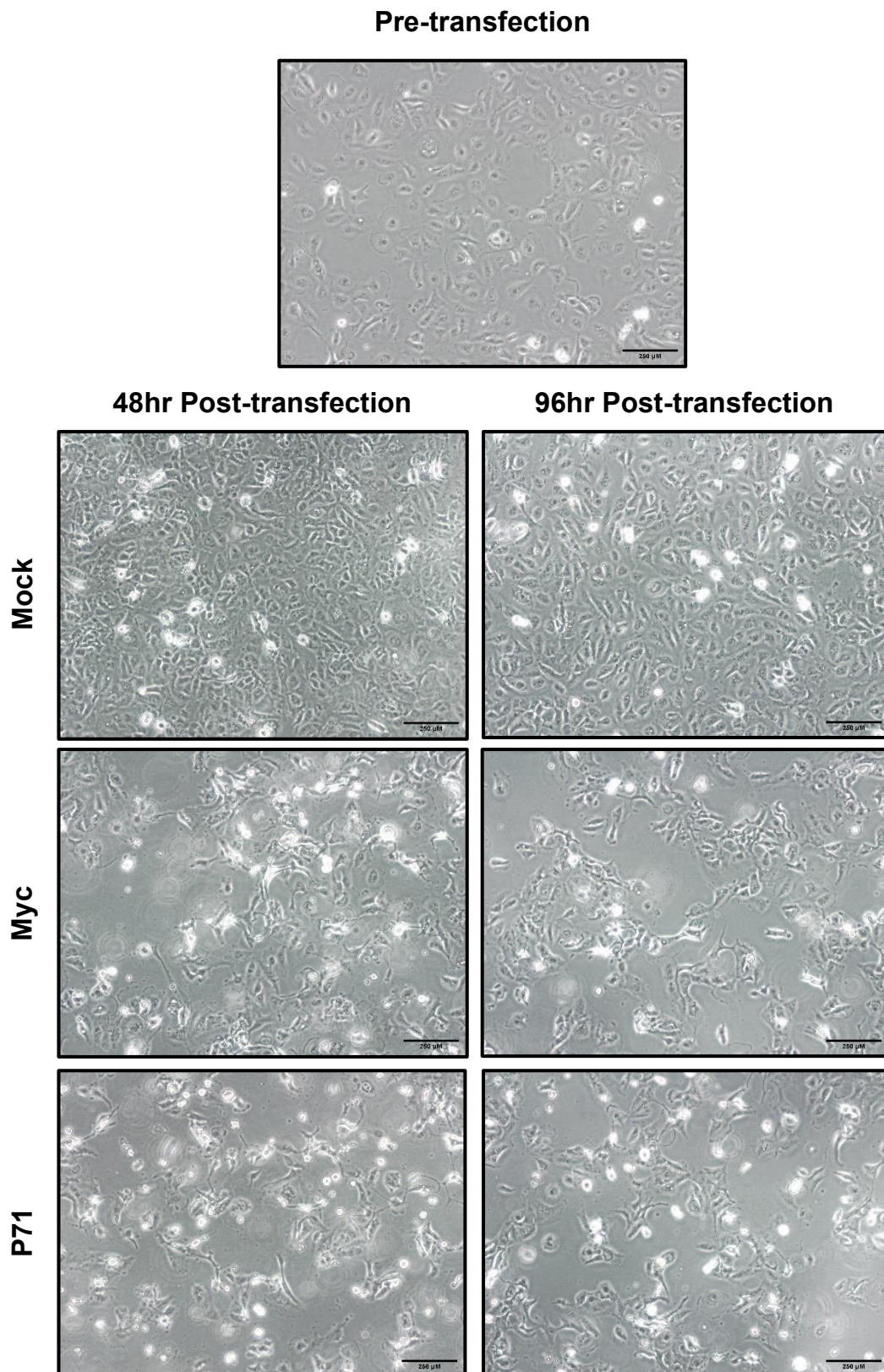


**Figure 4.23: Stable transfection of WEE1 expressing plasmid to HCC38 cells.** High levels of tox seen in both p71 and Myc cells following transfection visible by reduced cell confluency and high numbers of floating cells. HCC38 cells were seeded in T25 flasks at  $2.6 \times 10^5$  cells per flask and left to incubate overnight. 6.5 $\mu$ g of each plasmid (Myc = Myc tag alone, P71 = WEE1 plasmid) was mixed in a 1:1 ( $\mu$ g/ $\mu$ l) ratio with lipofectamine 2000 in a total of 650 $\mu$ l opti-mem and incubated for 10 minutes at room temperature before applying to cells. Cells were transfected for 4 hours before media was refreshed. 24hrs after transfection high levels of cell death was seen in all conditions other than the mock control, cells were allowed to recover for 96hrs before transfer to 6-well plates for Geneticin selection. Mock flasks were passaged to avoid overgrowth and cell death. Pictures of cells taken at 40x magnification.



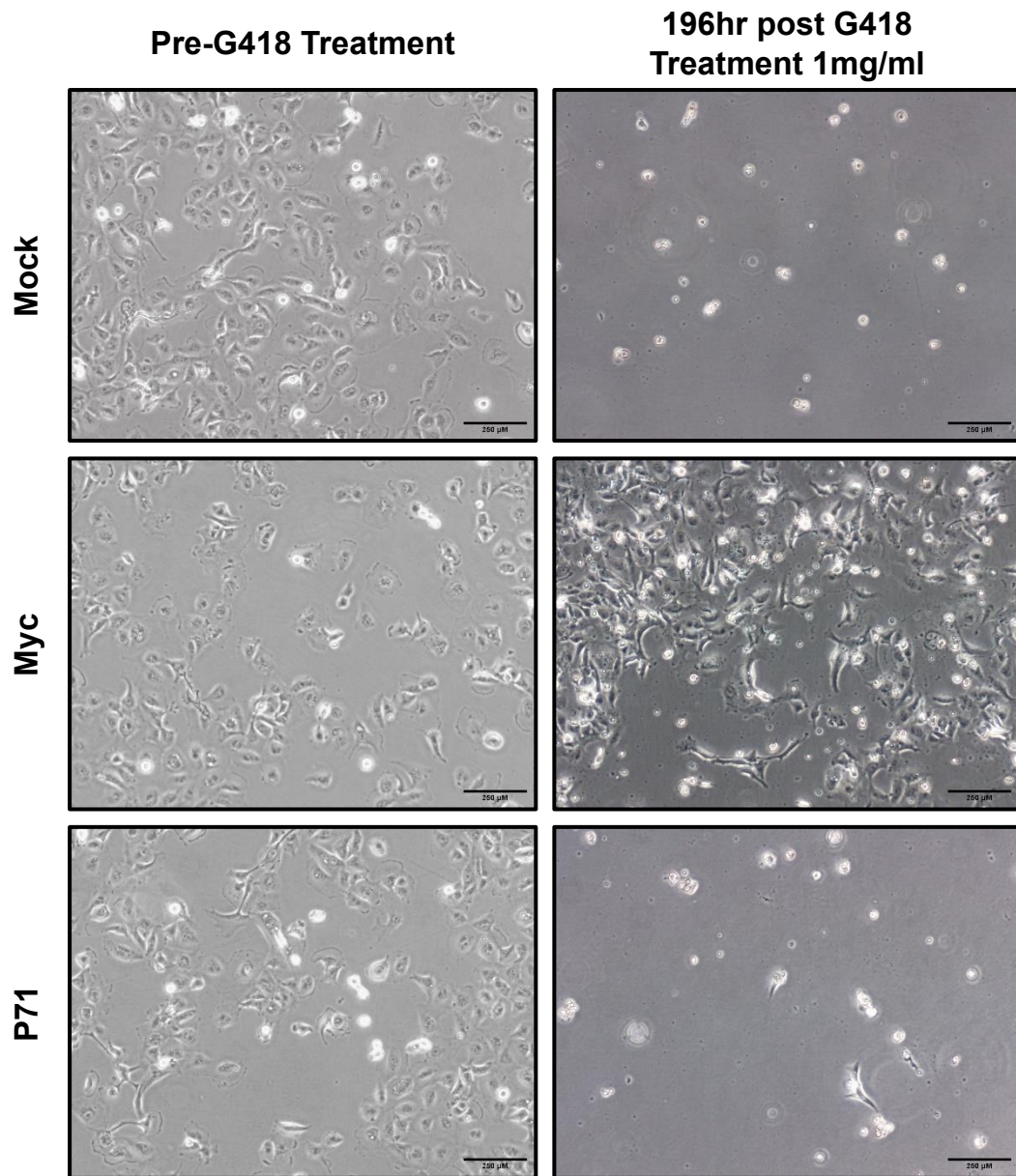


**Figure 4.24: Selection of stable cell lines with Geneticin.** P71 transfected cells failed to generate viable stably expressing colonies while Myc control vector successfully developed stably expressing cells. After transfection and 96hr incubation cells were seeded into 6-well plates at  $1 \times 10^5$  cells/well and allowed to adhere overnight. The following day media was replaced with 2ml IMDM + Geneticin (G418) 1mg/ml and incubated for a week. Media + G418 was replaced every 2 days or when the media showed signs of depletion. Pictures of cells taken at 40x magnification.

#### 4.2.5 Investigating WEE1 expression and CHK1i sensitivity in a TNBC cell line panel

To further test the hypothesis of WEE1 overexpression driving resistance to CHK1 inhibitors WEE1 protein levels were analysed in a panel of 14 TNBC cell lines obtained from the Resistant Cancer Cell Line (RCCL) collection (<https://research.kent.ac.uk/industrial-biotechnology-centre/the-resistant-cancer-cell-line-rccl-collection/>; Michaelis, Wass and Cinatl, 2019). These consisted of 3 chemo-naïve cell lines HCC38, HCC1806, and MDA-MB-468 and their drug adapted sublines to various DNA damaging agents such as Cisplatin, 5-fluoracil, Gemcitabine and Doxorubicin. Western blot analysis revealed HCC1806 cell lines exhibited very high levels of WEE1 protein while HCC38 and MDA-MB-468 cell lines show lower WEE1 levels (**Figure 4.25**). Interestingly MDA-CDDP cells appear to have downregulated WEE1 expression compared with MDA-MB-468 cells while MDA-Doxo appears to have upregulated WEE1 (**Figure 4.25**). In this blot, HPrexR cells no longer seem show higher WEE1 levels than HCC38 cells which contradicts previous blots seen in (**Figure 3.22**). Despite this H737R still shows high levels of WEE1 relative to HCC38 (**Figure 4.25**). As this data is only preliminary with no other repeat experiments, it is difficult to determine if low HPrexR WEE1 levels is caused by technical error or perhaps due to some inherent variability in HPrexR WEE1 expression.

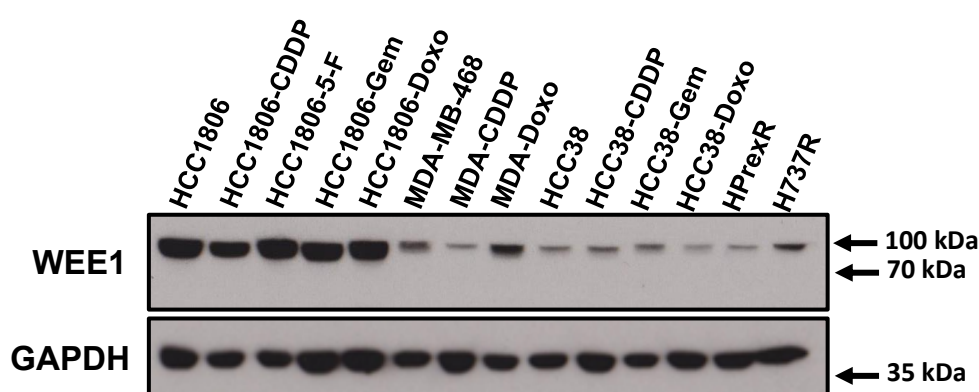


**Figure 4.25: Western blots of TNBC cell line panel.** 3 TNBC cell lines and their drug resistant sublines were analysed via western blot for WEE1 protein levels and GAPDH as a loading control. Preliminary data - only representative of n=1 experiment.

GI<sub>50</sub> determination of the TNBC cell line panel to multiple CHK1 inhibitors and Adavosertib was carried out by Dr Helen Grimsley (120-hour MTT assay, Garrett lab) and compared here with WEE1 expression in these cell lines (Grimsley, H, 2020) **(Figures 4.26 & 4.27)**. Interestingly, HCC1806 cell lines which showed the highest expression of WEE1 show high sensitivity to CHK1 inhibitors such as SRA737, Prexasertib, and Rabusertib **(Figures 4.26 A, B & 4.27 A)**. Within HCC1806 drug resistant sublines there is some variability, with Gemcitabine and Doxorubicin resistant cells showing greater resistance to MK-8776 than the chemo-naïve, Cisplatin resistant and 5-fluoracil resistant cell lines **(Figure 4.26 C)**. 144-hour H737R and HPrexR GI<sub>50</sub> determinations were carried out via SRB assay and not the MTT assay used in the data generated by H Grimsley, making them less comparable. Despite this, H737R and HPrexR show the highest GI<sub>50</sub> values to SRA737, Prexasertib and Adavosertib **(Figures 4.26 A, B & 4.27 B)** showing these cell lines are highly resistant while also demonstrating some of the lowest levels of WEE1 expression relative to the rest of the panel **(Figure 4.25)**. WEE1 protein expression was quantified by densitometry and normalised to the GAPDH loading control and plotted against GI<sub>50</sub> values for each drug tested **(Figure 4.26 & 4.27)**. Unsurprisingly no correlation was found between WEE1 expression and GI<sub>50</sub> values to CHK1 and WEE1 inhibitors suggesting that overexpression of WEE1 is likely not a driver of drug resistance to CHK1 and WEE1 inhibitors in these cell lines.

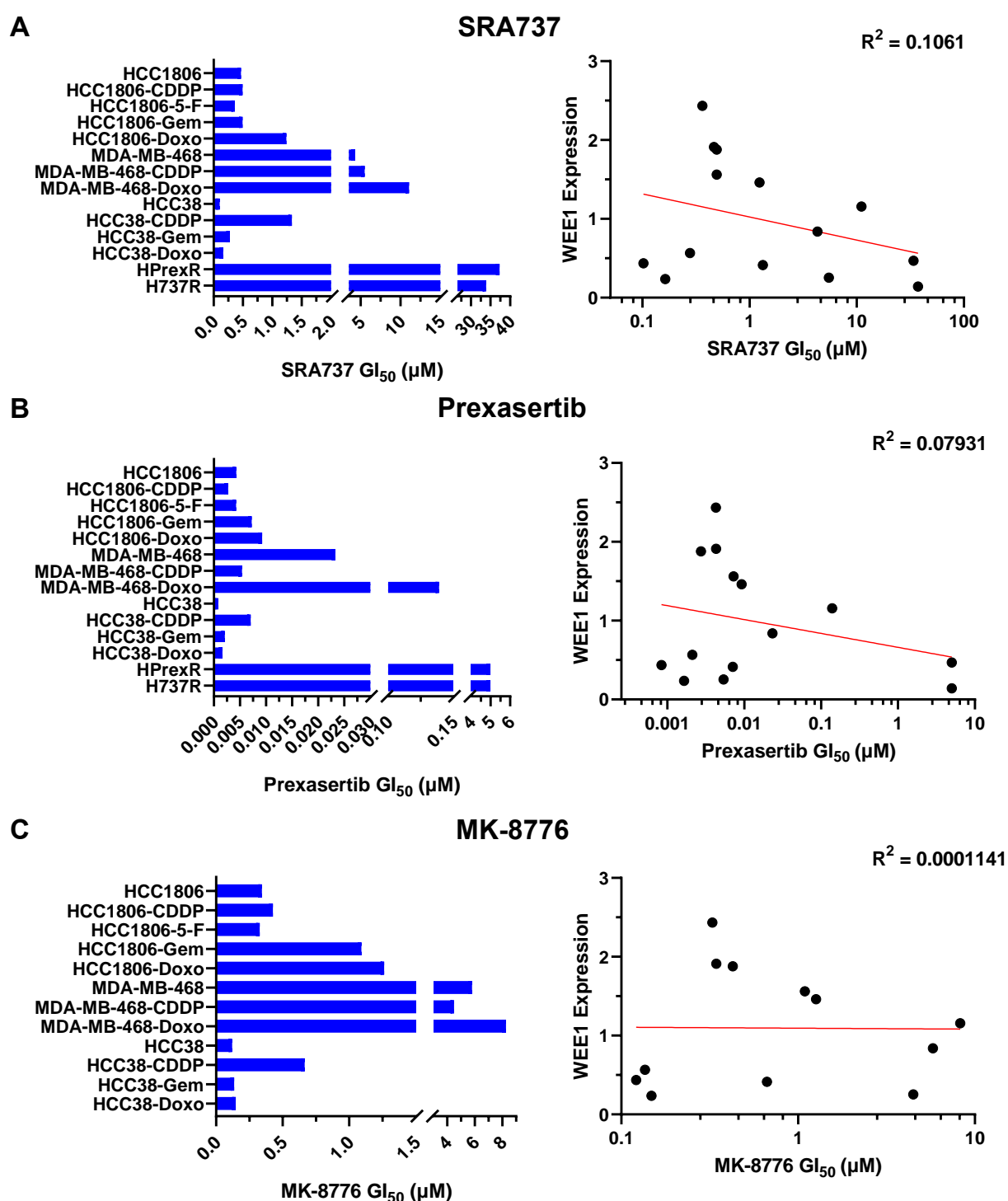


**Figure 4.26: Comparison of TNBC panel GI<sub>50</sub> data to WEE1 expression levels.** TNBC cell line panel GI<sub>50</sub> data for CHK1 inhibitors SRA737, Prexasertib and MK-8776 was determined via 120-hour MTT assay and analysed via Graphpad Prism 6 by Dr Helen Grimsley (Garrett lab). GI<sub>50</sub> data for H737R and HPrexR cell lines was determined via a 144-hour SRB assay. Bar graphs represent the average GI<sub>50</sub> from  $n \geq 3$  experiments. Scatter plots compare WEE1 expression determined by densitometry of TNBC cell line panel (**Figure 4.25**) to GI<sub>50</sub> data for CHK1 inhibitors **A) SRA737 B) Prexasertib C) MK-8776**. Linear regression and  $R^2$  value determined via Graphpad Prism 6.

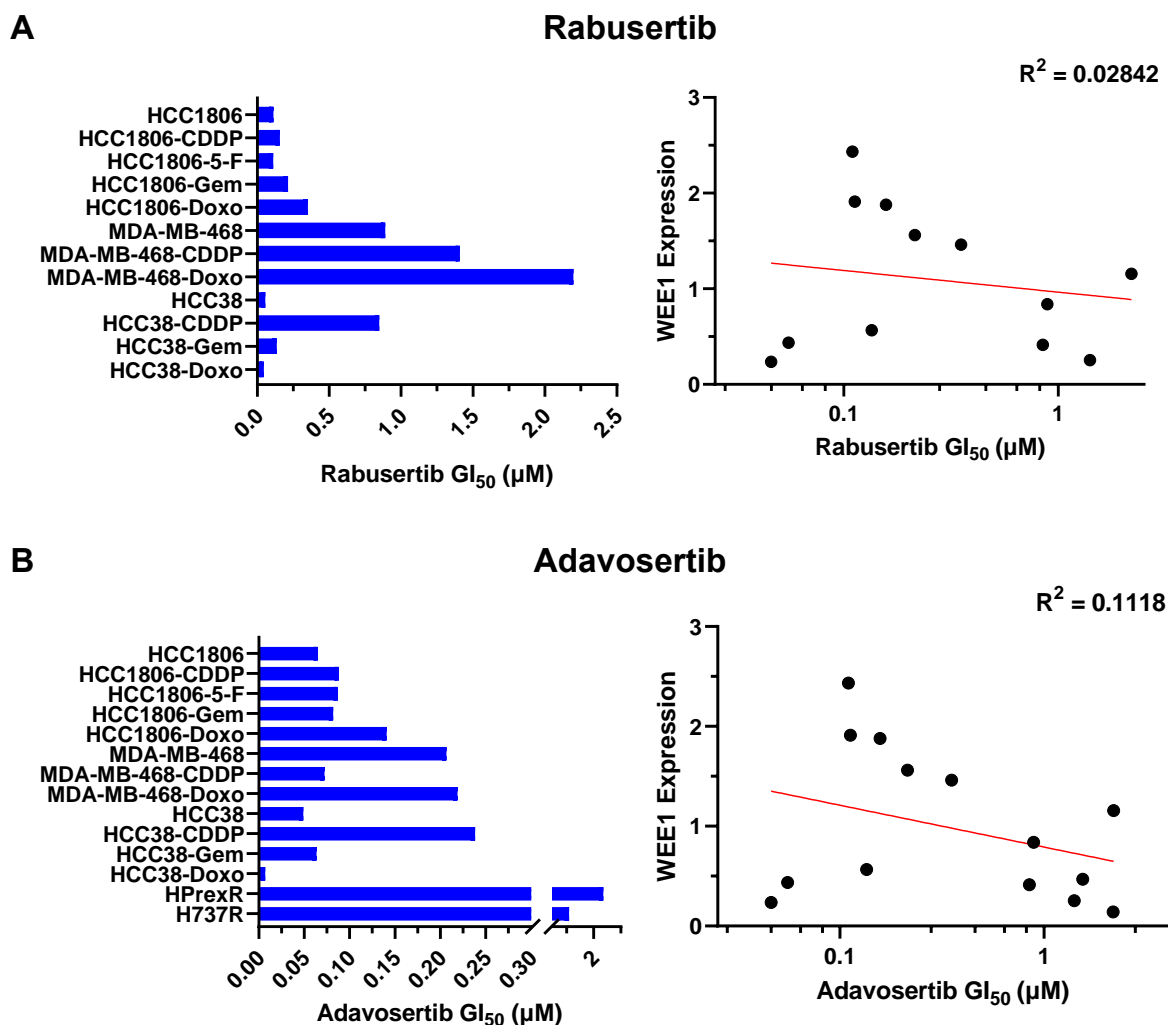


**Figure 4.27: Comparison of TNBC panel  $GI_{50}$  data to WEE1 expression levels.** TNBC cell line panel  $GI_{50}$  data for CHK1 inhibitor Rabusertib and WEE1 inhibitor Adavosertib was determined via 120-hour MTT assay and analysed via Graphpad Prism 6 by Dr Helen Grimsley (Garrett lab).  $GI_{50}$  data for H737R and HPrexR cell lines was determined via a 144-hour SRB assay. Bar graphs represent the average  $GI_{50}$  from  $n = \geq 3$  experiments. Scatter plots compare WEE1 expression determined by densitometry of TNBC cell line panel (**Figure 4.25**) to  $GI_{50}$  data for CHK1 and WEE1 inhibitors **A**) Rabusertib **B**) Adavosertib. Linear regression and  $R^2$  value determined via Graphpad Prism 6.



### 4.3 Discussion

In this chapter the role of WEE1 in resistance to CHK1 inhibitors was explored in more detail. Cycloheximide incubation and western blot of HCC38, H737R and HPrexR cell lines showed that WEE1 degradation is likely decreased leading to increased levels of WEE1 protein (**Figure 4.6 & 4.7**). Interestingly WEE1 inhibition by Adavosertib was well tolerated in H737R cells showing lower levels of DNA damage marker  $\gamma$ H2AX and normal progression of the cell cycle compared to the HCC38 cell line (**Figure 4.8, 4.10 & 4.11**). Excitingly, combined inhibition of CHK1 and WEE1 caused resensitisation of H737R and HPrexR cells to CHK1 inhibition leading to decreased cell viability, induction of  $\gamma$ H2AX and disruption of the cell cycle (**Figure 4.9-4.14**). Cross-profiling with another WEE1 inhibitor PD0166285 failed to yield similar results (**Figure 4.16**). Additionally, knockdown of WEE1 via SiRNA in H737R cells and exogenous overexpression of WEE1 in HCC38 cells was unsuccessful due to difficulties with transfection optimisation (**Figure 4.19 & 4.24**). As a result, WEE1 could not be successfully validated as a resistance mechanism. Nevertheless, this chapter shows combined inhibition of CHK1 and WEE1 holds promise as a method of overcoming CHK1i resistance.

Initial observations in **chapter 3** identified drug resistance to WEE1 inhibitor Adavosertib (**Figure 3.14**) as well as an increased expression of WEE1 protein (**Figure 3.22**) in H737R and HPrexR cell lines. CHK1 and WEE1 both regulate CDK1/2 activity and loss of either CHK1 or WEE1 is known to force cells into unscheduled mitosis and increase replication stress in S-phase (Matheson, Backos and Reigan, 2016; Neizer-Ashun and Bhattacharya, 2021). Therefore, we hypothesised that increased expression of WEE1 may be able to compensate for the loss of CHK1 activity through inhibition of CDK1/2 activity.

Western blotting experiments showed H737R cells did not induce  $\gamma$ H2AX and pCHK1 S345 during treatment with SRA737 while HCC38 cells did (**Figures 4.2 & 4.3**). pCHK1 S345 is phosphorylated in an ATR dependent manner following DNA damage induction (Bressenot *et al.*, 2008). Phosphorylation of Histone H2AX on S139 forming  $\gamma$ H2AX foci is an important

process in the DDR pathway, signalling the site of DNA double stranded breaks (DSB) for recruitment of proteins involved in DSB repair such as nonhomologous end joining (NHEJ) and homologous recombination (HR) (Sharma, Singh and Almasan, 2012).  $\gamma$ H2AX is also heavily phosphorylated during apoptosis resulting in a ring of  $\gamma$ H2AX which gradually spreads across the nucleus becoming pan-nuclear as DNA is degraded (Solier and Pommier, 2014). Therefore, it is difficult to determine if  $\gamma$ H2AX signal is due to high levels of apoptosis or DNA damage by western blot alone and future work should identify if increased  $\gamma$ H2AX seen via western blot is indicative of increased DNA damage (foci) or increased apoptosis (pan-nuclear staining) (Rogers *et al.*, 2020). Despite this,  $\gamma$ H2AX levels have been used as a marker of DNA damage and response to CHK1 inhibitors alone and in combination with other agents in multiple studies and is likely a strong indicator of response to CHK1 inhibition (Sakurikar *et al.*, 2016; Walton *et al.*, 2016b; Rogers *et al.*, 2020).

As CHK1 is capable of suppressing apoptosis (Myers *et al.*, 2009) it is possible that CHK1 inhibition via SRA737 leads to apoptosis in some cells, especially as C-PARP (cleaved PARP), a marker of apoptosis (Bressenot *et al.*, 2008), is increased in HCC38 cells treated with SRA737 (**Figures 4.2 & 4.3**). Interestingly cell cycle analysis did not show an increase in the Sub-G1 populations of cells with SRA737 treatment suggesting cells were not undergoing apoptosis (**Figures 4.4 & 4.5**). However, only cells adhered to the bottom of the flask were collected likely resulting in detached apoptotic cells being lost from the analysis.

Interestingly, C-PARP levels only increased in HCC38 cells at 24 hours of SRA737 incubation but  $\gamma$ H2AX and pCHK1 S345 signals were increased after 1hr (**Figure 4.3**). A study on the CHK1 inhibitor V158411 showed the HT29 colorectal adenocarcinoma cell line highly induced  $\gamma$ H2AX during CHK1 inhibition only in S-phase cells and  $\gamma$ H2AX induction was an early event of CHK1 inhibition (Wayne, Brooks and Massey, 2016). They also showed that induction of  $\gamma$ H2AX, and caspase-associated apoptosis are cellular outcomes mutually exclusive from one another with cells expressing either high  $\gamma$ H2AX or cleaved caspase-3 but rarely both markers simultaneously. They also showed caspase-associated apoptosis resulting from CHK1

inhibition was linked to p53 WT cells while p53 mutated cells undergo permanent cell cycle arrest and high  $\gamma$ H2AX induction (Wayne, Brooks and Massey, 2016). As HCC38 exhibits a mutated TP53 gene (**Table 3.1**) and appear to arrest in S-phase after 24-hour incubation in SRA737 (**Figures 4.4 & 4.5**), it's likely that  $\gamma$ H2AX is a marker of CHK1 inhibition-induced DNA damage rather than that of apoptosis. However, it is possible a sub population of cells are undergoing apoptosis leading to the increase in C-PARP at the 24-hour timepoint (**Figure 4.3**).

H737R cells exhibit an unperturbed cell cycle during SRA737 incubation (**Figures 4.4 & 4.5**) and do not induce markers of DNA damage (**Figures 4.2 & 4.3**). CHK1i induced DNA damage has been associated with collapse of DNA replication forks and unscheduled firing of replication origins (Syljuåsen *et al.*, 2005; Durkin *et al.*, 2006) and is dependent on the activity of CDC25A a phosphatase inhibited by CHK1 to maintain inactivity of CDK1/2 (Beck *et al.*, 2010). **Figure 4.2** shows phosphorylation of pCDK1/2 Y15 is lost at 1 $\mu$ M & 3 $\mu$ M SRA737 in HCC38 cells but maintained in H737R cells. This could explain why DNA damage is not induced in H737R cells as CDK activity is inhibited by phosphorylation of Y15 (Bridget T. Hughes *et al.*, 2013). However, this effect is less pronounced in **Figure 4.3** making it difficult to tell if pCDK1/2 Y15 is up in H737R relative to HCC38 cells at 24-hours. This may indicate that pCDK1/2 Y15 maintenance is not required for SRA737 resistance as DNA damage markers are not induced in H737R cells despite similar pCDK1 Y15 levels to the parental cell line.

H737R and HPrexR cells both exhibit higher WEE1 protein levels than the parental HCC38 cell line (**Figure 3.22**). Cells may increase protein levels by increasing gene expression or reducing the rate of protein degradation. The latter was investigated in parental HCC38 versus the H737R and HPrexR drug resistant cell lines via incubation with the protein synthesis inhibitor cycloheximide. Both H737R and PrexR cells demonstrated a reduced rate of WEE1 protein turnover following cycloheximide treatment compared to the HCC38 cell line (**Figures 4.6 & 4.7**). HPrexR does show slightly lower WEE1 expression than H737R cells (**Figure 3.22**)

which could explain the disparity in rates of WEE1 degradation. Expression of the *WEE1* gene was also investigated via RNA sequencing and details of this process are covered in **Chapter 6**. However, no significant difference was found in *WEE1* gene expression between HCC38 cell lines (**Appendix 6.4 & 6.5**) suggesting that the high levels of WEE1 protein in the H737R and PrexR cell line versus the parental cell lines is caused solely by a decrease in the rate of WEE1 protein degradation. Interestingly, another study looking at resistance to Prexasertib in SCLC showed Prex-resistant cells exhibited increased WEE1 mRNA and DNA copy number and was correlated with CHK1i resistance (Zhao, I. K. Kim, *et al.*, 2021). This showed WEE1 overexpression can also be mediated at the expression level but no experiments were conducted to look at WEE1 degradation (Zhao, I. K. Kim, *et al.*, 2021).

In dose response experiments H737R cells treated with the WEE1 inhibitor Adavosertib showed a similar response to parental HCC38 cells with  $\gamma$ H2AX and pCHK1 S345 increasing with increasing concentrations of inhibitor but to a lesser extent in H737R cells (**Figure 4.8**). pCDK1/2 Y15 levels decreased with increasing concentrations of Adavosertib in both parental HCC38 and H737R cell lines. However, despite the level of pCDK1/2 Y15 decreasing at similar doses in both cell lines, the DNA damage marker  $\gamma$ H2AX and pCHK1 S345 (phosphorylated by ATR in response to replication stress and DNA damage) are not induced in H737R to the same levels seen in HCC38 parental cells (**Figure 4.8**). This is different to the effects seen in **figure 4.2**, where pCDK1/2 Y15 is maintained in H737R cells and  $\gamma$ H2AX/pCHK1 S345 are not induced when treated with CHK1 inhibitor SRA737. This suggests that during inhibition of CHK1 only CDK activity is restrained, likely contributing to CHK1 inhibitor resistance. However, resistance to Adavosertib suggests H737R cells have also developed resilience to aberrant activation of CDK's and potentially have strategies to overcome checkpoint abrogation or CDK induced replication stress. Interestingly, CDK1 protein levels are reduced in HCC38 but not H737R in higher concentrations of Adavosertib (**Figure 4.8**). This may suggest a negative feedback mechanism in which CDK1 is degraded following overactivation

by Adavosertib, or perhaps this is a response linked to high levels of cell death likely present in HCC38 cells indicated by the relatively higher C-PARP levels vs H737R cells (**Figure 4.8**).

Our findings demonstrate SRA737 and Adavosertib sensitise HCC38, H737R and HPrexR cell lines to SRA737. This sensitivity is likely via their synergistic activity when used combination. A useful analogy for describing drug synergy was discussed by Roell, et al, who described an additive drug effect as  $1+1=2$ , whereas a synergistic effect may be thought as  $1+0=2$  (Roell, Reif and Motsinger-Reif, 2017). This describes the basic concept of drug synergy, in which a drug combination exhibits a synergistic effect if the combined effect of two drugs is greater than the combined additive effect of each drugs single agent activity. We have not conducted any experiments that directly measure synergy such as a Chou-Talalay assay (Chou, 2010), but we do see a strong effect of SRA737 and Adavosertib when used in combination in terms of the molecular response, cell viability, and disruption to the cell cycle.

SRA737 + Adavosertib combination greatly increases  $\gamma$ H2AX in H737R cells the response is still lower than seen in HCC38 cells under the same conditions (**Figure 4.9**) suggesting H737R cells exhibit some drug resistance to this drug combination. This is supported by the fact that the cell cycle of H737R cells is not disrupted by the drug combination to the same degree seen in HCC38 cells (**Figures 4.10 to 4.13**). Despite this, pCDK1/2 Y15 is still lost in both HCC38 and H737R cell lines during treatment with SRA737 + Adavosertib (**Figure 4.9**) suggesting resistance to dual inhibition of CHK1 and WEE1 is influenced but not driven by maintenance of CDK1/2 inactivation.

Interestingly, cell viability experiments show H737R and HPrexR cell lines are more sensitive to lower concentrations of SRA737 than HCC38 cells when treated in combination with Adavosertib (**Figure 4.14**). However, at concentrations exceeding 1-5 $\mu$ M SRA737, H737R and HPrexR cells are more resistant than HCC38 (**Figure 4.14**). At approximately 10 $\mu$ M SRA737 the dose response curve forms a “bump” before complete loss of cell viability (**Figure 4.14**). This bump is likely caused by self-limiting off target effects identified in SRA737, which has been shown to inhibit CDK2 and probably CDK1 activity at high concentrations (Ditano

and Eastman, 2021) supporting the idea that CDK inhibition can influence resistance to dual inhibition of CHK1 and WEE1.

Knockdown of WEE1 by SiRNA failed to sensitise H737R and HPrexR cell lines to SRA737 (**Figure 4.20**). While knockdown was achieved across the 96-hour period of the experiment, WEE1 was still present at levels higher than seen in parental HCC38 cells (**Figure 4.19**). This may account for the lack of synergism seen in combination with a CHK1 inhibitor which has been documented in other cell lines (Wang, Decker and Sebolt-Leopold, 2004; Chilà *et al.*, 2015). This was likely due to limited transfection efficiency (**Figure 4.19**) as Lipofectamine 2000 was highly toxic for HCC38 cell lines (**Figures 4.17 & 4.18**) making optimisation of transfection conditions difficult. Future experiments should try different transfection reagents/methods that are less cytotoxic to improve efficiency and achieve greater levels of knockdown. However, as H737R and HPrexR cells are resistant to pharmacological inhibition of both CHK1 and WEE1 (**Figure 4.9-4.14**) it is likely they are resistant to WEE1 knockdown too. Therefore, it is probable greater knockdown is required to mirror the effects seen with pharmacological inhibition of WEE1.

The synergistic effects of combined CHK1 and WEE1 inhibition have been documented in the past. WEE1 was identified in an SiRNA screen to find genes that demonstrated synthetic lethality with CHK1 inhibitors in breast, ovarian, colon and prostate cancer cell lines (Carrassa *et al.*, 2012). Non-toxic combinations of the CHK1 inhibitor PF-00477736 and WEE1 inhibitor MK-1775 (now named Adavosertib) showed synergy independent of p53 status in both cell line models and OVCAR-5 mouse xenografts (Carrassa *et al.*, 2012). This has also been shown in neuroblastoma, acute myeloid leukaemia and mantle cell lymphoma (Russell *et al.*, 2013; Chaudhuri, Vincelette, Koh, Naylor, Flatten, Peterson, McNally, Gojo, Karp, Ruben A Mesa, *et al.*, 2014; Chilà *et al.*, 2015).

Hauge, *et al* showed pharmacological inhibition of both CHK1 and WEE1 kinases led to a synergistic induction of S-phase DNA damage (Hauge *et al.*, 2017). Although both kinases influence the activity of CDKs, it was shown that WEE1 had greater control over CDK activity

and therefore its inhibition led to a larger increase in CDK activation than seen with CHK1 inhibitors (Hauge *et al.*, 2017). In addition, they identified a CDK independent effect of CHK1 on CDC45 loading. It is the combination of the high CDK activity in S-phase with the CDK independent loading of CDC45 that led to excessive replication initiation and massive DNA damage in S-phase (Hauge *et al.*, 2017).

To test if the synergy between SRA737 and Adavosertib extends to other WEE1 inhibitors, we investigated the effects of WEE1 inhibitor PD0166285 alone and in combination with SRA737 on our cell lines (**Figures 4.15 & 4.16**). Surprisingly, no significant difference was seen in dose response to PD0166285 alone between HCC38, H737R and HPrexR cell lines (**Figure 4.15**) despite H737R and HPrexR cells showing cross resistance to Adavosertib (**Figure 3.14**). Additionally, the drug combination of SRA737 + PD0166285 did not show a strong response in H737R cells (**Figure 4.16**) (HPrexR cells were not tested). At approximately 0.8 $\mu$ M SRA737 the cell viability of H737R cells treated with the drug combination does not appear any lower than the PD0166285 control, suggesting these drugs may not be working synergistically (**Figure 4.16**). However, an assay that specifically measures drug synergy such as a Chou-Talalay assay would be required to accurately determine if synergy is present between these two drugs (Chou, 2010).

The differences in dose response between Adavosertib and PD0166285 were unexpected as both drugs have been shown to inhibit WEE1, successfully leading to a loss of inhibitory Y15 phosphorylation on CDK1 (O *et al.*, 2006; Hirai *et al.*, 2009). PD0166285 inhibits WEE1 with an IC<sub>50</sub> of 24nM and has also been shown to inhibit MYT1 kinase with an IC<sub>50</sub> of 72nM and CHK1 with an IC<sub>50</sub> of 3.4 $\mu$ M (Wang *et al.*, 2001), while Adavosertib shows an IC<sub>50</sub> of 5.2nM against WEE1 kinase and >100-fold selectivity over MYT1 (Hirai *et al.*, 2009). MYT1 is a kinase that phosphorylates CDK1 but not CDK2 on T14 contributing to inactivation of CDK1 (Booher, Holman and Fattaey, 1997). No data has been published on PD0166285 and synergy with CHK1 inhibitors. Interestingly, most publications on PD0166285 focus on its interaction with CDK1 and the G2/M checkpoint and do not mention an effect on S-phase and DNA

replication (Wang *et al.*, 2001; Mir *et al.*, 2010; J *et al.*, 2011). Contrastingly, the effect of Adavosertib on both G2/M and S-phase has been well documented (Hirai *et al.*, 2009; Amy D. Guertin *et al.*, 2013), with S-phase disruption shown to be behind the synergistic effects seen with CHK1 inhibitors (Hauge *et al.*, 2017).

Synergistic DNA damage has been seen with SiRNA knockdown of WEE1 in combination with a CHK1 inhibitor suggesting that Adavosertib's inhibition of WEE1 is responsible for synergy rather than a potential off target effect (Carrassa *et al.*, 2012). This may indicate a difference in the way PD0166285 and Adavosertib differentially effect the cell cycle. Potentially, PD0166285 is more disruptive to the G2/M checkpoint than S-phase, due to the inactivation of both WEE1 and MYT1 leading to greater activation of CDK1 over CDK2. If resistance mechanisms to CHK1 inhibition in H737R and HPrexR cell lines rely on more CDK2 and S-phase dependent mechanisms, this may explain why cells are resistant to Adavosertib but not PD0166285. Future experiments should investigate the effects of PD0166285 on the cell cycle in HCC38 and H737R cell lines. Cells may accumulate in G2/M due to complications in cell division caused by unscheduled progression into mitosis. Or perhaps cells may accumulate in G0/G1 or Sub-G1 populations after suffering mitotic catastrophe, leading to cell death or senescence (Vitale *et al.*, 2011).

WEE1 protein levels from a panel of 3 TNBC cell lines and 11 of their sublines adapted to various DNA damaging agents were compared and contrasted with their GI<sub>50</sub> values to various CHK1 inhibitors and Adavosertib. Interestingly, no correlation was observed between WEE1 protein levels and response to CHK1 inhibitors (**Figures 4.25-4.27**). HCC1806 cell lines showed WEE1 expression higher than that of H737R cells but demonstrated considerably lower GI<sub>50</sub> values to both SRA737, Prexasertib and Adavosertib. This suggests that WEE1 may not be a strong biomarker of resistance to CHK1 inhibition in TNBC. However, it is possible that WEE1 overexpression may only confer resistance to CHK1 inhibition in the right cellular context, as WEE1 up-regulation has recently been shown to be involved in acquired resistance to Prexasertib in small cell lung cancer (Zhao, I. Kim, *et al.*, 2021). These results



should be considered carefully as western blot data is only n=1 and only a few cell lines were used. Future experiments should expand the number of TNBC cell lines while considering cellular context such as mutation status of various DDR-related genes.

Unfortunately, we were unable to generate stable cell lines that ectopically expressed WEE1 within the time allowed. This was due to difficulty in the optimisation of transfection conditions and likely toxic overexpression of WEE1 (**Figure 4.21**). Future experiments should try to reduce WEE1 expression, possibly through use of a weaker promoter or through titration of the WEE1 plasmid to reduce total plasmid uptake and ectopic expression of WEE1.

In summary, the data presented in this chapter suggests that the CHK1 inhibitor SRA737 kills HCC38 cell lines through the accumulation of excessive DNA damage in S-phase (**Figure 4.2 & 4.3**). While H737R and perhaps HPrexR cells are adapted to manage the S-phase associated DNA damage caused by CHK1 inhibition, in part by inhibiting CDK activity (**Figure 4.2**). Cross resistance with the WEE1 inhibitor Adavosertib (**Figure 3.14**) and increased expression of the kinase (**Figure 3.22**) indicated WEE1 in H737R and HPrexR cells was potentially driving resistance. Initially up-regulation of WEE1 was thought to cause resistance to Adavosertib due to the increased levels of WEE1 available for inhibition. However, H737R and HPrexR cells were not cross resistant to both Adavosertib and PD0166285 (**Figures 3.14 & 4.15**), suggesting increased WEE1 protein is not the cause of resistance to WEE1 inhibition. Flow cytometry and dose response westerns to Adavosertib revealed S-phase DNA damage was the likely the cause of cell death in HCC38 cells treated with Adavosertib (**Figures 4.8, 4.10 & 4.12**) while H737R cells did not exhibit this response (**Figures 4.8, 4.11 & 4.13**). However, this appeared to be independent of pCDK1/2 Y15 maintenance, which was lost in both HCC38 and H737R cells with Adavosertib treatment (**Figure 4.8**). While H737R cells did accumulate in S-phase and undergo high levels of DNA damage with a combination treatment of SRA737 + Adavosertib, they were still more resistant to the combination than HCC38 cells (**Figure 4.9-4.13**). This suggests that while maintenance of CDK activity plays a role in resistance, another mechanism of resistance to both CHK1 and WEE1 inhibition lies

downstream of CDK activation. Up-regulated DNA repair pathways or tighter control of the unscheduled firing of replication origins may allow H737R and HPrexR cells to cope with CHK1/WEE1 inhibitor associated replication stress. The following chapter explores the role of replication stress in CHK1 inhibitor resistance in more detail.

---

# **Chapter 5**

## **Examining the Role of Replication Stress in CHK1 Inhibitor Resistance**

# 5. Examining the Role of Replication Stress in CHK1 Inhibitor Resistance

## 5.1 Introduction

Cyclin-dependent kinases (CDKs) are serine/threonine kinases that control key processes within the cell cycle. Binding of CDKs with cyclins positively regulate CDK activity and drive progression through the cell cycle, while CDK inhibitors (CKIs) negatively regulate CDK activity leading to the activation of cell cycle checkpoints. The first cyclin dependent kinase, CDK1 (*cdc2*), was discovered in *S. pombe* & *S. cerevisiae* yeast and found to regulate the transition between cell cycle phases (Nurse, Thuriaux and Nasmyth, 1976; Nurse and Thuriaux, 1980; Beach, Durkacz and Nurse, 1982; Reed, Ferguson and Groppe, 1982). They are required for the cell cycle in mammalian cells but have since been shown to regulate many processes such as transcription, DNA damage repair, proteolytic degradation, epigenetic regulation, metabolism, stem cell self-renewal, neuronal functions and spermatogenesis (Lim and Kaldis, 2013). Cyclins bind CDKs and positively regulate their activity, they aid in timing the progression of the cell cycle via their cyclical synthesis and degradation, signalling the transition of cell cycle phases (Pines, 1993).

While different combinations of cyclins and CDKs have been shown to drive select cellular processes (i.e. CDK1-cyclin B for timing of G2 transition into mitosis or the ability for CDK2-cyclin E to regulate G1-S phase transition (Bertoli, Skotheim and De Bruin, 2013)) studies have shown redundancy between CDKs demonstrating the ability for cells to proliferate in the absence of multiple interphase CDKs such as CDK2, CDK4 and CDK6 (Malumbres *et al.*, 2004; Berthet *et al.*, 2006; Barrière *et al.*, 2007). One study showed mouse embryonic fibroblasts lacking all interphase CDKs (CDK2, CDK3, CDK4 and CDK6) were still capable of cell proliferation *in vitro* and CDK1 could bind all cyclin types, showing CDK1 was capable of

executing all events required for cell division (Santamaría *et al.*, 2007). This demonstrates a degree of redundancy and flexibility inherent to CDKs that is likely dependent on cellular context.

Replication stress is the slowing or stalling of replication fork progression during DNA synthesis (Gaillard, García-Muse and Aguilera, 2015) leading to DNA damage and genomic instability (Gaillard, García-Muse and Aguilera, 2015). Replication stress typically results in long stretches of ssDNA coated with replication protein A (RPA) caused by the uncoupling of the stalled polymerase from the helicase as it continues to unwind DNA (Gaillard, García-Muse and Aguilera, 2015). Causes of replication stress include DNA lesions, misincorporated ribonucleotides, collisions between replication and transcription complexes and limitation of essential replication factors i.e. insufficient pools of nucleotides for the replication machinery (Zeman and Cimprich, 2014). Long stretches of ssDNA bound by RPA signal for the binding of ATR-ATR-interacting protein (ATR-ATRIP) complex and subsequent checkpoint signalling and DNA damage response (Zou and Elledge, 2003; Rao *et al.*, 2017).

CHK1 is activated by ATR in response to DNA damage or replication stress and indirectly inhibits the activity of CDK1/2 via the phosphorylation and subsequent ubiquitin dependent degradation of CDC25 phosphatases (Sanchez *et al.*, 1997; Sørensen and Syljuåsen, 2012). This leads to decreased removal of the inhibitory Y15 phosphorylation on CDK1/2 which is maintained by WEE1 (Sørensen and Syljuåsen, 2012). In addition, p21<sup>Cip1/Waf1</sup> competes with CDC25 for binding on CDK2 inhibiting the dephosphorylation of CDK2 (Saha *et al.*, 1997). However, p21<sup>Cip1/Waf1</sup> has also been shown to inhibit CDK1 in the absence of CDK2 to maintain the G1/S phase checkpoint (Satyanarayana, Hilton and Kaldis, 2008) further demonstrating the flexible nature of these kinases. Deregulation of CDK activity via CHK1 and WEE1 inhibitors has been shown to cause replication stress and premature mitosis (Aarts *et al.*, 2012; Koppenhafer *et al.*, 2020; McNeely, Beckmann and Bence Lin, 2014). Unscheduled mitosis is thought to occur via a CDK1 dependent mechanism (Kohn *et al.*, 2002; Aarts *et al.*, 2012) while increased replication stress is generally linked to deregulated CDK2 activity in S-

phase (Bridget T Hughes *et al.*, 2013; Bačević *et al.*, 2017; Daigh *et al.*, 2018; Koppenhafer *et al.*, 2020). However, CDK1 inhibition has also been shown to promote DNA damage in S-phase again demonstrating overlap between these kinases (Liao *et al.*, 2017).

This chapter aims to investigate the role of CDKs 1 and 2 in replication stress and resistance to CHK1 inhibition. To this end, HCC38, H737R and HPrexR cell lines were tested with CDK1/2 inhibitors RO-3306 and Roscovitine in combination with CHK1 inhibitor SRA737 and WEE1 inhibitor Adavosertib and markers of replication stress examined. In addition, replication stress inducing agents Gemcitabine and Hydroxyurea were also tested on these cell lines to investigate if CHK1i resistant cell lines have become generally more resistant to replication stress. As CHK1 inhibitors are also known to potentiate the effects of Gemcitabine (McNeely, Beckmann and Bence Lin, 2014) this drug combination was also tested in HCC38, H737R and HPrexR cell lines.

### **Chapter aims and objectives**

- Investigate the role of replication stress in resistance to CHK1 inhibitors.
  - Cross profile parental and resistant cell lines with replication stress inducing agents Gemcitabine and Hydroxyurea.
  - Western blot markers of replication stress in response to CHK1 and WEE1 inhibitors.
- Investigate the role of CDK1/2 in resistance to CHK1 inhibitors in parental and resistant cell lines.
  - Cross profile parental and resistant cell lines with CDK1/2 inhibitors R0-3306 and Roscovitine as a monotherapy and in combination with CHK1 and WEE1 inhibitors.

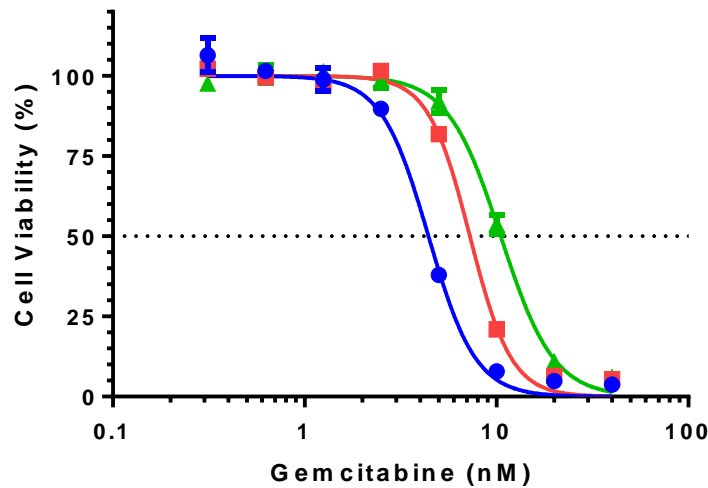
## 5.2 Results

### 5.2.1 Response of H737R and HPrexR to inducers of replication stress

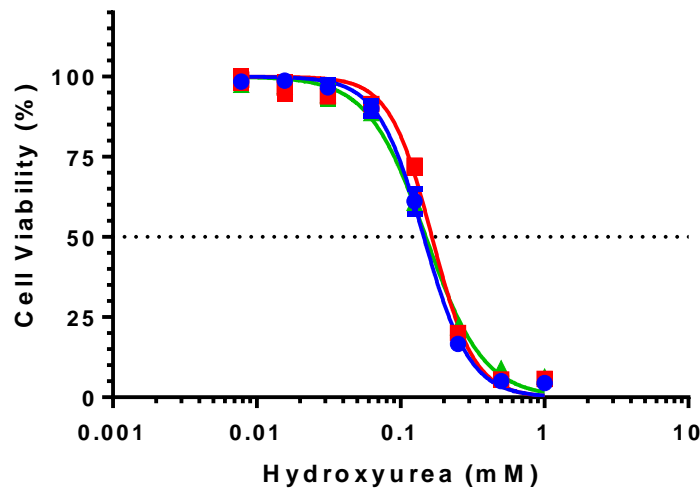
Gemcitabine and Hydroxyurea have both been shown to induce replication stress, likely via the inhibition of ribonucleotide reductase (RNR) leading to nucleotide depletion and slowing and stalling of DNA replication forks (JW, 1992; Karnitz *et al.*, 2005). In addition, Gemcitabine triphosphate (an active metabolite of Gemcitabine) is incorporated into DNA during replication followed by one deoxynucleotide, forming a masked termination stopping proofreading enzymes from removing Gemcitabine (Plunkett, Huang and Gandhi, 1995). As inhibition of both CHK1 and WEE1 appears to induce replication stress in HCC38 but not H737R and potentially HPrexR cells, we hypothesised H737R and HPrexR cells may also be resistant to compounds that induce replication stress directly. Therefore, the dose response of Gemcitabine and Hydroxyurea was determined in HCC38, H737R and HPrexR cell lines. H737R and HPrexR cell lines were significantly more resistant to Gemcitabine than HCC38 cells (**Figure 5.1 A**). HCC38, H737R and HPrexR exhibited GI<sub>50</sub> values of 4.12nM, 11.35nM and 7.95nM respectively for gemcitabine, demonstrating approximately 3-fold and 2-fold resistance to gemcitabine for H737R and HPrexR cell lines respectively versus parental cells (**Figure 5.1 C**). In response to Hydroxyurea, no significant difference in GI<sub>50</sub> was detected between HCC38, H737R and HPrexR cell lines (**Figure 5.1 B**).

### HCC38 GI<sub>50</sub> Determination

**A**



**B**



● HCC38 Parental    ■ HCC38 PrexR    ▲ HCC38 737R

**C**

HCC38		Parental	H737R		HPrexR	
		GI <sub>50</sub> ± SD	GI <sub>50</sub> ± SD	RF	GI <sub>50</sub> ± SD	RF
Gemcitabine (nM)	DNA Damage	4.12 ± 0.31 (n=3)	11.35 ± 1.27 (n=3) *	2.75	7.95 ± 0.86 (n=3) *	1.93
Hydroxyurea (mM)	RNR	0.12 ± 0.01 (n=3)	0.15 ± 0.02 (n=3)	1.25	0.16 ± 0.01 (n=3)	1.33

**Figure 5.1:** GI<sub>50</sub> determination of HCC38, H737R and HPrexR to Gemcitabine and Ribonucleotide Reductase inhibitor Hydroxyurea. Cells were plated at 3200 cells/well in a 96-well plate and grown for 48 hours before treatment with a serial dilution of Gemcitabine or Hydroxyurea for 96 hours and analysed via SRB assay. A) Gemcitabine and B) Hydroxyurea dose response curves calculated with Graphpad Prism 6 using non-linear regression. Dotted line marks the GI<sub>50</sub>. Data points represent the mean ± SD from one representative experiment. C) Table summarises the mean ± SD n = 3 experiments. Statistical significance was calculated using a student's t-test, \* = p ≤ 0.05.

Subunits of RNR, ribonucleotide reductase M1 (RRM1) and ribonucleotide reductase M2 (RRM2) and the critical kinase in Gemcitabine metabolism deoxycytidine kinase (dCK) (OHASHI *et al.*, 2008) were investigated by RNA sequencing and differential analysis of



HCC38, H737R and HPrexR cells detailed in **chapter 6**. RRM1 was significantly upregulated in H737R and HPrexR cells showing a fold change of 1.71 and 1.39 respectively (**Table 5.1**). In HPrexR but not H737R RRM2 and dCK were upregulated by fold changes of 1.28 & 1.29 for respectively (**Table 5.1**).

Gene	H737R		HPrexR	
	Fold Change	padj	Fold Change	padj
dCK	1.02	0.86	1.28	$8.25 \times 10^{-5}$
RRM1	1.71	$3.28 \times 10^{-38}$	1.39	$1.22 \times 10^{-14}$
RRM2	1.13	0.21	1.29	$4.49 \times 10^{-3}$

**Table 5.1: Fold change of genes expressed in H737R and HPrexR cell lines from HCC38 cells.** RNA sequencing and differential expression analysis of HCC38, H737R and HPrexR cell lines carried out as shown in **chapter 6**. Data taken from **Appendix 6.4 & 6.5**.

CHK1 inhibitors have been shown to sensitise cancer cells to DNA damaging agents such as gemcitabine. As H737R and HPrexR cell lines demonstrated resistance to Gemcitabine we investigated the response to a combination of SRA737 and Gemcitabine in HCC38, H737R and HPrexR cells. Two gemcitabine concentrations were tested that caused little to no loss in cell viability of H737R and HPrexR cells in combination with a titration of SRA737 across a standard SRB dose response assay. Interestingly, both H737R and HPrexR were more resistant to the drug combination than HCC38 cells (**Figure 5.2**). H737R showed a higher degree of resistance than HPrexR to the drug combination as seen with Gemcitabine alone (**Figures 5.1-5.3**). At 125nM SRA737, 4nM Gemcitabine caused near complete loss of cell viability in HCC38 cells while H737R cells still showed approximately 60% cell viability under the same conditions (**Figure 5.3**). HPrexR cells showed similar levels of resistance to 2nM Gemcitabine as H737R cells as both maintained 100% cell viability, however HPrexR was more sensitive to 4nM Gemcitabine with a cell viability of approximately 15-20% (**Figure 5.3**). Despite this Gemcitabine highly resensitised H737R and HPrexR to SRA737 especially at

4nM which surpassed the levels of sensitivity seen in HCC38 to SRA737 as a single agent (Figure 5.2 & 5.3).

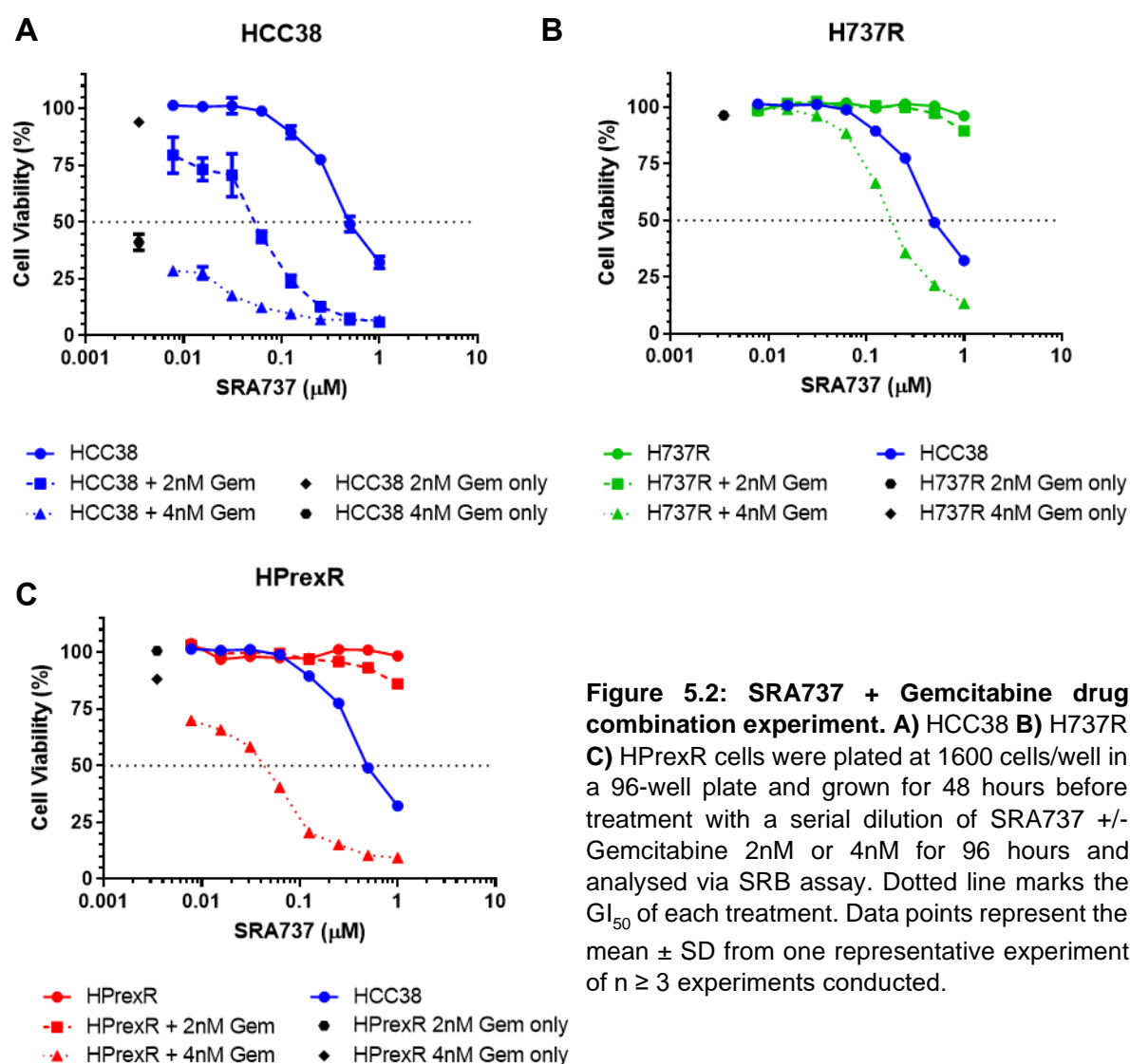


**Figure 5.2: SRA737 + Gemcitabine drug combination experiment.** A) HCC38 B) H737R C) HPrexR cells were plated at 1600 cells/well in a 96-well plate and grown for 48 hours before treatment with a serial dilution of SRA737 +/- Gemcitabine 2nM or 4nM for 96 hours and analysed via SRB assay. Dotted line marks the  $GI_{50}$  of each treatment. Data points represent the mean  $\pm$  SD from one representative experiment of  $n \geq 3$  experiments conducted.

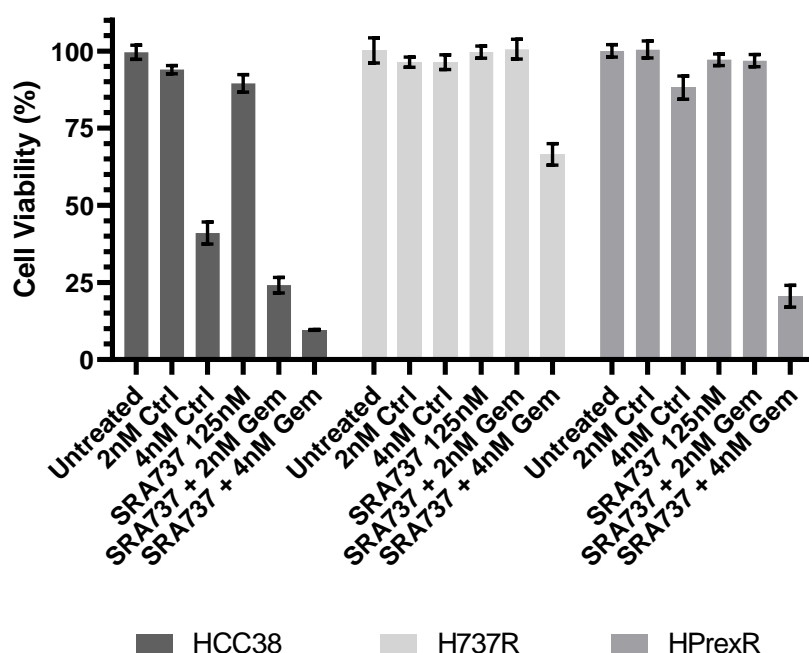


**Figure 5.3: Bar chart of SRA737 + Gemcitabine drug combination experiment.** HCC38, H737R and HPrexR cells were plated at 1600 cells/well in a 96-well plate and grown for 48 hours before treatment with a serial dilution of SRA737 +/- Gemcitabine 2nM or 4nM for 96 hours and analysed via SRB assay. Each bar represents the mean cell viability across treatment conditions at 125nM of SRA737. Error bars show the standard deviation from one representative experiment of  $n \geq 3$  experiments conducted.

In summary, H737R and HPrexR cell lines demonstrate resistance to Gemcitabine, a DNA damaging agent that causes high levels of replication stress via RNR inhibition and incorporation into DNA during replication. However, H737R and HPrexR are not resistant to Hydroxyurea which only inhibits RNR. It could be argued that Gemcitabine sensitised CHK1 resistant cell lines to SRA737, as low concentrations of Gemcitabine (4nM) were able to significantly reduce cell viability of H737R and HPrexR cells (**Figures 5.2 & 5.3**). However, lower concentrations of Gemcitabine (2nM) achieved greater effect in HCC38 cells versus H737R and HPrexR cells (**Figures 5.2 & 5.3**). This supports the idea that H737R and HPrexR cells are better adapted to manage DNA damage/replication stress. Potentially via improved DNA damage repair mechanisms or maintenance of stalled replication forks.

### 5.2.2 The effect of CHK1 and WEE1 inhibition on replication stress in H737R and HPrexR cells

To investigate the role of replication stress in response to CHK1 and WEE1 inhibition the level of Replication protein A 32 kDa subunit (RPA32) was examined via western blot in HCC38 and H737R cell lines in response to SRA737, Adavosertib and a combination of both drugs (**Figures 5.4-5.6**). RPA32 is phosphorylated on multiple sites in response to replication stress, which can be visualised by a band shift on a western blot. In HCC38 cells, RPA32 band shifting increases with increasing doses of SRA737. In contrast with HCC38 cells, band shifting is visible in the H737R cell line across all conditions, but the intensity of the higher bands does not increase with increasing doses of SRA737 (**Figure 5.4**). The increasing intensity of shifted RPA32 bands coincides with increased  $\gamma$ H2AX signal (DNA damage marker) and Cleaved-PARP (C-PARP, marker of apoptosis) in HCC38 cell lines, but these signals aren't greatly induced in H737R in response to SRA737 (**Figure 5.4**). As discussed in **chapter 4**, C-PARP bands are not very well defined between HCC38 and H737R cells, making it difficult to draw a clear distinction between them. However, **appendix 4.1** shows higher levels of C-PARP in HCC38 cells relative to H737R in 2 out of 3 experiments. Levels of the CDK inhibitor  $p21^{Cip1/Waf1}$  were also investigated and showed variability between concentrations but appear to be unchanged at 3 $\mu$ M SRA737 to levels matching the untreated control, suggesting  $p21^{Cip1/Waf1}$  is maintained in the presence of SRA737 (**Figure 5.4**). H737R also shows higher expression of  $p21^{Cip1/Waf1}$  versus HCC38 cells (**Figure 5.4**). Interestingly, loss of pCDK1/2 Y15 also coincides with increased RPA32 band shifting in HCC38 cell lines, while H737R shows no band shifting of RPA32 and maintains pCDK1/2 Y15 phosphorylation (**Figure 5.4**).

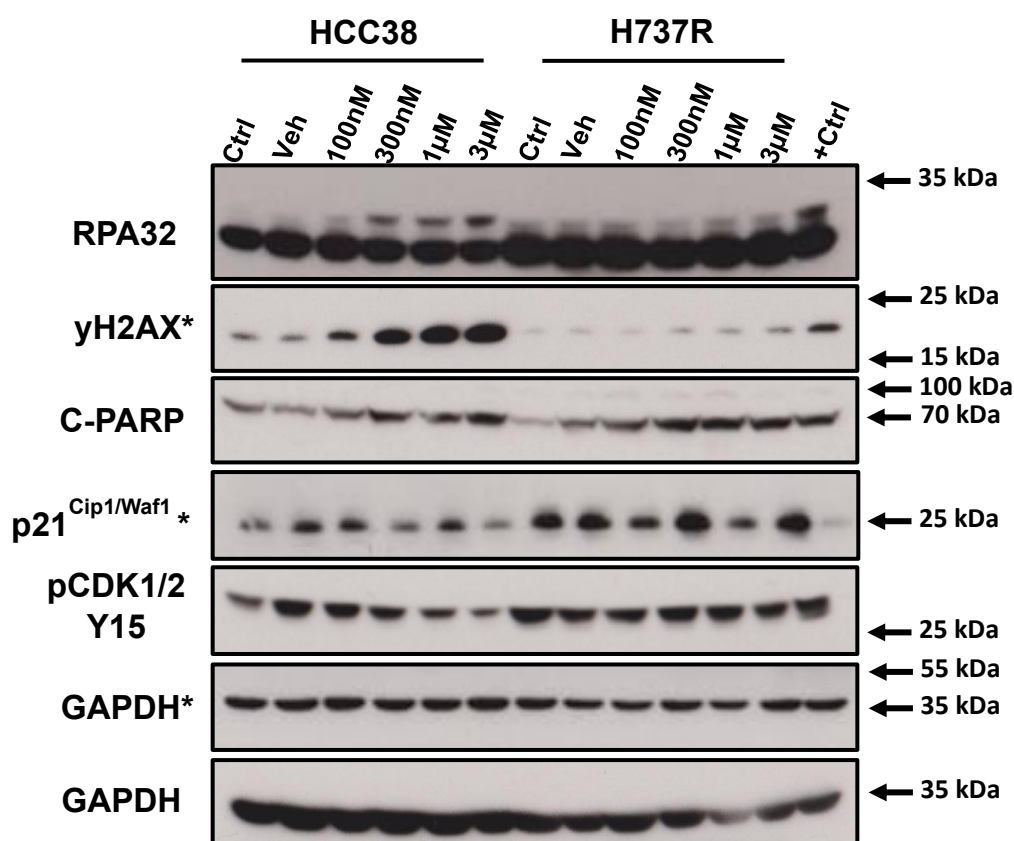


**Figure 5.4: Markers of replication stress and cell death to SRA737 treatment in HCC38 and H737R cells.** Cells were plated in 7cm dishes and left to adhere overnight before incubation with SRA737 at the concentrations indicated for 24 hours before lysis and analysis via western blot. GAPDH = loading Control. Ctrl = Untreated cells. Veh = Vehicle control (DMSO). +Ctrl = HCC38 cells treated with 5μM Cisplatin for 24 hours as a positive DNA damage control. \* Indicates which loading control corresponds with each target. Blots are representative of n=3 experiments. yH2AX, C-PARP, and pCDK1/2 Y15 blots taken from figure 4.2. Blot was re-probed for RPA32 and p21<sup>Cip1/Waf1</sup> signals.

The response to WEE1 inhibitor Adavosertib in HCC38 and H737R cell lines is similar to the response seen with SRA737. RPA32 band shifting, yH2AX and C-PARP all increase with increasing doses of Adavosertib in HCC38 cells (**Figure 5.5**). RPA32, yH2AX and C-PARP do not increase greatly in H737R cell lines, except at 1μM and 2μM of Adavosertib, but this response is much lower than seen in HCC38 cells (**Figure 5.5**). In contrast with **figure 5.4**, p21<sup>Cip1/Waf1</sup> appears to decrease with increasing concentrations of Adavosertib, whereas p21<sup>Cip1/Waf1</sup> levels were maintained with increasing concentrations of SRA737. Additionally, pCDK1/2 Y15 is not maintained in H737R which coincides with lower p21<sup>Cip1/Waf1</sup> levels and increasing RPA32 band shifting, yH2AX and C-PARP levels.

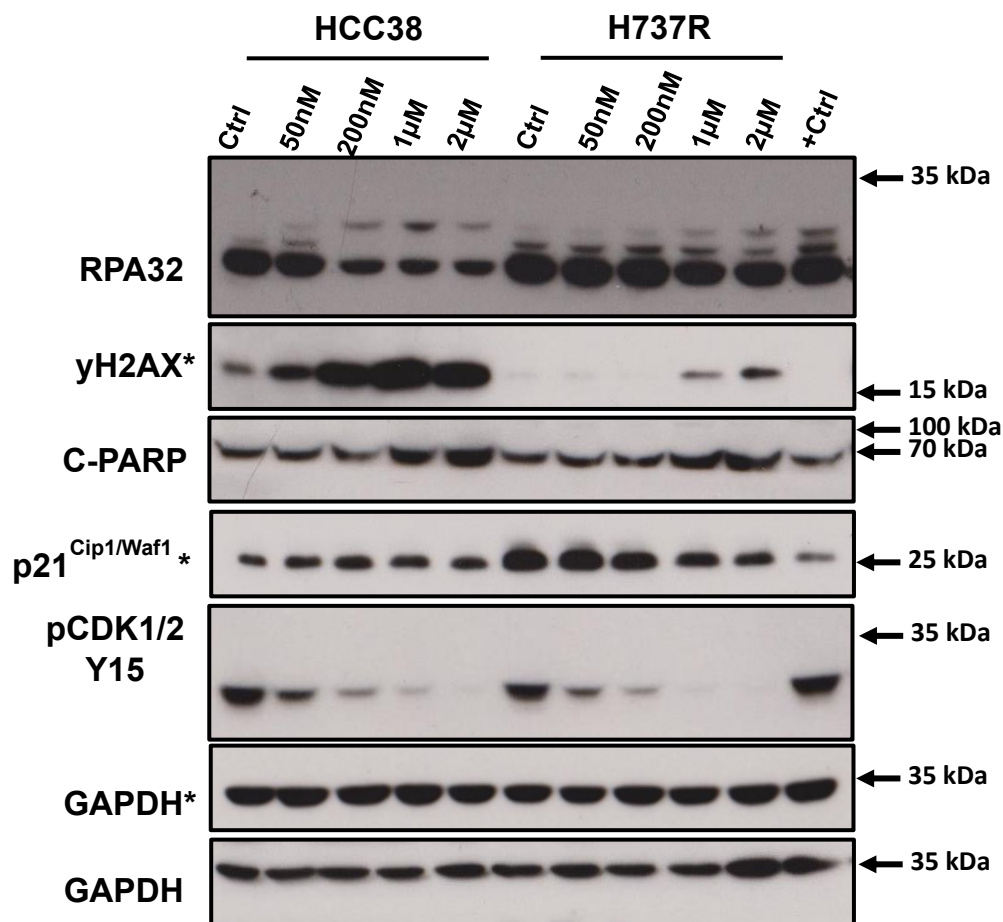


**Figure 5.5: Markers of replication stress and cell death to Adavosertib treatment in HCC38 and H737R cells.** Cells were plated in 7cm dishes and left to adhere overnight before incubation with Adavosertib at the concentrations indicated for 24 hours before lysis and analysis via western blot for the proteins indicated above. GAPDH = loading control. Ctrl = untreated cells. +Ctrl = HCC38 cells treated with Cisplatin 5 $\mu$ M for 24 hours as a positive control for DNA damage. \* Indicates which loading control corresponds with each target. Blots are representative of n=3 experiments.

In response to the combination of both SRA737 and Adavosertib band shifting of RPA32 is greatly increased in both HCC38 and H737R cell lines (**Figure 5.6**). Alongside,  $\gamma$ H2AX and C-PARP are also increased in both HCC38 and H737R cells, however  $\gamma$ H2AX is not as strongly induced in H737R cells versus HCC38 (**Figure 5.6**). This suggests H737R cells are more capable of dealing with replication stress by avoiding subsequent DNA damage. However, C-PARP levels are still high in both HCC38 and H737R indicating these cells may be undergoing apoptosis and that the drug combination is still highly damaging to H737R cells suggesting H737R cells are re-sensitised to SRA737 (**Figure 5.6**) p21<sup>Cip1/Waf1</sup> and pCDK1/2 Y15 levels are decreased in both HCC38 and H737R cell lines with the drug combination (**Figure 5.6**).

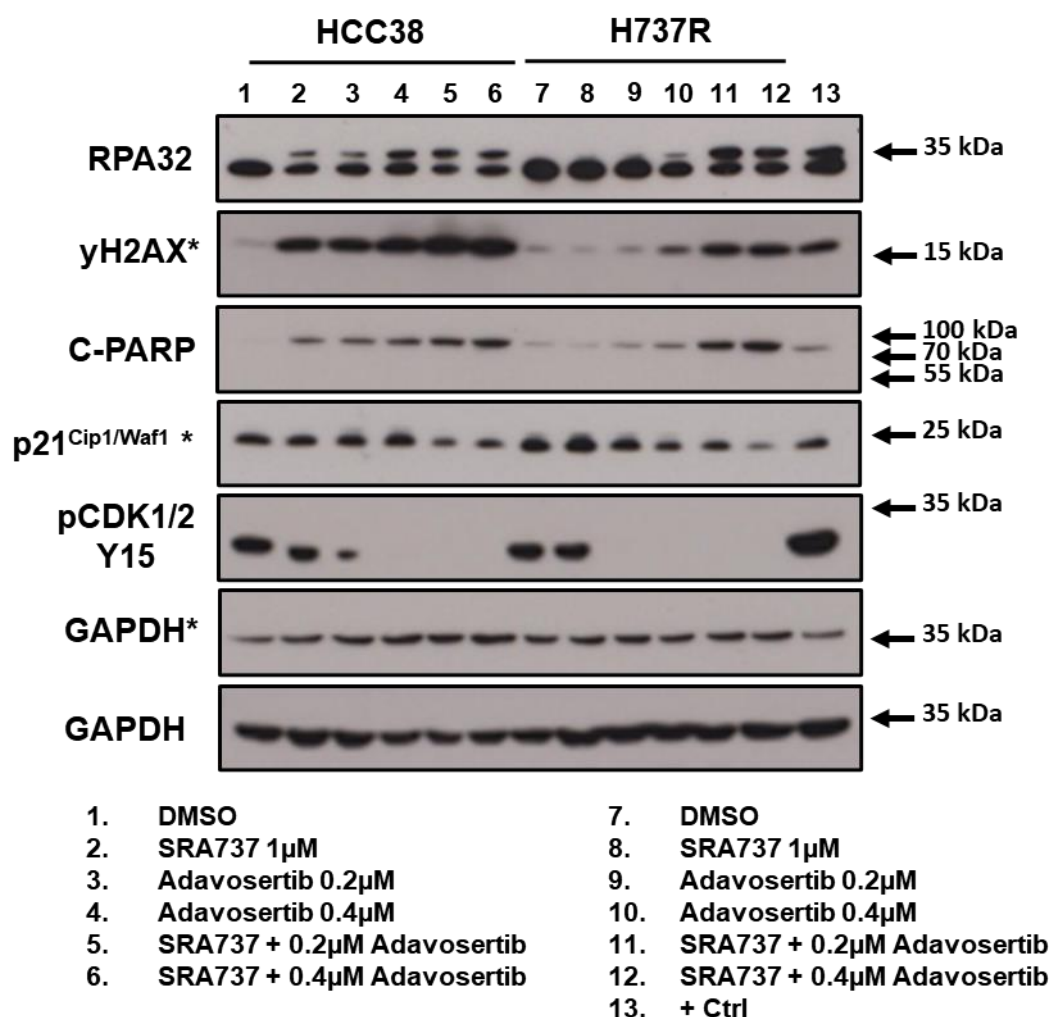


**Figure 5.6: SRA737 + Adavosertib drug combination western blot in HCC38 and H737R cell lines.** Cells were plated in 7cm dishes and left to adhere overnight before incubation with SRA737, Adavosertib or a combination of both drugs at the concentrations indicated for 24 hours before lysis and analysis via western blot of proteins indicated above. GAPDH = loading control. Veh = Vehicle control (DMSO). \* Indicates which loading control corresponds with each target. Blots are representative of n=3 experiments.

In summary, SRA737 and Adavosertib cause replication stress indicated by band shifting of RPA32 and induction of γH2AX in HCC38 but not in H737R cells (**Figures 5.4 & 5.5**). However, a combination of both drugs increases replication stress in H737R cells (**Figure 5.6**) and potentially HPrexR cells suggested by the dose response experiments in **figure 4.14** that show Adavosertib sensitises HPrexR cells to SRA737. Interestingly the CDK inhibitor p21<sup>Cip1/Waf1</sup> is elevated in H737R cells but reduced by inhibition of WEE1 or during dual inhibition of CHK1 and WEE1 in both cell lines but not by CHK1 inhibition alone. Potentially,

overactivation of CDKs by Adavosertib or SRA737 + Adavosertib in combination leads to CDK dependent degradation of p21<sup>Cip1/Waf1</sup>. If so, this would suggest SRA737 does not strongly activate CDKs while Adavosertib does and might explain why pCDK1 Y15 is maintained in H737R cells treated with SRA737 and not Adavosertib or the drug combination (**Figures 5.4-5.6**). While H737R showed a high induction of  $\gamma$ H2AX, indicative of DNA damage with the drug combination,  $\gamma$ H2AX was still lower than seen under the same conditions in HCC38 cells (**Figure 5.6**). This suggests that H737R cells are more resistant to the drug combination than HCC38 cells, possibly via a mechanism that allows the cells to better respond to replication stress or DNA damage.

### 5.2.3 The role of CDK activity in resistance to CHK1 inhibition

A study investigating resistance to the CHK1 inhibitor Prexasertib showed the CDK1 inhibitor RO-3306 was able to rescue viability of Ovarian cancer cell lines from treatment with Prexasertib and suggested this was due to a prolonged G2 delay enforced by CDK1 inhibition (Nair *et al.*, 2020). CHK1 and WEE1 inhibitors have been shown to reduce the inhibitory phosphorylation Y15 of CDK1/2 in our HCC38 cell lines, suggesting that CDK1/2 activity is increased. Therefore, it was hypothesised that inhibition of CDK activity by RO-3306 should confer resistance to CHK1 inhibition in HCC38 cells via inhibition of CDK1. Initially, the GI<sub>50</sub> value of the small-molecule CDK1 inhibitor RO-3306 was determined in HCC38, H737R and HPrexR cell lines. RO-3306 has been shown to inhibit both CDK1 and CDK2 but did not strongly interfere with S-phase processes in HeLa cells, suggesting its CDK2 inhibitory activity is limited and its activity is predominantly due to CDK1 inhibition (Vassilev *et al.*, 2006). No significant difference in RO-3306 GI<sub>50</sub> value was seen in either H737R or HPrexR compared with parental HCC38 cells (**Figure 5.7**).



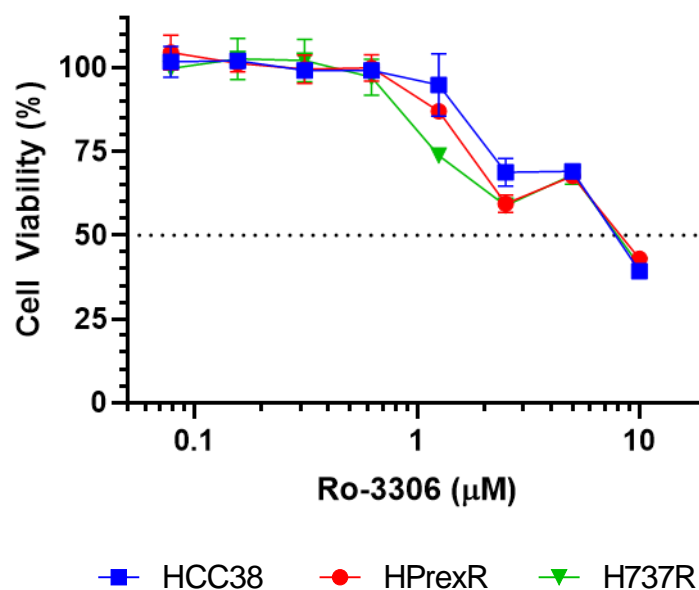
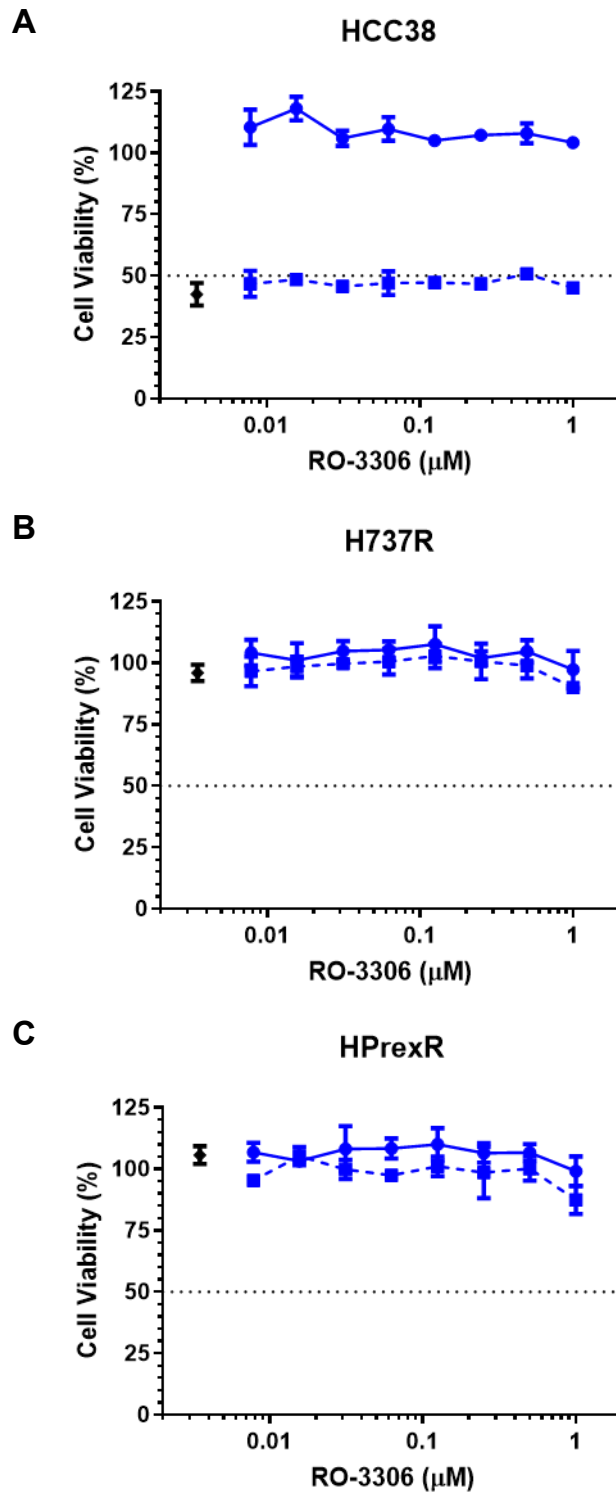


**Figure 5.7: GI<sub>50</sub> determination of HCC38, H737R and HPrexR cell lines to CDK1 inhibitor RO-3306.** HCC38, H737R and HPrexR cells were plated at 1600 cells/well in a 96-well plate and grown for 48 hours before treatment with a serial dilution of RO-3306 for 96 hours and analysed via SRB assay. Dotted line marks the GI<sub>50</sub> of RO-3306, data points represent the mean  $\pm$  SD from one experiment representative of  $n \geq 3$  experiments.

Additionally, RO-3306 failed to rescue cell viability in HCC38 cells from CHK1 inhibition via SRA737 (**Figure 5.8 A**). This suggests that the cell killing effects of SRA737 are not dependent on CDK1 activity or abrogation of the G2/M checkpoint. No difference was seen in H737R and HPrexR cell lines to combined inhibition of CHK1 and CDK1 (**Figures 5.8 B & C**), which is expected as these cells are already highly resistant to SRA737.



◆ 5μM SRA737 Ctrl    ● RO-3306 Only    ■ RO-3306 + 5μM SRA737

**Figure 5.8: RO-3306 + SRA737 drug combination experiment.** A) HCC38, B) H737R and C) HPrexR cells were plated at 1600 cells/well in a 96-well plate and grown for 48 hours before treatment with a serial dilution of RO-3306 +/- 5μM of SRA737 for 96 hours and analysed via SRB assay. Dotted line marks the  $GI_{50}$  of RO-3306, data points represent the mean  $\pm$  SD from one experiment representative of  $n \geq 3$  experiments.

As the CDK1 inhibitor RO-3306 failed to restore cell viability in HCC38 cells, we hypothesised a resistance to CHK1 and WEE1 inhibition may be dependent on CDK2 activity instead. To test this hypothesis, the CDK inhibitor Roscovitine was also tested on HCC38, H737R and HPrexR cell lines in combination with SRA737 and the SRA737 + Adavosertib combination. Roscovitine has been shown to inhibit CDK1/Cyclin B, CDK2/Cyclin A/E and CDK5/p35 with  $IC_{50}$  values of 0.65 $\mu$ M, 0.7 $\mu$ M and 0.16 $\mu$ M respectively (Meijer *et al.*, 1997). Initially, the  $GI_{50}$  values for Roscovitine were determined in HCC38, H737R and HPrexR cell lines and no significant difference was detected (**Figure 5.9**). Prior western blotting experiments have shown an increase in replication stress markers to SRA737 as a single agent in HCC38 cells (**Figure 5.1**). H737R cells do not respond to SRA737 as a single agent but combined treatment with SRA737 and Adavosertib induces markers of replication stress and increases sensitivity to SRA737 (**Figures 4.14 & 5.3**). It was hypothesised that inhibition of CDK2 with Roscovitine should rescue the replication stress response and the loss of cell viability caused by SRA737 and Adavosertib combination treatment.

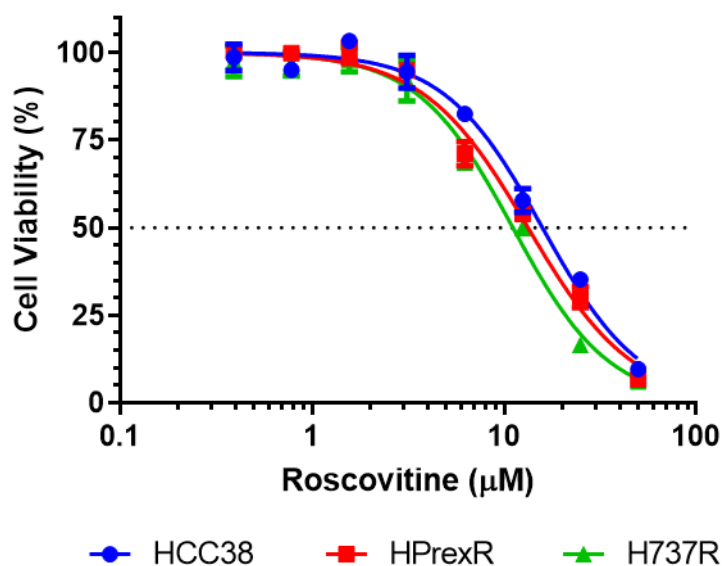


**Figure 5.9:  $GI_{50}$  determination of HCC38, H737R and HPrexR cell lines to CDK2/1 inhibitor Roscovitine.** HCC38, H737R and HPrexR cells were plated at 1600 cells/well in a 96-well plate and grown for 48 hours before treatment with a serial dilution of Roscovitine for 96 hours and analysed via SRB assay. Dose response curves calculated with Graphpad Prism 6 using non-linear regression. Dotted line marks the  $GI_{50}$  of RO-3306, data points represent the mean  $\pm$  SD from one experiment representative of  $n \geq 3$  experiments.

HCC38, H737R and HPrxR cells were treated in a drug combination experiment with SRA737 +/- Adavosertib and Roscovitine. In contrast to RO-3306, Roscovitine increased cell viability in HCC38 cells treated with SRA737 (**Figure 5.10**). HCC38 cell lines treated with the SRA737 + Adavosertib drug combination showed almost complete loss of viability even at low concentrations of SRA737 (**Figure 5.10**). Strikingly, Roscovitine was able to partially rescue this effect in a dose dependent manner (**Figure 5.10**). In contrast to HCC38 cells, Roscovitine didn't rescue the effects of SRA737 in H737R cells and at 5 $\mu$ M even reduced cell viability (**Figure 5.11**) although, this is likely explained due to H737R cells already exhibiting high levels of resistance to SRA737. However, Roscovitine did partially rescue H737R cells from the combination treatment of SRA737 + Adavosertib, but there was little difference between 1 $\mu$ M and 5 $\mu$ M concentrations of Roscovitine (**Figure 5.11**). The response of HPrxR cells mirrored that of the H737R cell line (**Figure 5.12**).

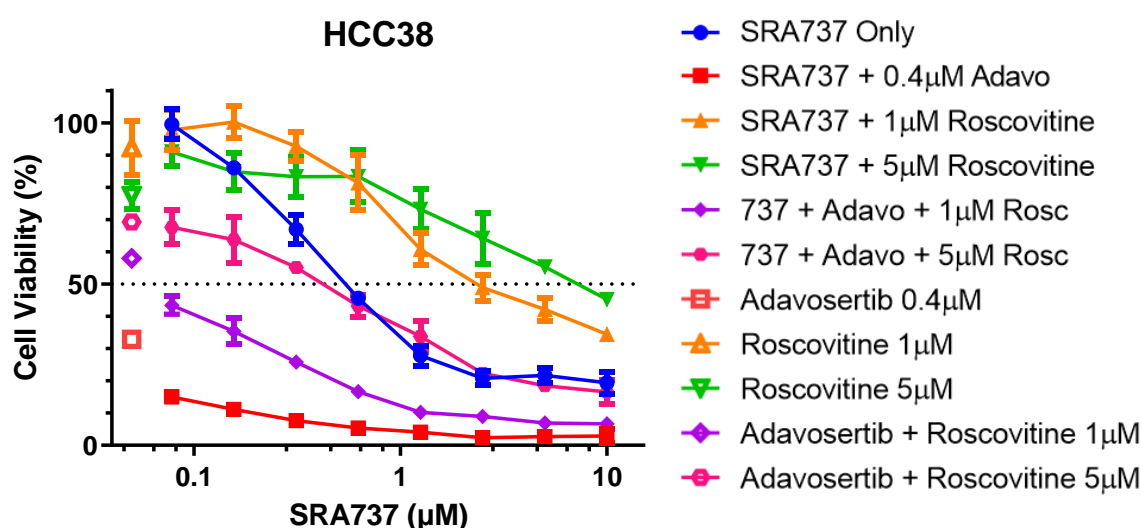


**Figure 5.10: HCC38 SRA737 + Adavosertib + Roscovitine drug combination experiment.** HCC38 cells were plated at 1600 cells/well in a 96-well plate and grown for 48 hours before treatment with a serial dilution of SRA737 +/- 0.4 $\mu$ M Adavosertib and +/- 1 $\mu$ M or 5 $\mu$ M Roscovitine for 96 hours and analysed via SRB assay. Dotted line marks the GI<sub>50</sub> of each treatment, data points represent the mean  $\pm$  SD from one experiment representative of  $n \geq 3$  experiments.

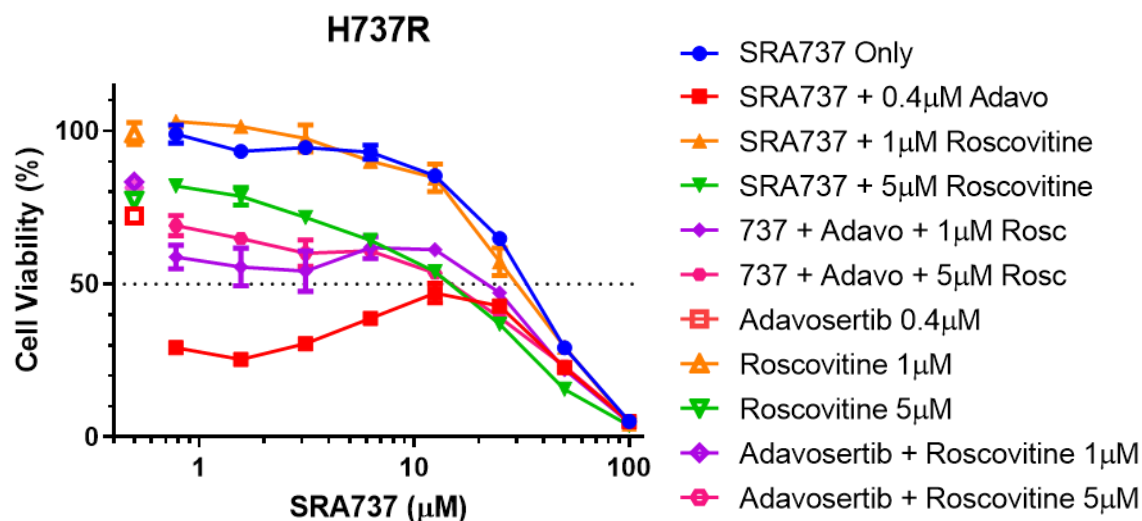


**Figure 5.11: H737R SRA737 + Adavosertib + Roscovitine drug combination experiment.** H737R cells were plated at 1600 cells/well in a 96-well plate and grown for 48 hours before treatment with a serial dilution of SRA737 +/- 0.4μM Adavosertib and +/- 1μM or 5μM Roscovitine for 96 hours and analysed via SRB assay. Dotted line marks the  $GI_{50}$  of each treatment, data points represent the mean  $\pm$  SD from one experiment representative of  $n \geq 3$  experiments.

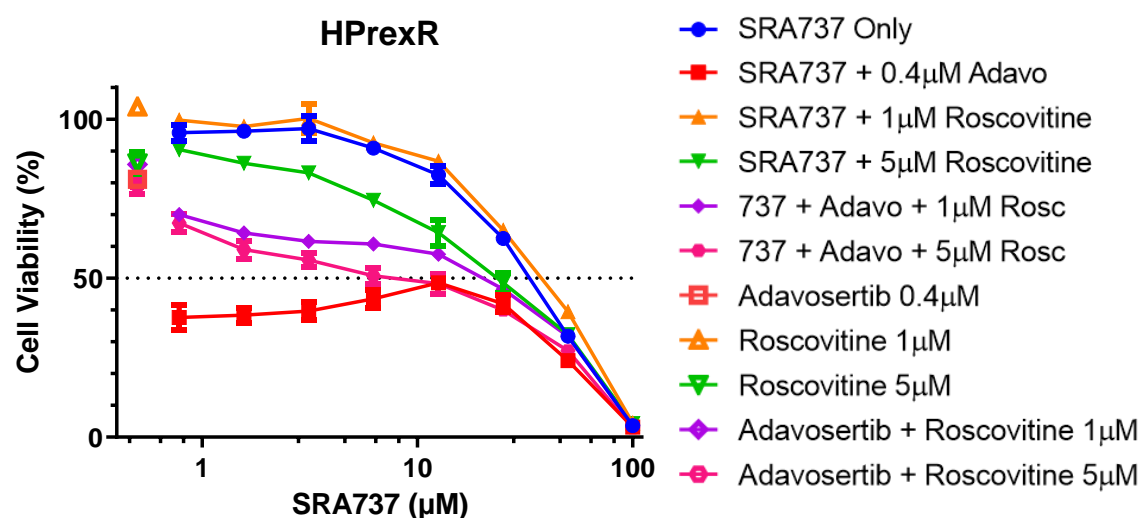
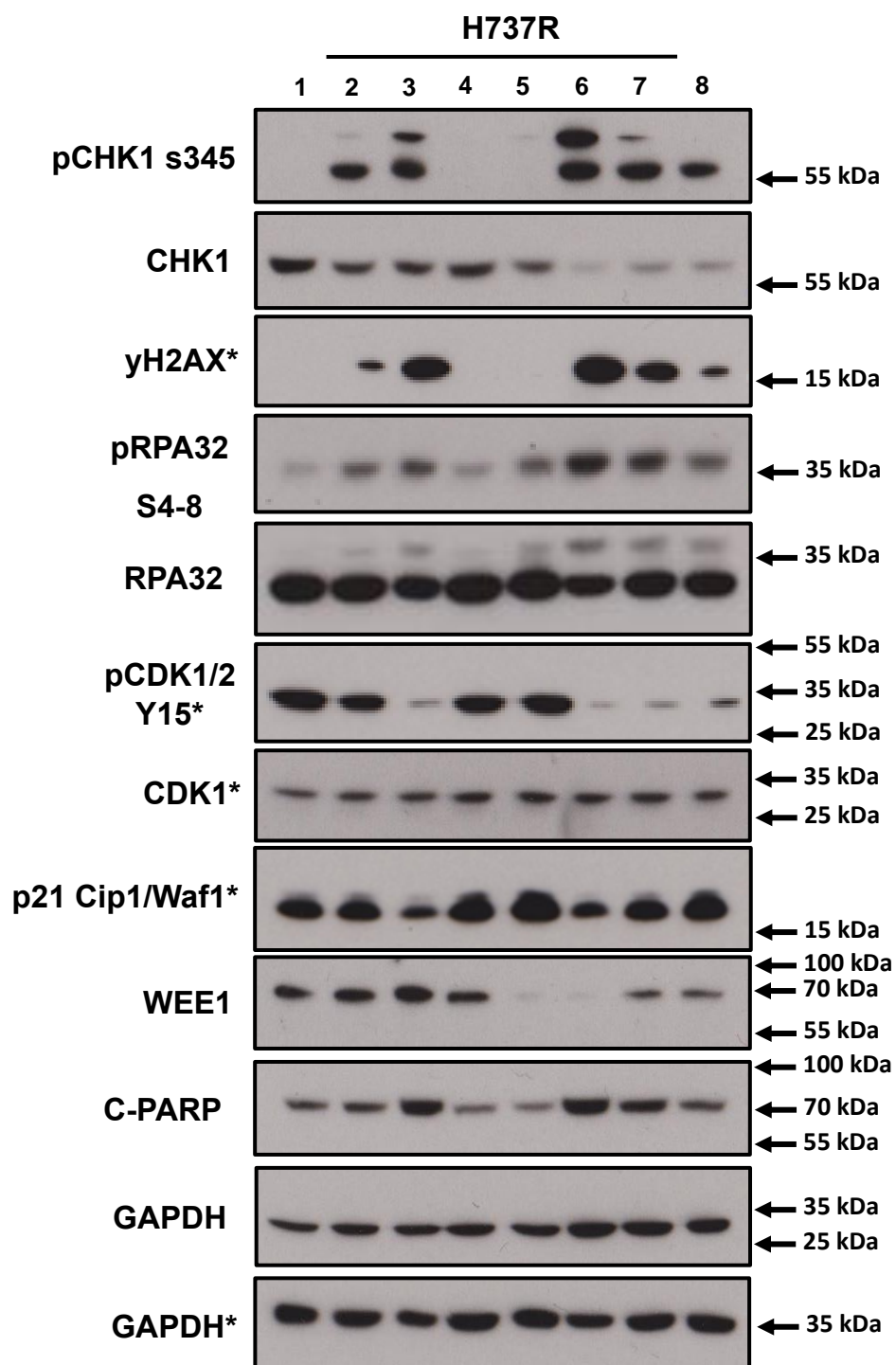


**Figure 5.12: HPrexR SRA737 + Adavosertib + Roscovitine drug combination experiment.** HPrexR cells were plated at 1600 cells/well in a 96-well plate and grown for 48 hours before treatment with a serial dilution of SRA737 +/- 0.4μM Adavosertib and +/- 1μM or 5μM Roscovitine for 96 hours and analysed via SRB assay. Dotted line marks the  $GI_{50}$  of each treatment, data points represent the mean  $\pm$  SD from one experiment representative of  $n \geq 3$  experiments.

The molecular effects of Roscovitine in combination with SRA737 and Adavosertib were investigated in H737R cells by western blot. pCHK1 s345 and yH2AX were both reduced in SRA737 + Adavosertib with the addition of Roscovitine, versus SRA737 + Adavosertib combination alone in a dose dependent manner (**Figure 5.13**). RPA32 band shifting and pRPA32 s4-8 levels, both markers of replication stress, were slightly reduced by the addition of Roscovitine to SRA737 + Adavosertib treated cells (**Figure 5.13**). pCDK1 Y15 and p21<sup>Cip1/Waf1</sup> increased with increasing concentrations of Roscovitine when added to the combination of SRA737+Adavosertib (**Figure 5.13**) and decreased with Adavosertib alone or in combination with SRA737, supporting the idea that CDK activation leads to p21<sup>Cip1/Waf1</sup> loss (**Figure 5.13**). Interestingly, WEE1 protein levels decreased in cells treated with SRA737 + Adavosertib but increased with the addition of Roscovitine to this combination, however 5µM of Roscovitine alone also caused a reduction of WEE1 levels (**Figure 5.13**). C-PARP, a marker of apoptosis also decreased with the addition of Roscovitine to the combination of SRA737 + Adavosertib in a dose dependent manner and was highest in cells treated with the CHK1i + WEE1i combination or Adavosertib alone (**Figure 5.13**).



- |                      |   |
|----------------------|---|
| 1. DMSO              | 5. 5μM Roscovitine                                  |
| 2. 3μM SRA737        | 6. 3μM SRA737 + 0.4μM Adavosertib                   |
| 3. 0.4μM Adavosertib | 7. 3μM SRA737 + 0.4μM Adavosertib + 1μM Roscovitine |
| 4. 1μM Roscovitine   | 8. 3μM SRA737 + 0.4μM Adavosertib + 5μM Roscovitine |

**Figure 5.13: SRA737 + Adavosertib + Roscovitine drug combination western blot in H737R cells.** Cells were plated in 6-well plates and left to adhere overnight before incubation in SRA737, Adavosertib and Roscovitine, or a combination of SRA737 + Adavosertib +/- Roscovitine at concentrations indicated for 24 hours before lysis and analysis via western blot of the proteins indicated above. \* Indicates which loading control corresponds with each target. Blots are representative of n=3 experiments.

To summarise, no difference in dose response was seen to CDK inhibitors RO-3306 or Roscovitine (**Figures 5.7 & 5.9**). However, Roscovitine but not RO-3306 rescued cell viability loss from SRA737 treatment in HCC38 cell lines (**Figures 5.8 & 5.10**). Moreover, Roscovitine partially rescued the effects of the drug combination SRA737 + Adavosertib in all cell lines tested (**Figures 5.10-5.12**) suggesting that the cell killing effect of SRA737 as a single agent and in combination with Adavosertib is at least in part tied to CDK2 but not CDK1 activation and therefore S-phase related rather than G2/M checkpoint related. Western blotting show that Roscovitine treatment reduced markers of DNA damage, replication stress and apoptosis induced by SRA737 + Adavosertib (**Figure 5.13**), suggesting over activation of CDK2 was driving replication stress and subsequent cell death. Levels of pCDK1 Y15, p21<sup>Cip1/Waf1</sup> and WEE1 increased with the addition of Roscovitine (**Figure 5.13**) suggesting WEE1 and p21<sup>Cip1/Waf1</sup> may be negatively regulated by CDK activity.



## 5.3 Discussion

In this chapter, the roles of replication stress and CDK1/2 were investigated in more detail. Western blotting showed SRA737 and Adavosertib cause replication stress in HCC38 but not H737R cells indicated by band shifting of RPA32 (**Figure 5.4 & 5.5**). However, combined inhibition of CHK1 and WEE1 increased replication stress in H737R cells (**Figure 5.6**). CDK inhibitor p21<sup>Cip1/Waf1</sup> was also seen in higher levels in H737R cells and appeared to decrease in both cell lines with combined treatment of SRA737 and Adavosertib (**Figure 5.6**). Replication stress inducing agents Gemcitabine and Hydroxyurea were also tested in HCC38, HPrexR and H737R cell lines. Both H737R and HPrexR demonstrated resistance to Gemcitabine but not Hydroxyurea (**Figure 5.1**). Excitingly, combined treatment of SRA737 and Gemcitabine highly resensitised H737R and HPrexR to CHK1 inhibition and greatly increased sensitivity in HCC38 cells (**Figure 5.2 & 5.3**).

To determine if sensitivity caused by Adavosertib was CDK1 or CDK2 dependent, CDK inhibitors RO-3306 and Roscovitine were tested in combination with SRA737 and/or Adavosertib. CDK1 inhibitor RO-3306 failed to reduce sensitivity to SRA737 in HCC38, H737R and HPrexR cell lines (**Figure 5.8**). CDK2 inhibitor Roscovitine increased SRA737 resistance in HCC38 cells and reduced the effects of the SRA737 + Adavosertib drug combination in HCC38, H737R and HPrexR cell lines (**Figure 5.10-5.12**). Molecular analysis of SRA737 by western blot showed Roscovitine reduced DNA damage marker  $\gamma$ H2AX, RPA32 band shifting, and apoptosis marker C-PARP, suggesting inhibition of CDK2 reduces the effects of replication stress and subsequent DNA damage and cell death caused by SRA737 and Adavosertib (**Figure 5.13**). These results are discussed in more detail below.

### 5.3.1 Investigating the role of replication stress in resistance to CHK1 inhibition

Since inhibition of both CHK1 and WEE1 appears to induce replication stress in HCC38 but not H737R and potentially HPrexR cells, we hypothesised H737R and HPrexR cells may also be resistant to compounds that induce replication stress. Since both Gemcitabine and HU are

known to induce replication stress they were both investigated for their effects on the viability of HCC38 parental cells versus H737R and HPrexR cell lines. Interestingly, H737R and HPrexR cell lines both showed cross resistance to Gemcitabine but not to Hydroxyurea despite the ability for both drugs to inhibit RNR (**Figure 5.1**)(JW, 1992; Plunkett, Huang and Gandhi, 1995) suggesting resistance to Gemcitabine may be dependent on its unique mechanism of action. Gemcitabine is an analogue of deoxycytidine and upon cell entry is rapidly phosphorylated by deoxycytidine kinase (dCK) forming the active Gemcitabine diphosphate and Gemcitabine triphosphate. Gemcitabine diphosphate inhibits RNR (Heinemann and Plunkett, 1989; CH *et al.*, 1991) while Gemcitabine triphosphate competes with deoxycytidine triphosphate for incorporation into DNA (Hertel *et al.*, 1989). Once incorporated into DNA, DNA polymerase adds one more deoxynucleotide hiding Gemcitabine triphosphate from proof reading enzymes in what is termed a masked termination (Plunkett, Huang and Gandhi, 1995) leading to increased replication stress (Karnitz *et al.*, 2005).

Resistance to Gemcitabine has been documented previously, one known mechanism is via the downregulation of dCK. Downregulation of this kinase by SiRNA has been shown to increase resistance to Gemcitabine (OHHASHI *et al.*, 2008), and a study adapting the ovarian cancer cell line A2780 to gemcitabine identified downregulation of dCK as the driver of acquired resistance (Al-Madhoun *et al.*, 2004) due to the requirement for dCK to phosphorylate Gemcitabine. Phosphorylation of dCK by ATM on Serine 74 has been shown to inhibit CDK1 activity and the help maintain the G2/M checkpoint in response to DNA damage by ionising radiation (Yang *et al.*, 2012) identifying an area of crosstalk between dCK and CHK1. However, ATR the main upstream kinase of CHK1, has also been shown to activate dCK during periods of replication stress (Beyaert *et al.*, 2016) suggesting CHK1 and dCK likely work together to maintain CDK1 inhibition during replication stress. In addition, RNA sequencing carried out in **chapter 6** identified dCK shows no significant difference in expression in H737R and a small increase in HPrexR with a fold difference of 1.44 in HPrexR cell lines (**Table 5.1**). Therefore, it seems unlikely that dCK downregulation is the cause of

Gemcitabine resistance in H737R and HPrexR cell lines, as this appears incompatible with both CHK1i and Gemcitabine resistance.

Although H737R and HPrexR cells appear to be resistant to the drug combination of Gemcitabine and SRA737, it is still important to acknowledge that low concentrations of Gemcitabine still sensitise H737R and HPrexR to SRA737 (**Figures 5.2 & 5.3**). At 4nM Gemcitabine dose response curves in H737R and HPrexR appear more sensitive than HCC38 treated with SRA737 alone (**Figure 5.2**) showing that Gemcitabine is still very effective at sensitising these cells to CHK1 inhibition. Once activated by dCK Gemcitabine can inhibit RNR, an important protein in the synthesis of dNTPs for DNA replication. Therefore, this may indicate RNR is critical to maintain resistance to CHK1 inhibition. However, the ability of Gemcitabine triphosphate to incorporate into DNA and form masked chain terminations should not be overlooked. It is possible H737R and HPrexR cell lines may be adapted to better manage DNA damage caused by Gemcitabine triphosphate incorporation. DNA damage repair pathways such as base excision repair (BER), nucleotide excision repair (NER), homologous recombination (HR) and non-homologous end joining (NHEJ) are supposedly incapable of modulating the cytotoxicity of Gemcitabine (M *et al.*, 2003). However, the Mre11 exonuclease part of the Mre11/Rad50/nbs1 (MRN) complex which is important in HR has been shown to remove gemcitabine from the nascent strand of DNA via its 3' to 5' exonuclease activity (Boeckemeier *et al.*, 2020). But in the context of CHK1 inhibition, loss of Mre11 has been shown to reduce the accumulation of ssDNA and double stranded breaks in cells treated with a CHK1 inhibitor as a single agent (Thompson, Montano and Eastman, 2012). This suggests that cross resistance to Gemcitabine and CHK1 inhibitors via Mre11 may be incompatible mechanisms of resistance.

RNR Catalytic Subunit M1 has also been associated with Gemcitabine resistance (Beyaert *et al.*, 2016) and it's inhibition by Gemcitabine is thought to contribute to the synergism seen when treatment is combined with a CHK1 inhibitor (Bennett *et al.*, 2012). RNA sequencing carried out in **chapter 6** identified significant overexpression of RRM1 in H737R and HPrexR

cell lines by a factor of 1.71 and 1.39 respectively (**Table 5.1**) (**Appendix 6.4 & 6.5**). While changes in RRM1 expression have not been confirmed at the protein level, RRM1 mRNA expression correlates with the difference in Gemcitabine resistance seen between H737R and HPrexR cell lines, with H737R showing greater levels of Gemcitabine resistance versus HPrexR (**Figure 5.1**). Increased RRM1 levels could also explain increased resistance to SRA737 + Gemcitabine synergy seen in H737R and HPrexR cells (**Figures 5.2 & 5.3**) as higher Gemcitabine concentrations may be required to inhibit greater levels of RRM1 to achieve the same synergy (Bennett *et al.*, 2012). This may also explain the lack of any resistance to HU in H737R and HPrexR cells (**Figure 5.1**) as HU inhibits RNR by scavenging the tyrosyl free radical of Ribonucleotide Reductase Catalytic Subunit M2 (RRM2), blocking RNR activity (Navarra and Preziosi, 1999) while Gemcitabine's inhibitory effects on RNR may be RRM1 dependent (Davidson *et al.*, 2004). No significant difference was observed in mRNA levels of RRM2 in H737R cells although a small significant increase was detected in HPrexR cells with a fold-difference of approximately 1.29 (**Table 5.1**) (**Appendix 6.4 & 6.5**). However, RRM2 may not be overexpressed enough to cause any meaningful change in HU dose response, or changes in gene expression may not translate to an increase in RRM2 protein.

Knockdown of RNR subunits by SiRNA has been shown to be synthetically lethal with CHK1 knockdown and pharmacological inhibition, leading to upregulation of  $\gamma$ H2AX and phosphorylation of RPA32 (Taricani *et al.*, 2014). Furthermore, a close interaction was proposed between RNR, CHK1 and DNA Polymerase  $\alpha$  (DNA Pol $\alpha$ ) at the replication complex evidenced by their co-immunoprecipitation suggesting their interaction is important for efficient communication between the replication machinery and replication checkpoint control (Taricani *et al.*, 2014). This is further supported by the known synthetic lethality between knockdown and inhibition of B-family DNA polymerases and CHK1 inhibitor SRA737 (Rogers *et al.*, 2020). In addition, another study identified inhibition of ATR-CHK1 or WEE1 depletes the RRM2 subunit of RNR by activation of CDK2 and subsequent phosphorylation of T33 on RRM2 leading to its degradation (Koppenhafer *et al.*, 2020). However, the ability for WEE1 and CHK1

inhibitors to activate CDK2 and cause replication stress differs and is likely linked to the distinct ways CHK1 and WEE1 regulate CDK activity and manage DNA replication in addition to other cell line dependent effects (Koppenhafer *et al.*, 2020).

Changes in the regulation of RNR either by reducing the ability for CDK2 activity to deplete RNR subunits or by overexpression of limiting RNR subunits may be able to compensate for inhibition of CHK1 and WEE1 by maintaining a suitable pool of dNTPs during CHK1i or WEE1i induced replication stress. As seen in **figures 5.4 & 5.5** replication stress is much lower in H737R cell lines when treated with SRA737 or Adavosertib relative to HCC38 cells. This is indicated by lower levels of  $\gamma$ H2AX and double banding of RPA32, indicative of heavy RPA32 phosphorylation. Interestingly, p21<sup>Cip1/Waf1</sup> decreases with increasing doses of Adavosertib but not SRA737 and appears at a much higher basal level in H737R cells versus HCC38 parental cells (**Figures 5.4 & 5.5**). p21<sup>Cip1/Waf1</sup> is a CDK inhibitor and competes with CDC25A for the same binding site of CDK2/Cyclin A complex and could reduce the ability for CHK1 inhibition to activate CDK2 (Saha *et al.*, 1997). Loss of WEE1 activity via Adavosertib would bypass competition between CDC25A and p21<sup>Cip1/Waf1</sup> and directly activate CDK2, leading to CDK2 dependent degradation of p21<sup>Cip1/Waf1</sup> (Zhu, Nie and Maki, 2005). This may also explain why H737R cells are more sensitive to WEE1 over CHK1 inhibition (**Figures 3.7 & 3.14**) as WEE1 inhibition results in greater activation of CDK2, highlighting a dependency on CDK2 inhibition for resistance to CHK1 inhibitors. The loss of p21<sup>Cip1/Waf1</sup> is even more noticeable in H737R cells treated with SRA737 and Adavosertib in combination (**Figure 5.6**) likely due to the greater increase in CDK activity caused by this drug combination (**Figure 5.14**)(Hauge *et al.*, 2017). Interestingly, a study looking at Prexasertib resistance in High-Grade Serous Ovarian Cancer (HGSOC) showed increased resistance to Gemcitabine between the OVCAR8 parental cell line and the OVCAR8R (Prexasertib resistant) cell line. However, both cell lines were highly sensitive to combined treatment with each drug mirroring our results seen with our TNBC cell lines (Nair *et al.*, 2020).

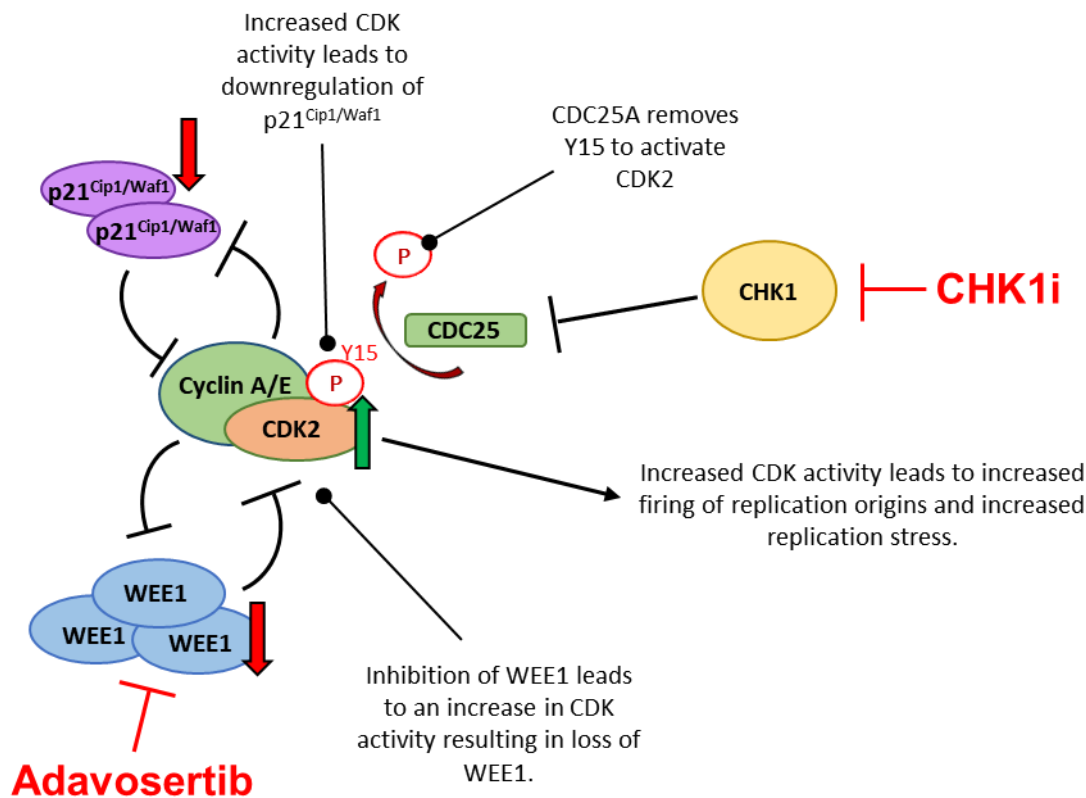


**Figure 5.14: Inhibition of both CHK1 and WEE1 greatly increases CDK activity and leads to reduction of p21<sup>Cip1/Waf1</sup> and WEE1 protein levels.**

### 5.3.2 Investigating the role of Cyclin Dependent kinases in resistance to CHK1 inhibition

To study the roles of CDK1/2 in resistance to CHK1 inhibition with SRA737 and WEE1 inhibition with Adavosertib HCC38, H737R and HPrexR cell lines were tested with CDK inhibitors RO-3306 and Roscovitine. As mentioned previously, RO-3306 inhibits both CDK1 and CDK2 though it is not thought to significantly interfere with CDK2 function in S-phase as it permits successful initiation of DNA replication (Vassilev *et al.*, 2006) and could therefore be considered a weak CDK2 inhibitor. On the other hand, Roscovitine inhibits CDK1, CDK2 and CDK5 (Meijer *et al.*, 1997), therefore care should be taken when interpreting experiments involving these inhibitors.

No difference in GI<sub>50</sub> value was detected in H737R or HPrexR cells versus HCC38 cells to either RO-3306 or Roscovitine (**Figures 5.7 & 5.9**). RO-3306 in combination with SRA737

also failed to rescue the loss of cell viability seen in HCC38 cell lines suggesting CDK1 activity is not required for SRA737 induced cell death (**Figure 5.8**). Interestingly, Roscovitine treatment made HCC38 cells resistant to SRA737 treatment (**Figure 5.10**) and partially rescued the effects of SRA737 + Adavosertib in all cell lines tested (**Figures 5.10-5.12**). These results suggest CDK1 activity is not important for the loss of viability seen with SRA737 as a single agent or in combination with Adavosertib and leaves CDK2 and CDK5 as potential candidates for Roscovitine's effect. H737R and HPrexR cell lines treated with the SRA737 and Adavosertib combination experience a characteristic “bump” in cell viability at approximately 10-12 $\mu$ M of SRA737 (**Figures 5.11 & 5.12**). This was noted in **chapter 4 figure 4.16** and may be linked to the self-limiting effects of SRA737 likely inhibiting CDK2 and CDK1 activity (Ditano and Eastman, 2021).

The ability for Roscovitine to rescue SRA737 + Adavosertib treatment appears to be via the reduction of replication stress. Western blots of H737R show a decrease in replication stress markers  $\gamma$ H2AX, pCHK1 s345, pRPA32 s4-8 and RPA32 double banding with an increasing concentration of Roscovitine in combination with SRA737 + Adavosertib (**Figure 5.13**). In addition, phosphorylation of pCDK1/2 Y15 increases alongside an increase of WEE1 and p21<sup>Cip1/Waf1</sup> (**Figure 5.13**). Unfortunately, the antibody for pCDK1/2 Y15 is non-selective for CDK1 and CDK2 so it isn't possible to distinguish between either kinase. However, increased pCDK1/2 Y15 may be due to relief of CDK dependent degradation of WEE1 and p21<sup>Cip1/Waf1</sup> thereby allowing inhibition of CDK1/2 (**Figure 5.14**)(Zhu, Nie and Maki, 2005; Hughes *et al.*, 2013).

Inhibition of CDK2 via phosphorylation of tyrosine 15 is essential for a normal cell response to replication stress allowing for activation of the S-phase checkpoint and is required for normal DNA replication dynamics (Bridget T Hughes *et al.*, 2013). One study using live single-cell image analysis shows CDK2 activity fluctuates during unperturbed S-phase and demonstrated cells experiencing increased replication stress suppress CDK2 activity to adjust global DNA synthesis rates, allowing for successful replication of DNA (Daigh *et al.*, 2018). In HeLa cells,

CDK5 activity was shown to be important in the cellular response to replication stress (Chiker *et al.*, 2015). Loss of CDK5 by shRNA resulted in higher sensitivity to replication stress inducing agents and S-phase irradiation despite not being directly implicated in DNA repair (Chiker *et al.*, 2015). This suggests inhibition of CDK5 by Roscovitine is likely detrimental to cell viability during inhibition with CHK1 and WEE1 and therefore unlikely to be the cause of Roscovitines rescuing effects (**Figures 5.10-5.13**). This may also explain why Roscovitine failed to completely rescue cell viability from SRA737 + Adavosertib as CDK5 inhibition likely increases replication stress, limiting Roscovitines effects.

Use of CDK inhibitors provides interesting mechanistic insights into the role of CDK activity in resistance to CHK1 inhibitors. However, most inhibitors are rarely very selective and target multiple CDKs at different concentrations making it difficult to draw solid conclusions from any data using these compounds (Sakurikar and Eastman, 2016). In addition, no antibodies are selective for the inhibitory phosphorylation Y15 of CDK1/2, making it difficult to determine the Y15 status of either kinase without separating them via immunoprecipitation (Sakurikar and Eastman, 2016). While RO-3306 did not rescue cell viability in HCC38 cells treated with SRA737, other studies have shown RO-3306 is capable of reducing  $\gamma$ H2AX in S-phase cells induced by CHK1 inhibitors (Sakurikar and Eastman, 2016; Sakurikar *et al.*, 2016), suggesting CDK2 is inhibited significantly by this compound. As none of our experiments investigated the effects of RO-3306 on SRA737 or Adavosertib induced  $\gamma$ H2AX we cannot be certain RO-3306 isn't significantly inhibiting CDK2 in these cell lines, only that RO-3306 does not restore cell viability to SRA737 as Roscovitine has been shown to do (**Figures 5.8 & 5.10-5.12**).

### 5.3.3 Summary

To summarise, CDK2 inhibition is required for normal cellular response to replication stress (Hughes *et al.*, 2013; Daigh *et al.*, 2018) and both SRA737 and Adavosertib have been shown to greatly increase replication stress in these cell lines likely via overactivation of CDK2 (**Figures 5.4-5.6 & 5.13**). The CDK1 inhibitor and weak CDK2 inhibitor RO-3306 (Vassilev *et al.*, 2006) failed to restore viability of HCC38 cells treated with SRA737 (**Figure 5.8**) and loss



of CDK5 has been shown to increase replication stress (Chiker *et al.*, 2015). Therefore, this suggests inhibition of CDK2 by Roscovitine is able rescue the effects of SRA737 +/- Adavosertib seen in HCC38, H737R and HPrexR cell lines (**Figures 5.10-5.13**). Flow cytometry experiments in **chapter 4** revealed HCC38 cells accumulate in S-phase after treatment with a CHK1 inhibitor and H737R cells also accumulate in S-phase when CHK1 and WEE1 are inhibited (**Figures 4.10-4.13**). This does not seem consistent with CHK1 induced activation of CDK1 in S-phase which has been shown to cause premature mitosis (Aarts *et al.*, 2012), however no markers of mitosis were investigated in our experiments. As overactivation of CDK2 is known to cause replication stress and stalling in S-phase (Sakurikar *et al.*, 2016), it follows that H737R and HPrexR cells may be resistant to CHK1i induced replication stress via the maintenance of CDK2 inhibition. P21<sup>Cip1/Waf1</sup> and WEE1 are overexpressed in H737R cells (**Figures 5.4-5.6 & 3.22**) therefore it is possible both proteins act to maintain CDK2 inactivity during single agent treatment with SRA737. However, H737R cells demonstrate cross resistance to Adavosertib, despite loss of pCDK1 Y15 during treatment (**Figure 5.5**) and both H737R and HPrexR are cross resistant to RNR inhibitor Gemcitabine (**Figure 5.1**). In addition, H737R cells show greater resistance to drug combinations of SRA737 + Adavosertib or to Gemcitabine alone but not HU than HCC38 cells (**Figures 4.9-4.13 & 5.1-5.3**). This suggests H737R (and potentially HPrexR cells too) may exhibit changes downstream of CDK2 that build resilience to CDK2 overactivation and replication stress, potentially via RNR. The RNR subunit RRM1 is slightly overexpressed at the RNA level in H737R and HPrexR cell lines (**Table 5.1**). If this translates to increased RRM1 protein levels H737R and HPrexR cell lines may have greater pools of dNTPs available for DNA replication promoting some resilience to replication stress. However, this requires further investigation.

---

# **Chapter 6**

## **Gene Expression Analysis of HCC38 Parental and Resistant Cell Lines**

## 6. Gene Expression Analysis of HCC38 Parental and Resistant Cell Lines

### 6.1 Introduction

Resistance to cancer therapies can occur via several different mechanisms. Cells may alter drug metabolism and activation, compartmentalise a drug away from its target, increase efflux or reduce drug uptake. Drug targets may be altered to stop activity altogether or alterations in compensatory pathways may render the target redundant. Cells may even deregulate apoptotic pathways and upregulate pro survival or DNA damage response pathways to cope with drug effects (Holohan *et al.*, 2013). Many of these adaptations may result in gene expression changes detectable through RNA sequencing.

Interpretation of gene expression data originally relied on low-throughput methods such as quantitative polymerase chain reaction (qPCR) and northern blots which are limited in the number of genes that can be measured. High-throughput technologies such as hybridisation-based microarrays allowed for genome wide studies to take place creating the field of transcriptomics, but were limited to genes already known to researchers and struggled to quantify at the extreme highs and lows of gene expression (Kukurba and Montgomery, 2015). Next generation sequencing (NGS) technologies revolutionised the study of gene expression with the development of RNA-sequencing. RNA sequences are isolated from genomic DNA, converted to complementary DNA (cDNA) and fragmented before sequencing with NGS technologies and mapping to a reference genome. Data can then be provided on the quantity of each RNA sequence in addition to sequence structure itself (Wang, Gerstein and Snyder, 2009). RNA-sequencing has a much higher dynamic range compared to older gene expression technologies, providing accurate quantification of high and low expressed genes and does not require prior knowledge of the genes being sequenced (Wang, Gerstein and Snyder, 2009).

RNA-sequencing has been a highly effective tool in understanding drug resistance in cancers, one study found that expression of circular RNA AKT3 (circAKT3) promoted Cisplatin resistance in gastric cancers. CircAKT3 acted as an inhibitor of micro-RNA-198 suppressing its inhibitory effect on *PI3KR1* expression, which encodes the p85 regulatory subunit of PI3Kinase. Activation of the PI3K/AKT pathway contributed to upregulation of BRCA1 facilitating resistance to CDDP-based DNA damage (Huang *et al.*, 2019). In arabinoside cytarabine (Ara-C) resistant acute myeloid leukaemia (AML) RNA-sequencing analysis identified large gene deletion and frame shift mutations in deoxycytidine kinase (dCK), a kinase of the dNTP salvage pathway. Mutation of dCK stopped the phosphorylation and activation of Ara-C, halting its incorporation into DNA and disruption of DNA synthesis (Rathe *et al.*, 2014). A cell line study investigating heterogeneity of human epithelial ovarian cancer (EOC) found subpopulations of cells which exhibit higher invasive and migratory capacities and identified activation of the PI3K/AKT/mTOR pathway to be associated with these cells. This was shown by the upregulation of many PI3K/AKT/mTOR components (Bai *et al.*, 2015). The aim of this chapter was to identify changes in gene expression between HCC38, H737R and HPrexR cell lines using RNA sequencing and differential expression analysis. Pathway enrichment analysis was used to identify biological pathways that are heavily altered in resistant cell lines. Enriched pathways may contain clues pertaining to CHK1i resistance mechanisms or biomarkers of resistance.

### **Chapter aims and objectives**

- Identify changes in gene expression between HCC38, H737R and HPrexR cell lines.
  - RNA sequencing and differential expression analysis.
- Identify potential pathways involved in CHK1i resistance.
  - Pathway enrichment analysis.

## 6.2 Results

### 6.2.1 RNA Sequencing and quality control of reads

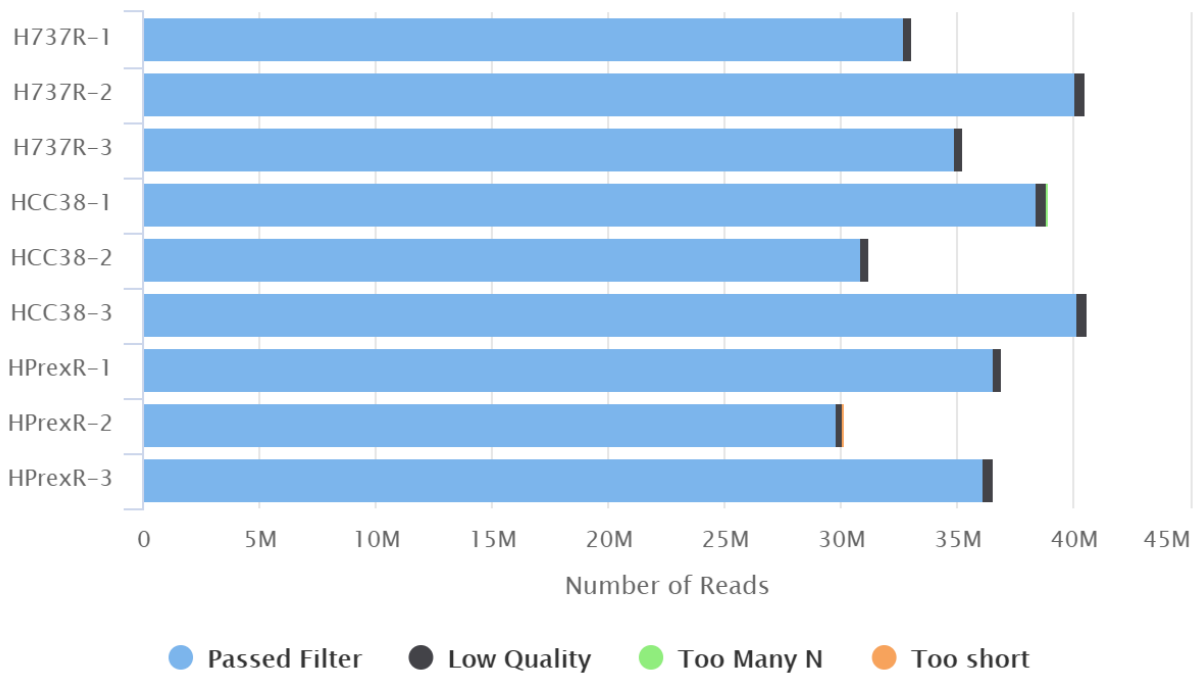
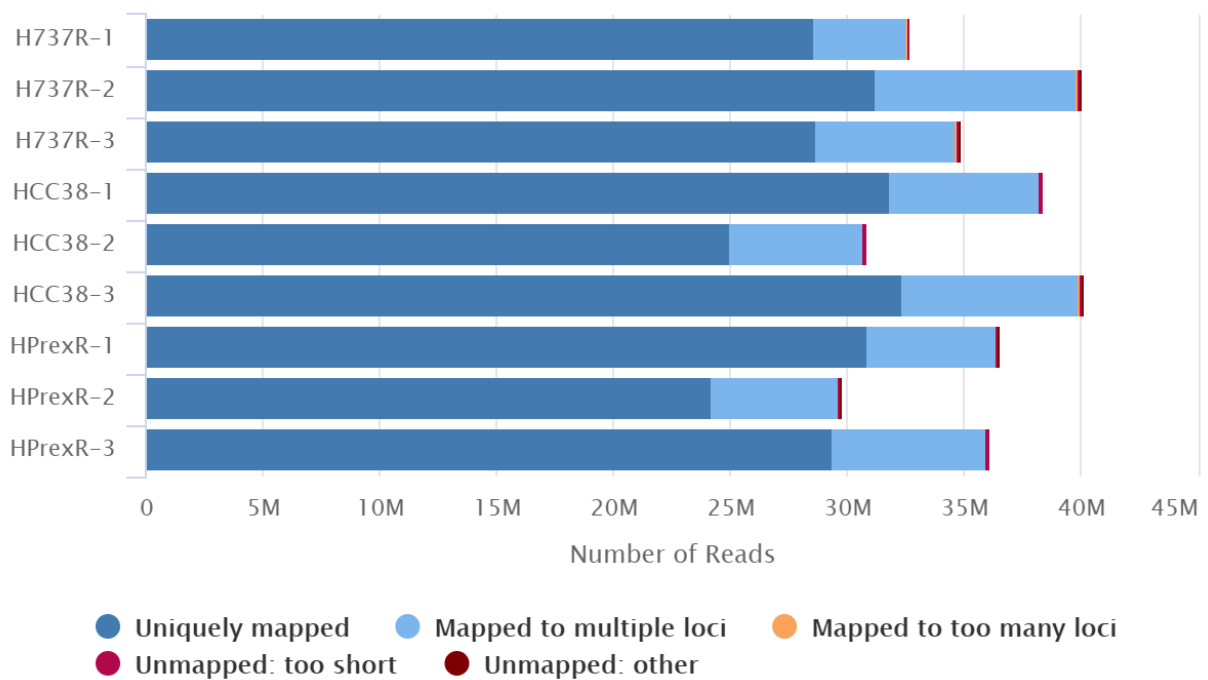
To identify changes in gene expression potentially driving resistance in CHK1i resistant cell lines, RNA was extracted from HCC38, H737R and HPrexR cells and sent to UCL Genomics (<https://www.ucl.ac.uk/child-health/research/genetics-and-genomic-medicine/ucl-genomics>) for sequencing. UCL Genomics carried data analysis of RNA sequencing data and produced an mRNA-Seq Quality control report (MultiQC report; **Appendix 6.1**). Additionally, UCL Genomics carried out the differential expression analysis with DESeq2 and produced a report describing the raw data and normalisation process (SARTools R report; **Appendix 6.2**). Both reports will be referred to in this chapter. Sequencing via the Kapa mRNA Hyper prep assay along with IDT xGen UDI/UMI adaptors allowed for samples to be pooled and run together on an Illumina NextSeq 500 system. Reads were later demultiplexed and assigned to the correct sample based on the assigned index sequence. The unique molecular identifiers (UMI), short sequences consisting of random 8mers were sequenced in conjunction with cDNA allowing for estimation of PCR bias. Complete data processing of read data is available in **appendix 6.1**.

Demultiplexed raw data was pre-processed to remove/trim poor-quality base-calls and contaminating Illumina adapter sequences using the software fastp. Approximately >98% of the reads passed the Fastp filter, reads shorter than 15 bases after trimming were discarded as these sequences were too short to be mapped uniquely to a gene (**Table 6.1, Figure 6.1 A**). Processed reads were aligned to the UCSC Human hg38 genome via STAR, all reads that mapped to more than 1 loci were discarded before downstream analysis (**Figure 6.1 B**).

Deduplication carried out on Picard identified approximately 4-8.5% of reads as duplications which were removed (**Table 6.1 A, Figure 6.2 A**). Further QC to check for Ribosomal contamination and reads that map to known mRNA features confirmed low levels of contamination and good overlap of UTR and coding regions (**Table 6.1 Figure 6.2 B**). Processed data was assembled in a .txt file listing genes and raw counts per sample to be used for downstream analysis (**Appendix 6.3**).

Sample Name	rRNA %	mRNA %	Duplications %	Aligned reads %	Aligned reads (Millions)	GC content %	Passed filter %
HCC38-3	2.20%	74.00%	8.30%	80.70%	32.4	48.00%	98.90%
HCC38-2	2.20%	73.10%	7.30%	81.00%	25	47.70%	98.90%
HCC38-1	1.70%	75.90%	8.50%	82.80%	31.8	47.90%	98.80%
H737R-3	1.80%	75.70%	5.70%	82.20%	28.7	47.70%	98.80%
H737R-2	2.80%	72.30%	8.70%	78.00%	31.3	48.00%	98.90%
H737R-1	0.70%	81.20%	4.30%	87.40%	28.6	47.00%	99.00%
HPrexR-3	2.10%	74.40%	7.10%	81.30%	29.4	47.70%	98.90%
HPrexR-2	2.10%	73.80%	7.40%	81.30%	24.2	47.50%	98.80%
HPrexR-1	1.40%	78.30%	5.70%	84.50%	30.9	47.50%	98.90%

**Table 6.1: General statistics for processing of raw RNA sequencing data.** rRNA % = Percentage of aligned bases which overlapped Ribosomal RNA regions. mRNA % = Percentage of aligned bases which overlapped untranslated regions and coding regions of mRNA transcripts. Duplications % = Percentage of duplicated reads which are identified as originating from a single fragment of DNA. Aligned reads % = Percentage of reads uniquely mapped to the genome. Aligned reads (Millions) = Total uniquely mapped reads in millions. GC content % = Percentage of guanine & cytosine nucleotide content in reads after filtering. Passed filter % = Percentage of reads which successfully passed the filtering process. Table adapted from data produced by UCL Genomics in the MultiQC report **Appendix 6.1**.

**A****Fastp: Filtered Reads****B****STAR: Alignment Scores**

**Figure 6.1: A) Filtering of raw data to remove poor-quality base calls.** Reads filtered by Fastp for low quality (Black) or too short (Orange) or contained too many ambiguous bases (Green) to be successfully mapped to a gene. >98% of reads passed the Fastp filter (Light blue). **B) Alignment of reads to the UCSC Human hg38 reference genome via STAR.** All reads mapped to more than 1 loci were discarded from downstream analysis. Both graphs taken from the MultiQC report generated by UCL Genomics, see **Appendix 6.1**.

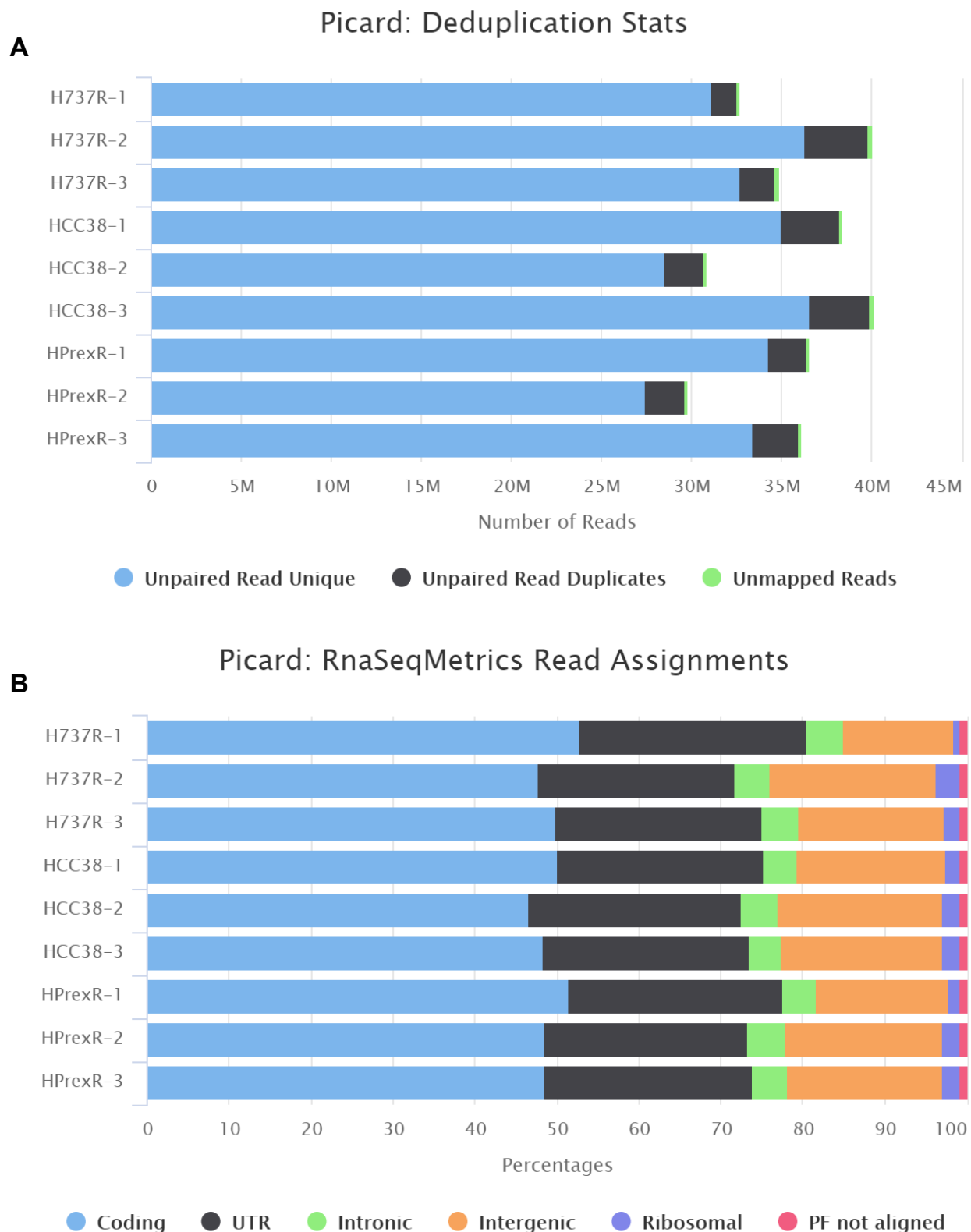


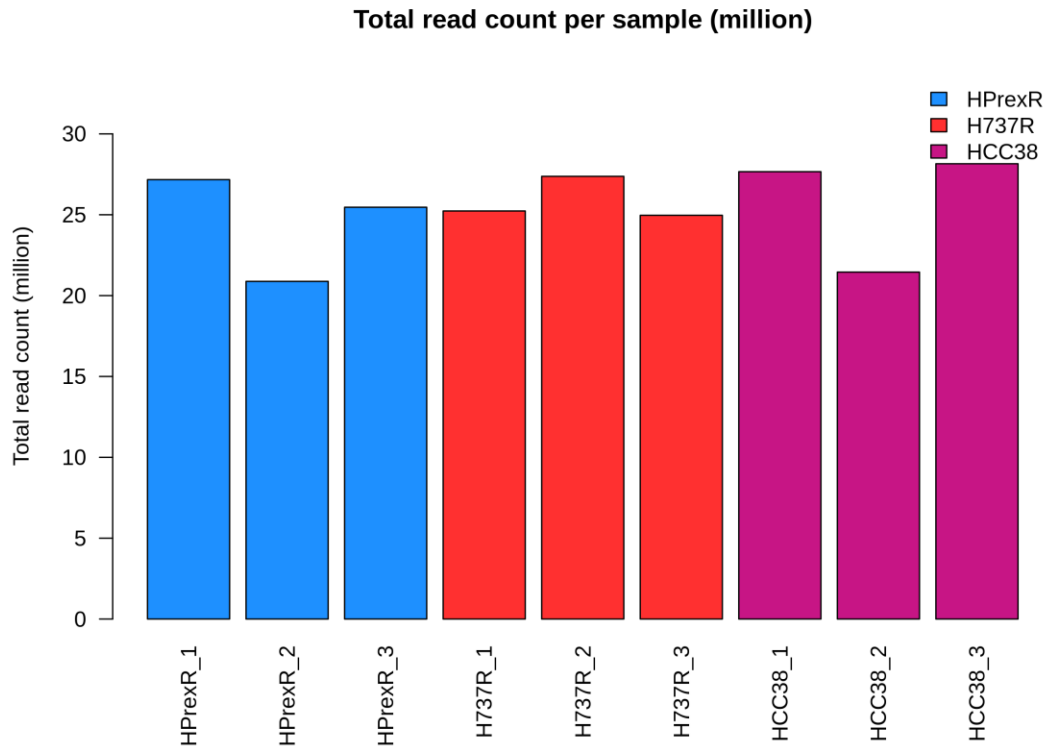
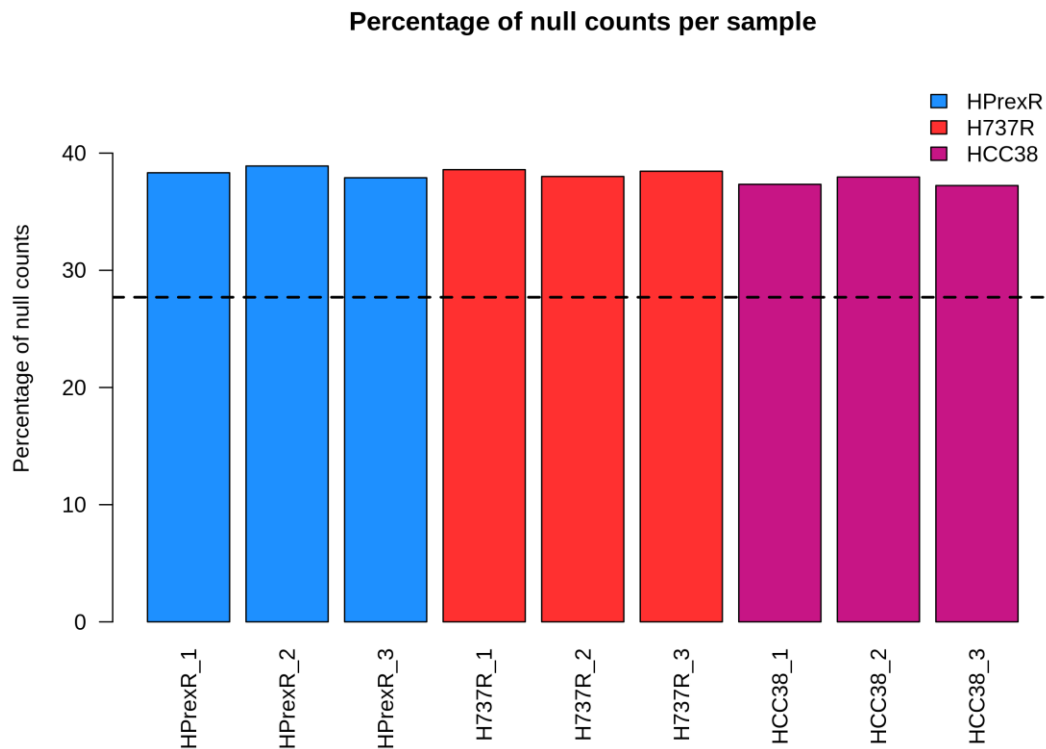
**Figure 6.2: A) Identified duplicate reads.** 4-8.5% of bases identified as duplicate reads were removed from further analysis. M = Million. **B) Assignment of RNA bases to known mRNA features.** Percentage of bases that align to regions of the reference genome. Regions include, Gene coding regions (Light blue), Untranslated regions (UTR; Black), Intronic (Non-coding regions removed during RNA splicing; Green), Intergenic (non-coding regions between genes; Orange), Ribosomal (Purple), PF not aligned (Reads that passed filter but were not aligned to the reference genome; Pink). Both graphs taken from the MultiQC report generated by UCL Genomics, see **Appendix 6.1**.



### 6.2.2 Identifying differentially expressed genes

Raw counts data were assessed and processed before normalisation and differential expression analysis (DEA) by UCL Genomics, complete data available in **Appendix 6.2**. Total read counts show some variability between samples which could be due to slight differences in library concentrations or levels of rRNA contamination, however this was not enough to adversely affect downstream analysis (**Figure 6.3 A**). Genes registering 0 reads were identified for each sample, in cases where a gene reads 0 for all 9 samples data was not considered for differential expression analysis and fold-change and p-values were set to NA in the data files (**Figure 6.3 B**).

Similarity between samples was investigated using a pairwise scatter plot of  $\log_2(\text{counts}+1)$  rather than raw counts. SERE statistic was used to produce a similarity index between RNA-Sequencing samples (Schulze *et al.*, 2012). This determines if variability is higher than random Poisson variability and pairwise SERE values are shown in the lower triangle of **figure 6.4**. The lower the pairwise value the less variable the samples, this shows biological replicates are sufficiently like one another but different from other cell lines.

**A****B**

**Figure 6.3: A) Total read counts.** Total number of mapped and counted reads for each sample. **B) Percentage of null counts per sample.** Genes that registered 0 reads for a given sample are identified as null counts. The percentage of null counts is expected to be similar within conditions. Genes that registered null counts on all 9 samples were not considered for analysis downstream with DESeq2. A total of 7337 genes (27.7%) fit into this category indicated by the dashed line. Graphs taken from the SARTools R Report generated by UCL Genomics, see **Appendix 6.2**.

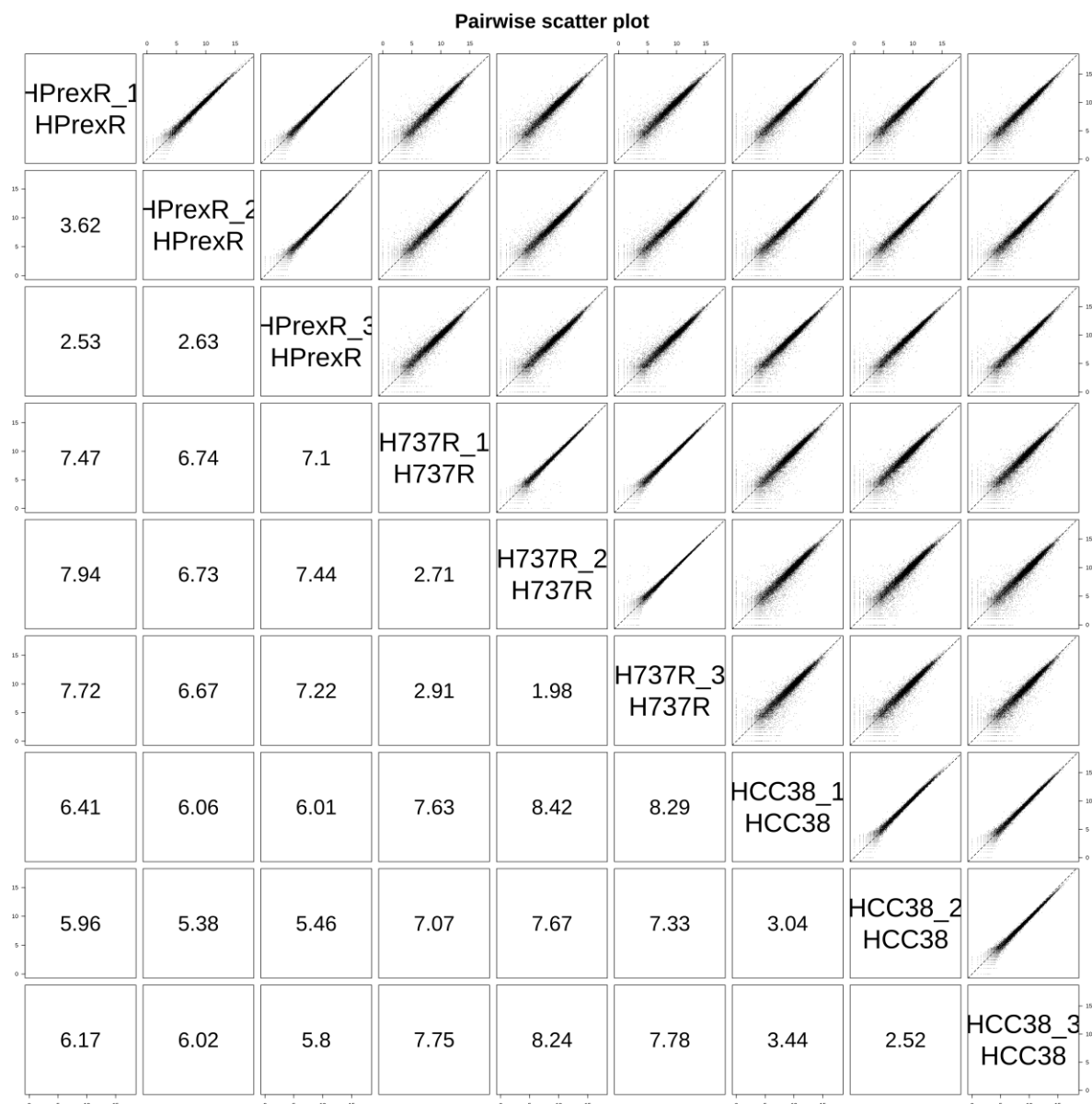


**Figure 6.4: Pairwise scatter plot and similarity index.** SERE statistics values in the lower left-hand side identify the degree of similarity between samples. Lower values indicate less variability. Technical repeats of samples show the lowest SERE scores while different biological conditions show the highest SERE values as expected. Taken from the SARTools R Report generated by UCL Genomics, see **Appendix 6.2**.

Principal component analysis was used to visualise the variance between cell lines. As expected, the first principal component (PC1) separated samples into their distinct biological conditions confirming that biological variability is the main source of variance while technical repeats cluster together (**Figure 6.5**).

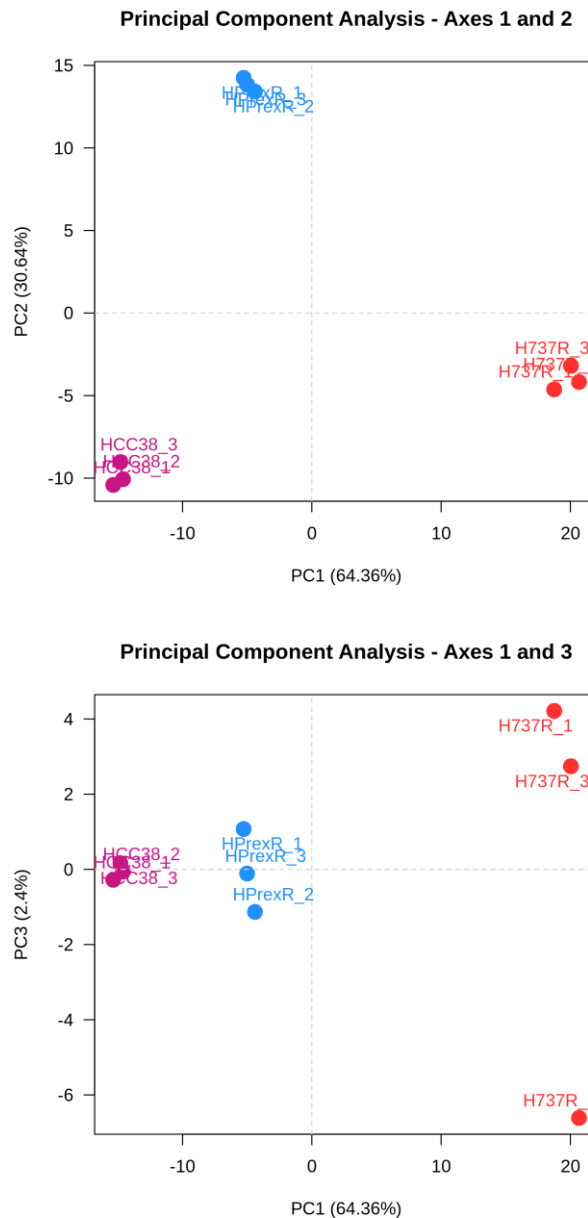


**Figure 6.5: Visualising experimental variability with Principal Component Analysis.** First 2 PCA's carried out account for the majority of variability within the experiment identifying biological variability is the largest source of variation between samples. Graphs taken from the SARTools R Report generated by UCL Genomics, see **Appendix 6.2**.

To make read counts comparable between samples, normalisation was carried out using DESeq2 which assumes that most genes are not differentially expressed in any given sample. The locfunc="median" method was used to calculate the scaling factors shown in **Table 6.2**.

	HCC38 - 1	HCC38 - 2	HCC38 - 3	H737R - 1	H737R - 2	H737R - 3	HPrexR - 1	HPrexR - 2	HPrexR - 3
Size Factor	1.09	0.84	1.04	1.01	1.1	0.99	1.07	0.85	1.09

**Table 6.2: Scaling factors determined by DESeq2 used to normalise RNA sequencing data.** Scaling factors lower than 1 will produce normalised counts higher than original raw counts while scaling factors higher than 1 will produce normalised counts lower than original raw counts. Table adapted from data produced by UCL Genomics in the SARTools R report **Appendix 6.2**.

Normalised read counts are then determined by dividing raw read counts by the scaling factor. Validation of the normalisation method is shown in **Figure 6.6** where the size factor is represented by a red line which is expected to be close the mode of the distribution of counts divided by their geometric means across all samples. After normalisation, count distributions are stabilised across samples as seen in **Figure 6.7**. Differential expression analysis (DEA) was carried out using DESeq2 to calculate the fold-change, p-values, and adjusted p-values for each gene. The Benjamini-Hochberg procedure was used to adjust the p-value to account for multiple testing. Differentially expressed genes (DEGs) were considered significant if the adjusted p-value was  $\leq 0.05$ . **Table 6.3** shows the total number of DEGs present in each comparison. Complete output of DEA available in **Appendix 6.3-6.5**.

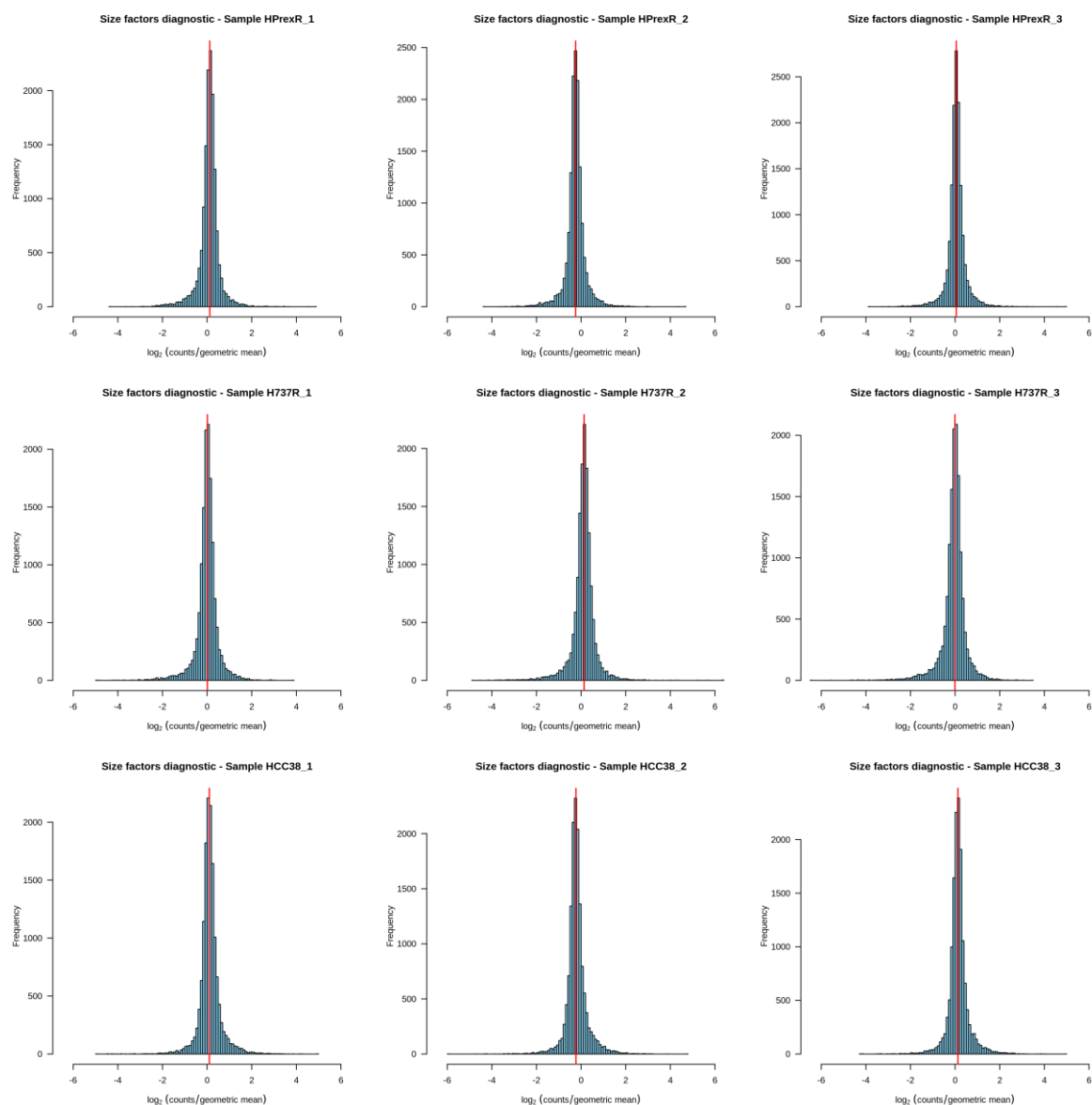


**Figure 6.6: Assessment of the estimation of size factors for normalisation of raw counts.** Red line indicates the scaling factor used to normalise each sample. Ideal scaling factors are expected to be close to the mode of the distribution of counts divided by their geometric means across samples. Graphs taken from the SARTools R Report generated by UCL Genomics, see **Appendix 6.2**.

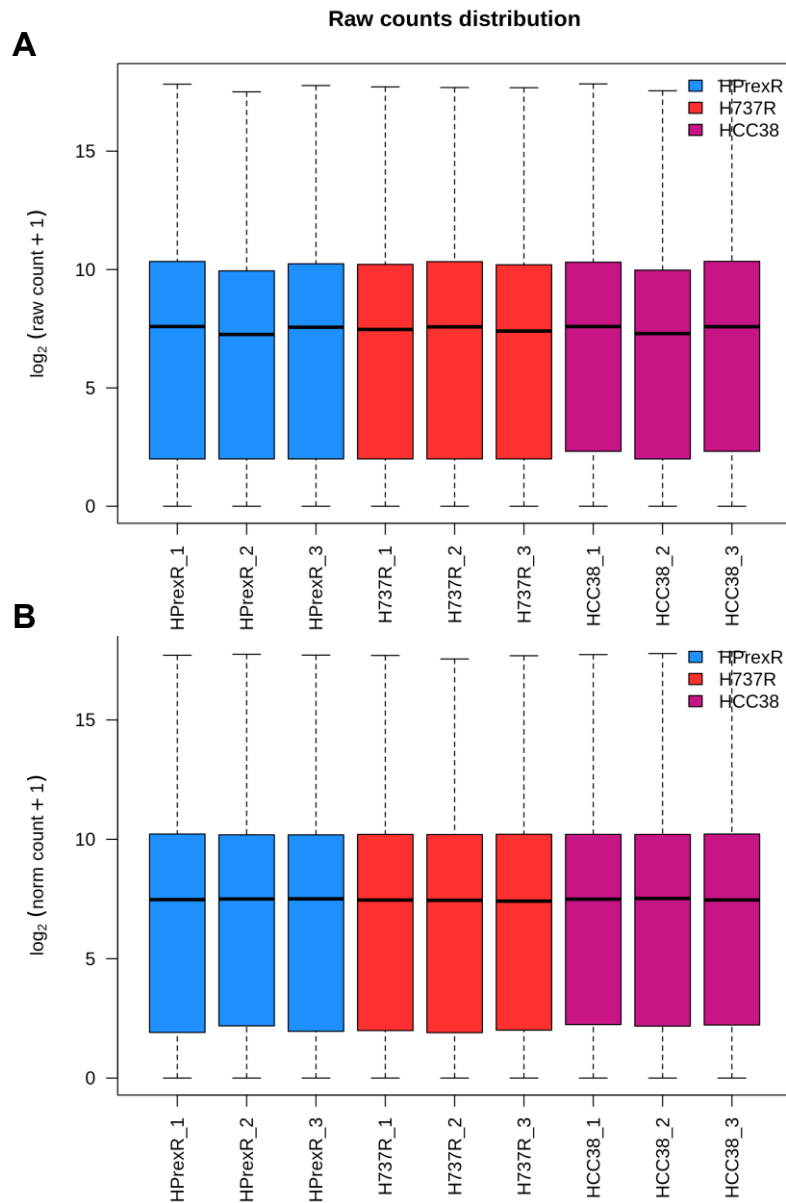


**Figure 6.7: Boxplots showing quality of normalisation of raw counts. A)** Un-normalised raw counts show slight variations in the distributions between samples. **B)** Once normalisation has been carried out, sample distributions are much more similar between samples. Graphs taken from the SARTools R Report generated by UCL Genomics, see **Appendix 6.2**.

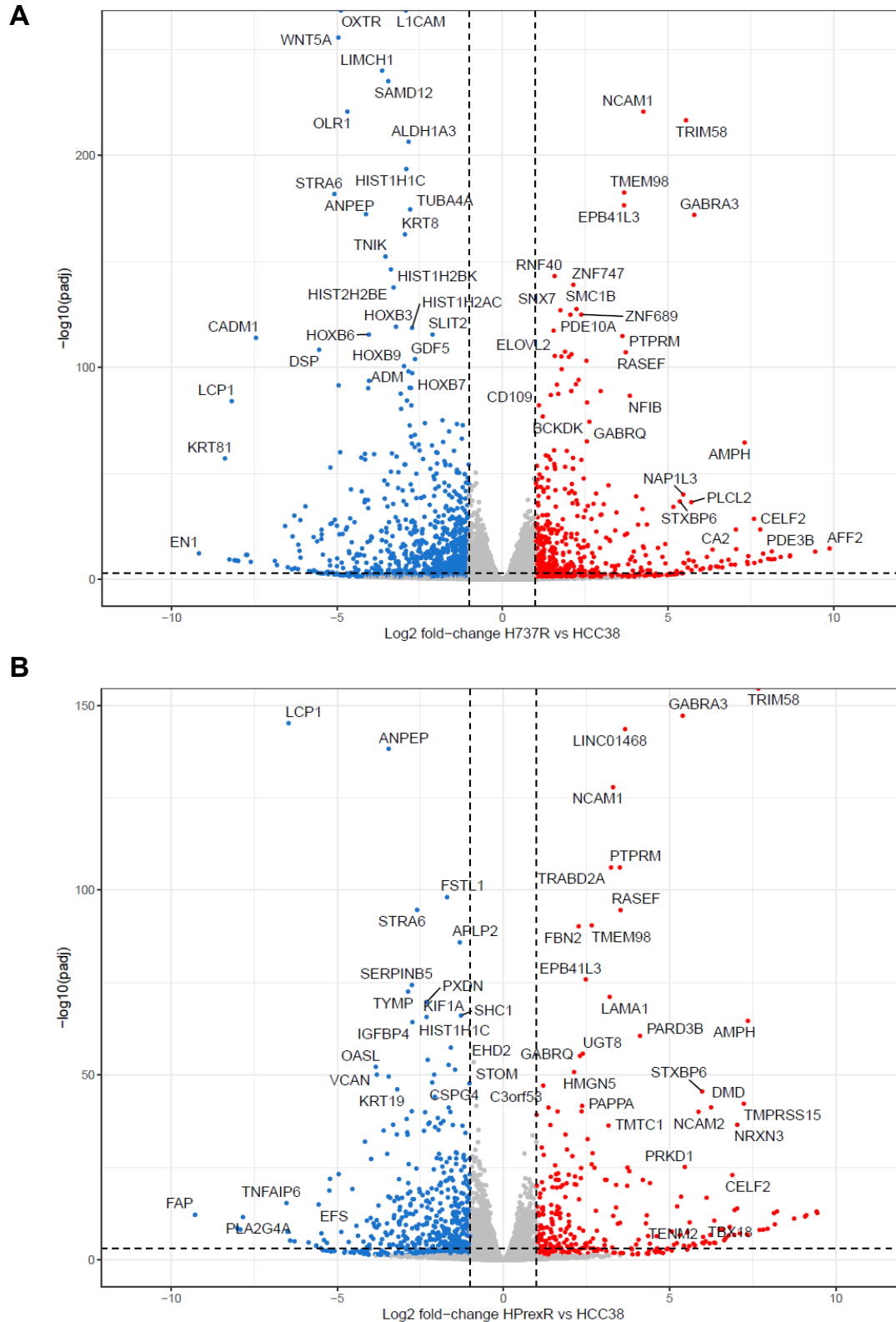
	Down DEGs	Up DEGs	Total DEGs
<b>HCC38 vs H737R</b>	3355	3505	6860
<b>HCC38 vs HPrexR</b>	2345	2582	4927
<b>H737R vs HPrexR</b>	3122	3090	6212

**Table 6.3: Total number of differentially expressed genes for each analysis.** Genes were only considered significantly differentially expressed if  $\text{padj} \leq 0.05$ . Table adapted from data produced by UCL Genomics in the SARTools R report **Appendix 6.2**.

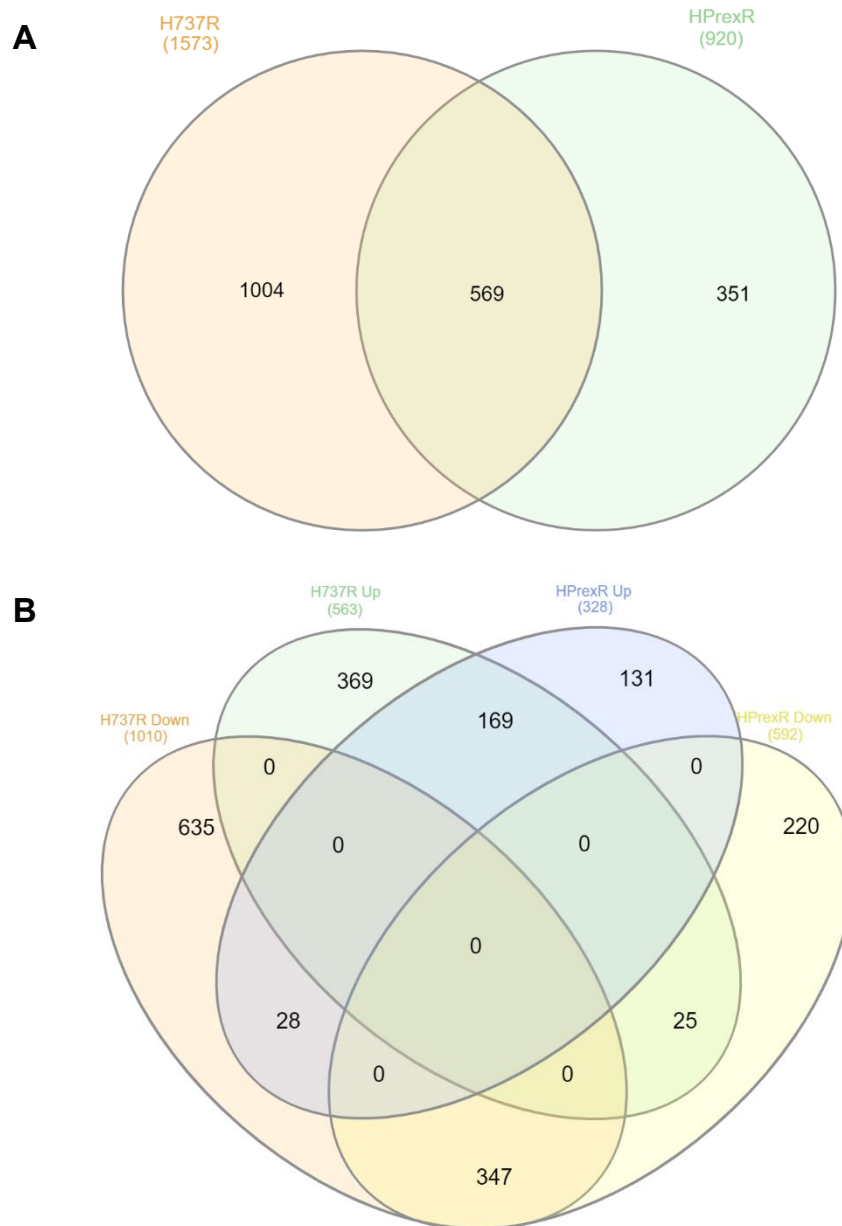
### 6.2.3 Identifying enriched pathways or biological processes

A cut off of  $\geq 2$ -fold-change in gene expression was applied to both H737R versus HCC38 and HPrexR versus HCC38 DEG to reduce the number of genes in the initial analysis. In H737R 1573 genes were differentially expressed at  $\geq 2$ -fold change compared to HPrexR 920 genes (**Figure 6.8, Appendix 6.6 & 6.7**). Of these DEGs, 569 were shared between the two cell lines leaving 1004 and 351 unique DEGs in H737R and HPrexR respectively (**Figure 6.9 A, Appendix 6.8**). DEGs were divided into groups of up and downregulation and compared. More genes were downregulated than upregulated in both cell lines, with H737R showing 1010 down versus 563 up DEGs and 592 down versus 328 up DEGs in HPrexR (**Figure 6.9 B, Appendix 6.9**). 169 upregulated DEGs and 347 downregulated DEGs were shared between the cell lines while 25 DEGs were upregulated in H737R but down in HPrexR and 28 DEGs were down in H737R but up in HPrexR (**Figure 6.9 B, Appendix 6.9**). The shared 569 DEGs are plotted in volcano plots in **figure 6.10**.

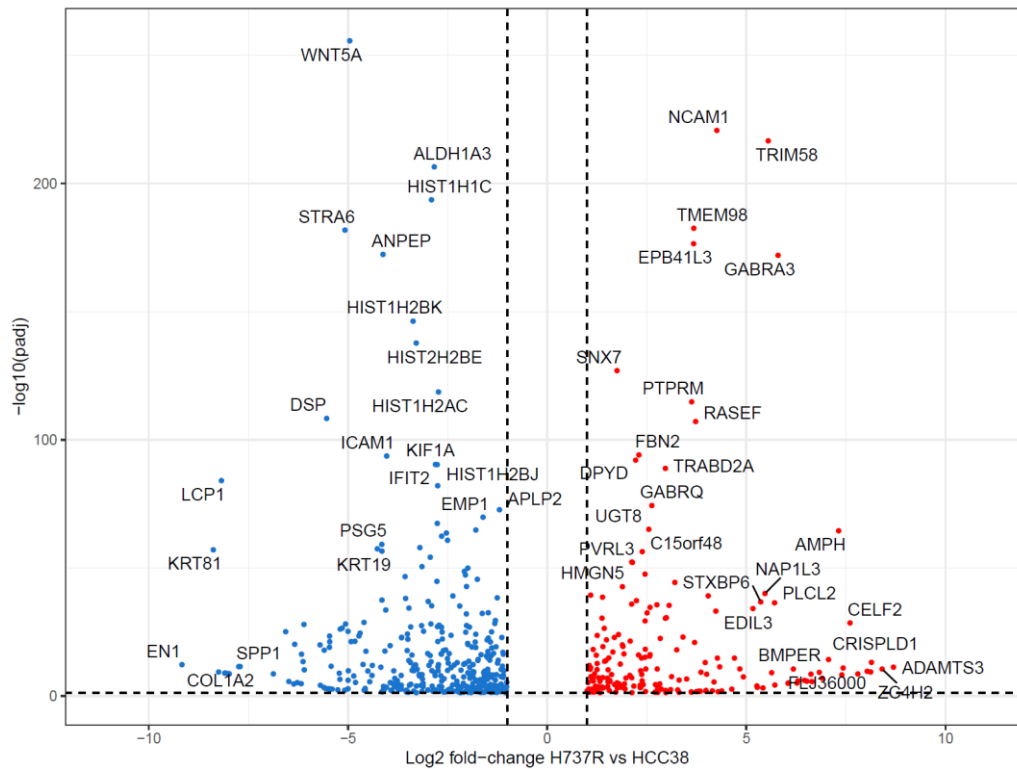
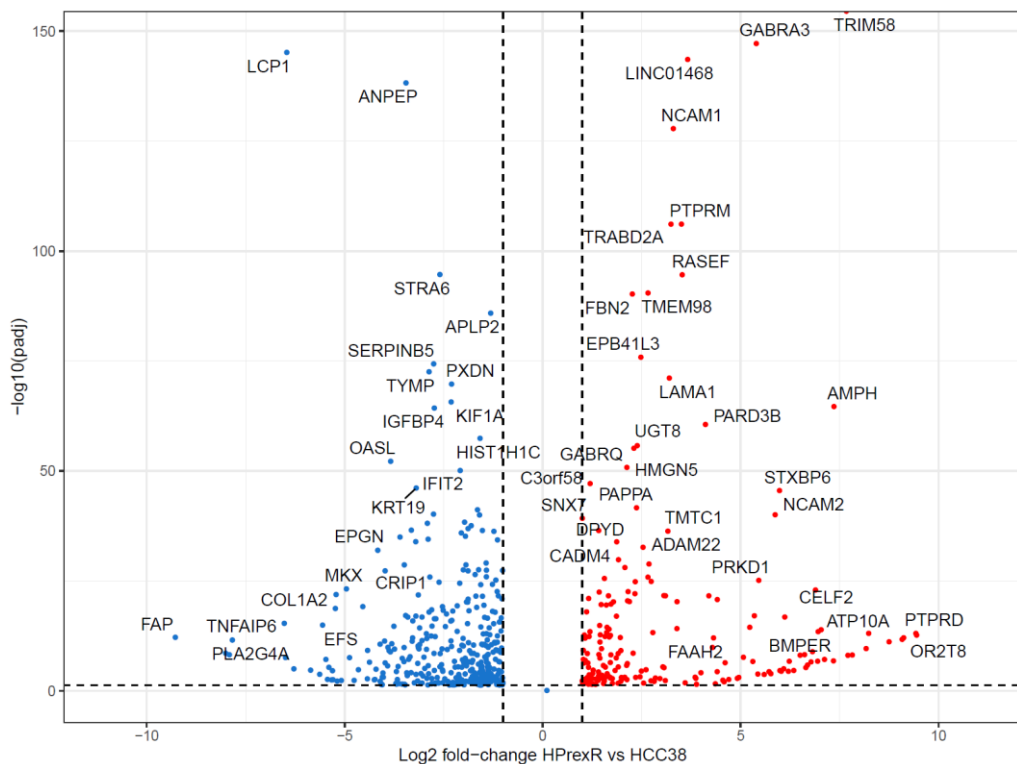




**Figure 6.8: Volcano plots of differentially expressed genes in H737R (A) and HPrexR (B) cell lines versus the parental HCC38 cell line.** All DEGs were plotted on a volcano plot for each differential expression analysis. Dotted line on the Y-axis indicates the padj cut-off of 0.05 while X-axis dotted lines indicate fold-change cut-off of 2. Downregulated genes above the threshold are coloured blue while upregulated genes above the threshold are red. All DEGs below the X and Y thresholds are shown in grey. **A)** H737R versus HCC38 **B)** HPrexR versus HCC38.



**Figure 6.9: Differentially expressed genes shared by H737R and HPrexR differential expression analysis. A)** DEGs of  $\geq 2$ -fold-change and a  $p_{adj}$  value of  $\leq 0.05$  were taken from H737R versus HCC38 and HPrexR versus HCC38 differential expression analyses and compared using iVenn. **B)** DEGs of  $\geq 2$ -fold-change and a  $p_{adj}$  value of  $\leq 0.05$  were taken from H737R versus HCC38 and HPrexR versus HCC38 differential expression analyses and split into groups of up or down regulation versus the parental cell line and compared with iVenn. Full list of DEGs in **Appendix 6.8 & 6.9**.

**A****B**

**Figure 6.10: Volcano plots of shared differentially expressed genes between H737R (A) and HPrexR (B) cell lines versus the parental HCC38 cell line.** 569 Shared DEGs from figure 6.16 were plotted on a volcano plot for each differential expression analyses. Dotted line on the Y-axis indicates the padj cut-off of 0.05 while X-axis dotted lines indicate fold-change cut-off of 2. Downregulated genes above the cut-off threshold are coloured blue while upregulated genes above the threshold are red. **A)** H737R versus HCC38 **B)** HPrexR versus HCC38. Fold-change data and padj values available in **Appendix 6.10**.

To identify pathways or biological processes altered by DEGs, pathway enrichment analysis was carried out via Metascape (Y *et al.*, 2019). Metascape analyses a list of DEGs and identifies genesets that significantly overlap with inputted genes to identify potential changes in biological processes and pathways. Of interest were the 569 DEGs shared between H737R and HPrexR. As both cell lines are cross resistant to CHK1 inhibitors it was thought that gene expression changes pertaining to resistance may be identified within the shared genes and genesets they enrich for. Epithelial to Mesenchymal transition (EMT) was the most significant geneset enriched by this analysis followed by many pathways involved in regulation of the extra cellular matrix (**Figure 6.11**). Some neuronal based pathways were also significantly enriched like axonogenesis, axon development and neuron projection morphogenesis in addition to pathways associated with cell motility and morphogenesis (**Figure 6.11**).

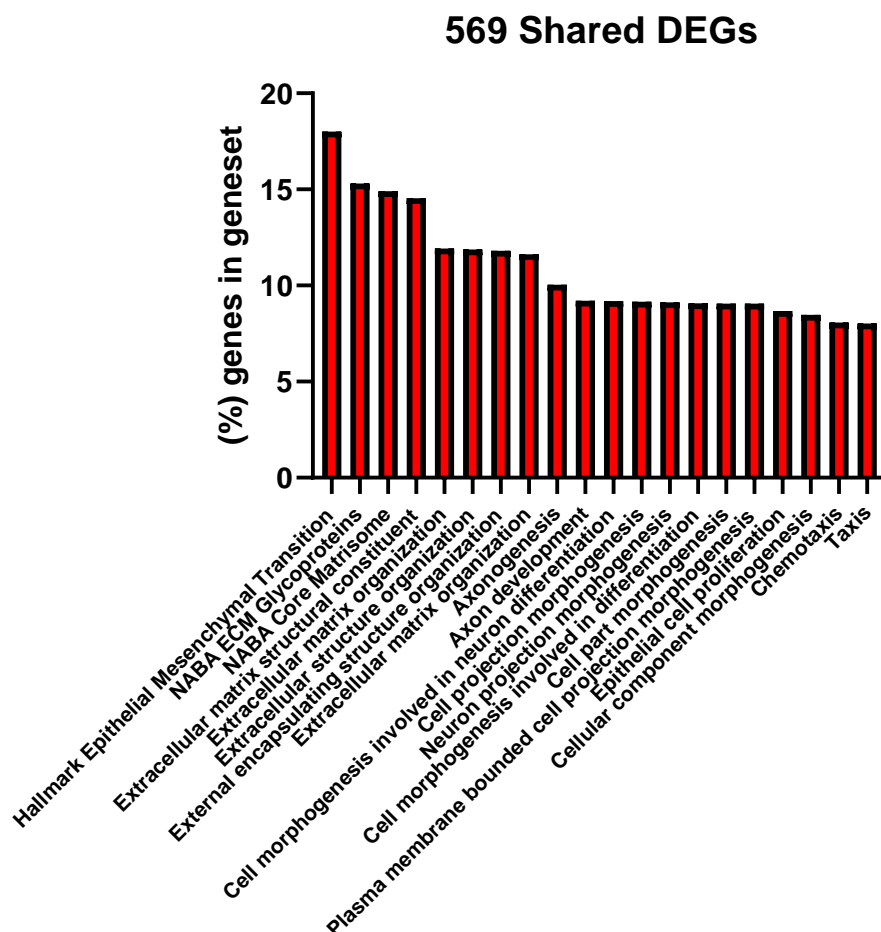


**Figure 6.11: Top 20 most significantly enriched genesets for 569 shared differentially expressed genes.** Geneset enrichment analysis of 569 DEGs shared by H737R and HPrexR carried out on Metascape and top 20 most significant genesets selected. Percentage shows the number of genes in the genesets present in the DEG list. For all genesets  $\text{Log}(\text{padj}) \leq -10$ . Full list of enriched genesets for 569 DEGs in **Appendix 6.11**.

To gain a deeper understanding of if these pathways, DEGs were separated into the shared 169 upregulated and 347 downregulated genes and reanalysed. Downregulated shared DEGs also enriched for EMT despite there being fewer genes present in the geneset (**Figure 6.12 A**) but this was not seen in upregulated DEGs (**Figure 6.12 B**) suggesting the majority of EMT associated genes are downregulated. Other interesting pathways enriched in downregulated DEGs included epithelial cell proliferation, wound healing and cell morphogenesis involved in differentiation which are pathways related to EMT (**Figure 6.12 A**). Overall fewer highly significant pathways were identified in the shared upregulated DEGs, but this should be expected based on the lower number of overall genes present in the analysis. However, one group of interest was the receptor-type tyrosine-protein phosphatases (RPTPs) in which *PTPRD* and *SLITRK2-5* were significantly upregulated (**Figure 6.12 B**). RPTPs are cell surface proteins with intracellular protein phosphatase activity and exhibit sequence homology to cell adhesion molecules (Xu and Fisher, 2012). *PTPRD* which showed no reads in the parental cell line was highly expressed in both H737R and HPrexR with Log2Fold-differences of 7.4 and 9.4 respectively and was the 2<sup>nd</sup> highest upregulated gene in HPrexR cells and 16<sup>th</sup> highest in H737R cells (**Appendix 6.20**). Knockdown of *PTPRD* has been shown to increase markers associated with EMT and breast cancer stem cells and so its expression may counteract transition to mesenchymal phenotypes (Yu *et al.*, 2017). *SLITRK* proteins are neural transmembrane proteins that are mainly found in brain tissue but have been seen in epithelial tumours (K *et al.*, 2016).

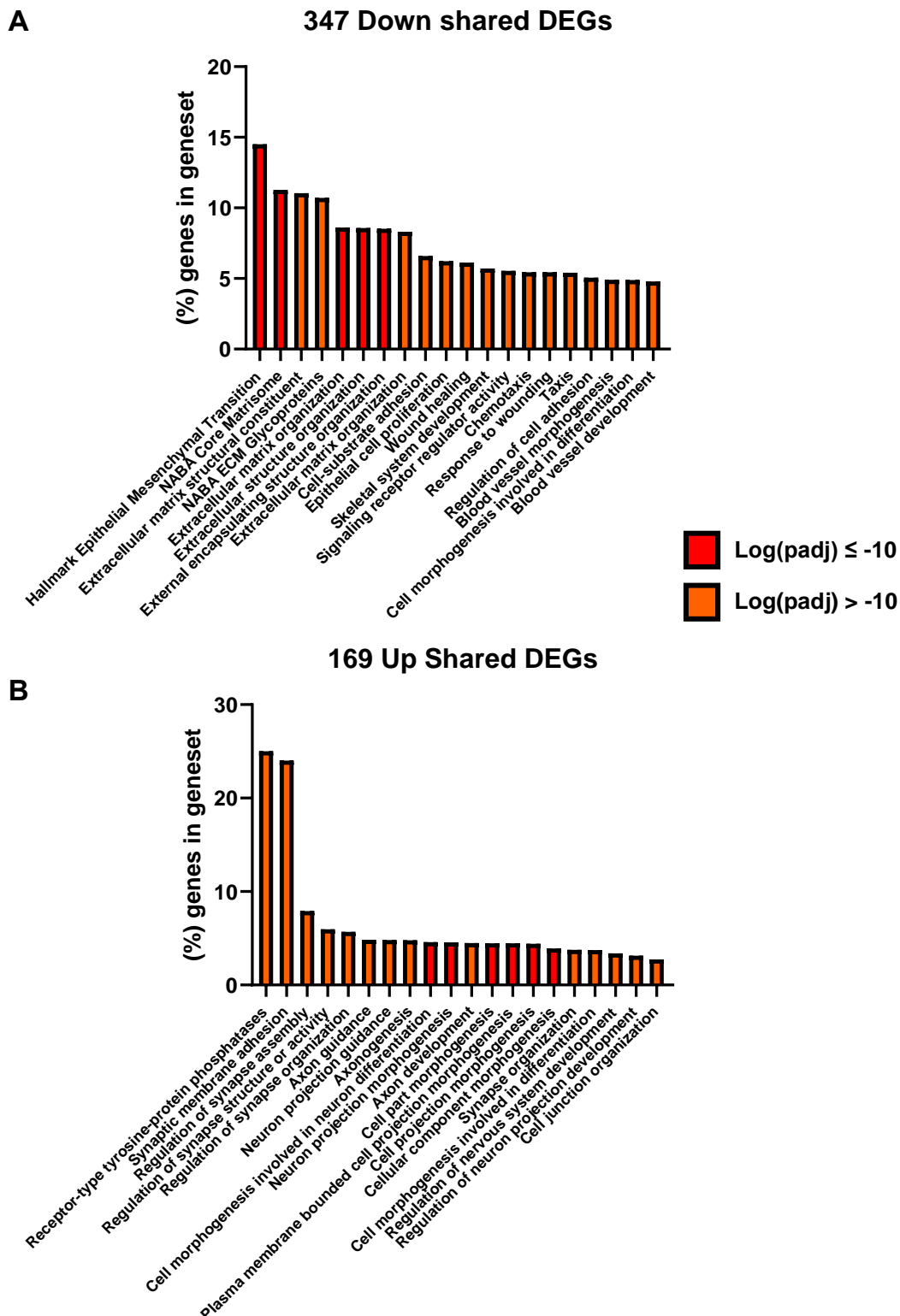


**Figure 6.12: Top 20 most significantly enriched genesets for up and down shared differentially expressed genes. A) 347 shared downregulated DEGs (Figure 6.19 B) and B) 169 upregulated DEGs (Figure 6.19 B).** Does not include shared DEGs that were up in H737R but down in HPrexR or DEGs down in H737R but up in HPrexR (Figure 6.19 B). Geneset enrichment analysis was run for each list on Metascape and top 20 most significant genesets selected. Percentage shows the number of genes in the genesets present in the DEG list. Full list of enriched genesets for A and B available in **Appendix 6.12 & 6.13**.

To get a fuller picture of gene expression changes related to EMT, pathway enrichment analysis was carried out on all DEGs instead of just the 569 shared DEGs. This was to make sure all DEGs involved in EMT could be identified for each cell line as the types of EMT DEGs that are downregulated may differ (**Figures 6.13**). **Figure 6.14** shows the expression profiles of all genes identified by Metascape as enriched for EMT in H737R and HPrexR. While H737R and HPrexR have similar levels of total downregulated genes (70 and 67 respectively), H737R has more genes that are highly downregulated ( $\geq 2$  FD) (**Table 6.4**). HPrexR had slightly more total upregulated EMT genes than H737R (17 in HPrexR to 14 in H737R) but similar numbers of highly upregulated DEGs (9 in HPrexR to 8 in H737R). Key regulators of EMT such as Transforming growth factor  $\beta$  (*TGF- $\beta$* ), Focal adhesion protein (*FAP*), *Prrx1* and *COL1A2* are all downregulated (**Figures 6.14 & Table 6.5**). Another important regulator of EMT called *Snai1* (Wang *et al.*, 2013) was also downregulated in H737R and HPrexR but not identified via Metascape analysis (**Tables 6.5 & Appendix 6.4, 6.5, 6.14 & 6.15**). *Snai1* was not picked up by Metascape as the geneset enriched by these lists of DEGs was M5930 which only contains *Snai2* (GSEA: Gene set M5930, 2021)(**Appendix 6.14-6.17**).

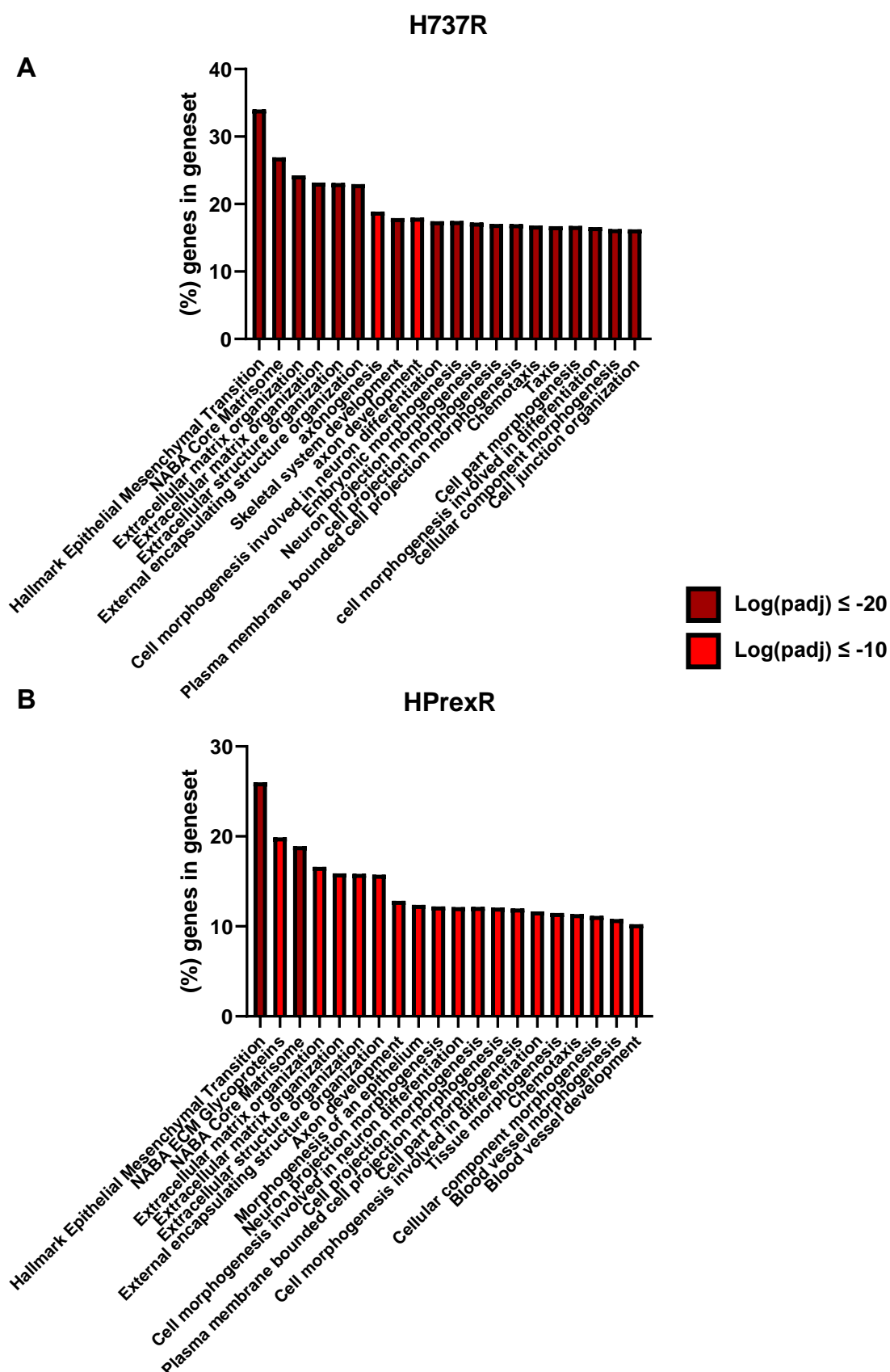


**Figure 6.13: Top 20 most significantly enriched genesets for all differentially expressed genes in H737R and HPrexR.** Geneset enrichment analysis of all DEGs in **A)** H737R and **B)** HPrexR carried out on Metascape and top 20 most significant genesets selected. Percentage shows the number of genes in the genesets present in the DEG list. Full list of genes enriched for EMT available in **Appendix 6.14 & 6.15**.



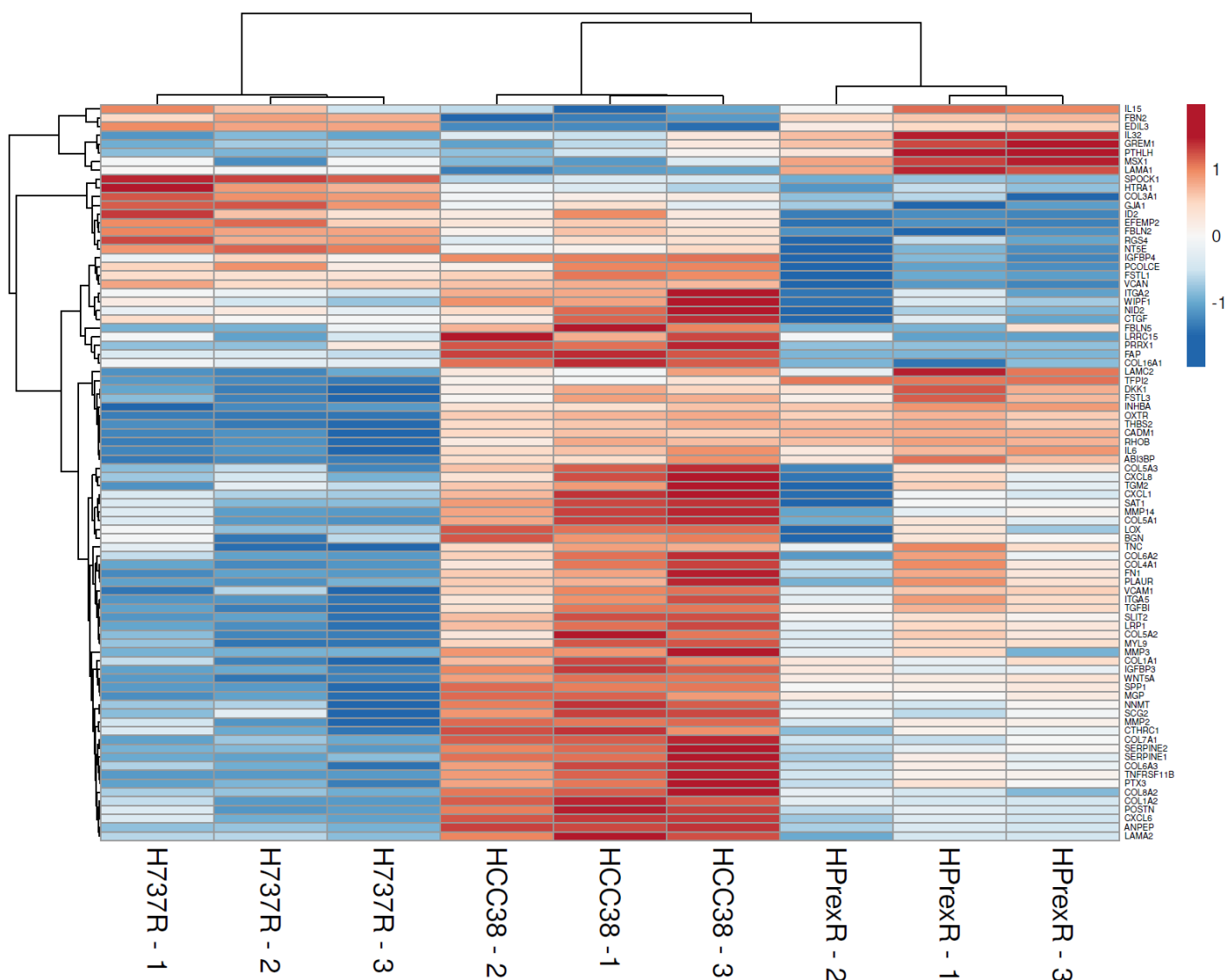


**Figure 6.14: Expression profile of EMT enriched genes in HCC38 parental and resistant cell lines.** DEGs identified to enrich for EMT in Metascape pathway enrichment analysis were isolated and their raw counts used to generate a heatmap in ClustVis. Full list of genes enriched for EMT available in **Appendix 6.16 & 6.17**.

	H737R	HPrexR
Total downregulated genes	70	67
Highly downregulated genes ( $\geq 2$ FD)	60	45
Total upregulated genes	14	17
Highly upregulated genes ( $\geq 2$ FD)	8	9

**Table 6.4: Numbers of Up and Down differentially expressed genes enriched for EMT.** FD = Fold difference. Full list of genes enriched for EMT available in **Appendix 6.16 & 6.17**.

	H737R		HPrexR	
	Log2FoldChange	padj	Log2FoldChange	padj
TGFB1	-0.597	2.400E-09	-0.7	4.560E-12
TGFB2	-1.017	5.570E-20	0.072	5.003E-01
TGFB3	-1.095	1.000E-05	-0.886	5.680E-04
TGFBR1	-1.023	2.370E-30	-0.535	5.569E-10
TGFBR2	-0.542	3.160E-07	-0.632	1.833E-10
TGFBR3	0.029	9.167E-01	-0.221	2.229E-01
Snai1	-1.123	3.290E-05	-0.703	1.361E-02
Prrx1	-3.29	3.317E-02	-5.295	2.860E-03
FAP	-6.167	4.690E-17	-9.276	6.660E-13
TNFRSF11B	-8.247	4.220E-10	-3.348	1.700E-08
COL1A2	-7.743	3.070E-12	-5.216	1.250E-22
MGP	-6.338	6.330E-21	-2.316	4.310E-12

**Table 6.5: Key EMT related genes Log2 fold changes and padj values.** Full list of DEGs available in **Appendix 6.4 & 6.5**.

As shown in **figure 6.11 and 6.12** the epithelial cell proliferation geneset was significantly enriched in the 569 shared DEGs and 347 downregulated shared DEGs but not in the 169 upregulated shared DEGs. **Figure 6.15** shows a heatmap of the DEGs enriched for the epithelial cell proliferation. Most genes in this geneset are downregulated in H737R and HPrexR compared to the parental cell line. However, one cluster of 4 genes *EDNRB*, *PTPRN*, *GJA1* and *SOX11* are upregulated in H737R and downregulated in HPrexR. Another cluster of 7 genes *PGR*, *NRP2*, *AGTR1*, *BMP2*, *PRKD1*, *PTPRM* and *BMPER* were upregulated in both H737R and HPrexR relative to the parental cell line (**Figure 6.15**). Of particular interest is the expression of the *PGR* gene in H737R and HPrexR which encodes for the Progesterone receptor. No reads for *PGR* were detected in HCC38, and this is consistent with its status as a Triple Negative breast cancer cell line. However, H737R and HPrexR both show reads for *PGR* but to a greater extent in H737R (Log2Fold-difference H737R 8.12 versus HPrexR 5.718). *PGR* is the 8<sup>th</sup> most upregulated gene in H737R cell lines but the 42<sup>nd</sup> highest upregulated in HPrexR cells (**Appendix 6.7 & 6.20**).

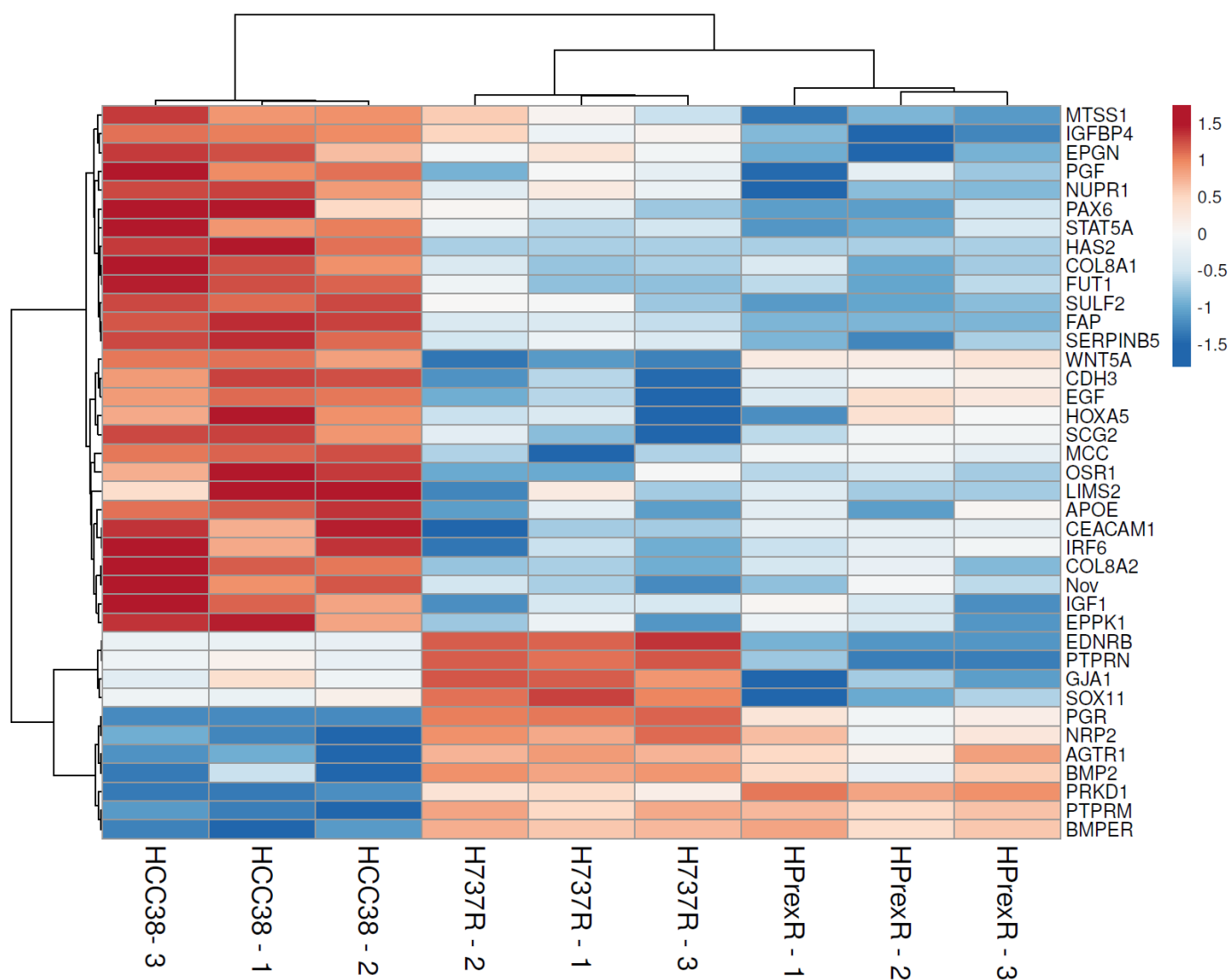


**Figure 6.15: Expression profile of Epithelial proliferation enriched genes in HCC38 parental and resistant cell lines.** DEGs identified to enrich for Epithelial cell proliferation in Metascape pathway enrichment analysis were isolated and their raw counts used to generate a heatmap in ClustVis. Full list of genes enriched for Epithelial proliferation in **Appendix 6.18 & 6.19.**

## 6.3 Discussion

In this chapter RNA was successfully extracted from HCC38, H737R and HPrexR and sequenced for global analysis of gene expression and pathway enrichment analysis. These data show Epithelial Mesenchymal transition was the most significantly enriched pathway and consisted mostly of downregulated DEGs in both H737R and HPrexR cell lines. Other enriched genesets included multiple neuronal pathways in addition to cell motility, extracellular matrix, wound healing, and morphogenesis. Of the 169 upregulated shared DEGs between HPrexR and H737R, 5 RPTPs were shown to be upregulated. Epithelial cell proliferation was also enriched with most genes being downregulated. However, a unique cluster of 4 genes EDNRB, PTPRN, GJA1 and SOX11 were upregulated in H737R but downregulated in HPrexR cells. In addition, HPrexR and H737R now express PGR, a gene otherwise absent in the parental triple negative breast cancer cell line, suggesting these cells may no longer possess a TNBC phenotype. These results are discussed in more detail below.

RNA sequencing and differential expression analysis was carried out by UCL Genomics and the resulting data passed on to the Garrett lab for downstream analysis by myself. Differential expression analysis identified many genes that were differentially expressed in H737R and HPrexR cell lines (**Appendix 6.4-6.6**). To reduce the amount of data and to focus on larger changes in gene expression only significant ( $\text{padj} \leq 0.05$ ) DEGs with a fold-difference of  $\geq 2$  were taken forward (**Appendix 6.7 & 6.8**). It should be acknowledged that while initial analysis may be simplified through this method, smaller but equally important fold changes that may accumulate in pathways would be missed.

H737R showed a much higher number of DEGs than HPrexR before and after filtering out of  $< 2$ -fold DEGs (**Table 6.3, Figure 6.8**). In addition, pairwise scatter plots and PCA show HPrexR variability is much closer to that of HCC38 than H737R suggesting the H737R cell line has diverged from the parental phenotype to a greater extent than HPrexR cells (**Figure 6.4 & 6.5**). As shown in **chapter 3**, H737R and HPrexR cells demonstrate similar levels of

cross resistance to each CHK1 inhibitor (**Figure 3.7**), and both display cross resistance to other targeted inhibitors such as Adavosertib (WEE1i) and Ceralasertib (ATR) (**Figure 3.14**) therefore it was thought that changes in gene expression pertaining to drug resistance may also be similar. Objectively, the disparity in the numbers of DEGs could have little impact on the mechanisms of resistance in both HPrexR and H737R and could have arisen independent of drug treatment. Due to the heterogenous nature of these cells' lines, certain sub populations may have been selected over subsequent passages leading to coincidental divergence. Equally of note is that H737R and HPrexR still share a significant number of genes, of the set taken forward for further analysis, 569 DEGs were shared (**Figure 6.9 B**). Although generation of CHK1i resistant cell lines happened independently from one another and with different types of drugs, it was thought that pathways involved in CHK1i resistance may be shared between cell lines. Therefore, initial analysis was directed at these 569 genes.

Interestingly, the most significantly enriched pathway in the 569 genes was epithelial mesenchymal transition (EMT) (**Figure 6.11**). EMT is described as the biological process allowing polarised epithelial cells to undergo transition to mesenchymal cells. Mesenchymal cell phenotypes are associated with enhanced migratory capacity, invasiveness of tissues, elevated resistance to apoptosis and greatly increased production of extracellular matrix components (Kalluri and Neilson, 2003). Degradation of the underlying basement membrane indicates the completion of EMT as the mesenchymal cell forms and migrates away from its epithelial layer of origin (Kalluri and Weinberg, 2009).

EMT is important in many different biological processes and has been split into 3 types. Type 1 EMTs are associated with embryo implantation, formation, and organ development (Acloque *et al.*, 2009). Type 2 EMTs relate to wound healing, tissue regeneration and organ fibrosis (Kalluri and Weinberg, 2009). Type 3 EMTs are associated with cancer and is thought to play a role cancer malignancy and eventual spread of cancer from the primary tumour via metastasis (Thiery, 2002). Given the diverse roles of EMT, enrichment of pathways involved

in the extracellular matrix, embryogenic development, cell motility and wound healing is unsurprising (**Figure 6.11-6.13**).

Deeper analysis revealed the majority of DEGs in H737R and HPrexR are downregulated relative to the parental cell line within the EMT pathway (**Figure 6.12 & 6.14**). It can be tempting to assume that as most genes are downregulated, cells have therefore downregulated EMT and transitioned to a more epithelial phenotype. However, signalling pathways may downregulate repressors of a pathway to promote activity highlighting the need for a deeper understanding of the pathway. Important EMT regulators Transforming Growth factor beta (TGF- $\beta$ ), Zinc finger protein Snai1, and Prrx1 transcription factors have been downregulated in both resistant cell lines, but to a greater extent in H737R (**Figure 6.14, Table 6.5, Appendix 6.4 & 6.5**).

TGF- $\beta$  has been shown regulate EMT through transcriptional activation of Snai1 (J, S and R, 2009). Snai1 is said to act as a strong repressor of the epithelial phenotype by silencing the expression of E-cadherin (Fazilaty *et al.*, 2019; Wang *et al.*, 2013). Prrx1 is also activated by TGF- $\beta$  but expression is delayed until after Snai1 and acts as a strong inducer of the mesenchymal phenotype. Despite association with EMT, high levels of Prrx1 have been associated with a favourable prognosis in TNBC patients as it is thought cells may be stuck in a mesenchymal state unable to revert to an epithelial cell type to restart proliferation and secondary tumour growth (Fazilaty *et al.*, 2019).

Other downregulated proteins involved in the EMT pathway include Focal adhesion protein (FAP), TNF receptor superfamily member 11B (TNFRSF11B), type 1 Collagen (COL1A2) and Matrix Gla protein (MGP) to name a few (**Figure 6.14 & Table 6.5**). FAP has been shown to act as a tumour promotor in Oral Squamous Cell Carcinoma via downregulation of DPP9 (Wu *et al.*, 2020) which is shown to be upregulated in H737R but not HPrexR (**Figure 6.14**). TNFRSF11B has been shown to activate WNT/beta-catenin signalling which induces and stabilises EMT activators (Coelho *et al.*, 2020; F *et al.*, 2020) and type 1 Collagen is an important regulator of EMT that promotes increased expression of Snai1 and LEF-1

transcription factors via ILK-dependent phosphorylation of I $\kappa$ B and activation of NF- $\kappa$ B (Medici and Nawshad, 2010). In TNBC MGP expression has also been shown to promote EMT and is associated with poor relapse free survival in TNBC patients (C *et al.*, 2019). HTRA1, a gene upregulated in H737R but slightly downregulated in HPrexR has been inversely associated with EMT progression as it's downregulation led to an increase in cell migration and metastasis in patients (F *et al.*, 2015).

Some downregulated genes enriched for the EMT pathway appear to promote EMT. CADM1 a cell adhesion protein is downregulated heavily in H737R but slightly upregulated in HPrexR. Increased expression of CADM1 has been shown to suppress EMT (EJ *et al.*, 2019). EDL3, an upregulated gene in both H737R and HPrexR which encodes for an extracellular matrix protein has been shown to stimulate EMT and resistance to paclitaxel via its interactions with integrin  $\alpha_5\beta_3$  (Gasca *et al.*, 2020). While these genes have been shown to promote EMT it is difficult to say what the overall effect on the pathway may be. In **chapter 3** it was mentioned that H737R and HPrexR cells may display a more epithelial phenotype relative to HCC38 cells. H737R and HPrexR appear be less flat and elongated and seem to grow in tighter groups (**Figure 3.9**). H737R also grow at a faster rate than HPrexR and HCC38 (**Figure 3.5**) cells suggesting a more proliferative epithelial-like phenotype.

The increased growth rate of H737R appears contrary to **figure 6.15** showing many genes are downregulated for epithelial proliferation in both H737R and HPrexR. An upregulated cluster of DEGs in H737R consisting of SRY-Box Transcription Factor 11 (*SOX11*), Endothelin receptor type B (*EDNRB*), Protein Tyrosine Phosphatase Receptor Type N (*PTPRN*) and Gap Junction Protein Alpha 1 (*GJA1*) may explain why H737R exhibits a faster growth rate compared with HCC38 and HPrexR cells. *SOX11* has been linked with proliferation in multiple cancer cell lines including ER-negative breast cancer, but may also inhibit proliferation via inhibition of the Wnt signalling pathway (Yang *et al.*, 2019). *EDNRB* has been associated with proliferation in both bladder cancer cells and regeneration (Fu *et al.*, 2019) along with proliferation of melanocyte stem cells and may interact with the Wnt signalling pathway (Takeo

*et al.*, 2016). *PTPRN* overexpression has been associated with poor prognosis and metastasis in lung adenocarcinoma patients in addition to promoting markers of EMT (X *et al.*, 2021). *GJA1* has been identified as both a tumour suppressor in colorectal cancer associated with positive prognosis (W *et al.*, 2020) and a prognostic marker of poor survival in cervical cancer patients (Meng *et al.*, 2020) and is also associated with EMT (CC *et al.*, 2018). The complex nature of these genes and their interactions with proliferative and EMT related pathways makes it difficult to determine the effect of their upregulation on epithelial proliferation, especially in TNBC cell lines and may warrant further analysis.

Interestingly Progesterone receptor, one of the defining features of TNBC by its absence is now expressed in H737R and HPrexR, but to a greater extent in H737R cell lines (**Figure 6.15**). This may also help to explain the increased proliferation seen in H737R cell lines as PGR is known to influence cell proliferation in breast cancers (Carnevale *et al.*, 2007). However, expression of PGR in ER negative cancer has been associated with a decrease in cell proliferation and stalling in G0/G1 phase of the cell cycle (C-L Lin *et al.*, 1999). This also implies that H737R and HPrexR cell lines no longer exhibit the TNBC phenotype. It will be important to determine if PGR gene expression translates into active PGR protein moving forward.

So far, the question of drug resistance to CHK1 inhibitors has not been addressed. Induction of EMT has been strongly associated with drug resistance in multiple cancers and drugs (BA *et al.*, 1996; X *et al.*, 2015; Du and Shim, 2016). However, it appears EMT has been downregulated in our CHK1 resistant cell lines. One study found knockdown of EMT transcription factor ZEB1 was able to sensitise cells to an ATR inhibitor VE-821 through lessening of migratory behaviour and AKT/ERK signalling driving EMT (Song *et al.*, 2018). They also revealed inhibition of ZEB1 promoted CHK1 phosphorylation and induced S-phase arrest by enhancement of TopBP1 expression proposing a mechanism by which EMT may influence CHK1 activity (Song *et al.*, 2018). Another study connects ZEB1 and EMT to the DNA damage response and radio resistance, but suggests this is via ATM stabilising ZEB1



which directly interacts with ZEB1 enhancing its ability to stabilise CHK1 (Zhang *et al.*, 2014). It is difficult to identify how downregulation of EMT may promote resistance to a CHK1 inhibitor, but it is clear there is some crosstalk between members of each pathway.

With the information available it's difficult to draw strong conclusions regarding CHK1i resistance. Results from RNA sequencing may be improved with a larger sample size to increase the power of the analysis which may reveal more subtle but important changes. Future work should also look to sequence cells treated with and without CHK1 inhibitors as resistance mechanisms may be invisible to RNA sequencing in untreated cells. Due to time constraints, we were unable to explore other types of analysis which may reveal more information. As a result, a blunt  $\geq 2$ -fold-difference cut off was applied to the data which may have excluded important DEGs with lower fold changes. Despite this, the data highlights the differences between H737R and HPrexR cells showing how HPrexR may be closer to the parental phenotype than H737R. In addition, the apparent downregulation of the EMT pathway provides an interesting explanation for the changes in growth and appearance of H737R and HPrexR cell lines. However, the relevance of these finding to CHK1i resistance remains to be seen.

---

# **Chapter 7**

## **General Discussion**

# 7. General Discussion

## 7.1 Introduction

Triple negative breast cancer (TNBC) is an aggressive and metastatic breast cancer subtype defined by the lack of oestrogen receptor (ER), progesterone receptor (PGR) and the human epidermal growth factor 2 receptor (HER2) proteins. Treatment options are limited as hormonal manipulation therapies commonly used to treat breast cancer are ineffective against TNBC (Wahba and El-Hadaad, 2015). Therefore, CHK1 inhibitors have been proposed as a means of exploiting the inherent genomic instability present in TNBC due to the high frequency of *TP53* mutations in this cancer subtype (Ma *et al.*, 2012). CHK1 inhibitors are currently progressing through the clinic for use as a single agent and in combination with other chemotherapeutics, however the problem of drug resistance remains.

Resistance to cancer therapies presents a major obstacle in the successful treatment of patients and can be innately present or acquired over prolonged exposure to the drug (Longley and Johnston, 2005). Preclinical models of drug resistance, i.e., cancer cell lines adapted to cancer drugs have already proved to be successful in identifying clinically relevant biomarkers and mechanisms of drug resistance (Garraway and Jänne, 2012). To this end, TNBC cell lines HCC38 and MDA-MB-468 were adapted to CHK1 inhibitors SRA737 and Prexasertib and underwent initial characterisation and cross-profiling with other inhibitors. This work explores the response to CHK1 inhibition in TNBC and the potential mechanisms of resistance that may arise in the clinic. This work also identifies potential treatments which may be used to combat resistance to CHK1 inhibitors and could be relevant to treatment of patients in the clinic.

This chapter discusses the key findings of this thesis, and the wider implications for the treatment of CHK1 inhibitor resistant TNBC and makes suggestions for future work to further the goals of this project. Namely the identification of CHK1 inhibitor biomarkers and

mechanisms of resistance, along with therapeutic strategies to overcome resistance to CHK1 inhibitors in TNBC.

## 7.2 Summary of main findings

### 7.2.1 Triple Negative breast cancer cell lines with acquired resistance to CHK1 inhibition

In order to investigate mechanisms of CHK1 inhibitor resistance, TNBC cell lines HCC38 and MDA-MB-468 were made resistant to CHK1 inhibitors SRA737 or Prexasertib producing 4 CHK1i resistant cell line models. In chapter 3, resistance was generated via dose escalation with each drug and CHK1i resistant cell lines characterised. Initial characterisation showed the MDA-MB-468 cell lines were more innately resistant to CHK1 inhibition versus HCC38 cells, demonstrating GI<sub>50</sub> values approximately 60-fold and 34-fold higher to SRA737 and Prexasertib respectively (**Figure 3.2**). Both cell lines were successfully adapted to growth in the presence of Prexasertib, showing a >33-fold increase in GI<sub>50</sub> in MDA-PrexR cells versus a 1250-fold increase in HPrexR cells (**Figures 3.7 & 3.8**). These resistant sublines had GI<sub>50</sub> values of approximately 5µM with the difference in resistance factor owing to their variation in innate resistance to CHK1 inhibition. MDA-MB-468 cells were unable to adapt to SRA737 suggesting MDA-MB-468 cell lines were innately resistant to SRA737 (**Figure 3.4**). However, prolonged exposure to SRA737 conferred cross resistance to Prexasertib suggesting some adaptations did take place (**Figure 3.8**). H737R and HPrexR cell lines showed similar levels of cross resistance to each CHK1 inhibitor (**Figure 3.7**), while the MDA-737R dose response curve showed greater sensitivity to Prexasertib than MDA-PrexR cells (**Figure 3.8**).

No increase in MDR1 (P-glycoprotein 1) drug efflux pump was identified H737R, HPrexR, MDA-737R or MDA-PrexR versus their respective parental cell lines (**Figure 3.11**). In addition, the P-glycoprotein 1 inhibitor Verapamil failed to resensitise H737R and HPrexR cell lines to SRA737 and Prexasertib (**Figure 3.13**), suggesting that drug efflux is an unlikely cause of resistance to these inhibitors. In addition, both HCC38 and MDA-MB-468 resistant cell lines

were cross resistant to Ceralasertib (**Figures 3.14 & 3.15**), which inhibits ATR, a kinase upstream of CHK1 that signals for its activation in response to replication stress and DNA damage. Furthermore, H737R and HPrexR cells are cross resistant to the drug Adavosertib (**Figures 3.14 & 3.15**) which inhibits the kinase WEE1. Both WEE1 and CHK1 regulate the activity of cyclin dependent kinases (CDK), therefore cross resistance to this drug highlighted regulation of CDK activity as a potential locus of resistance in H737R and HPrexR cells. Consequently, cross resistance to these inhibitors suggests mechanistic alterations in the CHK1 signalling pathway or a related pathways are more likely the cause of drug resistance than upregulation of drug efflux pumps.

H737R and HPrexR cells lines exhibit shorter doubling times of 31.3 and 35.15 hours respectively compared with 47.58 hours in HCC38 cell lines at 1600 cells per well (**Figure 3.5**). MDA-737R and MDA-PrexR have slightly longer doubling times at 29.9 and 30.59 hours respectively compared with 27.02 hours MDA-MB-468 cells at 3200 cells per well (**Figure 3.6**). However, only H737R and MDA-PrexR cells showed a significant difference in doubling time ( $p=0.05$ ), but this is likely due to the limited number of biological repeats ( $n=2$ ) making it difficult to identify subtle significant differences. Interestingly, as shown in **chapter 6**, H737R and HPrexR cell lines have downregulated genes involved in the epithelial to mesenchymal transition (**Figure 6.14**), suggesting H737R and HPrexR may exhibit a more epithelial phenotype relative to HCC38 cells. This may be linked to the shorter doubling times seen in these cells, as epithelial cell types are typically more proliferative (Kalluri and Weinberg, 2009). Two studies investigating acquired resistance to Prexasertib both showed an increase in cell doubling times, which was attributed to prolongation of the G2/M phase in small cell lung cancer (SCLC) (Zhao, I. K. Kim, *et al.*, 2021) and BRCA wild-type ovarian cancer cell lines (Nair *et al.*, 2020). However, no acquired resistance study published to date has shown a CHK1i resistant cell line model with a shorter doubling time.

## 7.2.2 Maintenance of CDK inhibition combined with elevated resilience to replication stress may drive CHK1i resistance

### 7.2.2.1 The role of WEE1 kinase and CDK inhibitor p21<sup>Cip1/Waf1</sup>.

In **chapters 3 & 5** western blot experiments showed that the CDK inhibitory kinase WEE1 and the CDK inhibitor p21<sup>Cip1/Waf1</sup> are upregulated in H737R cells (**Figures 3.22 & 5.4-5.6**), while in HPrexR cells WEE1 was slightly increased (**Figure 3.22**) and p21<sup>Cip1/Waf1</sup> was not investigated in HPrexR cells. A cycloheximide time course experiment investigating changes in H737R and HPrexR cells showed WEE1 turnover was reduced in both cell lines, but to a greater extent in H737R cells, likely leading to its upregulation of WEE1 in both cell lines (**Figures 4.6 & 4.7**). Interestingly, no difference in WEE1 mRNA was detected by RNA sequencing in either H737R or HPrexR versus the HCC38 parental cells (**Appendix 6.4 & 6.5**). Taken together, this would suggest that WEE1 kinase is predominantly regulated at the protein level via its phosphorylation and subsequent ubiquitination and degradation, although this has not been formally proven (Smith *et al.*, 2007). However, the E2F1 transcription factor has been shown to promote WEE1 expression (Bhar *et al.*, 2013), and E2F1 knockdown causes a significant reduction in WEE1 expression in small cell lung cancer cell lines (SCLC)(Zhao, I. K. Kim, *et al.*, 2021). 14-3-3 proteins have also been shown to promote WEE1 stability, an interaction likely encouraged by CHK1 dependent phosphorylation of WEE1 (Lee, Kumagai and Dunphy, 2001; Rothblum-Oviatt, Ryan and Piwnicka-Worms, 2001). p21<sup>Cip1/Waf1</sup> is known to be transcriptionally regulated by p53 (Kagawa *et al.*, 1997; Hill *et al.*, 2008), which is inactive in these cell lines (**Table 3.1**). However, multiple p53-independent pathways regulate p21<sup>Cip1/Waf1</sup> including RAS and transforming growth factor-beta (TGF-beta) signalling pathways, which influence p21<sup>Cip1/Waf1</sup> transcription (Kivinen *et al.*, 1999; Datto *et al.*, 1995). The cause of p21<sup>Cip1/Waf1</sup> overexpression was not investigated, however as an inhibitor of CDKs, it was thought p21<sup>Cip1/Waf1</sup> may contribute to resistance.

In **chapter 5**, loss of the inhibitory phosphorylation on Y15 of CDK1/2, was increased in response to SRA737 + Adavosertib treatment (**Figure 5.13**). This led to a reduction in both p21<sup>Cip1/Waf1</sup> and WEE1 (**Figure 5.13**). The addition of Roscovitine reversed the effects of the drug combination, increasing both WEE1 and p21<sup>Cip1/Waf1</sup> levels and increased pCDK1/2 Y15 signal, likely due to the restoration of the WEE1 kinase (**Figure 5.13**). This suggests a mechanism by which CDK1/2 signals for WEE1 and p21<sup>Cip1/Waf1</sup> degradation. Indeed, CDK1 and CDK2 have been shown to phosphorylate WEE1 for proteasomal degradation (Li *et al.*, 2010; Hughes *et al.*, 2013) creating a positive feedback loop that is likely essential for the unidirectional progression of cells through mitosis (Pomerening, Sun and Ferrell, 2005; Madoux *et al.*, 2010). In addition, CDK2 is known to destabilise p21<sup>Cip1/Waf1</sup> by phosphorylation on S130 (Zhu, Nie and Maki, 2005).

As WEE1, p21<sup>Cip1/Waf1</sup> and CHK1 regulate CDK activity we hypothesised resistance to CHK1 inhibition may arise via up-regulation of WEE1 kinase and/or p21<sup>Cip1/Waf1</sup> (**Figure 7.1**). There was not enough time to investigate the role of p21<sup>Cip1/Waf1</sup> in CHK1 inhibitor resistance for this project, but **chapter 4** investigated the role of WEE1. Unfortunately, these results remain inconclusive. Attempts to overexpress ectopic WEE1 in HCC38 cells (**Figures 5.21-4.24**) were unsuccessful and knockdown of WEE1 via siRNA did not resensitise H737R and HPrexR cell lines to SRA737 (**Figure 4.20**). However, these results are not in agreement with published studies showing knockdown of WEE1 was synergistic with CHK1 inhibition/knockdown (Carrassa *et al.*, 2012; Wang, Decker and Sebolt-Leopold, 2004). Therefore, it seems likely that failure to resensitise H737R & HPrexR to SRA737 via WEE1 siRNA may be due to insufficient knockdown of WEE1 kinase expression (**Figure 4.21**). H737R and HPrexR both show cross resistance to the WEE1 inhibitor Adavosertib showing 7.8- and 10.9-fold greater resistance versus HCC38 cells respectively (**Figure 3.14**). Additionally, Adavosertib partially resensitised H737R and HPrexR cells to CHK1 inhibition, suggesting WEE1 kinase was important for CHK1i resistance (**Figure 4.14**). Surprisingly, H737R and HPrexR cell lines did not show resistance to the WEE1 inhibitor PD0166285 (**Figure 4.15**) and was not synergistic

in combination with the CHK1 inhibitor SRA737 in H737R cells (**Figure 4.16**). Multiple studies have attributed Adavosertib single agent activity and synergistic effects with CHK1 inhibitors to inhibition of WEE1 (Guertin *et al.*, 2012; Hauge *et al.*, 2017; Krehling *et al.*, 2012; Guertin *et al.*, 2013; Chaudhuri *et al.*, 2014). Therefore, it seems unlikely the response to Adavosertib seen in H737R and HPrexR cell lines is due to an off-target effect of Adavosertib.

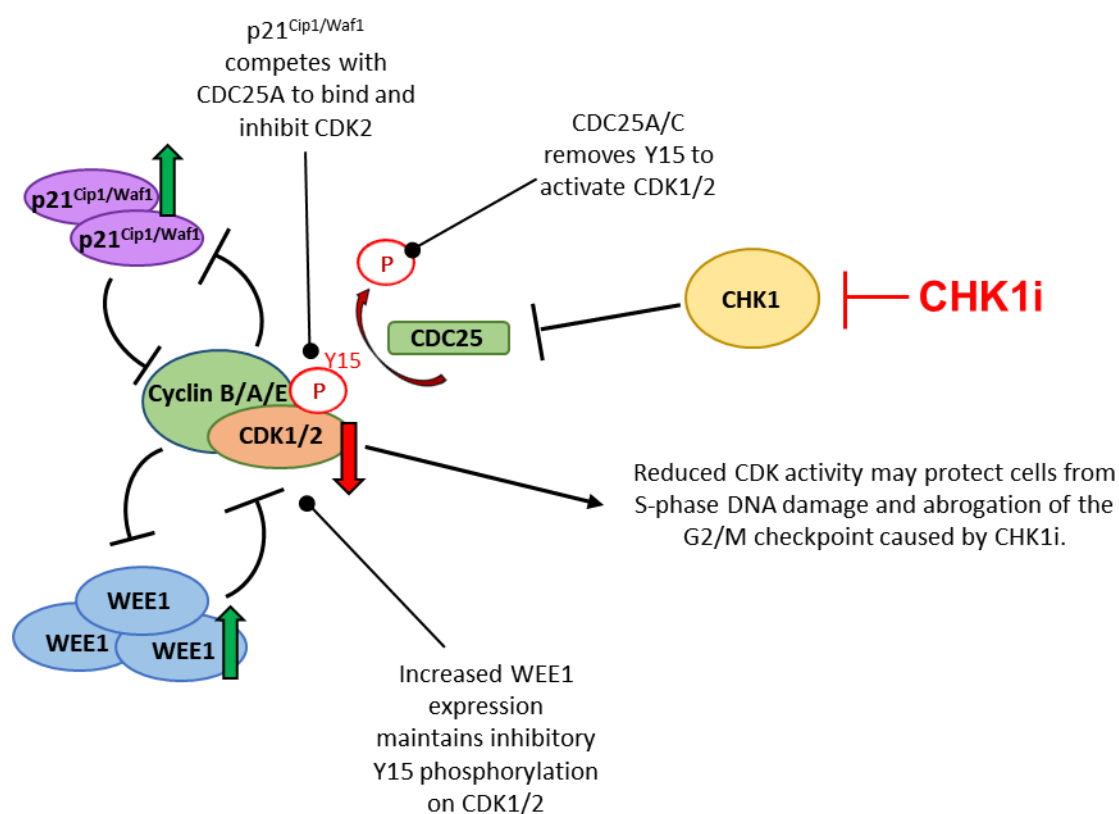


**Figure 7.1: Overexpression of WEE1 and p21<sup>Cip1/Waf1</sup> may compensate for CHK1 inhibition by maintaining CDK inhibition.** CDC25C dephosphorylates CDK1. CDC25A dephosphorylates CDK2.

In **chapter 4** the difference in response between Adavosertib and PD0166285 was discussed. Adavosertib is a more potent WEE1 inhibitor than PD0166285 with IC<sub>50</sub> values of 5.2nM and 24nM respectively (Wang *et al.*, 2001; Hirai *et al.*, 2009). Additionally, PD0166285 inhibits the MYT1 dual specificity kinase with an IC<sub>50</sub> of 72nM which phosphorylates CDK1 on T14 and Y15 (Wang *et al.*, 2001; Booher, Holman and Fattaey, 1997). It is possible for MYT1 to phosphorylate CDK2 on T14 if already phosphorylated at Y15, but Booher *et al.* suggest



WEE1 is the major kinase that suppresses CDK2 activity (Booher, Holman and Fattaey, 1997). While Hirai *et al.* do not specify the IC<sub>50</sub> value of Adavosertib for the with MYT1 kinase, they state that it is >100-fold more selective for WEE1 than MYT1 (Hirai *et al.*, 2009). Additionally, PD0166285 is a weak inhibitor of CHK1 with an IC<sub>50</sub> of 3.4μM (Wang *et al.*, 2001).

The accumulation of cells in S-phase associated with Adavosertib, in addition to its ability to abrogate the G2/M checkpoint are well documented (Hirai *et al.*, 2009; Amy D. Guertin *et al.*, 2013). HCC38 and H737R cells accumulate in S-phase after treatment with Adavosertib (**Figures 4.10-4.13**) and induce the DNA damage marker γH2AX (**Figure 4.8**) suggesting overactivation of CDKs via WEE1 inhibition, results in increased DNA damage and replication stress. However as mentioned in **chapter 4**, no publication investigating PD0166285 has shown an S-phase associated effect, focusing only on abrogation of the G2/M checkpoint (Wang *et al.*, 2001; Mir *et al.*, 2010; J *et al.*, 2011). Additionally, the synergistic effects of Adavosertib and CHK1 inhibitors have been linked to high induction of DNA damage in S-phase (Hauge *et al.*, 2017). As PD0166285 does not show a synergistic effect in combination with SRA737 or Prexasertib, it is possible that its effects are limited to abrogation of G2/M rather than S-phase (**Figure 4.16**).

Potentially, a lack of resistance to the WEE1 inhibitor PD0166285 in H737R and HPrexR versus HCC38 cells (**Figure 4.15**), and an absence of synergy shown between PD0166285 and CHK1 inhibitor SRA737 (**Figure 4.16**) could be explained by an ability of PD0166285 to activate CDK1 over CDK2. This would result in cell death by abrogation of the G2/M checkpoint as joint inactivation of WEE1 and MYT1 is potentially more effective at activating CDK1 prematurely over CDK2. Flow cytometry data showing S-phase accumulation in HCC38 cells treated with SRA737 while the H737R cell cycle is unperturbed (**Figures 4.10-4.13**) in addition to western blot data showing an increase in DNA damage and replication stress markers with CHK1 inhibition in HCC38 but not H737R cells (**Figures 4.2 & 5.4**) suggests these cell lines are better adapted to managing S-phase disruption than G2/M checkpoint abrogation. Therefore, it makes sense that H737R and HPrexR cells are not resistant to

PD0166285 if this drug kills cells by abrogation of the G2/M checkpoint, as they are likely more adapted to disruption of S-phase and DNA replication (**Figure 7.2**).

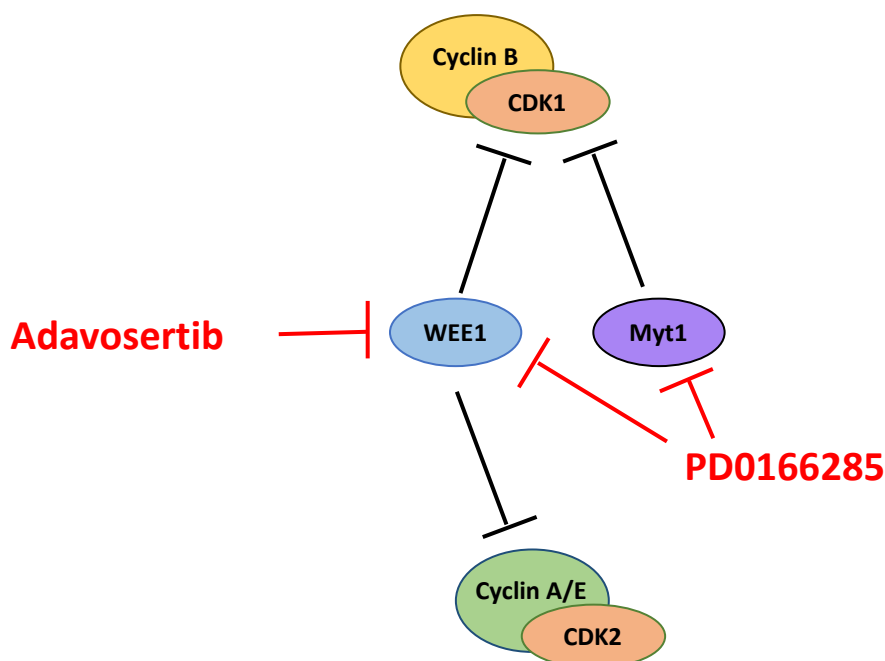


**Figure 7.2: Difference in response to WEE1 inhibitors Adavosertib and PD0166285 may be explained by PD0166285 ability to inhibit Myt1.** H737R and HPrexR cells may be adapted to CHK1i ability to disrupt S-phase over disruption of the G2/M checkpoint. Therefore PD0166285, a WEE1 inhibitor that predominantly kills cells by G2/M checkpoint abrogation, due to its inhibition of two CDK1 inhibitory kinases (Y et al., 2001), may not exhibit cross resistance in these cell lines.

As PD0166285 also weakly inhibits CHK1 with an  $IC_{50}$  of 3.4 $\mu$ M (Wang *et al.*, 2001), it's important to consider if this could explain why H737R & HPrexR cells exhibit resistance to WEE1 inhibitor Adavosertib but not PD0166285 (**Figures 3.14 & 4.15**), as dual inhibition of WEE1 and CHK1 may increase sensitivity to PD0166285 over Adavosertib. However, this seems unlikely as both H737R and HPrexR cells demonstrate greater resistance to the drug combination of SRA737 + Adavosertib compared with HCC38 cell lines (**Figures 5.10-5.12**). Therefore, if these cells are experiencing sufficient dual inhibition of CHK1 and WEE1, resistance to PD0166285 in H737R and HPrexR cells may still be expected. It also seems unlikely that the off-target inhibition of CHK1 explains the lack of synergy seen in **figure 4.16**.

This is because H737R cells are treated with 30nM of PD0166285 whereas the IC<sub>50</sub> for CHK1 inhibition by this drug is 3.4μM and therefore may not be greatly inhibiting CHK1 in cells. However, the effect on PD0166285 on CHK1 activity in our cell lines is not known. Additionally, if PD0166285 was inhibiting CHK1 to a sufficient degree it seems more likely this would enhance the effect of the drug combination with the CHK1 inhibitor SRA737 than inhibit potential synergistic effects caused by inhibiting WEE1 and CHK1 in combination.

While the exact role of WEE1 in CHK1i resistance is unclear in H737R and HPrexR cell lines, a study investigating resistance to CHK1 inhibitor Prexasertib in SCLC has shown that up-regulation of WEE1 confers resistance to CHK1 inhibition (Zhao, I. K. Kim, *et al.*, 2021). Zhao *et al.* show knockdown of WEE1 via siRNA in Prexasertib resistant SCLC cell lines resensitises cells to CHK1 inhibition, in addition ectopic expression of WEE1 in CHK1i naïve cells induces resistance to Prexasertib showing that WEE1 overexpression is a possible mechanism of resistance to CHK1 (Zhao, I. K. Kim, *et al.*, 2021). More work is required before WEE1's role in CHK1i resistance of H737R and HPrexR cell lines can be determined. Specifically, generation of ectopically overexpressing WEE1 HCC38 cell lines and sufficient knockdown of WEE1 in H737R and HPrexR cell lines. However, the downstream effects of CDK inhibition are investigated further in the next section.

#### **7.2.2.2 Understanding the role of CDK activity in resistance to CHK1 inhibition**

As discussed in the previous section, the difference in response to PD0166285 and Adavosertib in H737R and HPrexR cell lines (**Figures 3.14 & 4.14-4.16**) was attributed to the dual inhibition of WEE1 and MYT1 by PD0166285, while Adavosertib only inhibited WEE1 (Y *et al.*, 2001; Hirai *et al.*, 2009). It was hypothesised that if H737R and HPrexR cells are resistant to the induction of S-phase DNA damage caused by CHK1 inhibition rather than abrogation of the G2/M checkpoint, they would not exhibit resistance to a WEE1 inhibitor that may activate CDK1 over CDK2. While this is only speculative, PD0166285 may be more likely to activate CDK1 via inhibition of MYT1, an inhibitory kinase of CDK1 but not CDK2, via phosphorylation of T14 (Booher, Holman and Fattaey, 1997). If true, this would suggest

resistance to CHK1 inhibition in H737R and HPrexR cell lines, may be dependent on maintenance of CDK2 inhibition over CDK1. SRA737 and Adavosertib together induced markers of DNA damage, replication stress and apoptosis in H737R cell lines (**Figure 4.9**) suggesting that this drug combination is highly toxic to these cells. These effects were partially reversed by the addition of the CDK1/2/5 inhibitor Roscovitine (**Figure 5.13**), showing the ability for Roscovitine to rescue the cell killing effects of the drug combination are linked to the reduction of replication stress induced DNA damage and cell death driven by activation of CDKs. This is in agreement with studies that have shown the synergistic effects of CHK1 and WEE1 inhibition is in part due to the overactivation of CDK1/2 in S-phase (Hauge *et al.*, 2017; Guertin *et al.*, 2012).

Unfortunately, it's very difficult to discriminate between CDK1 and CDK2 activity. One method commonly used as a marker of CDK activation status is to measure the inhibitory phosphorylation Y15. Antibodies marketed as selective for pCDK1 Y15 cannot specifically bind Y15 on either pCDK1 or pCDK2 due to the location of the residue being in the middle of a conserved 13 amino acid sequence in the ATP binding pocket of the kinase (Sakurikar and Eastman, 2016). In addition, there are currently very few truly selective CDK inhibitors, making it difficult to say if effects seen using these compounds are due specifically to inhibition of CDK1 or CDK2. This is a limitation faced by our study, as the two CDK inhibitors RO-3306 and Roscovitine both inhibit CDK1 and CDK2. However, Roscovitine also inhibits CDK5 as mentioned previously. In **chapter 5**, it was reasoned RO-3306 may be a “weak” CDK2 inhibitor due to a study showing RO-3306 permitted successful initiation of DNA replication in HeLa cells (Vassilev *et al.*, 2006). They mention the dissociation constant ( $K_i$ ) of CDK1/Cyclin B complex is 35nM *in vitro* and state this is 10-fold more selective for CDK2/Cyclin E and >50-fold more selective than CDK4/Cyclin D (Vassilev *et al.*, 2006). A study investigating kinase inhibition of Roscovitine shows inhibition of CDK1/Cyclin B, CDK2/Cyclin A, CDK2/Cyclin E and CDK5/p35 with  $IC_{50}$ 's of 0.65 $\mu$ M, 0.7 $\mu$ M, 0.7 $\mu$ M and 0.16 $\mu$ M respectively (Meijer *et al.*, 1997). Therefore, it is very difficult to consider either of these inhibitors selective. Despite the

apparent crossover of RO-3306 and Roscovitine, these inhibitors show very different effects in combination with the CHK1 inhibitor SRA737 in our cell lines (**Figures 5.8 & 5.9**).

A study investigating acquired resistance to the CHK1 inhibitor Prexasertib in high grade serous ovarian cancer (HGSOC) used RO-3306 to demonstrate resistance to Prexasertib could be generated by reducing CDK1/Cyclin B activity (Nair *et al.*, 2020). This was also confirmed by showing depletion of Cyclin B by siRNA conferred resistance by limiting CDK1 activation (Nair *et al.*, 2020). Another study investigating resistance to the CHK1 inhibitor Prexasertib in small cell lung cancer (SCLC) identified WEE1 up-regulation was involved in resistance to CHK1 inhibition via maintenance of CDK1 inactivity (Zhao, I. K. Kim, *et al.*, 2021). They showed RO-3306 rescues the effects of Prexasertib treatment but this is not seen with the CDK2 inhibitor K03861 (Zhao, I. K. Kim, *et al.*, 2021). K03861 is a type II CDK inhibitor is selective for CDK2 with a  $K_d$  of 50nM (Łukasik *et al.*, 2021). Type II CDK inhibitors have been shown to compete with activating cyclins as their mechanism of action, stopping CDK/Cyclin complex activity (Alexander *et al.*, 2015). Relative to type I CDK inhibitors such as Roscovitine and RO-3306 which compete for binding at the ATP bind site of CDKs, these inhibitors are much more selective (Łukasik *et al.*, 2021). Additionally, Zhao *et al* show that the CDK7 inhibitor THZ1, a Type VI inhibitor for CDK7 due to its ability to covalently bind the active kinase domain (Łukasik *et al.*, 2021), caused resistance to Prexasertib treatment in CHK1i naïve cells (Zhao, I. K. Kim, *et al.*, 2021). CDK7 is known to promote activation of CDK1 and G2/M transition via the phosphorylation of CDK1 at T161 (Fujii *et al.*, 2011), therefore inhibition of this kinase likely causes CDK1 to remain inactive. Taken together these data suggest CDK1 activity over CDK2 activity is important for resistance to Prexasertib in these SCLC cell line models (Zhao, I. K. Kim, *et al.*, 2021).

Interestingly, this effect was not seen in our experiments with SRA737 and RO-3306 suggesting maintenance of the G2/M checkpoint is not required for survival to CHK1 inhibitors in our HCC38 TNBC cell line. If this is the case, it is likely that Roscovitines ability to rescue cell death in HCC38 cells treated with SRA737 (**Figure 5.10**) and HCC38, H737R and HPrexR

cells treated with SRA737 and Adavosertib (**Figures 5.10-5.12**) is due to inactivation of CDK2 suggesting acquired resistance to CHK1 inhibition in H737R and HPrexR is at least partially dependent on inhibition of CDK2 activity, potentially via up-regulation of WEE1 or p21<sup>Cip1/Waf1</sup>.

#### 7.2.2.3 Replication stress and mechanisms of resistance to CHK1 inhibition

**Chapter 5** investigated the response of HCC38, H737R and HPrexR cell lines to replication stress inducing agents Gemcitabine and Hydroxyurea (HU). These drugs cause replication stress via inhibition of ribonucleotide reductase (RNR) (JW, 1992; Plunkett, Huang and Gandhi, 1995). RNR is a heterotetrametric complex consisting of Ribonucleotide reductase catalytic subunits M1 & M2 (RRM1 & RRM2) that catalyses the reduction of ribonucleotide diphosphate (NDPs) into deoxyribonucleotides (dNDPs) for use in DNA replication (Zhou *et al.*, 2013). Interestingly, H737R and HPrexR cell lines demonstrated significant resistance to Gemcitabine showing a fold-increase in GI<sub>50</sub> of 2.8 and 1.93 respectively, but no significant resistance was detected to HU (**Figure 5.1**). RNA sequencing identified significant increases in RNR subunits (**Table 5.1**). H737R demonstrated a greater fold increase of RRM1 versus HPrexR cells of 1.71- and 1.39-fold respectively, whereas only HPrexR significantly overexpressed RRM2 with a 1.29-fold increase in expression (**Table 5.1**). Upregulation of RRM1 and RRM2 expression has not been confirmed at a protein level, therefore it is unknown if this will confer any phenotypic change. However, if RRM1 protein is upregulated this may explain resistance to Gemcitabine in H737R and HPrexR, as upregulation of RRM1 has been associated with resistance to Gemcitabine previously (Beyaert *et al.*, 2016). The difference in expression between RRM1 and RRM2 may explain why H737R and HPrexR are resistant to Gemcitabine but not HU. This is because Hydroxyurea specifically interacts with RRM2 for its RNR inhibitory activity (Navarra and Preziosi, 1999), whereas Gemcitabine's inhibition of RNR is thought to be RRM1 dependent (Davidson *et al.*, 2004).

In **chapter 5**, it was hypothesised that upregulation of RRM1 may confer resistance to CHK1 inhibition by increasing the levels of dNTPs available. However, one study assessed the total cellular dNTP levels in cells transfected with an RRM1 expression vector and saw no change

in available dNTPs relative to the non-transfected control cells, suggesting RRM1 expression alone cannot alter dNTP levels (Gautam, Li and Bepler, 2003). Phosphorylation of S559 on RRM1 has been shown to increase dNTP production by RNR, however this is regulated by CDK2/Cyclin A activity (Shu *et al.*, 2020). Since one hypothesis is that CDK2 inhibition is maintained in H737R and HPrexR cells as a mechanism of CHK1i resistance in section **7.2.2.2**, it seems contrary that RNR activity may be upregulated via increased phosphorylation on RRM1 S559. However, CDK2 has also been shown to regulate RNR by phosphorylation of RRM2 on T33, leading to its degradation (Koppenhafer *et al.*, 2020). Potentially, the CDK2 dependent regulation of RNR depends on timing and intensity of CDK2 activation as WEE1 inhibition by Adavosertib has been shown to deplete the pool of available dNTPs via loss of RRM2 (Pfister *et al.*, 2015), a process likely caused by unscheduled overactivation of CDK2. Therefore, if H737R and HPrexR cells maintain a more 'normal' function of CDK2 during CHK1 inhibition then they may be able to promote the activity of RNR leading to increased pools of dNTPs. However, future work should first identify if RRM1/RRM2 are upregulated at the protein level in addition to determining if pools of dNTPs are increased in H737R & HPrexR cell lines.

In section **7.2.2.2**, the ability for Adavosertib to partially resensitise H737R and HPrexR cells was attributed to overactivation of CDK2. This was supported by experiments showing RO-3306 (CDK1/weak CDK2 inhibitor (Vassilev *et al.*, 2006)) failed to rescue the effects of SRA737 in HCC38 cell lines, whereas Roscovitine (CDK1/2/5 inhibitor (Meijer *et al.*, 1997)) was able to rescue the effects of SRA737 in HCC38 and SRA737 + Adavosertib in HCC38, H737R and HPrexR cells (**Figures 5.10-5.12**). However, Roscovitine was not able to completely restore viability to SRA737 + Adavosertib treatment (**Figures 5.10 -5.12**). In addition, markers of replication stress such as  $\gamma$ H2AX, pRPA32 s4-8, RPA32 band shifting, and pCHK1 s345 were still up relative to control H737R cells with SRA737 & Adavosertib + Roscovitine treatment (**Figure 5.13**). This could suggest multiple things, either that Roscovitine was not able to completely inhibit CDK2, Roscovitine itself is causing some level

of replication stress, and/or inhibition of CDK2 is not sufficient to counteract the replication stress induced by SRA737 + Adavosertib. Indeed, inhibition of CDK5, a kinase that Roscovitine strongly inhibits (Meijer *et al.*, 1997), likely induced replication stress as knockdown of this CDK has been shown to increase replication stress in Hela cells (Chiker *et al.*, 2015). Additionally, Hauge *et al.* shows that the synergistic effects of SRA737 + Adavosertib are caused by overactivation of CDKs in addition to deregulation of CHK1s CDK-independent control over CDC45 loading (Hauge *et al.*, 2017).

CDC45 is an essential part of the CMG replicative helicase complex made up of CDC45-Mcm2-7-GINS proteins and is required for the initial unwinding and firing of replication origins (Köhler *et al.*, 2016; Seo and Kang, 2018). A study investigating CDC45 overexpression found increased CDC45 protein led to RPA exhaustion and subsequent replication catastrophe suggesting CDC45 played a rate limiting role in replication initiation (Köhler *et al.*, 2016). CDK activity has been shown to influence loading of CDC45 as the CDK inhibitor Roscovitine reduced the association of CDC45 with chromatin (Falck *et al.*, 2002). However, Hauge *et al.* showed the CHK1 inhibitor AZD7762 increased CDC45 loading to a greater extent than the WEE1 inhibitor Adavosertib (Hauge *et al.*, 2017) suggesting that CHK1 has tighter control over replication initiation that is not dependent on CDK activity. This may explain why Roscovitine fails to completely rescue the cell killing effects of SRA737 + Adavosertib in H737R and HPrexR cell lines (**Figure 5.13**), as inhibition of CDK activity may be unable to counteract increased CDC45 loading by CHK1 inhibition.

As shown in **chapter 4**, HCC38 and H737R cells stall in S-phase after combined inhibition of CHK1 and WEE1 but to a lesser degree in H737R cells (**Figures 4.10-4.13**). Interestingly, H737R cell cycle profile when treated with SRA737 + Adavosertib is more like HCC38 treated with SRA737 alone as HCC38 and H737R show approximately 50% of cells in S-phase (**Figures 4.12 & 4.13**). In comparison, HCC38 cells treated with SRA737 + Adavosertib show approximately 75% of cells in S-phase (**Figure 4.12**) demonstrating that H737R cells are also resistant to combined inhibition of CHK1 and WEE1. Therefore, another mechanism in



addition to inhibition of CDK2 activity must be present to allow H737R cells to cope with combined inhibition of CHK1 and WEE1. If RNR activity is indeed upregulated as mentioned earlier, an increased pool of dNTPs may increase H737R and HPrexR cells resilience to combined inhibition of CHK1 and WEE1 explaining why H737R and HPrexR cells are more resistant to combined treatment of SRA737 + Adavosertib than HCC38 cells.

#### **7.2.2.4 A model of CHK1 inhibitor resistance in H737R & HPrexR cell lines**

The data presented in this thesis suggests that the combined effects of CDK2 inhibition and an increase in resilience to replication stress confers resistance to CHK1 inhibition as described in **figure 7.3**. Upstream of CDK2, the WEE1 kinase and CDK inhibitor p21<sup>Cip1/Waf1</sup> are upregulated and potentially inhibit CDK activity to compensate for CHK1 inhibition and activation of the CDC25 phosphatase. Additionally, RNR activity may be upregulated leading to increased pools of dNTPs compensating for increased firing of replication origins caused by CHK1 inhibition, ensuring sufficient dNTPs are available for DNA replication thereby avoiding replication stress and DNA damage (**Figure 7.3 A**). H737R and HPrexR cell lines are both resistant to WEE1 inhibition by Adavosertib. However, western blot analysis of H737R cell lines show Adavosertib induces higher levels of DNA damage than SRA737 (**Figures 4.2 & 4.8**). As WEE1 directly inhibits CDK2 activity via phosphorylation of Y15, its inhibition leads to greater activation of CDK2 than CHK1 inhibition (**Figures 4.2 & 4.8**). The activation of CDK2 leads to CDK dependent degradation of p21<sup>Cip1/Waf1</sup> (**Figure 5.5**). However, active CHK1 and increased pool of dNTPs limit the effects of replication stress caused by WEE1 inhibition leading to low levels of DNA damage relative to HCC38 cell lines (**Figures 4.8, 5.5 & 7.3 B**). Combined inhibition of WEE1 and CHK1 greatly increases CDK activity and replication initiation leading to high levels of replication stress and subsequent DNA damage. However, increased pools of dNTPs likely increase H737R and HPrexR capacity for replication stress leading to less DNA damage from the drug combination relative to HCC38 cell lines (**Figures 4.9 & 7.3 C**). Finally, Gemcitabine is most effective at restoring sensitivity to SRA737 (**Figures 5.2-5.3**). Inhibition of RNR by Gemcitabine leads to depletion of the dNTP pool resulting in

insufficient dNTPs for successful DNA replication. Simultaneously, CHK1 inhibition leads to increased CDK activity and unscheduled firing of replication origins via increased loading of CDC45. While WEE1 and p21<sup>Cip1/Waf1</sup> may still reduce CDK activity to a greater extent than seen in HCC38 cell lines, this is unable to compensate for insufficient levels of dNTP eventually leading to high levels of DNA damage (**Figure 7.3 D**).

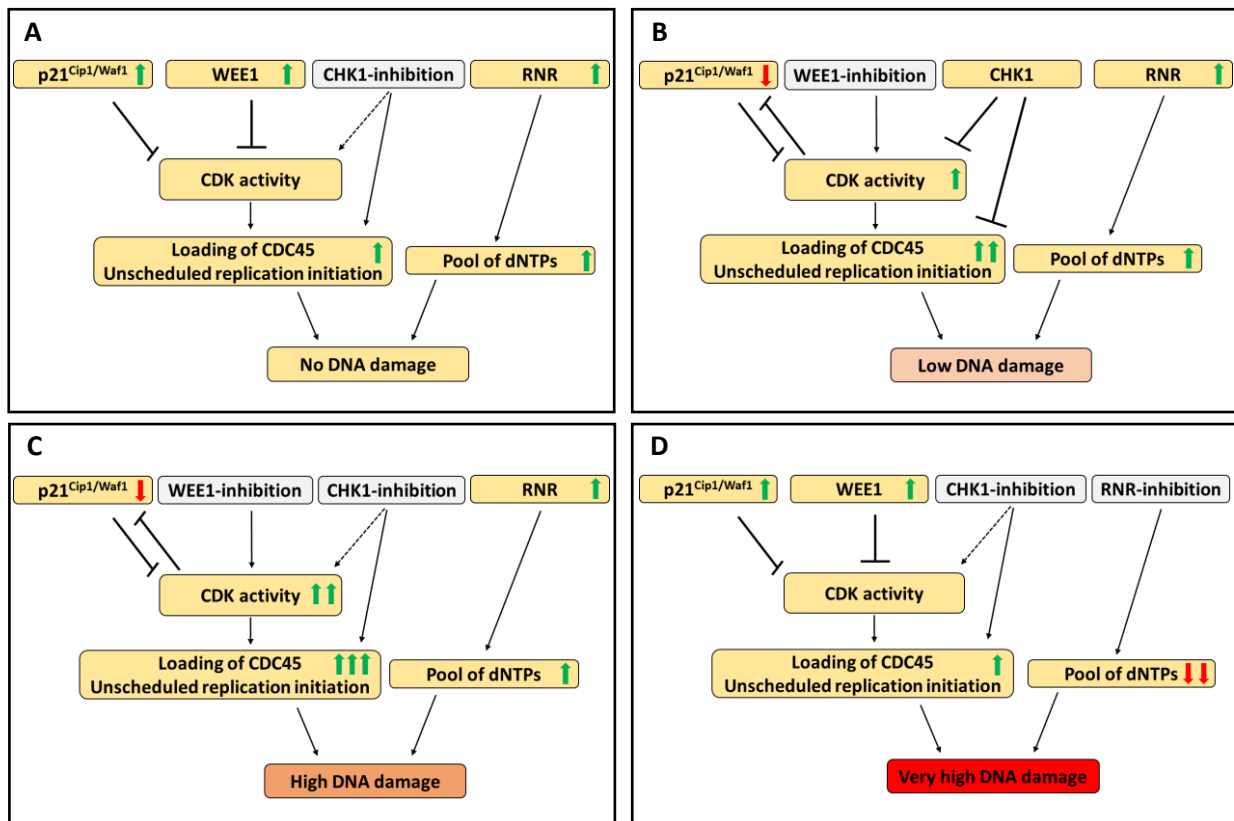


**Figure 7.3: Possible model for CHK1 inhibitor resistance and response to combined treatment of CHK1 + WEE1 inhibitors or CHK1 + Gemcitabine.** **A)** CHK1 inhibition is compensated for by an increase in CDK inhibitors WEE1 and p21<sup>Cip1/Waf1</sup> maintaining CDK inhibition. In addition, increased activity of RNR may compensate for a CDK independent increase in replication initiation caused by CHK1 inhibition by increasing the pool of available dNTPs. **B)** WEE1 inhibition leads to a greater increase in CDK activity than CHK1 inhibition and causes CDK dependent degradation of p21<sup>Cip1/Waf1</sup>. However, CHK1 may compensate for loss of WEE1's inhibition of CDK via inhibition of the CDC25 phosphatase and CDC45 loading, reducing unscheduled replication initiation (Hauge *et al.*, 2017) alongside increased RNR activity and dNTPs available for DNA replication. **C)** Combined inhibition of WEE1 and CHK1 leads to high levels of DNA damage due to the combined effects on CDK activity and unscheduled initiation of replication. However, increased activity of RNR may slightly compensate for this with higher pools of available dNTPs making H737R and HPrexR cells more resilient to this treatment than HCC38 cells. **D)** Combined inhibition of CHK1 and RNR by CHK1 inhibitors and gemcitabine highly resensitises cells to CHK1 inhibition potentially causing massive replication stress and DNA damage via dNTP depletion. Upregulation of CDK inhibitors may compensate slightly for gemcitabine induced replication stress but reduced CDK activity alone cannot compensate for depletion of dNTP pool. Therefore, resistance to Gemcitabine and the drug combination with a CHK1 inhibitor in H737R/HPrexR cell lines is limited.

This model proposes resistance to CHK1 inhibition likely arises by the combined effect of increased inhibition of CDK2 activity and upregulation of RNR activity leading to increased pools of dNTP available for DNA replication (**Figure 7.3**). However, investigations into the role of WEE1 were inconclusive. Upregulation of WEE1 has already been implicated in resistance to the CHK1 inhibitor Prexasertib (Zhao, I. K. Kim, *et al.*, 2021). In addition, the synergistic effects of WEE1 + CHK1 inhibition have already been described in some detail (Guertin *et al.*, 2012; Chilà *et al.*, 2015; Hauge *et al.*, 2017; Rorà *et al.*, 2019), showing WEE1 has the potential to influence the cellular response to CHK1 inhibition in H737R and HPrexR cell lines. At this stage, it is unknown if increased expression of RNR subunits shown in **chapter 5 (Figure 5.1)** is indicative of higher levels of dNTPs available for DNA replication and is therefore purely speculative. It is possible other pathways are altered to contribute to resistance such as upregulation of DNA repair or pro-survival/growth and proliferation pathways not investigated in this thesis. However, more work is required to elucidate further mechanisms of resistance.

### 7.3 Future work

The data presented in this thesis provides insights into potential mechanisms of CHK1 inhibition, suggesting cells maintain inhibition of CDK2 during CHK1i treatment to avoid replication stress and DNA damage. While WEE1 and p21<sup>Cip1/Waf1</sup> have been proposed as potential drivers of resistance, there is currently insufficient evidence to draw any solid conclusions. Additionally, the inability to completely resensitise H737R and HPrexR cell lines to CHK1i with Adavosertib suggests alternative mechanisms may exist, which compensates for deregulation of CDK2. We have already speculated that upregulation of RNR activity may contribute to resistance by increasing dNTPs available for DNA replication, but this remains untested. Potentially, ssDNA repair pathways may be upregulated in these cell lines such as base excision repair (BER) and mismatch repair (MMR) as shown by Nair *et al.* in BRCA wild-type CHK1 resistant HGSOc patient biopsies. This suggested CHK1i resistant cells may be repairing ssDNA breaks before they can generate double stranded DNA breakages (Nair *et*

*al.*, 2020). In addition, analysis of replication fork progression via DNA fibre analysis may provide useful insights into the progression of DNA replication and identify if CHK1 inhibition still perturbs DNA replication in H737R and HPrexR cell lines.

Initially, resistance was generated in the two TNBC cell lines HCC38 and MDA-MB-468, but MDA-MB-468 cells demonstrated high innate resistance to both SRA737 and Prexasertib. Due to time constraints, MDA-MB-468 cell lines were not investigated past their initial characterisation in **chapter 3** and HCC38 cell lines parental and resistant cell lines were taken forward. This was due to greater fold-increase in resistance to SRA737 and Prexasertib seen in the HCC38 CHK1i resistant cell lines, suggesting resistant cells had undergone substantial adaptations making differences easier to identify versus the parental cell line. Future work should investigate MDA-MB-468 cell lines for adaptations spotted in HCC38 cells, namely maintenance of CDK2 inhibition as a mechanism of drug resistance. Additionally, a study investigating innate resistance to Prexasertib has shown EGFR is highly expressed in MDA-MB-468 cell lines and likely contributes to innate resistance via suppression of pro-apoptotic pathways (Lee *et al.*, 2020). Future studies should investigate the role of EGFR and the RAS/RAF/MEK/ERK pathway to see if this is upregulated in instances of acquired resistance, adaptations in these pathways may contribute alongside regulation of CDK activity to CHK1 inhibitor resistance.

Other studies have identified low CDK1 activity as a driver of Prexasertib resistance in other cancer types (Nair *et al.*, 2020; Zhao, I. K. Kim, *et al.*, 2021) and this has been linked with reduced levels of Cyclin B in HGSOC cells (Nair *et al.*, 2020). Therefore, it would be interesting to see if certain cell lines are more likely to rely on CDK1 over CDK2 for resistance to CHK1 inhibition. Could this be an effect specific to TNBC? Or could certain biomarkers, like overexpression of cyclins B or E act as determinants for how a cell line may acquire resistance after successive treatments? Cyclins B has already been identified as a biomarker for sensitivity to CHK1 inhibition, while high cyclin E levels have been identified as a marker of sensitivity to WEE1 inhibitors (Xiao *et al.*, 2008; Chen *et al.*, 2018). It seems plausible that

cells overexpressing cyclin E may more sensitive to S-phase associated effects CHK1/WEE1 inhibitors (Chen *et al.*, 2018), whereas cyclin B overexpressing cells may be more sensitive to abrogation of the G2/M checkpoint (Xiao *et al.*, 2008). Perhaps these markers of sensitivity may predict future mechanisms of acquired resistance, as cyclin B overexpressing cell lines may tend to lower CDK1 activity whereas cyclin E overexpressing cells will lower CDK2 activity to survive CHK1 inhibition. Therefore, future acquired resistance studies should adapt TNBC cell lines taking note of parental cyclin E/B levels to see what different resistance mechanisms may emerge and if this can be linked to known markers of sensitivity.

RNA sequencing data was limited by the small sample size of 3 biological repeats per cell line, meaning significant differences were potentially deemed non-significant due to the low statistical power of the analysis. Due to time constraints differential expression analysis used a blunt  $\geq 2$ -fold cut off to isolate genes that were highly overexpressed meaning subtle but important differences in gene expression may be missed. Future RNA sequencing studies should investigate response in parental and resistant cells exposed to CHK1 inhibitor treatment as this may help to identify differences in the dynamic response to CHK1 inhibition between cell lines. Additionally, RNA sequencing can obtain mutational data which could reveal mutations that may confer drug resistance. Future studies should aim to investigate CHK1i resistant cell lines for resistance conferring mutations.

Despite the limitations, RNA sequencing produced some interesting findings. Namely, H737R and HPrexR resistant cell lines appeared to revert from a mesenchymal phenotype to an epithelial phenotype. This was determined due to the downregulation of many EMT associated genes identified by gene set enrichment analysis. Additionally, H737R cells demonstrate shorter doubling times and both H737R and HPrexR appear to exhibit a more rounded morphology relative to HCC38 cell lines. This is far from conclusive but does provide an interesting avenue for further investigation. It may be the case that genes enriched for EMT overlap with other pathways of interest. This was not investigated in detail and so further work should be done to see which pathways may overlap with the EMT geneset. Furthermore, *PGR*,

a hormone receptor absent from TNBC is now highly expressed in H737R and HPrexR cell lines. However, this has yet to be confirmed at the protein level. Additionally, it is unknown what effect this may have on the cell lines or if this has any role to play in resistance to CHK1 inhibitors. Interestingly, a study investigating the role of PGR showed cells that are ER and PGR negative but then ectopically express PGR experience growth inhibitory effects in the presence of progestins and attribute the reduced cell growth with an accumulation of cells in G0/G1 phase (C-L Lin *et al.*, 1999). Therefore, it would be interesting to see if ectopic expression of PGR in HCC38/MDA-MB-468 cell lines modulates the response to CHK1 inhibition in addition to performing SiRNA knockdown on H737R and HPrexR cell lines to determine if loss of PGR increases sensitivity to CHK1 inhibitors.

## **7.4 Clinical impact -Therapeutic strategies to combat CHK1 inhibitor resistance**

In addition to developing an understanding of the mechanistic drivers of CHK1 inhibitor resistance, this project has identified potential therapeutic strategies that may be used to overcome resistance. Namely, the combination of CHK1 inhibitors with either Adavosertib or Gemcitabine. As discussed, Adavosertib was synergistic with CHK1 inhibitor SRA737 in HCC38 parental and drug resistant cell lines (**Figures 4.9-4.14**). The synergistic effects of combined inhibition of CHK1 and WEE1 has been widely reported in the literature (Guertin *et al.*, 2012; Chaudhuri *et al.*, 2014; Carrassa *et al.*, 2012). Synergy is attributed to the deregulation of WEE1 and CHK1s ability to inhibit CDK1/2 activity in combination with a CHK1i specific effect increased firing of replication origins which combined with excess CDK1/2 activity leads to excessive replication stress, DNA damage and cell death (Hauge *et al.*, 2017). As mentioned previously, WEE1 has already been identified as a driver of resistance in SCLC cells that acquired resistance to CHK1 inhibitor Prexasertib, and combination treatment with Adavosertib was able to resensitise cells to CHK1 inhibition (Zhao, I. K. Kim, *et al.*, 2021). However, in our TNBC cell lines H737R and HPrexR, Adavosertib was only able to partially

resensitise cells and HPrexR was less responsive to this drug combination than H737R cells **(Figure 4.14)**.

In our cell lines, Gemcitabine showed the most potent resensitising effect to CHK1 inhibition **(Figure 5.1)**. Again, synergy between CHK1 inhibitors and Gemcitabine has been reported in the past. In pancreatic cancer cell lines with inactive p53, the combined effect of both drugs prolonged S-phase leading to senescence and apoptosis (Koh *et al.*, 2015). Additionally the G2/M checkpoint would be abrogated leading to mitotic death and mitotic catastrophe (Koh *et al.*, 2015). Nair *et al.*, demonstrated Gemcitabine could resensitise CHK1i resistant HGSOC cell lines to Prexasertib and hypothesised this is due to CHK1 being required to induce RAD51-mediated HR, thereby sensitising these cells to the DNA damaging effects of Gemcitabine (Nair *et al.*, 2020). We hypothesise our CHK1i resistant cell lines are vulnerable to CHK1i + Gemcitabine treatment because adaptations that enabled cross resistance to both CHK1 and WEE1 inhibitors, namely improved management of S-phase CDK2 activity and subsequent replication stress, are unable to compensate for depletion of dNTPs **(Figure 7.3)**. However, as we haven't investigated the role of various DNA repair pathways in resistance to CHK1 inhibition, it is possible deregulation of HR is also responsible for the observed synergy.

CHK1 inhibitors SRA737 (NCT02797964) and Prexasertib (NCT04032080) are currently progressing through clinical trials, in addition to the WEE1 inhibitor Adavosertib (NCT05008913, NCT02659241). Additionally, Gemcitabine is already an approved drug and its use in combination with SRA737 & Prexasertib is being tested in the clinic (SRA737: NCT02797977 Prexasertib: NCT04023669)(*ClinicalTrials.gov*, 2021). If CHK1 inhibitors are approved for use as single agent therapies in TNBC, it is likely these drugs will already be available to treat the emergence of drug resistance and as demonstrated by recent studies, these combination therapies will likely be effective at treating CHK1i resistance in other cancer types (Zhao *et al.*, 2021; Nair *et al.*, 2020).

## 7.5 Concluding remarks

The aim of this thesis is to develop an understanding of acquired resistance to CHK1 inhibition in triple negative breast cancer. As H737R and HPrexR cell lines can be partially resensitised to SRA737 with the use of WEE1 inhibitor Adavosertib it seems likely that WEE1 has an important role to play in resistance, however further validation is required. Additionally, Gemcitabine has been shown to be very effective at restoring sensitivity to CHK1 inhibitors, suggesting resistance mechanisms to CHK1 inhibition may not be able to overcome severe replication stress caused by CHK1 and Gemcitabine in combination. The use of CDK inhibitors has helped to explicate the role of cyclin dependent kinases in H737R and HPrexR cell lines and suggests resistance to CHK1 inhibition is likely dependent on inactivation of CDK2 over CDK1. Additionally, upregulation of the CDK inhibitor p21<sup>Cip1/Waf1</sup> in H737R identifies another potential avenue of resistance which could be working in concert with WEE1 to maintain CDK inhibition. In addition to regulation of CDK2, cells may rely on improved management of replication stress or upregulation of DNA repair and survival/growth pathways to compensate for loss of CHK1. These areas require further investigation and may unlock a deeper understanding in the mechanics of replication stress, DNA repair and CHK1 inhibitor resistance. Finally, this study has demonstrated that patients exhibiting resistance to CHK1 inhibitors may benefit from the combined treatment of a CHK1 inhibitor with either Gemcitabine or Adavosertib. Presenting new therapeutic strategies for overcoming CHK1 inhibitor resistance in the clinic.



# Appendix list

Appendix 4.1: Comparison of C-PARP between SRA737 Dose response western blots.

Appendix 4.2: Comparison of SRA737 + Adavosertib drug combination experiment in H737R and HPrexR cell lines.

Appendix 4.3: Effect of WEE1 knockdown by SiRNA on SRA737 sensitivity in H737R and HPrexR cell lines.

Appendix 6.1: MultiQC RNA Sequencing quality control report – produced by UCL Genomics.

Appendix 6.2: SARTools Report, description of raw RNA sequencing data, normalisation process and differential expression analysis by DESeq2 – produced by UCL Genomics.

Appendix 6.3: Raw gene counts per sample.

Appendix 6.4: H737R vs HCC38 differential expression analysis results

Appendix 6.5: HPrexR vs HCC38 differential expression analysis results

Appendix 6.6: H737R vs HCC38 differential expression analysis results -  $\geq 2$  FD &  $\leq 0.05$  padj

Appendix 6.7: HPrexR vs HCC38 differential expression analysis results -  $\geq 2$  FD &  $\leq 0.05$  padj

Appendix 6.8: List of shared and non-shared DEGs between H737R and HPrexR

Appendix 6.9: List of shared up and down regulated DEGs between H737R and HPrexR

Appendix 6.10: 569 shared DEGs Log2 fold change and padj for each gene

Appendix 6.11: Metascape geneset enrichment analysis results of shared 569 DEGs.

Appendix 6.12: Metascape geneset enrichment analysis results on shared 347 downregulated DEGs.

Appendix 6.13: Metascape geneset enrichment analysis results on shared 169 upregulated DEGs.

Appendix 6.14: Metascape geneset enrichment analysis results on all H737R DEGs.

Appendix 6.15: Metascape geneset enrichment analysis results on all HPrexR DEGs.

Appendix 6.16: DEGs identified as deregulated in EMT pathway, H737R vs HCC38 differential expression analysis data.

Appendix 6.17: DEGs identified as deregulated in EMT pathway, HPrexR vs HCC38 differential expression analysis data.

Appendix 6.18: DEGs identified as deregulated in epithelial proliferation pathway, H737R vs HCC38 differential expression analysis data.

Appendix 6.19: DEGs identified as deregulated in epithelial proliferation pathway, HPrexR vs HCC38 differential expression analysis data.

Appendix 6.20: List of top 20 up and downregulated genes for H737R and HPrexR cell lines.

# References

- Aarts, M. *et al.* (2012) 'Forced Mitotic Entry of S-Phase Cells as a Therapeutic Strategy Induced by Inhibition of WEE1', *Cancer Discovery*. American Association for Cancer Research, 2(6), pp. 524–539. doi: 10.1158/2159-8290.CD-11-0320.
- Abukhdeir, A. and Park, B. (2008) 'p21 and p27: Roles in carcinogenesis and drug resistance', *Expert Reviews in Molecular Medicine*. NIH Public Access. doi: 10.1017/S1462399408000744.
- Acloque, H. *et al.* (2009) 'Epithelial-mesenchymal transitions: the importance of changing cell state in development and disease', *The Journal of Clinical Investigation*. American Society for Clinical Investigation, 119(6), pp. 1438–1449. doi: 10.1172/JCI38019.
- Aird, K. M. *et al.* (2010) 'X-Linked Inhibitor of Apoptosis Protein Inhibits Apoptosis in Inflammatory Breast Cancer Cells with Acquired Resistance to an ErbB1/2 Tyrosine Kinase Inhibitor', *Molecular cancer therapeutics*. NIH Public Access, 9(5), p. 1432. doi: 10.1158/1535-7163.MCT-10-0160.
- Al-Madhoun, A. S. *et al.* (2004) 'Detection of an alternatively spliced form of deoxycytidine kinase mRNA in the 2'-2'-difluorodeoxycytidine (gemcitabine)-resistant human ovarian cancer cell line AG6000', *Biochemical Pharmacology*, 68(4), pp. 601–609. doi: 10.1016/J.BCP.2004.05.007.
- Albiges, L. *et al.* (2014) 'Chk1 as a new therapeutic target in triple-negative breast cancer', *The Breast*, 23, pp. 250–258. doi: 10.1016/j.breast.2014.02.004.
- Alexander, L. T. *et al.* (2015) 'Type II Inhibitors Targeting CDK2', *ACS Chemical Biology*. American Chemical Society, 10(9), pp. 2116–2125. doi: 10.1021/ACSCHEMBIO.5B00398/SUPPL\_FILE/CB5B00398\_SI\_002.XLSX.
- Aligue, R., Akhavan-Niak, H. and Russell, P. (1994) 'A role for Hsp90 in cell cycle control: Wee1 tyrosine kinase activity requires interaction with Hsp90.', *The EMBO Journal*. John Wiley & Sons, Ltd, 13(24), pp. 6099–6106. doi: 10.1002/J.1460-2075.1994.TB06956.X.
- Van Allen, E. M. *et al.* (2014) 'The Genetic Landscape of Clinical Resistance to RAF Inhibition in Metastatic Melanoma', *Cancer Discovery*. American Association for Cancer Research, 4(1), pp. 94–109. doi: 10.1158/2159-8290.CD-13-0617.
- Anderson, V. E. *et al.* (2011) 'CCT241533 is a potent and selective inhibitor of CHK2 that potentiates the cytotoxicity of PARP inhibitors', *Cancer Research*. Europe PMC Funders, 71(2), pp. 463–472. doi: 10.1158/0008-5472.CAN-10-1252.
- Antoni, L. *et al.* (2007) 'CHK2 kinase: Cancer susceptibility and cancer therapy - Two sides of the same coin?', *Nature Reviews Cancer*. Nature Publishing Group, pp. 925–936. doi: 10.1038/nrc2251.
- Arora, V. K. *et al.* (2013) 'Glucocorticoid Receptor Confers Resistance to Antiandrogens by Bypassing Androgen Receptor Blockade', *Cell*. Cell Press, 155(6), pp. 1309–1322. doi: 10.1016/J.CELL.2013.11.012.
- Azorsa, D. O. *et al.* (2009) 'Synthetic lethal RNAi screening identifies sensitizing targets for gemcitabine therapy in pancreatic cancer', *Journal of Translational Medicine*. BioMed Central, 7(1), pp. 1–12. doi: 10.1186/1479-5876-7-43/FIGURES/6.
- BA, T. *et al.* (1996) 'Transforming growth factor-beta in in vivo resistance', *Cancer chemotherapy and pharmacology*. Cancer Chemother Pharmacol, 37(6), pp. 601–609. doi: 10.1007/S002800050435.
- Bačević, K. *et al.* (2017) 'Cdk2 strengthens the intra-S checkpoint and counteracts cell cycle exit induced by DNA damage', *Scientific Reports 2017 7:1*. Nature Publishing Group, 7(1), pp. 1–14. doi: 10.1038/s41598-017-12868-5.
- Backert, S. *et al.* (1999) 'DIFFERENTIAL GENE EXPRESSION IN COLON CARCINOMA CELLS AND TISSUES DETECTED WITH A cDNA ARRAY', *J. Cancer*. Wiley-Liss, Inc, 82, pp. 868–874. doi: 10.1002/(SICI)1097-0215(19990909)82:6.

- Bagrodia, S., Smeal, T. and Abraham, R. T. (2012) 'Mechanisms of intrinsic and acquired resistance to kinase-targeted therapies', *Pigment Cell & Melanoma Research*. John Wiley & Sons, Ltd, 25(6), pp. 819–831. doi: 10.1111/PCMR.12007.
- Bahassi, E. M. *et al.* (2008) 'The checkpoint kinases Chk1 and Chk2 regulate the functional associations between hBRCA2 and Rad51 in response to DNA damage', *Oncogene*. Nature Publishing Group, 27(28), pp. 3977–3985. doi: 10.1038/onc.2008.17.
- Bai, H. *et al.* (2015) 'The PI3K/AKT/mTOR pathway is a potential predictor of distinct invasive and migratory capacities in human ovarian cancer cell lines', *Oncotarget*. Impact Journals, LLC, 6(28), p. 25520. doi: 10.18632/ONCOTARGET.4550.
- Balestrini, A. *et al.* (2010) 'GEMC1 is a TopBP1-interacting protein required for chromosomal DNA replication', *Nature cell biology*. Nat Cell Biol, 12(5), pp. 484–491. doi: 10.1038/NCB2050.
- Banerji, U. *et al.* (2019) 'A phase I/II first-in-human trial of oral SRA737 (a Chk1 inhibitor) given in combination with low-dose gemcitabine in subjects with advanced cancer.', [https://doi.org/10.1200/JCO.2019.37.15\\_suppl.3095](https://doi.org/10.1200/JCO.2019.37.15_suppl.3095). American Society of Clinical Oncology, 37(15\_suppl), pp. 3095–3095. doi: 10.1200/JCO.2019.37.15\_SUPPL.3095.
- Bardelli, A. *et al.* (2013) 'Amplification of the MET Receptor Drives Resistance to Anti-EGFR Therapies in Colorectal Cancer', *Cancer Discovery*. American Association for Cancer Research, 3(6), pp. 658–673. doi: 10.1158/2159-8290.CD-12-0558.
- Barlow, J. H. *et al.* (2013) 'Identification of Early Replicating Fragile Sites that Contribute to Genome Instability', *Cell*. Cell Press, 152(3), pp. 620–632. doi: 10.1016/J.CELL.2013.01.006.
- Barretina, J. *et al.* (2012) 'The Cancer Cell Line Encyclopedia enables predictive modelling of anticancer drug sensitivity', *Nature*. Nature Publishing Group, 483(7391), pp. 603–607. doi: 10.1038/nature11003.
- Barrière, C. *et al.* (2007) 'Mice thrive without Cdk4 and Cdk2', *Molecular Oncology*. No longer published by Elsevier, 1(1), pp. 72–83. doi: 10.1016/J.MOLONC.2007.03.001.
- Barroso-Sousa, R. *et al.* (2020) 'Prevalence and mutational determinants of high tumor mutation burden in breast cancer', *Annals of Oncology*. Elsevier Ltd, 31(3), pp. 387–394. doi: 10.1016/J.ANNONC.2019.11.010.
- Bartek, J. and Lukas, J. (2003) 'Chk1 and Chk2 kinases in checkpoint control and cancer', *Cancer Cell*. Cell Press, pp. 421–429. doi: 10.1016/S1535-6108(03)00110-7.
- Bartek, J. and Lukas, J. (2007) 'DNA damage checkpoints: from initiation to recovery or adaptation', *Current opinion in cell biology*. Curr Opin Cell Biol, 19(2), pp. 238–245. doi: 10.1016/J.CEB.2007.02.009.
- Beach, D., Durkacz, B. and Nurse, P. (1982) 'Functionally homologous cell cycle control genes in budding and fission yeast', *Nature* 1982 300:5894. Nature Publishing Group, 300(5894), pp. 706–709. doi: 10.1038/300706a0.
- Beck, H. *et al.* (2010) 'Regulators of cyclin-dependent kinases are crucial for maintaining genome integrity in S phase', *Journal of Cell Biology*. The Rockefeller University Press, 188(5), pp. 629–638. doi: 10.1083/JCB.200905059.
- Benada, J. and Macurek, L. (2015) 'Targeting the checkpoint to kill cancer cells', *Biomolecules*. MDPI AG, pp. 1912–1937. doi: 10.3390/biom5031912.
- Bennett, C. N. *et al.* (2012) 'Cross-species genomic and functional analyses identify a combination therapy using a CHK1 inhibitor and a ribonucleotide reductase inhibitor to treat triple-negative breast cancer', *Breast Cancer Research* 2012 14:4. BioMed Central, 14(4), pp. 1–17. doi: 10.1186/BCR3230.
- Bergin, A. R. T. and Loi, S. (2019) 'Triple-negative breast cancer: recent treatment advances', *F1000Research*. Faculty of 1000 Ltd, 8. doi: 10.12688/F1000RESEARCH.18888.1.
- Bermejo, R. *et al.* (2009) 'Genome-Organizing Factors Top2 and Hmo1 Prevent Chromosome

- Fragility at Sites of S phase Transcription', *Cell*. Cell Press, 138(5), pp. 870–884. doi: 10.1016/J.CELL.2009.06.022.
- Bermejo, R. *et al.* (2011) 'The Replication Checkpoint Protects Fork Stability by Releasing Transcribed Genes from Nuclear Pores', *Cell*. Cell Press, 146(2), pp. 233–246. doi: 10.1016/J.CELL.2011.06.033.
- Bermejo, R., Lai, M. S. and Foiani, M. (2012) 'Preventing Replication Stress to Maintain Genome Stability: Resolving Conflicts between Replication and Transcription', *Molecular Cell*. Cell Press, 45(6), pp. 710–718. doi: 10.1016/J.MOLCEL.2012.03.001.
- Berthet, C. *et al.* (2006) 'Combined Loss of Cdk2 and Cdk4 Results in Embryonic Lethality and Rb Hypophosphorylation', *Developmental Cell*. Cell Press, 10(5), pp. 563–573. doi: 10.1016/J.DEVCEL.2006.03.004.
- Bertoli, C. *et al.* (2013) 'Chk1 inhibits E2F6 repressor function in response to replication stress to maintain cell-cycle transcription', *Current biology : CB*. Curr Biol, 23(17), pp. 1629–1637. doi: 10.1016/J.CUB.2013.06.063.
- Bertoli, C., Skotheim, J. M. and De Bruin, R. A. M. (2013) 'Control of cell cycle transcription during G1 and S phases', *Nature reviews. Molecular cell biology*. NIH Public Access, 14(8), p. 518. doi: 10.1038/NRM3629.
- Besteiro, M. A. G. *et al.* (2019) 'Chk1 loss creates replication barriers that compromise cell survival independently of excess origin firing', *The EMBO Journal*. John Wiley & Sons, Ltd, 38(16), p. e101284. doi: 10.15252/EMBJ.2018101284.
- Bester, A. C. *et al.* (2011) 'Nucleotide Deficiency Promotes Genomic Instability in Early Stages of Cancer Development', *Cell*. Cell Press, 145(3), pp. 435–446. doi: 10.1016/J.CELL.2011.03.044.
- Beyaert, M. *et al.* (2016) 'A crucial role for ATR in the regulation of deoxycytidine kinase activity', *Biochemical Pharmacology*. Elsevier, 100, pp. 40–50. doi: 10.1016/J.BCP.2015.11.022.
- Bhar, A. *et al.* (2013) 'Coexpression and coregulation analysis of time-series gene expression data in estrogen-induced breast cancer cell', *Algorithms for Molecular Biology : AMB*. BioMed Central, 8(1), p. 9. doi: 10.1186/1748-7188-8-9.
- Bhattacharya, A. *et al.* (2012) 'Regulation of cell cycle checkpoint kinase WEE1 by miR-195 in malignant melanoma', *Oncogene* 2013 32:26. Nature Publishing Group, 32(26), pp. 3175–3183. doi: 10.1038/onc.2012.324.
- Blasina, A. *et al.* (2008) 'Breaching the DNA damage checkpoint via PF-00477736, a novel small-molecule inhibitor of checkpoint kinase 1', *Molecular Cancer Therapeutics*. American Association for Cancer Research, 7(8), pp. 2394–2404. doi: 10.1158/1535-7163.MCT-07-2391.
- Blow, J. J., Ge, X. Q. and Jackson, D. A. (2011) 'How dormant origins promote complete genome replication', *Trends in Biochemical Sciences*. Elsevier Current Trends, 36(8), pp. 405–414. doi: 10.1016/J.TIBS.2011.05.002.
- Bochman, M. L., Paeschke, K. and Zakian, V. A. (2012) 'DNA secondary structures: stability and function of G-quadruplex structures', *Nature Reviews Genetics* 2012 13:11. Nature Publishing Group, 13(11), pp. 770–780. doi: 10.1038/nrg3296.
- Boeckemeier, L. *et al.* (2020) 'Mre11 exonuclease activity removes the chain-terminating nucleoside analog gemcitabine from the nascent strand during DNA replication', *Science Advances*. American Association for the Advancement of Science, 6(22), p. 4126. doi: 10.1126/SCIADV.AAZ4126.
- Booher, R. N., Holman, P. S. and Fattaey, A. (1997) 'Human Myt1 Is a Cell Cycle-regulated Kinase That Inhibits Cdc2 but Not Cdk2 Activity \*', *Journal of Biological Chemistry*. Elsevier, 272(35), pp. 22300–22306. doi: 10.1074/JBC.272.35.22300.
- Bradford, M. M. (1976) 'A rapid and sensitive method for the quantitation of microgram quantities of protein utilizing the principle of protein-dye binding', *Analytical Biochemistry*. Academic Press, 72(1–2), pp. 248–254. doi: 10.1016/0003-2697(76)90527-3.

Branzei, D. and Psakhye, I. (2016) 'DNA damage tolerance', *Current Opinion in Cell Biology*. Elsevier Current Trends, 40, pp. 137–144. doi: 10.1016/J.CEB.2016.03.015.

Bray, F. *et al.* (2018) 'Global cancer statistics 2018: GLOBOCAN estimates of incidence and mortality worldwide for 36 cancers in 185 countries', *CA: A Cancer Journal for Clinicians*. American Cancer Society, 68(6), pp. 394–424. doi: 10.3322/CAAC.21492.

Bressenot, A. *et al.* (2008) 'Assessment of Apoptosis by Immunohistochemistry to Active Caspase-3, Active Caspase-7, or Cleaved PARP in Monolayer Cells and Spheroid and Subcutaneous Xenografts of Human Carcinoma', <http://dx.doi.org/10.1369/jhc.2008.952044>. SAGE PublicationsSage CA: Los Angeles, CA, 57(4), pp. 289–300. doi: 10.1369/JHC.2008.952044.

Brooks, K. *et al.* (2013) 'A potent Chk1 inhibitor is selectively cytotoxic in melanomas with high levels of replicative stress', *Oncogene*. Oncogene, 32(6), pp. 788–796. doi: 10.1038/ONC.2012.72.

Bryant, C., Rawlinson, R. and Massey, A. J. (2014) 'Chk1 Inhibition as a novel therapeutic strategy for treating triple-negative breast and ovarian cancers', *BMC Cancer*. BioMed Central Ltd., 14(1), pp. 1–14. doi: 10.1186/1471-2407-14-570/FIGURES/6.

Buchanan, B. W. *et al.* (2016) 'Cycloheximide Chase Analysis of Protein Degradation in *Saccharomyces cerevisiae*', *Journal of Visualized Experiments : JoVE*. MyJoVE Corporation, 2016(110), p. 53975. doi: 10.3791/53975.

Bunch, R. T. and Eastman, A. (1996) 'Enhancement of cisplatin-induced cytotoxicity by 7-hydroxystaurosporine (UCN-01), a new G2-checkpoint inhibitor.', *Clinical Cancer Research*, 2(5).

Burrows, A. E. and Elledge, S. J. (2008) 'How ATR turns on: TopBP1 goes on ATRIP with ATR', *Genes & Development*. Cold Spring Harbor Laboratory Press, 22(11), p. 1416. doi: 10.1101/GAD.1685108.

Busby, E. C. *et al.* (2000) 'The Radiosensitizing Agent 7-Hydroxystaurosporine (UCN-01) Inhibits the DNA Damage Checkpoint Kinase hChk1 1', *CANCER RESEARCH*, 60, pp. 2108–2112.

C-L Lin, V. *et al.* (1999) 'Progestins Inhibit the Growth of MDA-MB-231 Cells Transfected with Progesterone Receptor Complementary DNA 1'.

C, G. *et al.* (2019) 'Upregulation of MGP by HOXC8 promotes the proliferation, migration, and EMT processes of triple-negative breast cancer', *Molecular carcinogenesis*. Mol Carcinog, 58(10), pp. 1863–1875. doi: 10.1002/MC.23079.

*Cancer incidence statistics | Cancer Research UK* (2017). Available at: <https://www.cancerresearchuk.org/health-professional/cancer-statistics/incidence#heading-One> (Accessed: 16 June 2020).

Capasso, H. *et al.* (2002) 'Phosphorylation activates Chk1 and is required for checkpoint-mediated cell cycle arrest', *Journal of cell science*. J Cell Sci, 115(Pt 23), pp. 4555–4564. doi: 10.1242/JCS.00133.

Carlino, M. S. *et al.* (2015) 'Preexisting MEK1P124 Mutations Diminish Response to BRAF Inhibitors in Metastatic Melanoma Patients', *Clinical Cancer Research*. American Association for Cancer Research, 21(1), pp. 98–105. doi: 10.1158/1078-0432.CCR-14-0759.

Carnevale, R. P. *et al.* (2007) 'Progestin Effects on Breast Cancer Cell Proliferation, Proteases Activation, and in Vivo Development of Metastatic Phenotype All Depend on Progesterone Receptor Capacity to Activate Cytoplasmic Signaling Pathways', *Molecular Endocrinology*. Oxford Academic, 21(6), pp. 1335–1358. doi: 10.1210/ME.2006-0304.

Carrassa, L. *et al.* (2004) 'Chk1, but not Chk2, is Involved in the Cellular Response to DNA Damaging Agents: Differential Activity in Cells Expressing, or not, p53', <http://dx.doi.org/10.4161/cc.3.9.1080>. Taylor & Francis, 3(9), pp. 1175–1179. doi: 10.4161/CC.3.9.1080.

Carrassa, L. *et al.* (2012) 'Combined inhibition of Chk1 and Wee1: In vitro synergistic effect translates to tumor growth inhibition in vivo', <http://dx.doi.org/10.4161/cc.20899>. Taylor & Francis, 11(13), pp. 2507–2517. doi: 10.4161/CC.20899.

- CC, J. *et al.* (2018) 'Altered translation initiation of Gja1 limits gap junction formation during epithelial-mesenchymal transition', *Molecular biology of the cell*. Mol Biol Cell, 29(7), pp. 797–808. doi: 10.1091/MBC.E17-06-0406.
- CH, B. *et al.* (1991) '2'-Deoxy-2'-methylenecytidine and 2'-deoxy-2',2'-difluorocytidine 5'-diphosphates: potent mechanism-based inhibitors of ribonucleotide reductase', *Journal of medicinal chemistry*. J Med Chem, 34(6), pp. 1879–1884. doi: 10.1021/JM00110A019.
- Chaudhuri, L., Vincelette, N. D., Koh, B. D., Naylor, R. M., Flatten, K. S., Peterson, K. L., McNally, A., Gojo, I., Karp, J. E., Mesa, Ruben A, *et al.* (2014) 'CHK1 and WEE1 inhibition combine synergistically to enhance therapeutic efficacy in acute myeloid leukemia ex vivo', *Haematologica*. Ferrata Storti Foundation, 99(4), p. 688. doi: 10.3324/HAEMATOL.2013.093187.
- Chaudhuri, L., Vincelette, N. D., Koh, B. D., Naylor, R. M., Flatten, K. S., Peterson, K. L., McNally, A., Gojo, I., Karp, J. E., Mesa, Ruben A., *et al.* (2014) 'CHK1 and WEE1 inhibition combine synergistically to enhance therapeutic efficacy in acute myeloid leukemia ex vivo', *Haematologica*. Ferrata Storti Foundation, 99(4), p. 688. doi: 10.3324/HAEMATOL.2013.093187.
- Chavez, K. J., Garimella, S. V. and Lipkowitz, S. (2010) 'Triple Negative Breast Cancer Cell Lines: One Tool in the Search for Better Treatment of Triple Negative Breast Cancer', *Breast disease*. NIH Public Access, 32(1–2), p. 35. doi: 10.3233/BD-2010-0307.
- Chen, C. D. *et al.* (2003) 'Molecular determinants of resistance to antiandrogen therapy', *Nature Medicine* 2004 10:1. Nature Publishing Group, 10(1), pp. 33–39. doi: 10.1038/nm972.
- Chen, F. *et al.* (2022) 'Clinical Progress of PD-1/L1 Inhibitors in Breast Cancer Immunotherapy', *Frontiers in Oncology*. Frontiers Media S.A., 11, p. 5485. doi: 10.3389/FONC.2021.724424/BIBTEX.
- Chen, X. *et al.* (2018) 'Cyclin E Overexpression Sensitizes Triple-Negative Breast Cancer to Wee1 Kinase Inhibition', *Clinical Cancer Research*. American Association for Cancer Research, 24(24), pp. 6594–6610. doi: 10.1158/1078-0432.CCR-18-1446.
- Chiker, S. *et al.* (2015) 'Cdk5 promotes DNA replication stress checkpoint activation through RPA-32 phosphorylation, and impacts on metastasis free survival in breast cancer patients', <https://doi.org/10.1080/15384101.2015.1078020>. Taylor & Francis, 14(19), pp. 3066–3078. doi: 10.1080/15384101.2015.1078020.
- Chilà, R. *et al.* (2013) 'Chk1-Mad2 interaction: A crosslink between the DNA damage checkpoint and the mitotic spindle checkpoint', *Cell Cycle*. Taylor and Francis Inc., 12(7), pp. 1083–1090. doi: 10.4161/CC.24090/SUPPL\_FILE/KCCY\_A\_10924090\_SM0001.ZIP.
- Chilà, R. *et al.* (2015) 'Combined inhibition of Chk1 and Wee1 as a new therapeutic strategy for mantle cell lymphoma', *Oncotarget*. Impact Journals, LLC, 6(5), p. 3394. doi: 10.18632/ONCOTARGET.2583.
- Chinai, J. M. *et al.* (2015) 'New immunotherapies targeting the PD-1 pathway', *Trends in Pharmacological Sciences*. Elsevier Current Trends, 36(9), pp. 587–595. doi: 10.1016/J.TIPS.2015.06.005.
- Choi, Y. L. *et al.* (2010) 'EML4-ALK Mutations in Lung Cancer That Confer Resistance to ALK Inhibitors', *New England Journal of Medicine*. New England Journal of Medicine (NEJM/MMS), 363(18), pp. 1734–1739. doi: 10.1056/NEJMOA1007478/SUPPL\_FILE/NEJMOA1007478\_DISCLOSURES.PDF.
- Chou, T. C. (2010) 'Drug Combination Studies and Their Synergy Quantification Using the Chou-Talalay Method', *Cancer Research*. American Association for Cancer Research, 70(2), pp. 440–446. doi: 10.1158/0008-5472.CAN-09-1947.
- Ciccio, A. and Elledge, S. J. (2010) 'The DNA Damage Response: Making It Safe to Play with Knives', *Molecular Cell*. Cell Press, 40(2), pp. 179–204. doi: 10.1016/J.MOLCEL.2010.09.019.
- Coelho, B. P. *et al.* (2020) 'Multifaceted WNT Signaling at the Crossroads Between Epithelial-Mesenchymal Transition and Autophagy in Glioblastoma', *Frontiers in Oncology*. Frontiers, 0, p. 2501. doi: 10.3389/FONC.2020.597743.

- Cole, K. A. *et al.* (2011) 'RNAi screen of the protein kinome identifies checkpoint kinase 1 (CHK1) as a therapeutic target in neuroblastoma', *Proceedings of the National Academy of Sciences of the United States of America*. National Academy of Sciences, 108(8), pp. 3336–3341. doi: 10.1073/PNAS.1012351108/-DCSUPPLEMENTAL.
- Converso, A. *et al.* (2009) 'Development of thioquinazolinones, allosteric Chk1 kinase inhibitors', *Bioorganic & medicinal chemistry letters*. Bioorg Med Chem Lett, 19(4), pp. 1240–1244. doi: 10.1016/J.BMCL.2008.12.076.
- Cortazar, P. *et al.* (2014) 'Pathological complete response and long-term clinical benefit in breast cancer: the CTNeoBC pooled analysis', *The Lancet*. Elsevier, 384(9938), pp. 164–172. doi: 10.1016/S0140-6736(13)62422-8.
- Cruz, C. *et al.* (2018) 'RAD51 foci as a functional biomarker of homologous recombination repair and PARP inhibitor resistance in germline BRCA-mutated breast cancer', *Annals of Oncology*. Elsevier, 29(5), pp. 1203–1210. doi: 10.1093/ANNONC/MDY099.
- Dai, Y. and Grant, S. (2010) 'New Insights into Checkpoint Kinase 1 in the DNA Damage Response Signaling Network', *Clinical Cancer Research*. American Association for Cancer Research, 16(2), pp. 376–383. doi: 10.1158/1078-0432.CCR-09-1029.
- Daigh, L. H. *et al.* (2018) 'Stochastic Endogenous Replication Stress Causes ATR-Triggered Fluctuations in CDK2 Activity that Dynamically Adjust Global DNA Synthesis Rates', *Cell Systems*. Cell Press, 7(1), pp. 17-27.e3. doi: 10.1016/J.CELS.2018.05.011.
- Dalgaard, J. Z. (2012) 'Causes and consequences of ribonucleotide incorporation into nuclear DNA', *Trends in Genetics*. Elsevier Current Trends, 28(12), pp. 592–597. doi: 10.1016/J.TIG.2012.07.008.
- Darzynkiewicz, Z. *et al.* (1996) 'Cytometry of Cyclin Proteins', *Cytometry Part A*, 25(1), pp. 1–13. doi: 10.1002/(SICI)1097-0320(19960901)25:1.
- Dasari, S. and Bernard Tchounwou, P. (2014) 'Cisplatin in cancer therapy: Molecular mechanisms of action', *European Journal of Pharmacology*. Elsevier, pp. 364–378. doi: 10.1016/j.ejphar.2014.07.025.
- Datto, M. B. *et al.* (1995) 'Transforming growth factor beta induces the cyclin-dependent kinase inhibitor p21 through a p53-independent mechanism', *Proceedings of the National Academy of Sciences*. National Academy of Sciences, 92(12), pp. 5545–5549. doi: 10.1073/PNAS.92.12.5545.
- Davidson, J. D. *et al.* (2004) 'An Increase in the Expression of Ribonucleotide Reductase Large Subunit 1 Is Associated with Gemcitabine Resistance in Non-Small Cell Lung Cancer Cell Lines', *Cancer Research*. American Association for Cancer Research, 64(11), pp. 3761–3766. doi: 10.1158/0008-5472.CAN-03-3363.
- Davies, K. D. *et al.* (2011) 'Chk1 inhibition and Wee1 inhibition combine synergistically to impede cellular proliferation View supplementary material', *Cancer Biology & Therapy*, 12, pp. 788–796. doi: 10.4161/cbt.12.9.17673.
- Debatisse, M. *et al.* (2012) 'Common fragile sites: mechanisms of instability revisited', *Trends in Genetics*. Elsevier Current Trends, 28(1), pp. 22–32. doi: 10.1016/J.TIG.2011.10.003.
- Deem, A. *et al.* (2011) 'Break-Induced Replication Is Highly Inaccurate', *PLOS Biology*. Public Library of Science, 9(2), p. e1000594. doi: 10.1371/JOURNAL.PBIO.1000594.
- Demetri, G. *et al.* (2006) 'Molecular Correlates of Imatinib Resistance in Gastrointestinal Stromal Tumors Related papers Mechanisms of resistance to imatinib mesylate in KIT-positive metastatic uveal melanoma Anne Hagemeyer Pathologic and Molecular Features Correlate With Long-Term Outcome After Adjuvant Therapy of Re... Molecular Correlates of Imatinib Resistance in Gastrointestinal Stromal Tumors', *J Clin Oncol*, 24, pp. 4764–4774. doi: 10.1200/JCO.2006.06.2265.
- Diaz, L. A. *et al.* (2012) 'The molecular evolution of acquired resistance to targeted EGFR blockade in colorectal cancers', *Nature* 2012 486:7404. Nature Publishing Group, 486(7404), pp. 537–540. doi: 10.1038/nature11219.
- Ditano, J. P. and Eastman, A. (2021) 'Comparative Activity and Off-Target Effects in Cells of the CHK1 Inhibitors MK-8776, SRA737, and LY2606368', *ACS Pharmacology and Translational Science*.



American Chemical Society, 2021, pp. 730–743. doi: 10.1021/acsptsci.0c00201.

Do, K. *et al.* (2015) 'Phase I study of single-agent AZD1775 (MK-1775), a wee1 kinase inhibitor, in patients with refractory solid tumors', *Journal of Clinical Oncology*. American Society of Clinical Oncology, 33(30), pp. 3409–3415. doi: 10.1200/JCO.2014.60.4009.

Do, K., Doroshow, J. H. and Kummar, S. (2013) 'Wee1 kinase as a target for cancer therapy', *Review Cell Cycle*, 12, pp. 3159–3164. doi: 10.4161/cc.26062.

Donjerkovic, D. and Scott, D. W. (2000) 'Regulation of the G1 phase of the mammalian cell cycle', *Cell Research 2000 10:1*. Nature Publishing Group, 10(1), pp. 1–16. doi: 10.1038/sj.cr.7290031.

Du, B. and Shim, J. S. (2016) 'Targeting Epithelial–Mesenchymal Transition (EMT) to Overcome Drug Resistance in Cancer', *Molecules 2016, Vol. 21, Page 965*. Multidisciplinary Digital Publishing Institute, 21(7), p. 965. doi: 10.3390/MOLECULES21070965.

Duan, M. *et al.* (2020) 'Role of Nucleotide Excision Repair in Cisplatin Resistance', *International Journal of Molecular Sciences 2020, Vol. 21, Page 9248*. Multidisciplinary Digital Publishing Institute, 21(23), p. 9248. doi: 10.3390/IJMS21239248.

Dungrawala, H. *et al.* (2015) 'The Replication Checkpoint Prevents Two Types of Fork Collapse without Regulating Replisome Stability', *Molecular Cell*. Cell Press, 59(6), pp. 998–1010. doi: 10.1016/J.MOLCEL.2015.07.030.

Durkin, S. G. *et al.* (2006) 'Depletion of CHK1, but not CHK2, induces chromosomal instability and breaks at common fragile sites', *Oncogene 2006 25:32*. Nature Publishing Group, 25(32), pp. 4381–4388. doi: 10.1038/sj.onc.1209466.

Ebert, P. J. R. *et al.* (2016) 'MAP Kinase Inhibition Promotes T Cell and Anti-tumor Activity in Combination with PD-L1 Checkpoint Blockade', *Immunity*. Cell Press, 44(3), pp. 609–621. doi: 10.1016/J.IMMUNI.2016.01.024.

Edmunds, C. E., Simpson, L. J. and Sale, J. E. (2008) 'PCNA ubiquitination and REV1 define temporally distinct mechanisms for controlling translesion synthesis in the avian cell line DT40', *Molecular cell*. Mol Cell, 30(4), pp. 519–529. doi: 10.1016/J.MOLCEL.2008.03.024.

Edwards, S. L. *et al.* (2008) 'Resistance to therapy caused by intragenic deletion in BRCA2', *Nature 2008 451:7182*. Nature Publishing Group, 451(7182), pp. 1111–1115. doi: 10.1038/nature06548.

EJ, H. *et al.* (2019) 'CADM1 is a TWIST1-regulated suppressor of invasion and survival', *Cell death & disease*. Cell Death Dis, 10(4). doi: 10.1038/S41419-019-1515-3.

Elango, R. *et al.* (2017) 'Break-induced replication promotes formation of lethal joint molecules dissolved by Srs2', *Nature Communications 2017 8:1*. Nature Publishing Group, 8(1), pp. 1–13. doi: 10.1038/s41467-017-01987-2.

Elbæk, C. R., Petrosius, V. and Sørensen, C. S. (2020) 'WEE1 kinase limits CDK activities to safeguard DNA replication and mitotic entry', *Mutation research*. Mutat Res, 819–820. doi: 10.1016/J.MRFMMM.2020.111694.

Elvers, I. *et al.* (2011) 'UV stalled replication forks restart by re-priming in human fibroblasts', *Nucleic Acids Research*. Oxford Academic, 39(16), pp. 7049–7057. doi: 10.1093/NAR/GKR420.

Van Emburgh, B. O. *et al.* (2016) 'Acquired RAS or EGFR mutations and duration of response to EGFR blockade in colorectal cancer', *Nature Communications 2016 7:1*. Nature Publishing Group, 7(1), pp. 1–9. doi: 10.1038/ncomms13665.

Emery, C. M. *et al.* (2009) 'MEK1 mutations confer resistance to MEK and B-Raf inhibition', *Proceedings of the National Academy of Sciences*. National Academy of Sciences, 106(48), pp. 20411–20416. doi: 10.1073/PNAS.0905833106.

Engelman, J. A. *et al.* (2007) 'MET amplification leads to gefitinib resistance in lung cancer by activating ERBB3 signaling', *Science*. American Association for the Advancement of Science, 316(5827), pp. 1039–1043. doi: 10.1126/SCIENCE.1141478/SUPPL\_FILE/PAP.PDF.

Enomoto, M. *et al.* (2009) 'Novel positive feedback loop between Cdk1 and Chk1 in the nucleus

during G2/M transition', *The Journal of biological chemistry*. J Biol Chem, 284(49), pp. 34223–34230. doi: 10.1074/JBC.C109.051540.

Errico, A. and Costanzo, V. (2012) 'Mechanisms of replication fork protection: a safeguard for genome stability', *Critical reviews in biochemistry and molecular biology*. Crit Rev Biochem Mol Biol, 47(3), pp. 222–235. doi: 10.3109/10409238.2012.655374.

Evans, T. *et al.* (1983) 'Cyclin: A protein specified by maternal mRNA in sea urchin eggs that is destroyed at each cleavage division', *Cell*. Cell Press, 33(2), pp. 389–396. doi: 10.1016/0092-8674(83)90420-8.

F, L. *et al.* (2020) 'TNFRSF11B activates Wnt/ $\beta$ -catenin signaling and promotes gastric cancer progression', *International journal of biological sciences*. Int J Biol Sci, 16(11), pp. 1956–1971. doi: 10.7150/IJBS.43630.

F, Z. *et al.* (2015) 'HtrA1 regulates epithelial-mesenchymal transition in hepatocellular carcinoma', *Biochemical and biophysical research communications*. Biochem Biophys Res Commun, 467(3), pp. 589–594. doi: 10.1016/J.BBRC.2015.09.105.

Falck, J. *et al.* (2002) 'The DNA damage-dependent intra-S phase checkpoint is regulated by parallel pathways', *Nature Genetics* 2002 30:3. Nature Publishing Group, 30(3), pp. 290–294. doi: 10.1038/ng845.

Fazilaty, H. *et al.* (2019) 'A gene regulatory network to control EMT programs in development and disease', *Nature Communications* 2019 10:1. Nature Publishing Group, 10(1), pp. 1–16. doi: 10.1038/s41467-019-13091-8.

Feijoo, C. *et al.* (2001) 'Activation of mammalian Chk1 during DNA replication arrest: a role for Chk1 in the intra-S phase checkpoint monitoring replication origin firing', *The Journal of cell biology*. J Cell Biol, 154(5), pp. 913–923. doi: 10.1083/JCB.200104099.

Ferrao, P. T. *et al.* (2011) 'Efficacy of CHK inhibitors as single agents in MYC-driven lymphoma cells', *Oncogene* 2012 31:13. Nature Publishing Group, 31(13), pp. 1661–1672. doi: 10.1038/onc.2011.358.

Filipits, M. (2004) 'Mechanisms of cancer: multidrug resistance', *Drug Discovery Today: Disease Mechanisms*. Elsevier, 1(2), pp. 229–234. doi: 10.1016/J.DDMEC.2004.10.001.

Flatten, K. *et al.* (2005) 'The Role of Checkpoint Kinase 1 in Sensitivity to Topoisomerase I Poisons \*', *Journal of Biological Chemistry*. Elsevier, 280(14), pp. 14349–14355. doi: 10.1074/JBC.M411890200.

Forment, J. V. *et al.* (2011) 'Structure-specific DNA endonuclease Mus81/Eme1 generates DNA damage caused by Chk1 inactivation', *PLoS one*. PLoS One, 6(8). doi: 10.1371/JOURNAL.PONE.0023517.

Foskolou, I. P. *et al.* (2017) 'Ribonucleotide Reductase Requires Subunit Switching in Hypoxia to Maintain DNA Replication', *Molecular Cell*. Cell Press, 66(2), pp. 206–220.e9. doi: 10.1016/J.MOLCEL.2017.03.005.

Foskolou, I. P. and Hammond, E. M. (2017) 'RRM2B: An oxygen-requiring protein with a role in hypoxia', *Molecular & cellular oncology*. Mol Cell Oncol, 4(5). doi: 10.1080/23723556.2017.1335272.

Fragkos, M. *et al.* (2015) 'DNA replication origin activation in space and time', *Nature Reviews Molecular Cell Biology* 2015 16:6. Nature Publishing Group, 16(6), pp. 360–374. doi: 10.1038/nrm4002.

Freedman, G. M. *et al.* (2009) 'Locoregional recurrence of triple-negative breast cancer after breast-conserving surgery and radiation', *Cancer*. Cancer, 115(5), pp. 946–951. doi: 10.1002/CNCR.24094.

Fry, D. W. *et al.* (2004) 'Specific inhibition of cyclin-dependent kinase 4/6 by PD 0332991 and associated antitumor activity in human tumor xenografts', *Molecular Cancer Therapeutics*, pp. 1427–1437.

Fu, W. *et al.* (2019) 'The effect of miR-124-3p on cell proliferation and apoptosis in bladder cancer by targeting EDNRB', *Archives of Medical Science : AMS*. Termedia Publishing, 15(5), p. 1154. doi: 10.5114/AOMS.2018.78743.

- Fujii, W. *et al.* (2011) 'CDK7 and CCNH Are Components of CDK-Activating Kinase and Are Required for Meiotic Progression of Pig Oocytes', *Biology of Reproduction*. Oxford Academic, 85(6), pp. 1124–1132. doi: 10.1095/BIOLREPROD.111.091801.
- Gabrielli, B. G. *et al.* (1992) 'Cdc25 regulates the phosphorylation and activity of the Xenopus cdk2 protein kinase complex.', *Journal of Biological Chemistry*. Elsevier, 267(25), pp. 18040–18046. doi: 10.1016/S0021-9258(19)37149-2.
- Gaillard, H., García-Muse, T. and Aguilera, A. (2015) 'Replication stress and cancer', *Nature Reviews Cancer* 2015 15:5. Nature Publishing Group, 15(5), pp. 276–289. doi: 10.1038/nrc3916.
- Ganzinelli, M. *et al.* (2008) 'Checkpoint kinase 1 down-regulation by an inducible small interfering RNA expression system sensitized in vivo tumors to treatment with 5-fluorouracil', *Clinical cancer research : an official journal of the American Association for Cancer Research*. Clin Cancer Res, 14(16), pp. 5131–5141. doi: 10.1158/1078-0432.CCR-08-0304.
- Garcia, T. B. *et al.* (2020) 'Increased HDAC Activity and c-MYC Expression Mediate Acquired Resistance to WEE1 Inhibition in Acute Leukemia', *Frontiers in Oncology*. Frontiers Media S.A., 10. doi: 10.3389/fonc.2020.00296.
- Garraway, L. A. and Jänne, P. A. (2012) 'Circumventing cancer drug resistance in the era of personalized medicine', *Cancer Discovery*. American Association for Cancer Research, pp. 214–226. doi: 10.1158/2159-8290.CD-12-0012.
- Garrett, M. D. and Collins, I. (2011) 'Anticancer therapy with checkpoint inhibitors: what, where and when?', *Trends in Pharmacological Sciences*. Elsevier Current Trends, 32(5), pp. 308–316. doi: 10.1016/J.TIPS.2011.02.014.
- Garrido-Castro, A. C., Lin, N. U. and Polyak, K. (2019) 'Insights into molecular classifications of triple-negative breast cancer: improving patient selection for treatment', *Cancer discovery*. NIH Public Access, 9(2), p. 176. doi: 10.1158/2159-8290.CD-18-1177.
- Gasca, J. *et al.* (2020) 'EDIL3 promotes epithelial–mesenchymal transition and paclitaxel resistance through its interaction with integrin  $\alpha V\beta 3$  in cancer cells', *Cell Death Discovery* 2020 6:1. Nature Publishing Group, 6(1), pp. 1–14. doi: 10.1038/s41420-020-00322-x.
- Gautam, A., Li, Z. R. and Bepler, G. (2003) 'RRM1-induced metastasis suppression through PTEN-regulated pathways', *Oncogene* 2003 22:14. Nature Publishing Group, 22(14), pp. 2135–2142. doi: 10.1038/sj.onc.1206232.
- Ge, X. Q. and Blow, J. J. (2010) 'Chk1 inhibits replication factory activation but allows dormant origin firing in existing factories', *The Journal of Cell Biology*. The Rockefeller University Press, 191(7), p. 1285. doi: 10.1083/JCB.201007074.
- Ge, X. Q., Jackson, D. A. and Blow, J. J. (2007) 'Dormant origins licensed by excess Mcm2-7 are required for human cells to survive replicative stress', *Genes & development*. Genes Dev, 21(24), pp. 3331–3341. doi: 10.1101/GAD.457807.
- Giacinti, C. and Giordano, A. (2006) 'RB and cell cycle progression', *Oncogene* 2006 25:38. Nature Publishing Group, 25(38), pp. 5220–5227. doi: 10.1038/sj.onc.1209615.
- Gillet, J. P. and Gottesman, M. M. (2010) 'Mechanisms of Multidrug Resistance in Cancer', *Methods in molecular biology (Clifton, N.J.)*. Humana Press, 596, pp. 47–76. doi: 10.1007/978-1-60761-416-6\_4.
- Giono, L. E. and Manfredi, J. J. (2006) 'The p53 tumor suppressor participates in multiple cell cycle checkpoints', *Journal of Cellular Physiology*. John Wiley & Sons, Ltd, 209(1), pp. 13–20. doi: 10.1002/JCP.20689.
- Girard, F. *et al.* (1991) 'Cyclin A is required for the onset of DNA replication in mammalian fibroblasts', *Cell*. Cell, 67(6), pp. 1169–1179. doi: 10.1016/0092-8674(91)90293-8.
- Girotti, M. R. *et al.* (2013) 'Inhibiting EGF Receptor or SRC Family Kinase Signaling Overcomes BRAF Inhibitor Resistance in Melanoma', *Cancer Discovery*. American Association for Cancer Research, 3(2), pp. 158–167. doi: 10.1158/2159-8290.CD-12-0386.

González Besteiro, M. A. and Gottifredi, V. (2015) 'The fork and the kinase: A DNA replication tale from a CHK1 perspective', *Mutation Research/Reviews in Mutation Research*. Elsevier, 763, pp. 168–180. doi: 10.1016/J.MRREV.2014.10.003.

Gorre, M. E. *et al.* (2001) 'Clinical resistance to STI-571 cancer therapy caused by BCR-ABL gene mutation or amplification', *Science*. American Association for the Advancement of Science, 293(5531), pp. 876–880. doi: 10.1126/SCIENCE.1062538/SUPPL\_FILE/PAP.PDF.

Gottesman, M. M., Fojo, T. and Bates, S. E. (2002) 'Multidrug resistance in cancer: role of ATP-dependent transporters', *Nature Reviews Cancer* 2002 2:1. Nature Publishing Group, 2(1), pp. 48–58. doi: 10.1038/nrc706.

GSEA: Gene set M5930 (2021). Available at: [https://www.gsea-msigdb.org/gsea/msigdb/cards/HALLMARK\\_EPITHELIAL\\_MESENCHYMAL\\_TRANSITION.html](https://www.gsea-msigdb.org/gsea/msigdb/cards/HALLMARK_EPITHELIAL_MESENCHYMAL_TRANSITION.html) (Accessed: 12 December 2021).

Gu, Y., Turck, C. W. and Morgan, D. O. (1993) 'Inhibition of CDK2 activity in vivo by an associated 20K regulatory subunit', *Nature* 1993 366:6456. Nature Publishing Group, 366(6456), pp. 707–710. doi: 10.1038/366707a0.

Guardavaccaro, D. and Pagano, M. (2006) 'Stabilizers and Destabilizers Controlling Cell Cycle Oscillators', *Molecular Cell*. Elsevier, 22(1), pp. 1–4. doi: 10.1016/J.MOLCEL.2006.03.017.

Guertin, A. D. *et al.* (2012) 'Unique functions of CHK1 and WEE1 underlie synergistic anti-tumor activity upon pharmacologic inhibition', *Cancer Cell International*. BioMed Central, 12(1), pp. 1–12. doi: 10.1186/1475-2867-12-45/FIGURES/8.

Guertin, A. D. *et al.* (2013) 'Preclinical Evaluation of the WEE1 Inhibitor MK-1775 as Single-Agent Anticancer Therapy', *Molecular Cancer Therapeutics*. American Association for Cancer Research, 12(8), pp. 1442–1452. doi: 10.1158/1535-7163.MCT-13-0025.

Guix, M. *et al.* (2008) 'Acquired resistance to EGFR tyrosine kinase inhibitors in cancer cells is mediated by loss of IGF-binding proteins', *The Journal of Clinical Investigation*. American Society for Clinical Investigation, 118(7), pp. 2609–2619. doi: 10.1172/JCI34588.

Guo, C. *et al.* (2015) 'Interaction of Chk1 with Treslin Negatively Regulates the Initiation of Chromosomal DNA Replication', *Molecular Cell*. Cell Press, 57(3), pp. 492–505. doi: 10.1016/J.MOLCEL.2014.12.003.

Gurpinar, E. and Vousden, K. H. (2015) 'Hitting cancers' weak spots: Vulnerabilities imposed by p53 mutation', *Trends in Cell Biology*. Elsevier Ltd, pp. 486–495. doi: 10.1016/j.tcb.2015.04.001.

Hakem, R. (2008) 'DNA-damage repair; the good, the bad, and the ugly', *The EMBO Journal*. European Molecular Biology Organization, 27(4), p. 589. doi: 10.1038/EMBOJ.2008.15.

Halazonetis, T. D., Gorgoulis, V. G. and Bartek, J. (2008) 'An oncogene-induced DNA damage model for cancer development', *Science*. American Association for the Advancement of Science, 319(5868), pp. 1352–1355. doi: 10.1126/SCIENCE.1140735/SUPPL\_FILE/HALAZONETIS.SOM.PDF.

Hanahan, D. and Weinberg, R. A. (2000) 'The hallmarks of cancer', *Cell*. Elsevier, pp. 57–70. doi: 10.1016/S0092-8674(00)81683-9.

Hanahan, D. and Weinberg, R. A. (2011) 'Hallmarks of cancer: the next generation.', *Cell*. Elsevier, 144(5), pp. 646–74. doi: 10.1016/j.cell.2011.02.013.

Hartwell, L. (1992) 'Defects in a cell cycle checkpoint may be responsible for the genomic instability of cancer cells', *Cell*. Elsevier, 71(4), pp. 543–546. doi: 10.1016/0092-8674(92)90586-2.

Hata, A. N. *et al.* (2016) 'Tumor cells can follow distinct evolutionary paths to become resistant to epidermal growth factor receptor inhibition', *Nature Medicine* 2016 22:3. Nature Publishing Group, 22(3), pp. 262–269. doi: 10.1038/nm.4040.

Hauge, S. *et al.* (2017) *Combined inhibition of Wee1 and Chk1 gives synergistic DNA damage in S-phase due to distinct regulation of CDK activity and CDC45 loading*, *Oncotarget*. Available at:

www.impactjournals.com/oncotarget/ (Accessed: 9 September 2019).

Heald, R., McLoughlin, M. and McKeon, F. (1993) 'Human wee1 maintains mitotic timing by protecting the nucleus from cytoplasmically activated cdc2 kinase', *Cell*. Cell Press, 74(3), pp. 463–474. doi: 10.1016/0092-8674(93)80048-J.

Heinemann, V. and Plunkett, W. (1989) 'Modulation of deoxynucleotide metabolism by the deoxycytidylate deaminase inhibitor 3,4,5,6-tetrahydrodeoxyuridine', *Biochemical Pharmacology*, 38(22), pp. 4115–4121. doi: 10.1016/0006-2952(89)90693-X.

Heller, R. C. *et al.* (2011) 'Eukaryotic origin-dependent DNA replication in vitro reveals sequential action of DDK and S-CDK kinases', *Cell*. Cell, 146(1), pp. 80–91. doi: 10.1016/J.CELL.2011.06.012.

Hertel, L. W. *et al.* (1989) '2', 2'-difluorodeoxycytidine metabolism and mechanism of action in human leukemia cells', *Nucleosides and Nucleotides*, 8(5–6), pp. 775–785. doi: 10.1080/07328318908054215.

Van Den Heuvel-Eibrink, M. M., Sonneveld, P. and Pieters, R. (2000) 'The prognostic significance of membrane transport-associated multidrug resistance (MDR) proteins in leukemia.', *International Journal of Clinical Pharmacology and Therapeutics*. Dustri-Verlag Dr. Karl Feistle, 38(3), pp. 94–110. doi: 10.5414/CPP38094.

Hill, R. *et al.* (2008) 'p53 binding to the p21 promoter is dependent on the nature of DNA damage', <http://dx.doi.org/10.4161/cc.7.16.6440>. Taylor & Francis, 7(16), pp. 2535–2543. doi: 10.4161/CC.7.16.6440.

Hills, S. A. and Diffley, J. F. X. (2014) 'DNA Replication and Oncogene-Induced Replicative Stress', *Current Biology*. Cell Press, 24(10), pp. R435–R444. doi: 10.1016/J.CUB.2014.04.012.

Hirai, H. *et al.* (2009) 'Small-molecule inhibition of Wee1 kinase by MK-1775 selectively sensitizes p53-deficient tumor cells to DNA-damaging agents', *Molecular Cancer Therapeutics*. American Association for Cancer Research, 8(11), pp. 2992–3000. doi: 10.1158/1535-7163.MCT-09-0463.

Hirai, H. *et al.* (2010) 'MK-1775, a small molecule Wee1 inhibitor, enhances antitumor efficacy of various DNA-damaging agents, including 5-fluorouracil', *Cancer Biology and Therapy*. Landes Bioscience, 9(7), pp. 514–522. doi: 10.4161/cbt.9.7.11115.

Holohan, C. *et al.* (2013) 'Cancer drug resistance: An evolving paradigm', *Nature Reviews Cancer*. Nature Publishing Group, pp. 714–726. doi: 10.1038/nrc3599.

Home - *ClinicalTrials.gov* (no date). Available at: <https://clinicaltrials.gov/> (Accessed: 1 December 2021).

Huang, X. *et al.* (2019) 'Circular RNA AKT3 upregulates PIK3R1 to enhance cisplatin resistance in gastric cancer via miR-198 suppression', *Molecular Cancer*. BioMed Central, 18(1). doi: 10.1186/S12943-019-0969-3.

Hughes, Bridget T. *et al.* (2013) 'Essential role for Cdk2 inhibitory phosphorylation during replication stress revealed by a human Cdk2 knockin mutation', *Proceedings of the National Academy of Sciences of the United States of America*. National Academy of Sciences, 110(22), p. 8954. doi: 10.1073/PNAS.1302927110.

Hughes, Bridget T *et al.* (2013) 'Essential role for Cdk2 inhibitory phosphorylation during replication stress revealed by a human Cdk2 knockin mutation', 110(22). doi: 10.1073/pnas.1302927110.

Ibarra, A., Schwob, E. and Méndez, J. (2008) 'Excess MCM proteins protect human cells from replicative stress by licensing backup origins of replication', *Proceedings of the National Academy of Sciences of the United States of America*. Proc Natl Acad Sci U S A, 105(26), pp. 8956–8961. doi: 10.1073/PNAS.0803978105.

Ilves, I. *et al.* (2010) 'Activation of the MCM2-7 helicase by association with Cdc45 and GINS proteins', *Molecular cell*. Mol Cell, 37(2), pp. 247–258. doi: 10.1016/J.MOLCEL.2009.12.030.

Ismail-Khan, R. and Bui, M. M. (2010) 'A review of triple-negative breast cancer', *Cancer Control*. H. Lee Moffitt Cancer Center and Research Institute, 17(3), pp. 173–176. doi:

10.1177/107327481001700305.

Iyer, D. R. and Rhind, N. (2017) 'The Intra-S Checkpoint Responses to DNA Damage', *Genes*. Multidisciplinary Digital Publishing Institute (MDPI), 8(2). doi: 10.3390/GENES8020074.

J, P. *et al.* (2011) 'WEE1 inhibition sensitizes osteosarcoma to radiotherapy', *BMC cancer*. BMC Cancer, 11. doi: 10.1186/1471-2407-11-156.

J, R. (2007) 'Cdc25 phosphatases: structure, specificity, and mechanism', *Biochemistry*. Biochemistry, 46(12), pp. 3595–3604. doi: 10.1021/BI700026J.

J, X., S, L. and R, D. (2009) 'TGF-beta-induced epithelial to mesenchymal transition', *Cell research*. Cell Res, 19(2), pp. 156–172. doi: 10.1038/CR.2009.5.

Janssen, A. *et al.* (2011) 'Chromosome segregation errors as a cause of DNA damage and structural chromosome aberrations', *Science (New York, N.Y.)*. Science, 333(6051), pp. 1895–1898. doi: 10.1126/SCIENCE.1210214.

Jiang, K. *et al.* (2003) 'Regulation of Chk1 includes chromatin association and 14-3-3 binding following phosphorylation on Ser-345', *The Journal of biological chemistry*. J Biol Chem, 278(27), pp. 25207–25217. doi: 10.1074/JBC.M300070200.

Jiang, Y. *et al.* (2009) 'Common fragile sites are characterized by histone hypoacetylation', *Human Molecular Genetics*. Oxford Academic, 18(23), pp. 4501–4512. doi: 10.1093/HMG/DDP410.

Jin, L. *et al.* (2018) 'MAST1 Drives Cisplatin Resistance in Human Cancers by Rewiring cRaf-Independent MEK Activation', *Cancer Cell*. Cell Press, 34(2), pp. 315-330.e7. doi: 10.1016/j.ccell.2018.06.012.

Johannessen, C. M. *et al.* (2013) 'A melanocyte lineage program confers resistance to MAP kinase pathway inhibition', *Nature* 2013 504:7478. Nature Publishing Group, 504(7478), pp. 138–142. doi: 10.1038/nature12688.

Jones, R. M. *et al.* (2012) 'Increased replication initiation and conflicts with transcription underlie Cyclin E-induced replication stress', *Oncogene* 2013 32:32. Nature Publishing Group, 32(32), pp. 3744–3753. doi: 10.1038/onc.2012.387.

JW, Y. (1992) 'Mechanism of action of hydroxyurea.', *Seminars in Oncology*, 19(3 Suppl 9), pp. 1–10. Available at: <https://europepmc.org/article/med/1641648> (Accessed: 26 October 2021).

K, M. *et al.* (2016) 'Development of ASG-15ME, a Novel Antibody-Drug Conjugate Targeting SLITRK6, a New Urothelial Cancer Biomarker', *Molecular cancer therapeutics*. Mol Cancer Ther, 15(6), pp. 1301–1310. doi: 10.1158/1535-7163.MCT-15-0570.

Kagawa, S. *et al.* (1997) 'p53 expression overcomes p21WAF1/CIP1-mediated G1 arrest and induces apoptosis in human cancer cells', *Oncogene*. Nature Publishing Group, 15(16), pp. 1903–1909. doi: 10.1038/sj.onc.1201362.

Kalluri, R. and Neilson, E. G. (2003) 'Epithelial-mesenchymal transition and its implications for fibrosis', *The Journal of Clinical Investigation*. American Society for Clinical Investigation, 112(12), pp. 1776–1784. doi: 10.1172/JCI20530.

Kalluri, R. and Weinberg, R. A. (2009) 'The basics of epithelial-mesenchymal transition', *The Journal of Clinical Investigation*. American Society for Clinical Investigation, 119(6), p. 1420. doi: 10.1172/JCI39104.

Karnitz, L. M. *et al.* (2005) 'Gemcitabine-Induced Activation of Checkpoint Signaling Pathways That Affect Tumor Cell Survival', *Molecular Pharmacology*. American Society for Pharmacology and Experimental Therapeutics, 68(6), pp. 1636–1644. doi: 10.1124/MOL.105.012716.

Kasahara, K. *et al.* (2010) '14-3-3gamma mediates Cdc25A proteolysis to block premature mitotic entry after DNA damage', *The EMBO journal*. EMBO J, 29(16), pp. 2802–2812. doi: 10.1038/EMBOJ.2010.157.

Kastan, M. B. and Bartek, J. (2004) 'Cell-cycle checkpoints and cancer', *Nature* 2004 432:7015. Nature Publishing Group, 432(7015), pp. 316–323. doi: 10.1038/nature03097.

- Katsuragi, Y. and Sagata, N. (2004) 'Regulation of Chk1 kinase by autoinhibition and ATR-mediated phosphorylation', *Molecular biology of the cell*. Mol Biol Cell, 15(4), pp. 1680–1689. doi: 10.1091/MBC.E03-12-0874.
- Kawabata, T. *et al.* (2011) 'Stalled Fork Rescue via Dormant Replication Origins in Unchallenged S Phase Promotes Proper Chromosome Segregation and Tumor Suppression', *Molecular Cell*. Cell Press, 41(5), pp. 543–553. doi: 10.1016/J.MOLCEL.2011.02.006.
- Kemp, M. G. *et al.* (2010) 'Tipin-Replication Protein A Interaction Mediates Chk1 Phosphorylation by ATR in Response to Genotoxic Stress \*', *Journal of Biological Chemistry*. Elsevier, 285(22), pp. 16562–16571. doi: 10.1074/JBC.M110.110304.
- King, C., Diaz, H. B., *et al.* (2015) 'LY2606368 causes replication catastrophe and antitumor effects through CHK1-dependent mechanisms', *Molecular Cancer Therapeutics*. American Association for Cancer Research Inc., 14(9), pp. 2004–2013. doi: 10.1158/1535-7163.MCT-14-1037.
- King, C., Diaz, H Bruce, *et al.* (2015) 'LY2606368 Causes Replication Catastrophe and Antitumor Effects through CHK1-Dependent Mechanisms', *Molecular Cancer Therapeutics*, 14(9), pp. 2004–2013. doi: 10.1158/1535-7163.MCT-14-1037.
- Kivinen, L. *et al.* (1999) 'Ras induces p21Cip1/Waf1 cyclin kinase inhibitor transcriptionally through Sp1-binding sites', *Oncogene* 1999 18:46. Nature Publishing Group, 18(46), pp. 6252–6261. doi: 10.1038/sj.onc.1203000.
- Ko, L. J. and Prives, C. (1996) 'p53: puzzle and paradigm', *Genes & Development*, 10, pp. 1054–1072.
- Kobayashi, S. *et al.* (2009) 'EGFR Mutation and Resistance of Non–Small-Cell Lung Cancer to Gefitinib', <http://dx.doi.org/10.1056/NEJMoa044238>. Massachusetts Medical Society , 352(8), pp. 786–792. doi: 10.1056/NEJMoa044238.
- Koboldt, D. C. *et al.* (2012) 'Comprehensive molecular portraits of human breast tumours', *Nature*. Nature, 490(7418), pp. 61–70. doi: 10.1038/NATURE11412.
- Koh, S.-B. *et al.* (2015) 'Therapeutics, Targets, and Chemical Biology CHK1 Inhibition Synergizes with Gemcitabine Initially by Destabilizing the DNA Replication Apparatus'. doi: 10.1158/0008-5472.CAN-14-3347.
- Köhler, C. *et al.* (2016) 'Cdc45 is limiting for replication initiation in humans', *Cell Cycle*. Taylor and Francis Inc., 15(7), pp. 974–985. doi: 10.1080/15384101.2016.1152424/SUPPL\_FILE/KCCY\_A\_1152424\_SM8211.ZIP.
- Kohn, E. A. *et al.* (2002) 'Abrogation of the S Phase DNA Damage Checkpoint Results in S Phase Progression or Premature Mitosis Depending on the Concentration of 7-Hydroxystaurosporine and the Kinetics of Cdc25C Activation \*', *Journal of Biological Chemistry*. Elsevier, 277(29), pp. 26553–26564. doi: 10.1074/JBC.M202040200.
- Konieczkowski, David J, Johannessen, C. M. and Garraway, L. A. (2018) 'A Convergence-Based Framework for Cancer Drug Resistance.', *Cancer cell*. Elsevier, 33(5), pp. 801–815. doi: 10.1016/j.ccell.2018.03.025.
- Konieczkowski, David J., Johannessen, C. M. and Garraway, L. A. (2018) 'A Convergence-Based Framework for Cancer Drug Resistance', *Cancer Cell*. Cell Press, 33(5), pp. 801–815. doi: 10.1016/J.CCELL.2018.03.025.
- Koppenhafer, S. L. *et al.* (2020) 'Inhibition of the ATR–CHK1 Pathway in Ewing Sarcoma Cells Causes DNA Damage and Apoptosis via the CDK2-Mediated Degradation of RRM2', *Molecular Cancer Research*. American Association for Cancer Research, 18(1), pp. 91–104. doi: 10.1158/1541-7786.MCR-19-0585.
- Kosoy, A. and O'Connell, M. J. (2008) 'Regulation of Chk1 by Its C-terminal Domain', *Molecular Biology of the Cell*. American Society for Cell Biology, 19(11), p. 4546. doi: 10.1091/MBC.E08-04-0444.
- Kreahling, J. M. *et al.* (2012) 'MK1775, a Selective Wee1 Inhibitor, Shows Single-Agent Antitumor

Activity against Sarcoma Cells', *Molecular Cancer Therapeutics*. American Association for Cancer Research, 11(1), pp. 174–182. doi: 10.1158/1535-7163.MCT-11-0529.

Kukurba, K. R. and Montgomery, S. B. (2015) 'RNA Sequencing and Analysis', *Cold Spring Harbor Protocols*. Cold Spring Harbor Laboratory Press, 2015(11), p. pdb.top084970. doi: 10.1101/PDB.TOP084970.

Kumagai, A. *et al.* (2010) 'Treslin collaborates with TopBP1 in triggering the initiation of DNA replication', *Cell*. Cell, 140(3), pp. 349–359. doi: 10.1016/J.CELL.2009.12.049.

Kumagai, A. and Dunphy, W. G. (2000) 'Claspin, a Novel Protein Required for the Activation of Chk1 during a DNA Replication Checkpoint Response in Xenopus Egg Extracts', *Molecular Cell*. Cell Press, 6(4), pp. 839–849. doi: 10.1016/S1097-2765(05)00092-4.

Kumagai, A. and Dunphy, W. G. (2003) 'Repeated phosphopeptide motifs in Claspin mediate the regulated binding of Chk1', *Nature Cell Biology* 2003 5:2. Nature Publishing Group, 5(2), pp. 161–165. doi: 10.1038/ncb921.

Kumar, P. and Aggarwal, R. (2015) 'An overview of triple-negative breast cancer', *Archives of Gynecology and Obstetrics* 2015 293:2. Springer, 293(2), pp. 247–269. doi: 10.1007/S00404-015-3859-Y.

Kummar, S. *et al.* (2012) 'Advances in using PARP inhibitors to treat cancer', *BMC Medicine*. BioMed Central, p. 25. doi: 10.1186/1741-7015-10-25.

Kwei, K. A. *et al.* (2010) 'Genomic instability in breast cancer: Pathogenesis and clinical implications', *Molecular Oncology*. No longer published by Elsevier, 4(3), pp. 255–266. doi: 10.1016/J.MOLONC.2010.04.001.

Lambert, S. and Carr, A. M. (no date) 'Impediments to replication fork movement: stabilisation, reactivation and genome instability'. doi: 10.1007/s00412-013-0398-9.

Lang, K. S. and Merrikh, H. (2021) 'Topological stress is responsible for the detrimental outcomes of head-on replication-transcription conflicts', *Cell Reports*. Cell Press, 34(9), p. 108797. doi: 10.1016/J.CELREP.2021.108797.

Lee, J., Kumagai, A. and Dunphy, W. G. (2001) 'Positive Regulation of Wee1 by Chk1 and 14-3-3 Proteins', *Molecular Biology of the Cell*. American Society for Cell Biology, 12(3), p. 551. doi: 10.1091/MBC.12.3.551.

Lee, K. J. *et al.* (2020) 'EGFR signaling promotes resistance to CHK1 inhibitor prexasertib in triple negative breast cancer', *Cancer Drug Resistance*. OAE Publishing Inc., 3(4), pp. 980–991. doi: 10.20517/CDR.2020.73.

Lehmann, A. R. and Fuchs, R. P. (2006) 'Gaps and forks in DNA replication: Rediscovering old models', *DNA repair*. DNA Repair (Amst), 5(12), pp. 1495–1498. doi: 10.1016/J.DNAREP.2006.07.002.

Leijen, S., Van Geel, R. M. J. M., Pavlick, A. C., *et al.* (2016) 'Phase I study evaluating WEE1 inhibitor AZD1775 as monotherapy and in combination with gemcitabine, cisplatin, or carboplatin in patients with advanced solid tumors', *Journal of Clinical Oncology*, 34(36). doi: 10.1200/JCO.2016.67.5991.

Leijen, S., Van Geel, R. M. J. M., Sonke, G. S., *et al.* (2016) 'Phase II study of WEE1 inhibitor AZD1775 plus carboplatin in patients with tp53-mutated ovarian cancer refractory or resistant to first-line therapy within 3 months', *Journal of Clinical Oncology*, 34(36). doi: 10.1200/JCO.2016.67.5942.

LeTallec, B. *et al.* (2013) 'Common Fragile Site Profiling in Epithelial and Erythroid Cells Reveals that Most Recurrent Cancer Deletions Lie in Fragile Sites Hosting Large Genes', *Cell Reports*. Cell Press, 4(3), pp. 420–428. doi: 10.1016/J.CELREP.2013.07.003.

Leung-Pineda, V., Ryan, C. E. and Piwnica-Worms, H. (2006) 'Phosphorylation of Chk1 by ATR is antagonized by a Chk1-regulated protein phosphatase 2A circuit', *Molecular and cellular biology*. Mol Cell Biol, 26(20), pp. 7529–7538. doi: 10.1128/MCB.00447-06.

Van Leung-Pineda, Huh, J. and Piwnica-Worms, H. (2009) 'DDB1 targets Chk1 to the Cul4 E3 ligase



complex in normal cycling cells and in cells experiencing replication stress', *Cancer research*. Cancer Res, 69(6), pp. 2630–2637. doi: 10.1158/0008-5472.CAN-08-3382.

Levesque, A. A. *et al.* (2005) 'Distinct roles for p53 transactivation and repression in preventing UCN-01-mediated abrogation of DNA damage-induced arrest at S and G2 cell cycle checkpoints', *Oncogene*. Nature Publishing Group, 24(23), pp. 3786–3796. doi: 10.1038/sj.onc.1208451.

Levine, A. J. (1997) 'p53, the Cellular Gatekeeper Review for Growth and Division', *Cell*, 88, pp. 323–331.

Li, C. *et al.* (2010) 'A bifunctional regulatory element in human somatic Wee1 mediates cyclin A/Cdk2 binding and Crm1-dependent nuclear export', *Molecular and cellular biology*. Mol Cell Biol, 30(1), pp. 116–130. doi: 10.1128/MCB.01876-08.

Li, X. and Heyer, W. D. (2008) 'Homologous recombination in DNA repair and DNA damage tolerance', *Cell Research 2008 18:1*. Nature Publishing Group, 18(1), pp. 99–113. doi: 10.1038/cr.2008.1.

Liao, H. *et al.* (2017) 'CDK1 promotes nascent DNA synthesis and induces resistance of cancer cells to DNA-damaging therapeutic agents', *Oncotarget*. Impact Journals, LLC, 8(53), p. 90662. doi: 10.18632/ONCOTARGET.21730.

Lieber, M. R. (2010) 'The Mechanism of Double-Strand DNA Break Repair by the Nonhomologous DNA End-Joining Pathway', <http://dx.doi.org/10.1146/annurev.biochem.052308.093131>. Annual Reviews , 79, pp. 181–211. doi: 10.1146/ANNUREV.BIOCHEM.052308.093131.

Lim, S. and Kaldis, P. (2013) 'Cdks, cyclins and CKIs: roles beyond cell cycle regulation', *Development*. The Company of Biologists, 140(15), pp. 3079–3093. doi: 10.1242/DEV.091744.

Lindqvist, A., Rodríguez-Bravo, V. and Medema, R. H. (2009) 'The decision to enter mitosis: feedback and redundancy in the mitotic entry network', *Journal of Cell Biology*. The Rockefeller University Press, 185(2), pp. 193–202. doi: 10.1083/JCB.200812045.

Lindsey-Boltz, L. A. *et al.* (2009) 'Reconstitution of Human Claspin-mediated Phosphorylation of Chk1 by the ATR (Ataxia Telangiectasia-mutated and Rad3-related) Checkpoint Kinase \*', *Journal of Biological Chemistry*. Elsevier, 284(48), pp. 33107–33114. doi: 10.1074/JBC.M109.064485.

Liu, S. *et al.* (2014) 'Breast Cancer Stem Cells Transition between Epithelial and Mesenchymal States Reflective of their Normal Counterparts', *Stem Cell Reports*. Elsevier, 2(1), p. 78. doi: 10.1016/J.STEMCR.2013.11.009.

Liu, X. *et al.* (2021) 'Efficacy and Safety of PARP Inhibitors in Advanced or Metastatic Triple-Negative Breast Cancer: A Systematic Review and Meta-Analysis', *Frontiers in Oncology*. Frontiers Media S.A., 11, p. 4363. doi: 10.3389/FONC.2021.742139/BIBTEX.

Longley, D. and Johnston, P. (2005) 'Molecular mechanisms of drug resistance', *The Journal of Pathology*. John Wiley & Sons, Ltd, 205(2), pp. 275–292. doi: 10.1002/path.1706.

Lopes, M., Foiani, M. and Sogo, J. M. (2006) 'Multiple Mechanisms Control Chromosome Integrity after Replication Fork Uncoupling and Restart at Irreparable UV Lesions', *Molecular Cell*. Cell Press, 21(1), pp. 15–27. doi: 10.1016/J.MOLCEL.2005.11.015.

Lord, C. J. and Ashworth, A. (2017) 'PARP Inhibitors: The First Synthetic Lethal Targeted Therapy', *Science (New York, N. Y.)*. Europe PMC Funders, 355(6330), p. 1152. doi: 10.1126/SCIENCE.AAM7344.

Lukas, C. *et al.* (2001) 'DNA Damage-activated Kinase Chk2 Is Independent of Proliferation or Differentiation Yet Correlates with Tissue Biology 1', *CANCER RESEARCH*. Cancer Society, 61, pp. 4990–4993. Available at: <http://aacrjournals.org/cancerres/article-pdf/61/13/4990/2485504/4990.pdf> (Accessed: 10 April 2022).

Łukasik, P. *et al.* (2021) 'Inhibitors of Cyclin-Dependent Kinases: Types and Their Mechanism of Action', *International Journal of Molecular Sciences*. Multidisciplinary Digital Publishing Institute (MDPI), 22(6), pp. 1–23. doi: 10.3390/IJMS22062806.

- M, C. *et al.* (2003) 'DNA repair mechanisms involved in gemcitabine cytotoxicity and in the interaction between gemcitabine and cisplatin', *Biochemical pharmacology*. Biochem Pharmacol, 65(2), pp. 275–282. doi: 10.1016/S0006-2952(02)01508-3.
- M, S. *et al.* (2018) 'The Tumor Suppressor MIG6 Controls Mitotic Progression and the G2/M DNA Damage Checkpoint by Stabilizing the WEE1 Kinase', *Cell reports*. Cell Rep, 24(5), pp. 1278–1289. doi: 10.1016/J.CELREP.2018.06.064.
- Ma, C. X. *et al.* (2012) 'Targeting Chk1 in p53-deficient triple-negative breast cancer is therapeutically beneficial in human-in-mouse tumor models', *The Journal of Clinical Investigation*. American Society for Clinical Investigation, 122(4), pp. 1541–1552. doi: 10.1172/JCI58765.
- Ma, C. X., Janetka, J. W. and Piwnica-Worms, H. (2011) 'Death by releasing the breaks: CHK1 inhibitors as cancer therapeutics', *Trends in Molecular Medicine*. Elsevier Current Trends, 17(2), pp. 88–96. doi: 10.1016/J.MOLMED.2010.10.009.
- MacDougall, C. A. *et al.* (2007) 'The structural determinants of checkpoint activation', *Genes & Development*. Cold Spring Harbor Laboratory Press, 21(8), pp. 898–903. doi: 10.1101/GAD.1522607.
- Madoux, F. *et al.* (2010) 'An ultra-high throughput cell-based screen for wee1 degradation inhibitors', *Journal of Biomolecular Screening*. SAGE PublicationsSage CA: Los Angeles, CA, 15(8), pp. 907–917. doi: 10.1177/1087057110375848.
- Maertens, O. *et al.* (2013) 'Elucidating Distinct Roles for NF1 in Melanomagenesis', *Cancer Discovery*. American Association for Cancer Research, 3(3), pp. 338–349. doi: 10.1158/2159-8290.CD-12-0313.
- Malumbres, M. *et al.* (2004) 'Mammalian Cells Cycle without the D-Type Cyclin-Dependent Kinases Cdk4 and Cdk6', *Cell*. Cell Press, 118(4), pp. 493–504. doi: 10.1016/J.CELL.2004.08.002.
- Malumbres, M. and Barbacid, M. (2009) 'Cell cycle, CDKs and cancer: a changing paradigm', *Nature Reviews Cancer* 2009 9:3. Nature Publishing Group, 9(3), pp. 153–166. doi: 10.1038/nrc2602.
- Masai, H. *et al.* (2010) 'Eukaryotic chromosome DNA replication: where, when, and how?', *Annual review of biochemistry*. Annu Rev Biochem, 79, pp. 89–130. doi: 10.1146/ANNUREV.BIOCHEM.052308.103205.
- Matheson, C. J., Backos, D. S. and Reigan, P. (2016) 'Targeting WEE1 Kinase in Cancer', *Trends in Pharmacological Sciences*. Elsevier Current Trends, 37(10), pp. 872–881. doi: 10.1016/J.TIPS.2016.06.006.
- Matsuura, K. *et al.* (2008) 'Cleavage-mediated Activation of Chk1 during Apoptosis \*', *Journal of Biological Chemistry*. Elsevier, 283(37), pp. 25485–25491. doi: 10.1074/JBC.M803111200.
- Matthews, T. P., Jones, A. M. and Collins, I. (2013) 'Structure-based design, discovery and development of checkpoint kinase inhibitors as potential anticancer therapies', *Expert Opinion on Drug Discovery*, 8(6), pp. 621–640. doi: 10.1517/17460441.2013.788496.
- Maya-Mendoza, A. *et al.* (2007) 'Chk1 regulates the density of active replication origins during the vertebrate S phase', *The EMBO Journal*. John Wiley & Sons, Ltd, 26(11), pp. 2719–2731. doi: 10.1038/SJ.EMBOJ.7601714.
- McDermott, M. *et al.* (2014) 'In vitro development of chemotherapy and targeted therapy drug-resistant cancer cell lines: a practical guide with case studies'. doi: 10.3389/fonc.2014.00040.
- McGranahan, N. and Swanton, C. (2017) 'Clonal Heterogeneity and Tumor Evolution: Past, Present, and the Future', *Cell*. Cell Press, 168(4), pp. 613–628. doi: 10.1016/J.CELL.2017.01.018.
- McNeely, S., Beckmann, R. and Bence Lin, A. K. (2014) 'CHEK again: Revisiting the development of CHK1 inhibitors for cancer therapy', *Pharmacology and Therapeutics*. Elsevier B.V., 142(1), pp. 1–10. doi: 10.1016/j.pharmthera.2013.10.005.
- Medema, R. H. and Macuerek, L. M. (2012) 'Checkpoint control and cancer', *Oncogene*, 31, pp. 2601–2613. doi: 10.1038/onc.2011.451.
- Medici, D. and Nawshad, A. (2010) 'Type I collagen promotes epithelial-mesenchymal transition

- through ILK-dependent activation of NF- $\kappa$ B and LEF-1', *Matrix biology : journal of the International Society for Matrix Biology*. NIH Public Access, 29(3), p. 161. doi: 10.1016/J.MATBIO.2009.12.003.
- Meijer, L. *et al.* (1997) 'Biochemical and Cellular Effects of Roscovitine, a Potent and Selective Inhibitor of the Cyclin-Dependent Kinases cdc2, cdk2 and cdk5', *European Journal of Biochemistry*. John Wiley & Sons, Ltd, 243(1–2), pp. 527–536. doi: 10.1111/J.1432-1033.1997.T01-2-00527.X.
- Meng, S. *et al.* (2020) 'GJA1 expression and its prognostic value in cervical cancer', *BioMed Research International*. Hindawi Limited, 2020. doi: 10.1155/2020/8827920.
- Michaelis, M., Wass, M. N. and Cinatl, J. (2019) 'Drug-adapted cancer cell lines as preclinical models of acquired resistance', *Cancer Drug Resistance*. OAE Publishing Inc., 2(3), pp. 447–456. doi: 10.20517/CDR.2019.005.
- Mini, E. *et al.* (2006) 'Cellular pharmacology of gemcitabine', *Annals of Oncology*. Elsevier, 17(SUPPL. 5), pp. v7–v12. doi: 10.1093/ANNONC/MDJ941.
- Mir, S. E. *et al.* (2010) 'In Silico Analysis of Kinase Expression Identifies WEE1 as a Gatekeeper against Mitotic Catastrophe in Glioblastoma', *Cancer cell*. NIH Public Access, 18(3), p. 244. doi: 10.1016/J.CCR.2010.08.011.
- Misale, S. *et al.* (2012) 'Emergence of KRAS mutations and acquired resistance to anti-EGFR therapy in colorectal cancer', *Nature* 2012 486:7404. Nature Publishing Group, 486(7404), pp. 532–536. doi: 10.1038/nature11156.
- Moiseeva, T. *et al.* (2017) 'ATR kinase inhibition induces unscheduled origin firing through a Cdc7-dependent association between GINS and And-1', *Nature Communications* 2017 8:1. Nature Publishing Group, 8(1), pp. 1–11. doi: 10.1038/s41467-017-01401-x.
- Moiseeva, T. N. *et al.* (2019) 'An ATR and CHK1 kinase signaling mechanism that limits origin firing during unperturbed DNA replication', *Proceedings of the National Academy of Sciences of the United States of America*. National Academy of Sciences, 116(27), pp. 13374–13383. doi: 10.1073/PNAS.1903418116/-DCSUPPLEMENTAL.
- Montano, R. *et al.* (2012) 'Preclinical Development of the Novel Chk1 Inhibitor SCH900776 in Combination with DNA-Damaging Agents and Antimetabolites', *Molecular Cancer Therapeutics*. American Association for Cancer Research, 11(2), pp. 427–438. doi: 10.1158/1535-7163.MCT-11-0406.
- Montano, R. *et al.* (2013) 'Sensitization of human cancer cells to gemcitabine by the Chk1 inhibitor MK-8776: Cell cycle perturbation and impact of administration schedule in vitro and in vivo', *BMC Cancer*. BioMed Central, 13(1), pp. 1–14. doi: 10.1186/1471-2407-13-604/FIGURES/5.
- Morimoto, Y. *et al.* (2020) 'Prexasertib increases the sensitivity of pancreatic cancer cells to gemcitabine and S-1', *Oncology Reports*. Spandidos Publications, 43(2), pp. 689–699. doi: 10.3892/OR.2019.7421/HTML.
- Mourón, S. *et al.* (2013) 'Repriming of DNA synthesis at stalled replication forks by human PrimPol', *Nature structural & molecular biology*. Nat Struct Mol Biol, 20(12), pp. 1383–1389. doi: 10.1038/NSMB.2719.
- Murai, J. *et al.* (2016) 'Resistance to PARP inhibitors by SLFN11 inactivation can be overcome by ATR inhibition', *Oncotarget*. Impact Journals LLC, 7(47), pp. 76534–76550. doi: 10.18632/oncotarget.12266.
- Murfun, I. *et al.* (2013) 'Survival of the replication checkpoint deficient cells requires MUS81-RAD52 function', *PLoS genetics*. PLoS Genet, 9(10). doi: 10.1371/JOURNAL.PGEN.1003910.
- Murga, M. *et al.* (2011) 'Exploiting oncogene-induced replicative stress for the selective killing of Myc-driven tumors', *Nature Structural & Molecular Biology* 2011 18:12. Nature Publishing Group, 18(12), pp. 1331–1335. doi: 10.1038/nsmb.2189.
- Myers, K. *et al.* (2009) 'ATR and Chk1 Suppress a Caspase-3–Dependent Apoptotic Response Following DNA Replication Stress', *PLOS Genetics*. Public Library of Science, 5(1), p. e1000324. doi: 10.1371/JOURNAL.PGEN.1000324.

- N, W. *et al.* (2004) 'M-phase kinases induce phospho-dependent ubiquitination of somatic Wee1 by SCFbeta-TrCP', *Proceedings of the National Academy of Sciences of the United States of America*. Proc Natl Acad Sci U S A, 101(13), pp. 4419–4424. doi: 10.1073/PNAS.0307700101.
- Nair, J. *et al.* (2020) 'Resistance to the CHK1 inhibitor prexasertib involves functionally distinct CHK1 activities in BRCA wild-type ovarian cancer', *Oncogene*. Springer US, 39(33), pp. 5520–5535. doi: 10.1038/s41388-020-1383-4.
- Nam, E. A. and Cortez, D. (2011) 'ATR signalling: more than meeting at the fork', *Biochemical Journal*. Portland Press, 436(3), pp. 527–536. doi: 10.1042/BJ20102162.
- Namiki, Y. and Zou, L. (2006) 'ATRIP associates with replication protein A-coated ssDNA through multiple interactions', *Proceedings of the National Academy of Sciences of the United States of America*. Proc Natl Acad Sci U S A, 103(3), pp. 580–585. doi: 10.1073/PNAS.0510223103.
- Navarra, P. and Preziosi, P. (1999) 'Hydroxyurea: new insights on an old drug', *Critical Reviews in Oncology/Hematology*. Elsevier, 29(3), pp. 249–255. doi: 10.1016/S1040-8428(98)00032-8.
- Nazarian, R. *et al.* (2010) 'Melanomas acquire resistance to B-RAF(V600E) inhibition by RTK or N-RAS upregulation', *Nature* 2010 468:7326. Nature Publishing Group, 468(7326), pp. 973–977. doi: 10.1038/nature09626.
- Neelsen, K. J. and Lopes, M. (2015) 'Replication fork reversal in eukaryotes: from dead end to dynamic response', *Nature Reviews Molecular Cell Biology* 2015 16:4. Nature Publishing Group, 16(4), pp. 207–220. doi: 10.1038/nrm3935.
- Negrini, S., Gorgoulis, V. G. and Halazonetis, T. D. (2010) 'Genomic instability — an evolving hallmark of cancer', *Nature Reviews Molecular Cell Biology* 2010 11:3. Nature Publishing Group, 11(3), pp. 220–228. doi: 10.1038/nrm2858.
- Neizer-Ashun, F. and Bhattacharya, R. (2021) 'Reality CHEK: Understanding the biology and clinical potential of CHK1', *Cancer Letters*. Elsevier Ireland Ltd, pp. 202–211. doi: 10.1016/j.canlet.2020.09.016.
- Nogales, V. *et al.* (2016) 'Epigenetic inactivation of the putative DNA/RNA helicase SLFN11 in human cancer confers resistance to platinum drugs', *Oncotarget*. Impact Journals LLC, 7(3), pp. 3084–3097. doi: 10.18632/oncotarget.6413.
- Norquist, B. *et al.* (2011) 'Secondary Somatic Mutations Restoring BRCA1/2 Predict Chemotherapy Resistance in Hereditary Ovarian Carcinomas', *Journal of Clinical Oncology*. American Society of Clinical Oncology, 29(22), p. 3008. doi: 10.1200/JCO.2010.34.2980.
- Nurse, P. and Thuriaux, P. (1980) 'REGULATORY GENES CONTROLLING MITOSIS IN THE FISSION YEAST SCHIZOSACCHAROMYCES POMBE', *Genetics*. Oxford Academic, 96(3), pp. 627–637. doi: 10.1093/GENETICS/96.3.627.
- Nurse, P., Thuriaux, P. and Nasmyth, K. (1976) 'Genetic control of the cell division cycle in the fission yeast Schizosaccharomyces pombe', *Molecular and General Genetics MGG* 1976 146:2. Springer, 146(2), pp. 167–178. doi: 10.1007/BF00268085.
- O'Day, S. J. *et al.* (2020) 'Abstract CT073: IMPRIME 1 (NCT02981303): A novel phase 2 study in second-line +, metastatic triple negative breast cancer patients shows promising clinical benefit for the combination of the immune checkpoint inhibitor, pembrolizumab (pembro), with the novel innate immune activator, Imprime PGG', *Cancer Research*. American Association for Cancer Research, 80(16\_Supplement), pp. CT073–CT073. doi: 10.1158/1538-7445.AM2020-CT073.
- O, H. *et al.* (2006) 'Cell cycle regulation by the Wee1 inhibitor PD0166285, pyrido [2,3-d] pyrimidine, in the B16 mouse melanoma cell line', *BMC cancer*. BMC Cancer, 6. doi: 10.1186/1471-2407-6-292.
- OHHASHI, S. *et al.* (2008) 'Down-regulation of Deoxycytidine Kinase Enhances Acquired Resistance to Gemcitabine in Pancreatic Cancer', *Anticancer Research*, 28(4B).
- Olivier, M., Hollstein, M. and Hainaut, P. (2010) 'TP53 Mutations in Human Cancers: Origins, Consequences, and Clinical Use', *Cold Spring Harbor Perspectives in Biology*. Cold Spring Harbor Laboratory Press, 2(1). doi: 10.1101/CSHPERSPECT.A001008.

- Oser, M. G. *et al.* (2015) 'Transformation from non-small-cell lung cancer to small-cell lung cancer: molecular drivers and cells of origin', *The Lancet Oncology*. Elsevier, 16(4), pp. e165–e172. doi: 10.1016/S1470-2045(14)71180-5.
- P, F. (1979) 'Epistatic gene interactions in the control of division in fission yeast', *Nature*. Nature, 279(5712), pp. 428–430. doi: 10.1038/279428A0.
- Pacek, M. and Walter, J. C. (2004) 'A requirement for MCM7 and Cdc45 in chromosome unwinding during eukaryotic DNA replication', *The EMBO journal*. EMBO J, 23(18), pp. 3667–3676. doi: 10.1038/SJ.EMBOJ.7600369.
- Paeschke, K. *et al.* (2013) 'Pif1 family helicases suppress genome instability at G-quadruplex motifs', *Nature* 2013 497:7450. Nature Publishing Group, 497(7450), pp. 458–462. doi: 10.1038/nature12149.
- Pan, Y. *et al.* (2009) 'Knockdown of Chk1 sensitizes human colon carcinoma HCT116 cells in a p53-dependent manner to lidamycin through abrogation of a G2/M checkpoint and induction of apoptosis', *Cancer biology & therapy*. Cancer Biol Ther, 8(16). doi: 10.4161/CBT.8.16.8955.
- Parker, L. L. and Piwnica-Worms, H. (1992) 'Inactivation of the p34cdc2-cyclin B complex by the human WEE1 tyrosine kinase', *Science*. American Association for the Advancement of Science, 257(5078), pp. 1955–1957. doi: 10.1126/science.1384126.
- Parmar, K. *et al.* (2019) 'The CHK1 Inhibitor Prexasertib Exhibits Monotherapy Activity in High-Grade Serous Ovarian Cancer Models and Sensitizes to PARP Inhibition', *Clinical Cancer Research*. American Association for Cancer Research, 25(20), pp. 6127–6140. doi: 10.1158/1078-0432.CCR-19-0448.
- Parrilla-Castellar, E. R., Arlander, S. J. H. and Karnitz, L. (2004) 'Dial 9-1-1 for DNA damage: the Rad9-Hus1-Rad1 (9-1-1) clamp complex', *DNA repair*. DNA Repair (Amst), 3(8–9), pp. 1009–1014. doi: 10.1016/J.DNAREP.2004.03.032.
- Perona, R. *et al.* (2008) 'Role of CHK2 in cancer development', *Clinical and Translational Oncology*. Springer, 10(9), pp. 538–542. doi: 10.1007/s12094-008-0248-5.
- Petermann, E., Woodcock, M. and Helleday, T. (2010) 'Chk1 promotes replication fork progression by controlling replication initiation.', *Proceedings of the National Academy of Sciences of the United States of America*. National Academy of Sciences, 107(37), pp. 16090–5. doi: 10.1073/pnas.1005031107.
- Pfister, S. X. *et al.* (2015) 'Inhibiting WEE1 Selectively Kills Histone H3K36me3-Deficient Cancers by dNTP Starvation', *Cancer Cell*. Cell Press, 28(5), pp. 557–568. doi: 10.1016/J.CCELL.2015.09.015.
- De Piccoli, G. *et al.* (2012) 'Replisome stability at defective DNA replication forks is independent of S phase checkpoint kinases', *Molecular cell*. Mol Cell, 45(5), pp. 696–704. doi: 10.1016/J.MOLCEL.2012.01.007.
- Pike, K. G. (2016) 'Abstract 4859: Identifying high quality, potent and selective inhibitors of ATM kinase: Discovery of AZD0156', in *Cancer Research*. American Association for Cancer Research (AACR), pp. 4859–4859. doi: 10.1158/1538-7445.am2016-4859.
- Pines, J. (1993) 'Cyclins and their associated cyclin-dependent kinases in the human cell cycle', *Biochemical Society Transactions*. Portland Press, 21(4), pp. 921–925. doi: 10.1042/BST0210921.
- Piotrowska, Z. *et al.* (2015) 'Heterogeneity Underlies the Emergence of EGFR T790M Wild-Type Clones Following Treatment of T790M-Positive Cancers with a Third-Generation EGFR Inhibitor', *Cancer Discovery*. American Association for Cancer Research, 5(7), pp. 713–722. doi: 10.1158/2159-8290.CD-15-0399.
- Plummer, E. R. *et al.* (2019) 'A first-in-human phase I/II trial of SRA737 (a Chk1 Inhibitor) in subjects with advanced cancer.', [https://doi.org/10.1200/JCO.2019.37.15\\_suppl.3094](https://doi.org/10.1200/JCO.2019.37.15_suppl.3094). American Society of Clinical Oncology, 37(15\_suppl), pp. 3094–3094. doi: 10.1200/JCO.2019.37.15\_SUPPL.3094.
- Plunkett, W., Huang, P. and Gandhi, V. (1995) 'Preclinical characteristics of gemcitabine', *Anti-Cancer Drugs*. Lippincott Williams and Wilkins, 6(SUPPL. 6), pp. 7–13. doi: 10.1097/00001813-199512006-00002.

- Pomerening, J. R., Sun, Y. K. and Ferrell, J. E. (2005) 'Systems-Level Dissection of the Cell-Cycle Oscillator: Bypassing Positive Feedback Produces Damped Oscillations', *Cell*. Cell Press, 122(4), pp. 565–578. doi: 10.1016/J.CELL.2005.06.016.
- Prakash, S., Johnson, R. E. and Prakash, L. (2005) 'Eukaryotic translesion synthesis DNA polymerases: specificity of structure and function', *Annual review of biochemistry*. Annu Rev Biochem, 74, pp. 317–353. doi: 10.1146/ANNUREV.BIOCHEM.74.082803.133250.
- Puc, J. *et al.* (2005) 'Lack of PTEN sequesters CHK1 and initiates genetic instability', *Cancer Cell*. Cell Press, 7(2), pp. 193–204. doi: 10.1016/J.CCR.2005.01.009.
- Qiu, S. *et al.* (2021) 'Replication Fork Reversal and Protection', *Frontiers in Cell and Developmental Biology*. Frontiers Media SA, 9. doi: 10.3389/FCELL.2021.670392.
- Rao, Q. *et al.* (2017) 'Cryo-EM structure of human ATR-ATRIP complex', *Cell Research* 2018 28:2. Nature Publishing Group, 28(2), pp. 143–156. doi: 10.1038/cr.2017.158.
- Rathe, S. K. *et al.* (2014) 'Using RNA-seq and targeted nucleases to identify mechanisms of drug resistance in acute myeloid leukemia', *Scientific Reports* 2014 4:1. Nature Publishing Group, 4(1), pp. 1–9. doi: 10.1038/srep06048.
- Reardon, J. T. *et al.* (1999) 'Efficient nucleotide excision repair of cisplatin, oxaliplatin, and bis-acetoamine-dichloro-cyclohexylamine-platinum(IV) (JM216) platinum intrastrand DNA diadducts', *Cancer Research*, 59(16), pp. 3968–3971.
- Reed, S. I., Ferguson, J. and Groppe, J. C. (1982) 'Preliminary characterization of the transcriptional and translational products of the *Saccharomyces cerevisiae* cell division cycle gene CDC28', *Molecular and Cellular Biology*. American Society for Microbiology, 2(4), pp. 412–425. doi: 10.1128/MCB.2.4.412-425.1982.
- Ribas, A. and Wolchok, J. D. (2018) 'Cancer immunotherapy using checkpoint blockade', *Science*. American Association for the Advancement of Science, 359(6382), pp. 1350–1355. doi: 10.1126/SCIENCE.AAR4060.
- Robinson, D. R. *et al.* (2013) 'Activating ESR1 mutations in hormone-resistant metastatic breast cancer', *Nature Genetics* 2013 45:12. Nature Publishing Group, 45(12), pp. 1446–1451. doi: 10.1038/ng.2823.
- Rogers, R. F. *et al.* (2020) 'CHK1 inhibition is synthetically lethal with loss of B-family DNA polymerase function in human lung and colorectal cancer cells', *Cancer Research*. American Association for Cancer Research Inc., 80(8), pp. 1735–1747. doi: 10.1158/0008-5472.CAN-19-1372.
- Ronco, C. *et al.* (2017) 'ATM, ATR, CHK1, CHK2 and WEE1 inhibitors in cancer and cancer stem cells', *MedChemComm*. Royal Society of Chemistry, 8(2), p. 295. doi: 10.1039/C6MD00439C.
- Ronson, G. E. *et al.* (2018) 'PARP1 and PARP2 stabilise replication forks at base excision repair intermediates through Fbh1-dependent Rad51 regulation', *Nature Communications* 2018 9:1. Nature Publishing Group, 9(1), pp. 1–12. doi: 10.1038/s41467-018-03159-2.
- Rorà, A. G. L. Di *et al.* (2019) 'Synergism Through WEE1 and CHK1 Inhibition in Acute Lymphoblastic Leukemia', *Cancers* 2019, Vol. 11, Page 1654. Multidisciplinary Digital Publishing Institute, 11(11), p. 1654. doi: 10.3390/CANCERS11111654.
- Rothblum-Oviatt, C. J., Ryan, C. E. and Piwnicka-Worms, H. (2001) '14-3-3 Binding regulates catalytic activity of human Wee1 kinase', *Cell Growth and Differentiation*. AACR, 12(12), pp. 581–589. Available at: <http://cgd.aacrjournals.org/cgi/content/full/12/12/581> (Accessed: 21 October 2021).
- Rugo, H. S. *et al.* (2016) 'Adaptive Randomization of Veliparib–Carboplatin Treatment in Breast Cancer', *New England Journal of Medicine*. New England Journal of Medicine (NEJM/MMS), 375(1), pp. 23–34. doi: 10.1056/NEJMOA1513749/SUPPL\_FILE/NEJMOA1513749\_DISCLOSURES.PDF.
- Russell, M. R. *et al.* (2013) 'Combination Therapy Targeting the Chk1 and Wee1 Kinases Shows Therapeutic Efficacy in Neuroblastoma', *Cancer Research*. American Association for Cancer Research, 73(2), pp. 776–784. doi: 10.1158/0008-5472.CAN-12-2669.

- Saha, P. *et al.* (1997) 'p21CIP1 and Cdc25A: competition between an inhibitor and an activator of cyclin-dependent kinases', *Molecular and cellular biology*. Mol Cell Biol, 17(8), pp. 4338–4345. doi: 10.1128/MCB.17.8.4338.
- Sakurikar, N. *et al.* (2016) 'A subset of cancer cell lines is acutely sensitive to the Chk1 inhibitor MK-8776 as monotherapy due to CDK2 activation in S phase', *Oncotarget*. Impact Journals, 7(2), pp. 1380–1394. doi: 10.18632/oncotarget.6364.
- Sakurikar, N. and Eastman, A. (2016) 'Cell Cycle Critical reanalysis of the methods that discriminate the activity of CDK2 from CDK1 Critical reanalysis of the methods that discriminate the activity of CDK2 from CDK1'. doi: 10.1080/15384101.2016.1160983.
- Sale, J. E. (2013) 'Translesion DNA Synthesis and Mutagenesis in Eukaryotes', *Cold Spring Harbor Perspectives in Biology*. Cold Spring Harbor Laboratory Press, 5(3), p. a012708. doi: 10.1101/CSHPERSPECT.A012708.
- Sanchez, Y. *et al.* (1997) 'Conservation of the Chk1 Checkpoint Pathway in Mammals: Linkage of DNA Damage to Cdk Regulation Through Cdc25', *Science*. American Association for the Advancement of Science, 277(5331), pp. 1497–1501. doi: 10.1126/SCIENCE.277.5331.1497.
- Santamaría, D. *et al.* (2007) 'Cdk1 is sufficient to drive the mammalian cell cycle', *Nature* 2007 448:7155. Nature Publishing Group, 448(7155), pp. 811–815. doi: 10.1038/nature06046.
- Sarcar, B. *et al.* (2011) 'Targeting Radiation-Induced G 2 Checkpoint Activation with the Wee-1 Inhibitor MK-1775 in Glioblastoma Cell Lines'. doi: 10.1158/1535-7163.MCT-11-0469.
- Satyanarayana, A., Hilton, M. B. and Kaldis, P. (2008) 'p21 Inhibits Cdk1 in the Absence of Cdk2 to Maintain the G1/S Phase DNA Damage Checkpoint', *Molecular Biology of the Cell*. American Society for Cell Biology, 19(1), p. 65. doi: 10.1091/MBC.E07-06-0525.
- Schafer, K. A. (1998) 'The Cell Cycle: A Review', *Veterinary Pathology*. American College of Veterinary Pathologists Inc., 35(6), pp. 461–478. doi: 10.1177/030098589803500601.
- Schmid, P. *et al.* (2021) 'Abstract PS12-28: Phase 1b study evaluating a triplet combination of ipatasertib (IPAT), atezolizumab, and a taxane as first-line therapy for locally advanced/metastatic triple-negative breast cancer (TNBC)', *Cancer Research*. American Association for Cancer Research, 81(4\_Supplement), pp. PS12-28. doi: 10.1158/1538-7445.SABCS20-PS12-28.
- Schneider-Poetsch, T. *et al.* (2010) 'Inhibition of eukaryotic translation elongation by cycloheximide and lactimidomycin', *Nature Chemical Biology*. Nature Publishing Group, 6(3), pp. 209–217. doi: 10.1038/NCHEMBIO.304.
- Schulze, S. K. *et al.* (2012) 'SERE: Single-parameter quality control and sample comparison for RNA-Seq', *BMC Genomics* 2012 13:1. BioMed Central, 13(1), pp. 1–9. doi: 10.1186/1471-2164-13-524.
- Sen, T. *et al.* (2019) 'Combination Treatment of the Oral CHK1 Inhibitor, SRA737, and Low-Dose Gemcitabine Enhances the Effect of Programmed Death Ligand 1 Blockade by Modulating the Immune Microenvironment in SCLC', *Journal of Thoracic Oncology*. Elsevier, 14(12), pp. 2152–2163. doi: 10.1016/J.JTHO.2019.08.009.
- Seo, Y. S. and Kang, Y. H. (2018) 'The human replicative helicase, the CMG complex, as a target for anti-cancer therapy', *Frontiers in Molecular Biosciences*. Frontiers Media S.A., 5(MAR), p. 26. doi: 10.3389/FMOLB.2018.00026/BIBTEX.
- Sequist, L. V. *et al.* (2011) 'Genotypic and histological evolution of lung cancers acquiring resistance to EGFR inhibitors', *Science Translational Medicine*. American Association for the Advancement of Science, 3(75). doi: 10.1126/SCITRANSLMED.3002003/SUPPL\_FILE/3-75RA26\_SM.PDF.
- Sharma, A., Singh, K. and Almasan, A. (2012) 'Histone H2AX Phosphorylation: A Marker for DNA Damage', *Methods in Molecular Biology*. Humana Press, Totowa, NJ, 920, pp. 613–626. doi: 10.1007/978-1-61779-998-3\_40.
- Sharma, P. (2016) 'Biology and Management of Patients With Triple-Negative Breast Cancer', *The Oncologist*. Wiley-Blackwell, 21(9), p. 1050. doi: 10.1634/THEONCOLOGIST.2016-0067.

- Shechter, D., Costanzo, V. and Gautier, J. (2004) 'ATR and ATM regulate the timing of DNA replication origin firing', *Nature Cell Biology*, 6(7), pp. 648–655. doi: 10.1038/ncb1145.
- Shimada, M. *et al.* (2008) 'Chk1 is a histone H3 threonine 11 kinase that regulates DNA damage-induced transcriptional repression', *Cell*, 132(2), pp. 221–232. doi: 10.1016/J.CELL.2007.12.013.
- Shu, Z. *et al.* (2020) 'Cell-cycle-dependent phosphorylation of RRM1 ensures efficient DNA replication and regulates cancer vulnerability to ATR inhibition', *Oncogene* 2020 39:35. Nature Publishing Group, 39(35), pp. 5721–5733. doi: 10.1038/s41388-020-01403-y.
- Siddik, Z. H. (2003) 'Cisplatin: Mode of cytotoxic action and molecular basis of resistance', *Oncogene*. Nature Publishing Group, pp. 7265–7279. doi: 10.1038/sj.onc.1206933.
- Siddiqui, K., On, K. F. and Diffley, J. F. X. (2013) 'Regulating DNA Replication in Eukarya', *Cold Spring Harbor Perspectives in Biology*. Cold Spring Harbor Laboratory Press, 5(9), p. a012930. doi: 10.1101/CSHPERSPECT.A012930.
- Sidi, S. *et al.* (2008) 'Chk1 Suppresses a Caspase-2 Apoptotic Response to DNA Damage that Bypasses p53, Bcl-2, and Caspase-3', *Cell*. Cell Press, 133(5), pp. 864–877. doi: 10.1016/J.CELL.2008.03.037.
- Skehan, P., Storeng, R., Scudiero, D., Monks, A., McMahon, J., Vistica, D., Warren, J.T., Bokesch, H., Kenney, S., Boyd, M. R. (1990) 'New colorimetric cytotoxicity assay for anti- cancer-drug screening.', *Journal of National Cancer Institute*, 82(November), p. 1107.
- Smith, A. *et al.* (2007) 'Redundant Ubiquitin Ligase Activities Regulate Wee1 Degradation and Mitotic Entry', <http://dx.doi.org/10.4161/cc.6.22.4919>. Taylor & Francis, 6(22), pp. 2795–2799. doi: 10.4161/CC.6.22.4919.
- Smith, P. K. *et al.* (1985) 'Measurement of protein using bicinchoninic acid', *Analytical Biochemistry*. Academic Press, 150(1), pp. 76–85. doi: 10.1016/0003-2697(85)90442-7.
- Smits, V. A. J. (2006) 'Spreading the signal: dissociation of Chk1 from chromatin', *Cell cycle (Georgetown, Tex.)*. Cell Cycle, 5(10), pp. 1039–1043. doi: 10.4161/CC.5.10.2761.
- Smits, V. A. J., Reaper, P. M. and Jackson, S. P. (2006) 'Rapid PIKK-dependent release of Chk1 from chromatin promotes the DNA-damage checkpoint response', *Current Biology*. Elsevier, 16(2), pp. 150–159. doi: 10.1016/J.CUB.2005.11.066/ATTACHMENT/4C5AB864-5B96-44D3-B126-93EC5911C7B5/MMC1.PDF.
- Smittenaar, C. R. *et al.* (2016) 'Cancer incidence and mortality projections in the UK until 2035', *British Journal of Cancer*. Nature Publishing Group, 115(9), pp. 1147–1155. doi: 10.1038/bjc.2016.304.
- Solier, S. and Pommier, Y. (2014) 'The nuclear  $\gamma$ -H2AX apoptotic ring: implications for cancers and autoimmune diseases', *Cellular and Molecular Life Sciences*. Birkhauser Verlag AG, 71(12), pp. 2289–2297. doi: 10.1007/s00018-013-1555-2.
- Song, N. *et al.* (2018) 'ZEB1 inhibition sensitizes cells to the ATR inhibitor VE-821 by abrogating epithelial–mesenchymal transition and enhancing DNA damage', <https://doi.org/10.1080/15384101.2017.1404206>. Taylor & Francis, 17(5), pp. 595–604. doi: 10.1080/15384101.2017.1404206.
- Sørensen, C. S. *et al.* (2005) 'The cell-cycle checkpoint kinase Chk1 is required for mammalian homologous recombination repair', *Nature cell biology*. Nat Cell Biol, 7(2), pp. 195–201. doi: 10.1038/NCB1212.
- Sørensen, C. S. *et al.* (2006) 'ATR, Claspin and the Rad9-Rad1-Hus1 Complex Regulate Chk1 and Cdc25A in the Absence of DNA Damage', <https://doi.org/10.4161/cc.3.7.972>. Taylor & Francis, 3(7), pp. 941–945. doi: 10.4161/CC.3.7.972.
- Sørensen, C. S. and Syljuåsen, R. G. (2012) 'Safeguarding genome integrity: the checkpoint kinases ATR, CHK1 and WEE1 restrain CDK activity during normal DNA replication', *Nucleic Acids Research*. Oxford Academic, 40(2), pp. 477–486. doi: 10.1093/NAR/GKR697.



- Sørli, T. *et al.* (2001) 'Gene expression patterns of breast carcinomas distinguish tumor subclasses with clinical implications.', *Proceedings of the National Academy of Sciences of the United States of America*. National Academy of Sciences, 98(19), pp. 10869–74. doi: 10.1073/pnas.191367098.
- Sousa, F. G. *et al.* (2015) 'Alterations of DNA repair genes in the NCI-60 cell lines and their predictive value for anticancer drug activity', *DNA Repair*. Elsevier, 28, pp. 107–115. doi: 10.1016/j.dnarep.2015.01.011.
- Sparks, J. L. *et al.* (2012) 'RNase H2-Initiated Ribonucleotide Excision Repair', *Molecular Cell*. Cell Press, 47(6), pp. 980–986. doi: 10.1016/J.MOLCEL.2012.06.035.
- Speroni, J. *et al.* (2012) 'Kinase-independent function of checkpoint kinase 1 (Chk1) in the replication of damaged DNA', *Proceedings of the National Academy of Sciences of the United States of America*. Proc Natl Acad Sci U S A, 109(19), pp. 7344–7349. doi: 10.1073/PNAS.1116345109/-DCSUPPLEMENTAL/PNAS.201116345SI.PDF.
- Squire, C. J. *et al.* (2005) 'Structure and Inhibition of the Human Cell Cycle Checkpoint Kinase, Wee1A Kinase: An Atypical Tyrosine Kinase with a Key Role in CDK1 Regulation', *Structure*. Cell Press, 13(4), pp. 541–550. doi: 10.1016/J.STR.2004.12.017.
- Srinivasan, S. V. *et al.* (2013) 'Cdc45 Is a Critical Effector of Myc-Dependent DNA Replication Stress', *Cell Reports*. Cell Press, 3(5), pp. 1629–1639. doi: 10.1016/J.CELREP.2013.04.002.
- Steel, M. (1994) 'Cyclins and cancer: wheels within wheels', *The Lancet*. Elsevier, 343(8903), pp. 931–932. doi: 10.1016/S0140-6736(94)90062-0.
- Straussman, R. *et al.* (2012) 'Tumour micro-environment elicits innate resistance to RAF inhibitors through HGF secretion', *Nature* 2012 487:7408. Nature Publishing Group, 487(7408), pp. 500–504. doi: 10.1038/nature11183.
- Sugimoto, N. *et al.* (2018) 'Genome-wide analysis of the spatiotemporal regulation of firing and dormant replication origins in human cells', *Nucleic Acids Research*. Oxford Academic, 46(13), pp. 6683–6696. doi: 10.1093/NAR/GKY476.
- Swanton, C. (2012) 'Intratumor heterogeneity: Evolution through space and time', *Cancer Research*, pp. 4875–4882. doi: 10.1158/0008-5472.CAN-12-2217.
- Syljuåsen, R. G. *et al.* (2005) 'Inhibition of Human Chk1 Causes Increased Initiation of DNA Replication, Phosphorylation of ATR Targets, and DNA Breakage', *Molecular and Cellular Biology*. American Society for Microbiology, 25(9), pp. 3553–3562. doi: 10.1128/MCB.25.9.3553-3562.2005/ASSET/915F0CC1-91B7-404E-86A1-61B0031E33B2/ASSETS/GRAPHIC/ZMB0090549330006.JPEG.
- Takai, H. *et al.* (2002) 'Chk2-deficient mice exhibit radioresistance and defective p53-mediated transcription', *EMBO Journal*, 21(19), pp. 5195–5205. doi: 10.1093/emboj/cdf506.
- Takeo, M. *et al.* (2016) 'EdnrB Governs Regenerative Response of Melanocyte Stem Cells by Crosstalk with Wnt Signaling', *Cell Reports*. Cell Press, 15(6), pp. 1291–1302. doi: 10.1016/J.CELREP.2016.04.006.
- Takezawa, K. *et al.* (2012) 'HER2 Amplification: A Potential Mechanism of Acquired Resistance to EGFR Inhibition in EGFR-Mutant Lung Cancers That Lack the Second-Site EGFR T790M Mutation', *Cancer Discovery*. American Association for Cancer Research, 2(10), pp. 922–933. doi: 10.1158/2159-8290.CD-12-0108.
- Tanaka, S. *et al.* (2006) 'CDK-dependent phosphorylation of Sld2 and Sld3 initiates DNA replication in budding yeast', *Nature* 2006 445:7125. Nature Publishing Group, 445(7125), pp. 328–332. doi: 10.1038/nature05465.
- Tapia-Alveal, C., Calonge, T. M. and O'Connell, M. J. (2009) 'Regulation of Chk1', *Cell Division*. BioMed Central, 4(1), pp. 1–7. doi: 10.1186/1747-1028-4-8/FIGURES/3.
- Taricani, L. *et al.* (2014) 'A Functional Approach Reveals a Genetic and Physical Interaction between Ribonucleotide Reductase and CHK1 in Mammalian Cells', *PLOS ONE*. Public Library of Science, 9(11), p. e111714. doi: 10.1371/JOURNAL.PONE.0111714.

- Terzi, M. Y., Izmirli, M. and Gogebakan, B. (2016) 'The cell fate: senescence or quiescence', *Molecular Biology Reports*. Springer Netherlands, 43(11), pp. 1213–1220. doi: 10.1007/S11033-016-4065-0/TABLES/1.
- Thiery, J. P. (2002) 'Epithelial–mesenchymal transitions in tumour progression', *Nature Reviews Cancer* 2:6. Nature Publishing Group, 2(6), pp. 442–454. doi: 10.1038/nrc822.
- Thompson, R. *et al.* (2012) 'Treatment with the Chk1 inhibitor Gö6976 enhances cisplatin cytotoxicity in SCLC cells', *International Journal of Oncology*. Spandidos Publications, 40(1), pp. 194–202. doi: 10.3892/IJO.2011.1187/HTML.
- Thompson, R. and Eastman, A. (2013) 'The cancer therapeutic potential of Chk1 inhibitors: how mechanistic studies impact on clinical trial design', *British Journal of Clinical Pharmacology*. John Wiley & Sons, Ltd, 76(3), pp. 358–369. doi: 10.1111/BCP.12139.
- Thompson, R., Montano, R. and Eastman, A. (2012) 'The Mre11 nuclease is critical for the sensitivity of cells to Chk1 inhibition', *PLoS one*. PLoS One, 7(8). doi: 10.1371/JOURNAL.PONE.0044021.
- Timofeev, O. *et al.* (2010) 'Cdc25 phosphatases are required for timely assembly of CDK1-cyclin B at the G2/M transition', *Journal of Biological Chemistry*. American Society for Biochemistry and Molecular Biology, 285(22), pp. 16978–16990. doi: 10.1074/jbc.M109.096552.
- Toledo, L., Neelsen, K. J. and Lukas, J. (2017) 'Replication Catastrophe: When a Checkpoint Fails because of Exhaustion', *Molecular Cell*. Cell Press, pp. 735–749. doi: 10.1016/j.molcel.2017.05.001.
- Toy, W. *et al.* (2013) 'ESR1 ligand-binding domain mutations in hormone-resistant breast cancer', *Nature Genetics* 2013 45:12. Nature Publishing Group, 45(12), pp. 1439–1445. doi: 10.1038/ng.2822.
- Tse, A. N. *et al.* (2007) 'CHIR-124, a novel potent inhibitor of Chk1, potentiates the cytotoxicity of topoisomerase I poisons in vitro and in vivo', *Clinical cancer research: an official journal of the American Association for Cancer Research*. Clin Cancer Res, 13(2 Pt 1), pp. 591–602. doi: 10.1158/1078-0432.CCR-06-1424.
- Tsuruo, T. *et al.* (1981) 'Overcoming of Vincristine Resistance in P388 Leukemia in Vivo and in Vitro through Enhanced Cytotoxicity of Vincristine and Vinblastine by Verapamil', *Cancer Research*, 41(5).
- Tuduri, S. *et al.* (2009) 'Topoisomerase I suppresses genomic instability by preventing interference between replication and transcription', *Nature Cell Biology* 2009 11:11. Nature Publishing Group, 11(11), pp. 1315–1324. doi: 10.1038/ncb1984.
- Turk, A. A. and Wisinski, K. B. (2018) 'PARP inhibitors in breast cancer: Bringing synthetic lethality to the bedside', *Cancer*. John Wiley & Sons, Ltd, 124(12), pp. 2498–2506. doi: 10.1002/CNCR.31307.
- Turner, N. *et al.* (2013) 'Targeting triple negative breast cancer: Is p53 the answer?' doi: 10.1016/j.ctrv.2012.12.001.
- Turner, N. C. and Reis-Filho, J. S. (2006) 'Basal-like breast cancer and the BRCA1 phenotype', *Oncogene* 2006 25:43. Nature Publishing Group, 25(43), pp. 5846–5853. doi: 10.1038/sj.onc.1209876.
- Turner, N. C. and Reis-Filho, J. S. (2012) 'Genetic heterogeneity and cancer drug resistance', *The Lancet Oncology*. Elsevier, 13(4), pp. e178–e185. doi: 10.1016/S1470-2045(11)70335-7.
- Uziel, T. *et al.* (2003) 'Requirement of the MRN complex for ATM activation by DNA damage', *EMBO Journal*, 22(20), pp. 5612–5621. doi: 10.1093/emboj/cdg541.
- Vanderpool, D. *et al.* (2009) 'Characterization of the CHK1 allosteric inhibitor binding site', *Biochemistry*. American Chemical Society, 48(41), pp. 9823–9830. doi: 10.1021/B1900258V/SUPPL\_FILE/B1900258V\_SI\_001.PDF.
- Vasan, N., Baselga, J. and Hyman, D. M. (2019) 'A view on drug resistance in cancer', *Nature*. Nature Publishing Group, pp. 299–309. doi: 10.1038/s41586-019-1730-1.
- Vassilev, L. T. *et al.* (2006) 'Selective small-molecule inhibitor reveals critical mitotic functions of human CDK1', *Proceedings of the National Academy of Sciences*. National Academy of Sciences, 103(28), pp. 10660–10665. doi: 10.1073/PNAS.0600447103.

- Vendetti, F. P. *et al.* (2015) 'The orally active and bioavailable ATR kinase inhibitor AZD6738 potentiates the anti-tumor effects of cisplatin to resolve ATM-deficient non-small cell lung cancer in vivo', *Oncotarget*. Impact Journals LLC, 6(42), pp. 44289–44305. doi: 10.18632/oncotarget.6247.
- Verlinden, L. *et al.* (2007) 'The E2F-regulated gene Chk1 is highly expressed in triple-negative estrogen receptor /progesterone receptor /HER-2 breast carcinomas', *Cancer research*. Cancer Res, 67(14), pp. 6574–6581. doi: 10.1158/0008-5472.CAN-06-3545.
- Vinayak, S. *et al.* (2019) 'Open-label Clinical Trial of Niraparib Combined With Pembrolizumab for Treatment of Advanced or Metastatic Triple-Negative Breast Cancer', *JAMA Oncology*. American Medical Association, 5(8), pp. 1132–1140. doi: 10.1001/JAMAONCOL.2019.1029.
- Visakorpi, T. *et al.* (1995) 'In vivo amplification of the androgen receptor gene and progression of human prostate cancer', *Nature Genetics* 1995 9:4. Nature Publishing Group, 9(4), pp. 401–406. doi: 10.1038/ng0495-401.
- Vitale, I. *et al.* (2011) 'Mitotic catastrophe: a mechanism for avoiding genomic instability', *Nature Reviews Molecular Cell Biology* 2011 12:6. Nature Publishing Group, 12(6), pp. 385–392. doi: 10.1038/nrm3115.
- Vogel, C. L. *et al.* (2002) 'Efficacy and safety of trastuzumab as a single agent in first-line treatment of HER2-overexpressing metastatic breast cancer', *Journal of clinical oncology : official journal of the American Society of Clinical Oncology*. J Clin Oncol, 20(3), pp. 719–726. doi: 10.1200/JCO.2002.20.3.719.
- W, H. *et al.* (2020) 'GJA1 is a Prognostic Biomarker and Correlated with Immune Infiltrates in Colorectal Cancer', *Cancer management and research*. Cancer Manag Res, 12, pp. 11649–11661. doi: 10.2147/CMAR.S235500.
- Wade Harper, J. *et al.* (1993) 'The p21 Cdk-interacting protein Cip1 is a potent inhibitor of G1 cyclin-dependent kinases', *Cell*. Cell, 75(4), pp. 805–816. doi: 10.1016/0092-8674(93)90499-G.
- Wagner, J. M. and Karnitz, L. M. (2009) 'Cisplatin-Induced DNA Damage Activates Replication Checkpoint Signaling Components that Differentially Affect Tumor Cell Survival', *Molecular Pharmacology*. American Society for Pharmacology and Experimental Therapeutics, 76(1), pp. 208–214. doi: 10.1124/MOL.109.055178.
- Wahba, H. A. and El-Hadaad, H. A. (2015) 'Current approaches in treatment of triple-negative breast cancer.', *Cancer biology & medicine*. Chinese Anti-Cancer Association, 12(2), pp. 106–16. doi: 10.7497/j.issn.2095-3941.2015.0030.
- Walker, M. *et al.* (2009) 'Chk1 C-terminal regulatory phosphorylation mediates checkpoint activation by de-repression of Chk1 catalytic activity', *Oncogene* 2009 28:24. Nature Publishing Group, 28(24), pp. 2314–2323. doi: 10.1038/onc.2009.102.
- Walton, M. I. *et al.* (2010) 'The Preclinical Pharmacology and Therapeutic Activity of the Novel CHK1 Inhibitor SAR-020106', *Molecular Cancer Therapeutics*. American Association for Cancer Research, 9(1), pp. 89–100. doi: 10.1158/1535-7163.MCT-09-0938.
- Walton, Mike I *et al.* (2012) 'CCT244747 is a novel potent and selective CHK1 inhibitor with oral efficacy alone and in combination with genotoxic anticancer drugs.', *Clinical cancer research : an official journal of the American Association for Cancer Research*. Europe PMC Funders, 18(20), pp. 5650–61. doi: 10.1158/1078-0432.CCR-12-1322.
- Walton, Mike I. *et al.* (2012) 'CCT244747 is a novel potent and selective CHK1 inhibitor with oral efficacy alone and in combination with genotoxic anticancer drugs', *Clinical cancer research : an official journal of the American Association for Cancer Research*. Clin Cancer Res, 18(20), pp. 5650–5661. doi: 10.1158/1078-0432.CCR-12-1322.
- Walton, M. I. *et al.* (2016a) 'The clinical development candidate CCT245737 is an orally active CHK1 inhibitor with preclinical activity in RAS mutant NSCLC and E&micro;-MYC driven B-cell lymphoma', *Oncotarget*, 7(3), pp. 2329–2342. doi: 10.18632/oncotarget.4919.
- Walton, M. I. *et al.* (2016b) 'The clinical development candidate CCT245737 is an orally active CHK1 inhibitor with preclinical activity in RAS mutant NSCLC and Eμ-MYC driven B-cell lymphoma',

*Oncotarget*. Impact Journals LLC, 7(3), pp. 2329–2342. doi: 10.18632/oncotarget.4919.

Wang, F. *et al.* (2005) 'Transcriptional repression of WEE1 by Kruppel-like factor 2 is involved in DNA damage-induced apoptosis', *Oncogene* 2005 24:24. Nature Publishing Group, 24(24), pp. 3875–3885. doi: 10.1038/sj.onc.1208546.

Wang, J. *et al.* (2012) 'Coupling cellular localization and function of checkpoint kinase 1 (Chk1) in checkpoints and cell viability', *Journal of Biological Chemistry*. Elsevier, 287(30), pp. 25501–25509. doi: 10.1074/JBC.M112.350397/ATTACHMENT/67A76993-CE26-4AFA-A18F-D9D8A45EFD39/MMC1.PDF.

Wang, J., Han, X. and Zhang, Y. (2012) 'Autoregulatory Mechanisms of Phosphorylation of Checkpoint Kinase 1', *Cancer Research*. American Association for Cancer Research, 72(15), pp. 3786–3794. doi: 10.1158/0008-5472.CAN-12-0523.

Wang, Q. *et al.* (1996) 'UCN-01: a potent abrogator of G2 checkpoint function in cancer cells with disrupted p53.', *Journal of the National Cancer Institute*, 88(14), pp. 956–65. doi: 10.1093/jnci/88.14.956.

Wang, Y. *et al.* (2000) 'Binding of 14-3-3{beta} to the Carboxyl Terminus of Wee1 Increases Wee1 Stability, Kinase Activity, and G2-M Cell Population', *Cell Growth & Differentiation*. AACR, 11(4), p. 211. Available at: <http://cgd.aacrjournals.org/cgi/content/full/11/4/211> (Accessed: 21 October 2021).

Wang, Y. *et al.* (2001) 'Radiosensitization of p53 Mutant Cells by PD0166285, a Novel G 2 Checkpoint Abrogator', *CANCER RESEARCH*, 61, pp. 8211–8217.

Wang, Y. *et al.* (2013) 'The Role of Snail in EMT and Tumorigenesis', *Current cancer drug targets*. NIH Public Access, 13(9), p. 963. Available at: [/pmc/articles/PMC4004763/](http://pmc/articles/PMC4004763/) (Accessed: 19 September 2021).

Wang, Y., Decker, S. J. and Sebolt-Leopold, J. (2004) 'Knockdown of Chk1, Wee1 and Myt1 by RNA Interference Abrogates G2 Checkpoint and Induces Apoptosis', *Cancer Biology & Therapy*, 3, pp. 305–313. doi: 10.4161/cbt.3.3.697.

Wang, Z., Gerstein, M. and Snyder, M. (2009) 'RNA-Seq: a revolutionary tool for transcriptomics', *Nature reviews. Genetics*. NIH Public Access, 10(1), p. 57. doi: 10.1038/NRG2484.

Warren, N. J. H. and Eastman, A. (2020) 'Comparison of the different mechanisms of cytotoxicity induced by Checkpoint Kinase I inhibitors when used as single agents or in combination with DNA damage', *Oncogene*. NIH Public Access, 39(7), p. 1389. doi: 10.1038/S41388-019-1079-9.

Wayne, J., Brooks, T. and Massey, A. J. (2016) 'Inhibition of Chk1 with the small molecule inhibitor V158411 induces DNA damage and cell death in an unperturbed S-phase', *Oncotarget*. Impact Journals LLC, 7(51), pp. 85033–85048. doi: 10.18632/oncotarget.13119.

Weigelt, B. *et al.* (2010) 'Breast cancer molecular profiling with single sample predictors: A retrospective analysis', *The Lancet Oncology*. Elsevier, 11(4), pp. 339–349. doi: 10.1016/S1470-2045(10)70008-5/ATTACHMENT/902F9E35-3529-4475-94DF-248727E3701F/MMC1.PDF.

Wilhelm, T. *et al.* (2014) 'Spontaneous slow replication fork progression elicits mitosis alterations in homologous recombination-deficient mammalian cells', *Proceedings of the National Academy of Sciences of the United States of America*. National Academy of Sciences, 111(2), pp. 763–768. doi: 10.1073/PNAS.1311520111/-DCSUPPLEMENTAL/SM03.MOV.

Wilsker, D. *et al.* (2008) 'Essential function of Chk1 can be uncoupled from DNA damage checkpoint and replication control', *Proceedings of the National Academy of Sciences*. National Academy of Sciences, 105(52), pp. 20752–20757. doi: 10.1073/PNAS.0806917106.

Wilson, T. R. *et al.* (2012) 'Widespread potential for growth-factor-driven resistance to anticancer kinase inhibitors', *Nature* 2012 487:7408. Nature Publishing Group, 487(7408), pp. 505–509. doi: 10.1038/nature11249.

Woodward, A. M. *et al.* (2006) 'Excess Mcm2-7 license dormant origins of replication that can be used under conditions of replicative stress', *The Journal of cell biology*. J Cell Biol, 173(5), pp. 673–683. doi: 10.1083/JCB.200602108.

World Health Organization (2020) *Breast cancer*. Available at: <https://www.who.int/news-room/fact-sheets/detail/breast-cancer> (Accessed: 20 April 2022).

*Worldwide cancer incidence statistics | Cancer Research UK* (2018). Available at: <https://www.cancerresearchuk.org/health-professional/cancer-statistics/worldwide-cancer/incidence> (Accessed: 16 June 2020).

Wu, Q. *et al.* (2020) 'Fibroblast Activation Protein (FAP) Overexpression Induces Epithelial–Mesenchymal Transition (EMT) in Oral Squamous Cell Carcinoma by Down-Regulating Dipeptidyl Peptidase 9 (DPP9)', *OncoTargets and therapy*. Dove Press, 13, p. 2599. doi: 10.2147/OTT.S243417.

Wu, X. and Chen, J. (2003) 'Autophosphorylation of checkpoint kinase 2 at serine 516 is required for radiation-induced apoptosis', *The Journal of biological chemistry*. J Biol Chem, 278(38), pp. 36163–36168. doi: 10.1074/JBC.M303795200.

X, S. *et al.* (2021) 'Overexpression of PTPRN Promotes Metastasis of Lung Adenocarcinoma and Suppresses NK Cell Cytotoxicity', *Frontiers in cell and developmental biology*. Front Cell Dev Biol, 9. doi: 10.3389/FCELL.2021.622018.

X, Z. *et al.* (2015) 'Epithelial-to-mesenchymal transition is dispensable for metastasis but induces chemoresistance in pancreatic cancer', *Nature*. Nature, 527(7579), pp. 525–530. doi: 10.1038/NATURE16064.

Xiao, Z. *et al.* (2006) 'Differential roles of checkpoint kinase 1, checkpoint kinase 2, and mitogen-activated protein kinase–activated protein kinase 2 in mediating DNA damage–induced cell cycle arrest: implications for cancer therapy', *Molecular Cancer Therapeutics*. American Association for Cancer Research, 5(8), pp. 1935–1943. doi: 10.1158/1535-7163.MCT-06-0077.

Xiao, Z. *et al.* (2008) 'Cyclin B1 is an efficacy-predicting biomarker for Chk1 inhibitors', <http://dx.doi.org/10.1080/13547500802063240>. Taylor & Francis, 13(6), pp. 579–596. doi: 10.1080/13547500802063240.

Xu, W. *et al.* (2014) 'JWA reverses cisplatin resistance via the CK2-XRCC1 pathway in human gastric cancer cells', *Cell Death and Disease*. Nature Publishing Group, 5(12), p. e1551. doi: 10.1038/cddis.2014.517.

Xu, Y. and Fisher, G. J. (2012) 'Receptor type protein tyrosine phosphatases (RPTPs) – roles in signal transduction and human disease', *Journal of Cell Communication and Signaling*. Springer, 6(3), p. 125. doi: 10.1007/S12079-012-0171-5.

Y, Z. *et al.* (2019) 'Metascape provides a biologist-oriented resource for the analysis of systems-level datasets', *Nature communications*. Nat Commun, 10(1). doi: 10.1038/S41467-019-09234-6.

Yam, C. H., Fung, T. K. and Poon, R. Y. C. (2002) 'Cyclin A in cell cycle control and cancer', *Cellular and molecular life sciences : CMLS*. Cell Mol Life Sci, 59(8), pp. 1317–1326. doi: 10.1007/S00018-002-8510-Y.

Yamada, M. *et al.* (2013) 'ATR-Chk1-APC/CCdh1-dependent stabilization of Cdc7-ASK (Dbf4) kinase is required for DNA lesion bypass under replication stress', *Genes & development*. Genes Dev, 27(22), pp. 2459–2472. doi: 10.1101/GAD.224568.113.

Yang, C. *et al.* (2012) 'Deoxycytidine kinase regulates the G2/M checkpoint through interaction with cyclin-dependent kinase 1 in response to DNA damage', *Nucleic Acids Research*. Oxford Academic, 40(19), pp. 9621–9632. doi: 10.1093/NAR/GKS707.

Yang, X. H. *et al.* (2008) 'Chk1 and Claspin potentiate PCNA ubiquitination', *Genes & development*. Genes Dev, 22(9), pp. 1147–1152. doi: 10.1101/GAD.1632808.

Yang, Z. *et al.* (2019) 'SOX11: friend or foe in tumor prevention and carcinogenesis?', *Therapeutic Advances in Medical Oncology*. SAGE Publications, 11. doi: 10.1177/1758835919853449.

Yersal, O. and Barutca, S. (2014) 'Biological subtypes of breast cancer: Prognostic and therapeutic implications', *World Journal of Clinical Oncology*. Baishideng Publishing Group Inc, 5(3), p. 412. doi: 10.5306/WJCO.V5.I3.412.

- Yonesaka, K. *et al.* (2011) 'Activation of ERBB2 signaling causes resistance to the EGFR-directed therapeutic antibody cetuximab', *Science Translational Medicine*. American Association for the Advancement of Science, 3(99). doi: 10.1126/SCITRANSLMED.3002442/SUPPL\_FILE/3-99RA86\_SM.PDF.
- Yoshida, T. *et al.* (2004) 'The clinical significance of Cyclin B1 and Wee1 expression in non-small-cell lung cancer', *Annals of Oncology*. Elsevier, 15(2), pp. 252–256. doi: 10.1093/ANNONC/MDH073.
- Yu, X. *et al.* (2017) 'Protein tyrosine phosphatase receptor-type  $\delta$  acts as a negative regulator suppressing breast cancer', *Oncotarget*. Impact Journals, LLC, 8(58), p. 98798. doi: 10.18632/ONCOTARGET.22000.
- Yusa, K. and Tsuruo, T. (1989) 'Reversal Mechanism of Multidrug Resistance by Verapamil: Direct Binding of Verapamil to P-Glycoprotein on Specific Sites and Transport of Verapamil Outward across the Plasma Membrane of K562/ADM Cells', *Cancer Research*, 49(18).
- Zabludoff, S. D. *et al.* (2008) 'AZD7762, a novel checkpoint kinase inhibitor, drives checkpoint abrogation and potentiates DNA-targeted therapies', *Molecular Cancer Therapeutics*. American Association for Cancer Research, 7(9), pp. 2955–2966. doi: 10.1158/1535-7163.MCT-08-0492.
- Zachos, G. *et al.* (2007) 'Chk1 Is Required for Spindle Checkpoint Function', *Developmental cell*. Europe PMC Funders, 12(2), p. 247. doi: 10.1016/J.DEVCEL.2007.01.003.
- Zeeberg, B. R. *et al.* (2012) 'Functional categories associated with clusters of genes that are co-expressed across the NCI-60 cancer cell lines', *PLoS ONE*. Public Library of Science, 7(1). doi: 10.1371/journal.pone.0030317.
- Zeman, M. K. and Cimprich, K. A. (2013) 'Causes and consequences of replication stress', *Nature Cell Biology* 2014 16:1. Nature Publishing Group, 16(1), pp. 2–9. doi: 10.1038/ncb2897.
- Zeman, M. K. and Cimprich, K. A. (2014) 'Causes and consequences of replication stress', *Nature Cell Biology*. doi: 10.1038/ncb2897.
- Zenvirt, S., Kravchenko-Balasha, N. and Levitzki, A. (2010) 'Status of p53 in human cancer cells does not predict efficacy of CHK1 kinase inhibitors combined with chemotherapeutic agents', *Oncogene*. Oncogene, 29(46), pp. 6149–6159. doi: 10.1038/ONC.2010.343.
- Zhang, P. *et al.* (2014) 'ATM-mediated stabilization of ZEB1 promotes DNA damage response and radioresistance through CHK1', *Nature Cell Biology* 2014 16:9. Nature Publishing Group, 16(9), pp. 864–875. doi: 10.1038/ncb3013.
- Zhang, Y. and Hunter, T. (2014) 'Roles of Chk1 in cell biology and cancer therapy', *International Journal of Cancer*. NIH Public Access, pp. 1013–1023. doi: 10.1002/ijc.28226.
- Zhang, Y. W. *et al.* (2005) 'Genotoxic stress targets human Chk1 for degradation by the ubiquitin-proteasome pathway', *Molecular Cell*. Elsevier, 19(5), pp. 607–618. doi: 10.1016/J.MOLCEL.2005.07.019/ATTACHMENT/C9069B6A-8747-4AB0-836A-15C4003E2144/MMC1.PDF.
- Zhang, Y. W. *et al.* (2009) 'The F box protein Fbx6 regulates Chk1 stability and cellular sensitivity to replication stress', *Molecular cell*. Mol Cell, 35(4), pp. 442–453. doi: 10.1016/J.MOLCEL.2009.06.030.
- Zhao, H., Watkins, J. L. and Piwnicka-Worms, H. (2002) 'Disruption of the checkpoint kinase 1/cell division cycle 25A pathway abrogates ionizing radiation-induced S and G2 checkpoints', *Proceedings of the National Academy of Sciences*. National Academy of Sciences, 99(23), pp. 14795–14800. doi: 10.1073/PNAS.182557299.
- Zhao, X., Kim, I. K., *et al.* (2021) 'Acquired small cell lung cancer resistance to Chk1 inhibitors involves Wee1 up-regulation', *Molecular Oncology*. John Wiley and Sons Ltd, 15(4), pp. 1130–1145. doi: 10.1002/1878-0261.12882/FORMAT/PDF.
- Zhao, X., Kim, I., *et al.* (2021) 'Acquired small cell lung cancer resistance to Chk1 inhibitors involves Wee1 up-regulation', *Molecular Oncology*. Wiley-Blackwell, 15(4), p. 1130. doi: 10.1002/1878-0261.12882.

Zhou, B. *et al.* (2013) 'A small-molecule blocking ribonucleotide reductase holoenzyme formation inhibits cancer cell growth and overcomes drug resistance', *Cancer research*. Cancer Res, 73(21), pp. 6484–6493. doi: 10.1158/0008-5472.CAN-13-1094.

Zhu, H. *et al.* (2020) 'PD-1/PD-L1 counterattack alliance: multiple strategies for treating triple-negative breast cancer', *Drug Discovery Today*. Elsevier Current Trends, 25(9), pp. 1762–1771. doi: 10.1016/J.DRUDIS.2020.07.006.

Zhu, H., Nie, L. and Maki, C. G. (2005) 'Cdk2-dependent Inhibition of p21 Stability via a C-terminal Cyclin-binding Motif \*', *Journal of Biological Chemistry*. Elsevier, 280(32), pp. 29282–29288. doi: 10.1074/JBC.M407352200.

Zoppoli, G. *et al.* (2012) 'Putative DNA/RNA helicase Schlafen-11 (SLFN11) sensitizes cancer cells to DNA-damaging agents', *Proceedings of the National Academy of Sciences of the United States of America*. National Academy of Sciences, 109(37), pp. 15030–15035. doi: 10.1073/pnas.1205943109.

Zou, L. and Elledge, S. J. (2003) 'Sensing DNA damage through ATRIP recognition of RPA-ssDNA complexes', *Science*. American Association for the Advancement of Science, 300(5625), pp. 1542–1548. doi: 10.1126/science.1083430.